



**HAL**  
open science

# Contribution to the partial pole placement problem for some classes of time-delay systems with applications

Amina Benarab

► **To cite this version:**

Amina Benarab. Contribution to the partial pole placement problem for some classes of time-delay systems with applications. Mathematics [math]. Université de Paris Saclay, 2022. English. NNT : . tel-03921608v1

**HAL Id: tel-03921608**

**<https://hal.science/tel-03921608v1>**

Submitted on 3 Jan 2023 (v1), last revised 17 Jan 2023 (v4)

**HAL** is a multi-disciplinary open access archive for the deposit and dissemination of scientific research documents, whether they are published or not. The documents may come from teaching and research institutions in France or abroad, or from public or private research centers.

L'archive ouverte pluridisciplinaire **HAL**, est destinée au dépôt et à la diffusion de documents scientifiques de niveau recherche, publiés ou non, émanant des établissements d'enseignement et de recherche français ou étrangers, des laboratoires publics ou privés.

Contribution to the partial pole  
placement problem for some classes of  
time-delay systems with applications  
*Contribution au problème du placement partiel des pôles  
pour certaines classes de systèmes à retard, avec  
applications*

**Thèse de doctorat de l'université Paris-Saclay**

École doctorale n°580 : Sciences et technologies de l'information et de la  
communication (STIC)

Spécialité de doctorat : Mathématiques et Informatique

Graduate School : Sciences de l'ingénieur et des systèmes (SIS),

Référent : Faculté des sciences d'Orsay

Thèse préparée dans l'unité de recherche Laboratoire des signaux et systèmes  
(Université Paris-Saclay, CNRS, CentraleSupélec), sous la direction de Islam  
BOUSSAASDA, Professeur IPSA, le co-encadrement de Catherine BONNET,  
Directrice de recherche Inria, le co-encadrement de Karim TRABELSI, Directeur  
Délégué à la Recherche IPSA

**Thèse soutenue à Paris-Saclay, le 30 novembre 2022, par**

**Amina BENARAB**

**Composition du jury**

**Jean Jacques Loiseau**

Directeur de recherche, CNRS & LS2N

**Tomas Vyhlidal**

Professeur, ČVUT

**Kaïs Ammari**

Professeur, Université de Monastir

**Federico Bribiesca Argomedo**

Maître de Conférences, INSA & Ampère

**Delphine Bresch-Pietri**

Professeur assistant, Mines Paris-PSL

**Sami Tiiba**

Maître de conférences, L2S

**Islam Boussaada**

Professeur, IPSA & L2S

Rapporteur

Rapporteur

Président

Examineur

Examinatrice

Examineur

Directeur de thèse

**Titre:** Contribution au problème du placement partiel des pôles pour certaines classes de systèmes à retard, avec applications.

**Mots clés:** Systèmes à retard, placement de pôles, stabilité exponentielle, équations différentielles fonctionnelles neutres, Multiplicity-Induced-Dominancy, oscillateur classique.

**Résumé:** Une des questions d'intérêt pour les systèmes linéaires à retard est de déterminer les conditions sur les paramètres de l'équation qui garantissent la stabilité exponentielle des solutions. En général, c'est un véritable défi d'établir des conditions sur les paramètres du système afin de garantir une telle stabilité. L'une des approches efficaces dans l'analyse de stabilité des systèmes à retard est l'approche fréquentielle. Dans le domaine de Laplace, l'analyse de stabilité revient à étudier la distribution des racines des fonctions quasipolynomiales caractéristiques. Une fois la stabilité d'un système à retard prouvée, il est important de caractériser le taux de décroissance exponentielle des solutions de ces systèmes. Dans le domaine fréquentiel, ce taux de décroissance correspond à la valeur spectrale dominante. Des travaux récents ont mis en évidence le lien entre la multiplicité maximale et les racines dominantes.

En effet, les conditions pour qu'une racine multiple donnée soit dominante sont étudiées, cette propriété est connue sous le nom de Multiplicity-Induced-Dominancy (MID). Dans cette thèse, trois sujets liés à la propriété MID sont étudiés. Premièrement, l'effet des racines multiples avec des multiplicités admissibles présentant, sous des conditions appropriées, la validité de la propriété MID pour les équations différentielles neutres du second ordre avec un seul retard est exploré. La stabilisation de l'oscillateur classique bénéficie des résultats obtenus. Deuxièmement, les effets des retards sur la stabilité des véhicules aériens sans pilote (UAV) sont exploités. À cet égard, une application symbolique/numérique de la propriété MID dans le contrôle des drones à rotor avec des retards est fournie. Enfin, la stabilisation d'une balance à roulettes par le biais de la propriété MID est considérée.

**Title:** Contribution to the partial pole placement problem for some classes of time-delay systems with applications.

**Keywords:** Time-delay systems, pole placement, exponential stability, neutral functional differential equations, Multiplicity-Induced-Dominancy, classical oscillator.

**Abstract:** One of the questions of ongoing interest for linear time-delay systems is to determine conditions on the equation's parameters that guarantee the exponential stability of solutions. In general, it is quite a challenge to establish conditions on the parameters of the system in order to guarantee such a stability. One of the effective approaches in the stability analysis of time-delay systems is the frequency domain approach. In the Laplace domain, the stability analysis amounts to study the distribution of characteristic quasipolynomial functions' roots. Once the stability of a delay system has been proven, it is important to characterize the exponential decay rate of the solutions of such systems. In the frequency domain, this decay rate corresponds to the dominant spectral value. Recent works emphasized the link between maximal multiplicity and dominant roots.

Indeed, conditions for a given multiple root to be dominant are investigated, this property is known as Multiplicity-Induced-Dominancy (MID). In this dissertation, three topics related to the MID property are investigated. Firstly, the effect of multiple roots with admissible multiplicities exhibiting, under appropriate conditions, the validity of the MID property for second-order neutral time-delay differential equations with a single delay is explored. The stabilization of the classical oscillator benefits from the obtained results. Secondly, the effects of time-delays on the stability of Unmanned Aerial Vehicles (UAVs) is exploited. In this regard, a symbolic/numeric application of the MID property in the control of UAV rotorcrafts featuring time-delays is provided. Lastly, the stabilization of a rolling balance board by means of the MID property is considered.

# Acknowledgement

My first thanks go to my supervisors: Mr. Islam Boussaada, professor at IPSA Paris; Ms. Catherine Bonnet, research director at Inria Saclay and Mr. Karim Trabelsi, research director at IPSA Paris. I want to thank them for their guidance, help, and availability. The judicious advice they gave me throughout these three years of my thesis allowed me to progress and complete this work in the best conditions.

I want to especially thank Islam Boussaada for his support and for opening many doors to the research and academic world for me. I thank him for bringing to my attention many interesting research subjects and motivating me to work on them.

I want to thank Catherine Bonnet for her time and devotion. She provided support from both a scientific point of view and a humane point of view. I'm thankful for her kindness, the valuable advice, and the comfort she provided.

I want to thank Karim Trabelsi for all his guidance in improving my English and the presentation of the results in my articles and thesis manuscript. He was always present when I needed help with administrative tasks regarding the enrolment procedures and when I needed advice in general terms.

I want to thank Mr. Silviu-Iulian Niculescu for the precious discussions that I had with him. These discussions were very enriching for me.

I am very honored that Mr. Jean Jacques Loiseau, research director at LS2N Nantes, and Mr. Tomas Vyhlidal, professor at ČVUT Prague, have accepted to report my work. I want to thank them for the quality of their reading. Special thanks to Jean Jacques Loiseau for his time to explain some of the issues. He freed himself from his busy schedule to discuss with Catherine and me and shed some light on pole placement via the algebraic approach.

It is a great honor that Kaïs Ammari, Federico Bribiesca Argomedo, Delphine Bresch-Pietri, and Sami Tliba accepted to be members among the examiners of my thesis, and I am very grateful to them. I want to thank Sami, who helped explain the control of vibrations and suggested a line of work that interests me a lot, which motivated me to exploit the approach I am currently working on within vibration control. He kindly accompanied me to the experiment room, where he showed me several manipulations, among which one is an aluminum-based beam embedded in a mobile support.

I want to thank my fellow doctoral students, Abdelhak, Alex, Csgenge, Didine, Elissa, Fanni, Kike, Midou, Muhammad, Pepe, and many others, for their support and friendship. Special mention must be given to Ali Diab, whom I thank for all the time we spent together and for all the fruitful discussions. I also want to thank the researcher Alejandro "Gosmis" Apaza Perez, who spent days and months helping and cheering me up during the most challenging times. Thank you very much for our mathematical and philosophical discussions.

Many thanks to IPSA for the financial support during my thesis and the excellent teaching opportunity. In this same regard, I thank all the staff of the L2S-CentraleSupélec, that was always available and supportive.

Most importantly, I owe very much to my family for their love and encouragement. To my brothers: Belkacem, Abdelkrim, and Hani. To my sisters: Saadia, Wassila, Bahia, Karen, and Aya, my little sister who drew the left Figure of a human stance on a uniaxial rolling balance board in Figure 2. I particularly thank Abdelkrim, Belkacem and Karen who came from far away to support me, attend my defence and celebrate my success with me. I lastly thank my closest cousin, Hakim, who has always appreciated and believed in me.

Many thanks to my dear husband, Tayeb, for his full support and love. His presence by my side is comforting and indispensable to me. I also want to thank my family-in-law, particularly Lounis. Their support is appreciated.

Last but not least, to my parents, who do not speak and understand English, I devote a heartfelt paragraph written in Kabyle (interpreted by Aya, my little sister):

Yemma-ynu atawizet ibedden yef  
uqaruy-iw  
DaDa-ynu atafat n tudert-iw  
Yemma εzizen aticert n rbeḥ-iw  
iyidεan deg tfejrit mi tṣen  
medden  
DaDa-ynu alefnar iyiceεlen  
abrid-iw ur yliy ass kecc deffir  
uzagur-iw  
Yemma-ynu atahnint , tbedeḍ yidi  
s imeslayen-im ufiy talwit  
DaDa Akkd yemma atigzert  
yefren asirem s yiswen wdey yer  
wayen iresmey deg temzi-w  
Tberkem felli ar almi seiy  
afriwen , teb3ey leqraya-w deg  
lyurba lameεna yas aken maca  
seg zegwen ittawiy lebyi  
ukemmel  
Tmuddem-iyi-d Ur tcuḥem felli  
deg lqewwa akkd tayri ...  
Sawdem-yi seg usaεef-nwen yer  
wassa , ass n lefreḥ d zhu Akk  
ayen iyiεnan d wayen iyimudden  
taḍssa  
Ass adawiy tawriq-t inetnadi  
fella-s di kraḍ yedney seg zik  
"rbeḥ-iw"  
Anecta zegwen id-yekka  
Yemma , DaDa d kunwi i d isni ara  
ad sersey sufel uqerruy-iw assa  
n tekfa di leqraya-w werjin d  
tacacit 🎓  
Tamslayt Ur tessekfay ayen  
txedmem yidi deg lxir meεna  
tanmirt-nwen s teyzi n  
leεmer-nwen  
Akenyahrez rebbi  
Hemley-kun atas

## Declaration of Authorship

I, Amina Benarab, declare that this thesis, titled "*Contribution to the partial pole placement problem for some classes of time-delay systems with applications*", and the work introduced herein are of my own authorship, thus I confirm that:

- This work was done during the pre-established time corresponding to the Ph.D. formation at University of Paris Saclay.
- Any part of this thesis has previously been submitted for a degree or any other qualification at this University or any other institution, this has been clearly stated.
- The publications where the results of this work have been presented are properly mentioned.
- Citations to this manuscript are properly done.
- Any source of help has been included in the acknowledgements of this manuscript.
- The work done in conjunction with others is clearly declared, highlighting the contributions of mine.

Amina Benarab

Signed at **Gif-sur-Yvette, France** on **November 30, 2022**

Copyright © of the papers may go to the corresponding publication institution



# Contents

List of Figures	10
List of Tables	11
List of Symbols and Acronyms	13
Introduction (Version Française)	15
Introduction (English Version)	23
Publications List	31
<b>I Prerequisites</b>	<b>33</b>
<b>1 Definitions, prerequisites, and basic results</b>	<b>35</b>
1.1 Linear time-delay systems with single delay and constant coefficients . . . . .	35
1.2 The Multiplicity-Induced-Dominancy approach . . . . .	38
1.2.1 GMID property for first-order scalar neutral equations . . . . .	39
1.2.2 IMID property for second-order scalar neutral equations . . . . .	40
1.3 Partial pole placement via delay action ( $P3\delta$ ) . . . . .	40
1.4 Special functions in control design: Confluent hypergeometric functions . . . . .	41
1.5 Insights on nonlinear time-delay systems . . . . .	43
<b>2 Existing pole placement paradigms</b>	<b>47</b>
2.1 Introduction . . . . .	47
2.2 Finite spectrum assignment . . . . .	49
2.3 Algebraic pole placement . . . . .	51
2.4 Continuous pole placement . . . . .	54
2.5 Partial pole placement . . . . .	56
2.6 Illustrative examples . . . . .	57
2.7 Chapter Summary . . . . .	63
<b>II Partial pole placement approach</b>	<b>65</b>
<b>3 The GMID property for second order neutral equation</b>	<b>67</b>
3.1 Introduction . . . . .	67
3.2 The MID methodology on a toy model: Codimension 3 . . . . .	67
3.3 Problem Setting . . . . .	71
3.4 Statement of the main results . . . . .	72



3.5	Proof of the main results . . . . .	73
3.6	Illustrative example: exponential stabilization of an oscillator using delay action . . . . .	77
3.7	Chapter Summary . . . . .	78
<b>4</b>	<b>The IMID property for second order neutral equation</b>	<b>81</b>
4.1	Introduction . . . . .	81
4.2	MID methodology on a toy model: Codimension 2 . . . . .	82
4.3	Problem setting . . . . .	86
4.4	Statement of the main result . . . . .	87
4.5	Proof of the main result . . . . .	90
4.6	Illustrative example: classical oscillator . . . . .	102
4.7	Further remarks on the IMID: codimension 2 . . . . .	105
4.8	Some insights on linear combinations of two kummer functions . . . . .	107
4.9	Chapter Summary . . . . .	111
<b>III</b>	<b>Applications</b>	<b>113</b>
<b>5</b>	<b>Applying the MID property in the control of aerial vehicles</b>	<b>115</b>
5.1	Introduction . . . . .	115
5.2	Quadrotor models . . . . .	116
5.3	UAV control: The typical quadrotor case . . . . .	118
5.3.1	MID-property-based controllers analysis . . . . .	120
5.3.2	Symbolic/Numeric analysis of the MID-based controller . . . . .	122
5.4	UAV control: the tilting-rotors case . . . . .	127
5.5	Simulation results . . . . .	130
5.5.1	The typical quadrotor case . . . . .	131
5.5.2	The tilting-rotors case . . . . .	133
5.6	Chapter Summary . . . . .	133
<b>6</b>	<b>Bio-mechanical perspectives: Modeling the CNS Action</b>	<b>135</b>
6.1	Introduction . . . . .	135
6.2	Mechanical model . . . . .	136
6.3	Mathematical model . . . . .	138
6.4	Main results . . . . .	140
6.5	Illustration example . . . . .	142
6.6	Chapter Summary . . . . .	144
<b>7</b>	<b>Conclusion and Prospects</b>	<b>145</b>
7.1	Conclusion . . . . .	145
7.2	Prospects . . . . .	146
<b>A</b>	<b>Proofs of some technical lemmas</b>	<b>151</b>

## List of Figures

1	(Gauche) Interaction des neurones. (Droite) Fraiseuse à commande numérique. . . . .	15
2	(Gauche) Équilibre humain sur une planche d'équilibre roulante. (Droite) Véhicule quadrirotor : Drone. . . . .	16
3	(Left) Neurons' interaction. (Right) Computer numerical control (CNC) milling. . . . .	23
4	(Left) Human stance on a uniaxial rolling balance board in the sagittal plane. (Right) Quadrotor vehicle: Drone. . . . .	24
1.1	Spectrum distribution of delay equations: retarded, neutral and advanced type. . . . .	36
1.2	Initial value problem. . . . .	44
2.1	Block diagram of the closed-loop system. . . . .	58
2.2	Rightmost eigenvalues of the system (2.46)–(2.47) as a function of the delay $k = [0.719 \ 1.04 \ 1.29]^T$ . . . . .	61
2.3	(Left) Rightmost eigenvalues of the system (2.46)–(2.47) as a function of the delay $\tau$ for $K = (0.712 \ 1.075 \ 0.831)^T$ at iteration 37. (Right) $K = (0.559 \ 0.770 \ 0.694)^T$ at iteration 110. . . . .	61
2.4	Translation of the spectrum distribution of $\Delta_0$ according to the delay change. . . . .	62
3.1	Diagram illustrating the proof methodology of the MID property for a second-order time-delay differential equation . . . . .	68
3.2	Spectrum distribution of the quasipolynomial $\hat{\Delta}$ in (3.35). . . . .	76
3.3	Response of the oscillator (3.45) subjected to the stabilizing MID property, with $\xi = \frac{1}{2}, \omega = 1$ . . . . .	79
4.1	Plot emphasizes the fact that an interesting frequency bound ( $0 < \omega < \pi$ ) may be found only for a positive $\vartheta$ satisfying $\vartheta \leq \frac{5}{2}$ . . . . .	86
4.2	Plot of the region $R_q$ in terms of the parameters $(\delta, \nu)$ as defined in (4.56), (4.57) and (4.58). . . . .	93
4.3	Plot represents region $R_{D^+} = R_1^{+-}$ . . . . .	97
4.4	Plot shows a zoom on the regions $P_i, i = 1..4$ . . . . .	97
4.5	Plot represents the region $R_{A^+} \cup R_{A^-}$ . . . . .	99
4.6	Plot represents region $R_{d^+}$ . . . . .	100
4.7	Plot represents regions $\tilde{P}_1, \tilde{P}_2$ and $\tilde{P}_3$ . . . . .	100
4.8	Plot shows that regions $P_i, i = 1..4$ obtained for an order zero truncation have been recovered and enlarged when we increased the truncation order. . . . .	101

4.9	For $\omega = 2$ , $\eta = \frac{1}{9}$ and $\tau = 1$ , the plot exhibits the spectrum distribution of the quasipolynomial $\Delta$ where the assigned rightmost triple root at $s_0 = -3$ and the roots with large modulus are asymptotic to a vertical line $\Re(s) \approx -\frac{1}{\tau} \log  \alpha  \approx -4.2$ ([97]). . . . .	105
4.10	For $\omega = 2$ , $\eta = \frac{1}{9}$ and $\tau = 1$ , the plot illustrates the oscillator response with initial condition taken to be $\varphi(t) = 1$ for $t \in [-\tau, 0)$ . . . . .	106
4.11	The plot illustrates for $\omega = 2$ , $\eta = 0.02$ the rightmost double root of $\Delta$ at $s_0 = -0.5$ and the roots with large modulus asymptotic to the vertical line $\Re(s) \approx -\frac{1}{\tau} \log  \alpha  \approx -1.88$ . . . . .	106
4.12	The plot is the time-response of a particular solution of (4.103) with $\omega = 2$ , $\eta = 0.02$ ; the initial condition is taken to be $\varphi(t) = t^3$ for $t \in [-\tau, 0)$ . . . . .	107
5.1	Quadrotor vehicle and vision-based tracking system (scheme conceived from figures available at <i>freepik.com</i> ) . . . . .	117
5.2	Block diagram representation of the typical quadrotor closed-loop system . . . . .	120
5.3	Behavior of $R_{3,x}^*(\zeta; \nu)$ within the interval $0 < \nu < 1$ . Numerical evidence of the dominance of the root $s_{0_x}$ within the intervals in (5.61)-(5.63) with $\tau = 0.1$ [s] . . . . .	127
5.4	Spectral distribution of the roots . . . . .	127
5.5	Time-domain solution . . . . .	128
5.6	Block diagram representation of the quadrotor with tilting-rotors closed-loop system . . . . .	130
5.7	Motion of the typical quadrotor vehicle: Left) Translational states. Right) Rotational states. . . . .	132
5.8	Motion of the quadrotor vehicle endowed with tilting-rotors: Left) Translational states. Right) Rotational states. . . . .	134
6.1	2-DOF mechanical model of human stance on a uniaxial rolling balance board in the sagittal plane. . . . .	137
6.2	2-DOF mechanical model of human stance on a uniaxial rolling balance board in the sagittal plane. . . . .	143
6.3	Spectrum distribution of the characteristic equation . . . . .	144
A.1	The discriminant $D$ of $f$ . . . . .	153
A.2	Graph of $\Omega_+$ (red) and $\Omega_-$ (blue). . . . .	153
A.3	Graphs of $P$ (red), $P'$ (blue), $P^2$ (brown) and $P^3$ (green). . . . .	155
A.4	Plot of solutions of the equation $\tan(\xi) = \frac{3\xi}{3-\xi^2}$ . . . . .	157
A.5	Diagram representing conditions in parameter space guaranteeing the constancy sign of $q_{\delta,\nu}$ . . . . .	160

## List of Tables

5.1	Parameters of the UAVs . . . . .	130
5.2	Control gains: Typical quadrotor . . . . .	130
5.3	Control gains: Quadrotor endowed with titling rotors . . . . .	131
6.1	Result of MID-based control design . . . . .	143



# List of Symbols and Acronyms

## List of Symbols

$\mathbb{R}$	The set of real numbers
$\mathbb{R}_+$	The set of positive real numbers
$\mathbb{R}_+^*$	The set of non-negative real numbers
$\mathbb{C}$	the set of complex numbers
$\mathbb{C}_+$	The right half complex plane
$\mathbb{C}_-$	The left half complex plane
$\Re(\cdot)$	the real part of a complex number
$\Im(\cdot)$	The imaginary part of a complex number
$\mathbb{I}_n$	the identity matrix of dimension $n$
$A^T$	the transpose matrix of $A$
$\mathcal{R}[s]$	The ring of polynomials in $s$ over $\mathcal{R}$
$\mathcal{R}(s)$	The quotient files of $\mathcal{R}[s]$
$\mathcal{R}[s, z]$	the ring of 2-D polynomials in $s$ and $z$ over $\mathcal{R}$
$\deg_s(P)$	The degree of $P$ with respect to the variable $s$
$PS_B$	Polya and Szegö bound
$\sigma(A)$	The spectrum of $A$
$P_\sigma(A)$	The point spectrum of $A$

## List of Acronyms

TDS	Time-Delay System
LTI	Linear Time Invariant
DDE	Delay-Differential Equation
PDE	Partial-Differential Equation
FSA	Finite Spectrum Assignment
CPP	Continuous Pole Placement
APP	Algebraic Pole Placement
PPP	Partial Pole Placement
P3 $\delta$	Partial Pole Placement via Delay Action
MID	Multiplicity-Induced-Dominancy
GMID	Generic Multiplicity-Induced-Dominancy
IMID	Intermediate Multiplicity-Induced-Dominancy
PD	Proportional-Derivative
PID	Proportional Integral Derivative
PDA	Proportional-Derivative-Acceleration
UAVs	Unmanned Aerial Vehicles
CNS	Central Nervous System
i-DOF	i-Degree-Of-Freedom



## Introduction (Version Française)

Les systèmes à retards fournissent des modèles utiles dans un grand nombre de domaines scientifiques et technologiques tels que la biologie (par exemple, les interactions entre les neurones), la chimie, l'économie, la physique (par exemple, les lasers à rétroaction optique) ou l'ingénierie (par exemple, les vibrations des machines-outils : les machines de découpe et de fraisage), où la présence des retards est inhérente aux phénomènes de propagation, tels que la matière, l'énergie ou l'information, avec une vitesse de propagation finie. Pour plus de détails sur les systèmes à retard et leurs applications, voir [1]–[13].



Figure 1: (Gauche) Interaction des neurones. (Droite) Fraiseuse à commande numérique.

Deux applications nous intéressent en particulier et seront discutées plus en détail par la suite. La première concerne la robotique, en particulier la commande de véhicules aériens sans pilote (UAVs) à rotor avec des retards. Parmi les divers problèmes qui nuisent aux performances des systèmes aériens, l'étude des effets des retards reste relativement inexplorée. Dans la pratique, les systèmes de contrôle des drones fonctionnent en présence de retards provenant du traitement de la perception, de la prise de décision, des commandes de contrôle et de la dynamique retardée des actionneurs. En fait, il a été prouvé que les retards induisent des phénomènes oscillatoires qui rendent le système instable. L'étude de ces systèmes dynamiques à retard reste un sujet populaire et stimulant au sein de la communauté scientifique des systèmes de contrôle et de la robotique. La commande de ces systèmes à retard a beaucoup progressé et a déjà été utile dans de nombreuses applications.

La deuxième application concerne la bio-mécanique, plus précisément le contrôle du système nerveux central (CNS). En fait, le déséquilibre peut être dû à une multitude de déclinés associés à l'âge dans la fonction sensorimotrice, notamment la somatosensation, la fonction vestibulaire, la vision, la cognition et la force [14].



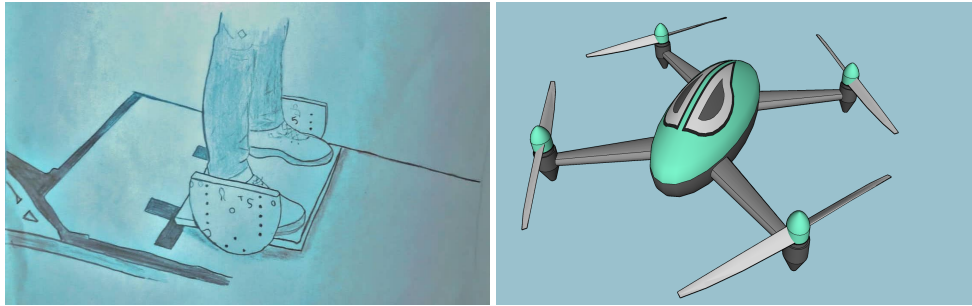


Figure 2: (Gauche) Équilibre humain sur une planche d'équilibre roulante. (Droite) Véhicule quadrirotor : Drone.

La stabilisation du corps humain et la planche d'équilibre est assurée par un processus de contrôle régi par le CNS. Les systèmes visuels, vestibulaires et somatosensoriels obtiennent des informations sur l'orientation spatiale du corps humain. Les informations sont transmises au cerveau, le CNS détermine l'interaction nécessaire pour maintenir l'équilibre après avoir traité les signaux et envoie une instruction à la musculature. Le processus décrit ci-dessus nécessite un temps défini appelé *temps de réaction*. Par conséquent, le modèle mathématique des tâches d'équilibrage implique une loi de commande retardée, ici une rétroaction proportionnelle-dérivée (PD) avec un retard de rétroaction constant [15]–[17], puisque les systèmes visuels et vestibulaires perçoivent respectivement la position et la vitesse. D'autres modèles de commande neuromusculaire fréquemment utilisés sont par exemple la rétroaction proportionnelle-dérivée-accélération (PDA) retardée [18], [19], contrôle intermittent [20]–[25] et la rétroaction du prédictiveur [18], [26]. Une question importante pour le contrôle de l'équilibre humain est traitée dans [27] où un contrôleur à temps discret et un contrôleur PDA retardé à temps continu sont considérés et la transition entre eux via la semi-discrétisation est établie. Il a été montré dans [28] et [29] qu'un terme intégral n'améliore pas la stabilisation du système en présence d'un retard de rétroaction, c'est pourquoi nous nous concentrons ici uniquement sur la rétroaction PD.

Il existe deux classes différentes de modèles : macroscopique (ou continuum) et microscopique (ou suivi de voiture). Le premier modèle décrit le trafic en termes de distributions continues de densité et de vitesse, tandis que le second modèle décrit le comportement des véhicules individuels. Notez que des retards peuvent également être inclus dans les modèles de continuum pour imiter le temps de réaction du conducteur. Ces retards peuvent modifier considérablement la dynamique du trafic, entraînant des instabilités pour les systèmes linéaires et non linéaires [30]. En revanche, certains systèmes qui ne sont pas stabilisables sans retard peuvent être stabilisés avec utilisation d'un retard artificiel dans la rétroaction de sortie statique (à temps continu) [31], [32].

Pour les systèmes linéaires à retard invariant dans le temps (LTI), l'une des idées les plus simples pour contrôler le comportement dynamique du système en boucle fermée consiste à placer les pôles du système à certains endroits souhaitables du plan complexe. Une telle méthode est appelée *placement de pôles* (voir par exemple [33]). Schématiquement, les principaux ingrédients du placement de pôle sont :

- la connaissance parfaite des variables d'état,
- certaines hypothèses de contrôlabilité appropriées sur le système, c'est-à-dire la possibilité de diriger un système dynamique d'un état initial arbitraire à un état final arbitraire au moyen d'un ensemble approprié de lois de contrôle admissibles.

Si cette méthode de placement de pôles est facile à comprendre et à appliquer dans le contrôle des systèmes LTI de dimension finie, son extension aux systèmes décrits par des équations différentielles à retard (DDEs) semble plus complexe. Plus précisément, deux questions doivent être abordées :

1. l'introduction d'une notion appropriée de contrôlabilité pour les systèmes à retard,
2. la compréhension approfondie de l'emplacement des pôles du système en boucle fermée en fonction des paramètres du contrôleur.

Pour une bonne introduction aux notions de contrôlabilité des systèmes à dimensions finies et infinies, y compris le cas des systèmes dynamiques représentés par des DDEs, nous renvoyons vers [34]. Une discussion plus approfondie des méthodes existantes pour caractériser les régions de stabilité dans l'espace des paramètres peut être trouvée dans [8]. Enfin, même pour certaines classes d'équations aux dérivées partielles (EDPs), le contrôle retardé a montré une certaine efficacité (voir par exemple [35], [36]). D'autre part, des reformulations d'EDPs et le *backstepping* ont été utilisées pour montrer qu'une loi de commande nominale compense les retards d'entrée en boucle fermée et fournit une stabilisation exponentielle nominale [37], [38]; voir également [39] où l'étude de la commande basée sur la prédiction portait sur des systèmes non linéaires soumis à des retards d'entrée ponctuels et à des retards d'état (potentiellement) distribués. [39].

À notre connaissance, les premiers résultats sur la localisation du spectre des systèmes linéaires représentés par des DDEs ont été publiés il y a un siècle. En effet, à la fin des années 20s, des travaux presque oubliés de [40] et [41] semblent être les premiers résultats à aborder un tel problème.

À la fin des années 70s, le concept de placement des pôles est apparu dans la théorie du contrôle sous la forme de *Assigment d'un spectre fini* (FSA); [42],

[43], dont le résultat était de contrebalancer l'effet du retard par une prédiction de l'état sur un intervalle de retard, réduisant ainsi le système en boucle fermée à un système de dimension finie; nous renvoyons vers [44] pour une vue d'ensemble des principaux ingrédients et une confrontation avec d'autres méthodes dédiées au contrôle de systèmes dynamiques présentant des retards dans l'entrée. En fait, la stratégie a été explorée en profondeur dans un cadre algébrique plus adéquat par [45] via l'introduction de l'anneau  $\mathcal{R}$ , c'est-à-dire, l'ensemble de toutes les fonctions méromorphes dans le plan complexe  $\mathbb{C}$  représenté génériquement comme  $\frac{P(s, e^{-\tau s})}{Q(s)}$ , où  $Q$  est un polynôme en la variable complexe de Laplace  $s$ ,  $P$  est un polynôme bivarié en  $s$  et  $e^{-\tau s}$ , et  $\tau$  est un nombre réel positif fixe. La conception algébrique de contrôleurs des systèmes différentiels à retard invariant dans le temps consiste en l'investigation algorithmique de l'anneau  $\mathcal{R}$ . Ces méthodes algébriques permettent une analyse de stabilité des systèmes à retard. Cependant, leur limitation a été observée au début des années 2000 dans [46]. Numériquement, la stabilité du système en boucle fermée est très sensible aux incertitudes infinitésimales. Ce dernier phénomène, connu sous le nom de *spillover*.

Le placement de pôles des systèmes à retard est plus qu'un problème d'interpolation quasipolynomial. En fait, dans [47],  $N$  pôles du système sont assignés à certaines positions souhaitées dans le plan complexe par  $N$  paramètres de rétroaction de la même manière que dans le cas en dimension finie. Néanmoins, afin d'éviter l'effet de *spillover*, il est bien connu qu'une telle interpolation est un placement efficace si, et seulement si, les valeurs spectrales restantes du système en boucle fermée sont situées à gauche du pôle le plus à droite des pôles assignés; c'est-à-dire que l'assignation réussit si ces derniers sont dominants. Cependant, cette caractéristique n'est pas garantie en général, comme le fait remarquer [48]; voir également [49], où l'on ne tente pas de prouver la dominance des pôles placés, mais où l'on applique plutôt une règle de bon sens par essais et erreurs pour plusieurs sélections de pôles assignés. Plus récemment, en s'appuyant sur l'effet des valeurs spectrales multiples sur la stabilité des DDEs, une nouvelle stratégie analytique de placement des pôles a été conçue dans [50]. Cette propriété a été évoquée dans [51], bien qu'illustrée par des cas simples d'ordre faible, sans tentative d'aborder le cas général. À notre connaissance, très peu de travaux ont abordé cette question de manière systématique jusqu'à récemment; voir [50], [52]–[58].

Considérons l'équation différentielle à retard (générique) :

$$\sum_{k=0}^n a_k x^{(k)}(t) + \alpha_k x^{(k)}(t - \tau) = 0, \quad (1)$$

où la fonction inconnue  $x$  est à valeurs réelles,  $a_k, \alpha_k \in \mathbb{R}$ , et le retard  $\tau > 0$ . Les systèmes linéaires avec retards sont décrits dans le domaine de Laplace par des fonctions de transfert impliquant des quasi-polynômes et admettent alors un nom-

bre infini de pôles. Ces quasi-polynômes ont été largement étudiés dans [59]–[61]. L'étude des propriétés de stabilité des systèmes de type *retardés* (ils admettent un nombre fini de pôles dans tout demi-plan droit) est beaucoup plus facile que l'étude de celles des systèmes de type *neutres* qui peuvent avoir un nombre infini de pôles, en chaînes asymptotiques à un axe vertical éventuellement situé dans le demi-plan droit ouvert ou sur l'axe imaginaire. Ces deux situations empêchent d'obtenir la stabilité exponentielle pour ces systèmes.

Il existe des études de stabilité des systèmes à retard, notamment des systèmes à retard constant unique ou multiple (voir par exemple [5]); des systèmes à retards combinés [62]; des équations aux différences à retard (voir par exemple [63]). Pour d'autres applications des méthodes spectrales, voir [64]–[66].

Pour effectuer l'analyse de stabilité, des méthodes efficaces ont été proposées dans le domaine fréquentiel, voir par exemple, [1], [5], [67]–[71]. Même avec les avancées significatives qui ont été rapportées sur ces sujets, la question de la détermination des conditions sur les paramètres du système qui garantissent la stabilité asymptotique des solutions des systèmes LTI à retard reste toujours *ouverte*.

Les méthodes spectrales, qui étudient la distribution du spectre des équations caractéristiques, constituent un outil puissant pour comprendre le comportement asymptotique des solutions des systèmes LTI à retard.

La fonction caractéristique de l'équation (1) est la fonction quasipolynomiale  $\Delta : \mathbb{C} \rightarrow \mathbb{C}$  définie pour  $s \in \mathbb{C}$  par:

$$\Delta(s) = \sum_{k=0}^n a_k s^k + \alpha_k s^k e^{-\tau s}. \quad (2)$$

La multiplicité d'une racine d'un quasi-polynôme est limitée par la *borne générique de Polya et Szegö* (notée  $PS_B$ ), qui est égale au *degré* du quasi-polynôme correspondant, c'est-à-dire la somme des degrés des polynômes impliqués plus le nombre des retards; voir par exemple [72, Problème 206.2, page 144 et page 347]. Il est intéressant de mentionner qu'une telle limite a été prouvée en utilisant des matrices structurées dans [73] plutôt que le principe d'argument comme dans [72]. En particulier, le degré de  $\Delta$  dans (2) est  $\deg_s(\Delta) = 2n + 1$ .

Pour le comportement exponentiel des solutions de (1), on s'intéresse à l'*abscisse spectrale* de la fonction caractéristique correspondante  $\Delta$  qui est le nombre réel

$$\rho = \sup\{\Re(s) \mid s \in \mathbb{C}, \Delta(s) = 0\}, \quad (3)$$

lié à la notion de taux de décroissance des solutions des systèmes à retard, voir [[1], Chapter 1, Theorem 6.2] pour plus de détails.

Du point de vue de la théorie du contrôle, on s'intéresse à une méthodologie récente de contrôle appelée *placement de pôle partiel* (PPP) [74], [75] et basée sur l'assignation du taux de décroissance de la solution dominante en boucle fermée. En effet, il s'avère que, pour les quasi-polynômes caractéristiques de certains systèmes à retard, les racines réelles de *multiplicité maximale* sont nécessairement *dominantes* (racines avec partie réelle la plus grande), cette propriété est connue sous le nom de "Generic Multiplicity-Induced-Dominancy" (GMID), elle se réfère à des conditions spéciales sur les paramètres libres du système (typiquement les paramètres de contrôle) où une racine caractéristique donnée correspond à l'abscisse spectrale telle que la valeur spectrale correspondante est dominante; voir par exemple [50], [76]. Dans le cas des racines multiples avec une multiplicité strictement intermédiaire, il faut chercher les conditions qui permettent de définir la région d'assignation admissible, propriété baptisée "Intermediate Multiplicity-Induced-Dominancy" (IMID); voir [50].

Grâce à cette propriété, une stratégie de contrôle asservi est proposée dans [50], [77], [78], qui consiste à assigner une racine avec une multiplicité admissible une fois que les conditions appropriées garantissant sa dominance sont déterminées. En outre, la propriété Multiplicity-Induced-Dominancy (MID) peut être utilisée pour régler les contrôleurs standards. Par exemple, dans [78], elle est appliquée au réglage systématique du contrôleur proportionnel-intégral-dérivé (PID) stabilisateur d'un système du premier ordre.

La propriété MID a été évoquée pour la première fois dans [51] pour certains cas d'ordre faible sans aucune tentative d'aborder la question générale; voir également [79] pour les équations scalaires spécifiques d'ordre 1. Des développements récents poursuivent l'étude de la propriété MID principalement dans le cas d'un seul retard, voir par exemple [50], [52]–[57], [78].

À notre connaissance, une preuve analytique de la caractérisation de l'abscisse spectrale pour l'équation scalaire avec un seul retard a été présentée et discutée pour la première fois dans les années 50s; voir [79]. La propriété de dominance est explorée et démontrée analytiquement pour les équations scalaires à retard dans [52], puis pour les systèmes du second ordre contrôlés par un contrôleur proportionnel retardé dans [53], [80], où son applicabilité à l'amortissement des vibrations actives pour une poutre piézo-actionnée est prouvée. Voir également [81], [82] qui présente une preuve analytique de la dominance de la valeur spectrale avec multiplicité maximale pour les systèmes du second ordre contrôlés par un contrôleur PD retardé.

Récemment, la propriété MID a été étendue aux équations différentielles neutres, d'abord dans [83] dans le contexte de la conception du contrôleur PID pour les systèmes retardés du premier ordre, puis dans [56] où la propriété MID ap-

paraît pour les valeurs spectrales avec une multiplicité maximale des équations différentielles scalaires génériques de type neutres .

La propriété MID peut être utilisée pour régler les contrôleurs standards. Par exemple, dans [78], elle est appliquée au réglage systématique du contrôleur PID stabilisateur d'un système de premier ordre.

Dans [84], on considère la stabilisation par rétroaction PDA retardée et rétroaction prédictive du pendule inversé, où la longueur critique du pendule qui limite la stabilisation est obtenue grâce à la propriété MID; voir aussi [85]. On montre également dans [86] que l'approche basée sur la MID permet d'obtenir le retard critique, et que les gains de contrôle associés sont facilement déduits de l'équation caractéristique et de ses dérivées.

Même si la GMID est complètement caractérisé dans [76], en général, la propriété MID reste une question ouverte et des développements supplémentaires sont nécessaires pour améliorer la compréhension de ses mécanismes et de ses avantages pour un objectif de contrôle.

Trois pistes principales restent à traiter pour la propriété MID:

1. le cas à plusieurs retards,
2. les valeurs spectrales avec des multiplicités admissibles non maximales,
3. le cas neutre.

À notre connaissance, le cas des retards multiples a été étudié pour la première fois dans [87], où l'on prouve que la propriété MID existe pour l'équation scalaire retardée du premier ordre avec *deux retards*. Ensuite, dans le contexte des valeurs spectrales avec des multiplicités admissibles strictement intermédiaires, on peut citer [50] où une MID paramétrique basée sur un discriminant a été étudiée dans le cas retardé du second ordre avec des valeurs spectrales de codimensions 3 et 4, et [77] où des conditions suffisantes et nécessaires sont fournies pour que la MID soit vérifiée pour les systèmes retardés d'ordre arbitraire sous certaines conditions. En outre, le cas neutre a été abordé dans certains cas particuliers; voir [56], [57], [78].

En fait, la propriété MID a été entièrement caractérisée, dans le cas où la multiplicité maximale est atteinte, pour l'équation neutre du premier ordre dans [56], pour le second ordre dans [57] et pour les systèmes d'ordre arbitraire dans [76]. Cependant, pour les valeurs spectrales avec des multiplicités admissibles strictement intermédiaires, *la seule contribution est fournie dans [78]*. En effet, la propriété MID est étendue à la codimension 4 pour les systèmes à retard de type neutre d'ordre 2, et une méthode systématique pour une stabilisation PID pour les systèmes à retard d'ordre faible est proposée.

L'objectif dans ce manuscrit est d'explorer l'effet des racines multiples avec des multiplicités admissibles présentant, sous des conditions appropriées, la validité de la propriété MID pour les équations différentielles neutres du second ordre avec un seul retard. Une fois que cela est fait, nous exploitons l'effet du retard sur la stabilité des drones en faisant une application symbolique/numérique de la propriété MID dans le contrôle des drones à rotor avec des retards. Ensuite, nous cherchons à assigner des racines réelles multiples dominantes avec des codimensions admissibles et nous utilisons la propriété MID pour le modèle mécanique de l'équilibre humain sur une planche d'équilibre roulante dans le plan sagittal.

La suite du manuscrit se présente de la manière suivante:

Dans la partie *I*, le chapitre 1 présente quelques résultats de base et des préliminaires pour les systèmes à retard. Dans le chapitre 2, nous discutons certaines extensions des méthodes de placement de pôles pour les systèmes linéaires décrits par des DDEs. Dans la partie *II*, le chapitre 3, considère la propriété GMID et se concentre sur les équations différentielles à retard neutres du second ordre avec un seul retard et avec la présence d'une racine réelle de multiplicité maximale. Ensuite, le chapitre 4, traite la stabilité exponentielle des systèmes linéaires à retard de type neutre en explorant l'effet des racines multiples avec des multiplicités admissibles montrant, sous des conditions appropriées, la validité de la propriété MID pour les équations différentielles à retard neutres du second ordre avec un seul retard. Enfin, la partie *III* représente deux applications de la propriété MID. Le chapitre 5 exploite une application symbolique/numérique de la propriété MID dans la commande retardée de Drone, tandis que le chapitre 6 étudie la stabilisation d'une planche d'équilibre roulante par le biais de la propriété MID.

## Introduction (English Version)

Systems with time delays provide useful models in a wide range of scientific and technological domains such as biology (e.g. interactions between neurons), chemistry, economics, physics (e.g. laser physics: lasers with optical feedback), or engineering (e.g. machine tool vibrations: cutting and milling machines), where the presence of the delays is inherent to propagation phenomena, such as of material, energy, or information, with a finite propagation speed. For more details on time-delay systems and their applications, we refer to [1]–[13].



Figure 3: (Left) Neurons' interaction. (Right) Computer numerical control (CNC) milling.

Two applications in particular, are of interest and will be discussed in more detail later. The first one deals with robotics, more particularly the control of Unmanned Aerial Vehicles (UAVs) rotorcrafts featuring time-delays. Among the variety of issues undermining the aerial systems performance, the study of time-delay effects remains relatively unexplored. In practice, UAVs' control systems operate in presence of time-delays arising from perception processing, decision-making, control commands and actuators' delayed dynamics. In fact, it has been proved that time-delays induce oscillatory phenomena rendering the system unstable. The study of dynamic systems with delays remains a popular and challenging subject within the scientific community of control systems and robotics. Controlling these delay systems has come a long way and has already been useful in many applications.

The second application concerns bio-mechanics, specifically the controller of the central nervous system (CNS). In fact, imbalance may be due to a multitude of age-associated declines in sensorimotor function, including somatosensation, vestibular function, vision, cognition and strength. Stabilization of the human body on the balance board is performed by a control process governed by the CNS. Visual, vestibular and somatosensory systems obtain information about the spatial orientation of the human body. The information is delivered to the brain,



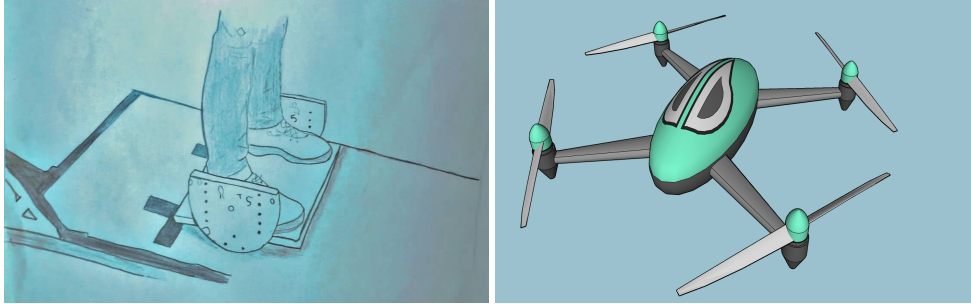


Figure 4: (Left) Human stance on a uniaxial rolling balance board in the sagittal plane. (Right) Quadrotor vehicle: Drone.

CNS determines the necessary interaction to maintain the balance after processing the signals and sends an instruction to the musculature. The process described above requires a definite time called *reaction time*. Consequently, the mathematical model of balancing tasks involves a delayed control law, here a proportional-derivative (PD) feedback with constant feedback delay [15]–[17], since the visual and vestibular system perceive position and velocity, respectively. Other frequently used neuromuscular control models are for instance delayed proportional-derivative-acceleration (PDA) feedback [18], [19], intermittent control [20]–[25] and predictor feedback [18], [26]. An important question for human stance control is treated in [27] where discrete-time and a continuous-time delayed PDA controller are considered and the transition between them by means of the semi-discretization is established. It was shown in [28] and [29] that an integral term does not improve the stabilizability of the system in the presence of feedback delay, therefore here we concentrate only on PD feedback.

There exist two different classes of models: macroscopic (or continuum) and microscopic (or car-following). The first model describes the traffic in terms of continuous density and velocity distributions, while the second model describes the behaviour of individual vehicles. Note that time-delays may also be included in continuum models to mimic driver reaction time. These delays can significantly alter the traffic dynamics, leading to instabilities for both linear and nonlinear systems [30]. In contrast, some systems that are not stabilizable without delay can be stabilized with the use of an artificial delay in the static output-feedback (continuous-time) [31], [32].

For linear time-invariant (LTI) systems, one of the simplest ideas to control the dynamical behavior of the closed-loop system is to place the poles of the system in some desirable loci in the complex plane. Such a method is called *pole placement* (e.g., [33]). Roughly speaking, the pole placement's main ingredients are:

- the perfect knowledge of the state variables,

- some appropriate *controllability* assumptions on the system, that is, the possibility to steer a dynamical system from an arbitrary initial state to an arbitrary final state by means of an apropos set of admissible control laws.

If the said method is easy to understand and to apply in the control of finite-dimensional LTI systems, its extension to systems described by delay-differential equations (DDEs) seems to be more involved. More precisely, two issues need to be addressed:

1. the introduction of a suitable notion of *controllability* for delay systems,
2. the *in-depth comprehension of the location of the poles of the closed-loop system in terms of the controller's parameters*.

For a thorough introduction to the controllability notions in finite- and infinite-dimensional systems, also including the case of dynamical systems represented by DDEs, we refer to [34]. A deeper discussion of the existing methods to characterize the stability regions in the parameter-space can be found in [8]. Finally, even for some class of partial differential equations (PDEs), delayed control has shown some effectiveness (see e.g. [35], [36]). On the other, reformulations of PDEs and backstepping have been used to show that a nominal control law compensates for the input delays in closed loop and provides nominal exponential stabilization [37], [38]; see also [39] where the investigation of prediction-based control was for nonlinear systems subject to both pointwise input- and (potentially) distributed state-delays.

Up to our knowledge, the first results on the spectrum location of linear systems represented by DDEs were published one century ago. Indeed, at the end of 1920s, the almost forgotten works of [40] and [41] seem to be the first results to address such a problem.

In the late 1970s, the concept of pole-placement emerged in control theory in the guise of *Finite spectrum assignment* (FSA); [42], [43], the upshot of which was to counterbalance the effect of delay by a prediction of the state over a delay interval, thereby downsizing the closed-loop system to a finite-dimensional plant; we refer to [44] for an overview of the main ingredients and confrontation with other methods dedicated to the control of dynamical systems featuring input delays. As a matter of fact, the strategy was thoroughly explored in a more adequate algebraic framework by [45] via the introduction of the ring  $\mathcal{R}$ , i.e., the set of all meromorphic functions in the complex plane  $\mathbb{C}$  generically represented as  $\frac{P(s, e^{-\tau s})}{Q(s)}$ , where  $Q$  is a polynomial in the Laplace complex variable  $s$ ,  $P$  is a bivariate polynomial in  $s$  and  $e^{-\tau s}$ , and  $\tau$  is a fixed positive real number. The algebraic design of controllers of delay differential systems consists in the algorithmic investigation of the ring  $\mathcal{R}$ . These algebraic methods enable the stability analysis of delay systems. However, their limitation was observed in the early 2000s in [46]. Numerically, the

closed-loop system's stability is highly sensitive to infinitesimal uncertainties. The latter phenomenon is known as the *spillover* problem.

There is more to pole placement for delay systems than a quasipolynomial interpolation problem. As a matter of fact, in [47],  $N$  poles of the system are assigned to (some) desired positions in the complex plane by  $N$  feedback parameters in the same fashion as in the finite-dimensional case. Nevertheless, in order to preclude the spillover effect, it is well-known that such an interpolation is an efficient placement if, and only if, the remaining spectral values of the closed-loop system are located to the left of the rightmost of assigned poles; that is, the assignment succeeds if the latter poles are dominant. However, this feature is not ensured in general as remarked in [48]; see also [49], where no attempt at proving the dominance of the placed poles is made, rather a trial-and-error commonsense rule is performed for several selections of assigned poles. More recently, building upon the effect of multiple spectral values on the stability of DDEs, a novel analytical pole placement strategy was devised in [50]. The property was hinted at in [51] albeit illustrated by simple low-order cases, with no endeavour to address the general case. Up to our knowledge, very few works have tackled this issue in a systematic fashion until recently; see [50], [52]–[58].

Let us consider the generic delay differential equation:

$$\sum_{k=0}^n a_k x^{(k)}(t) + \alpha_k x^{(k)}(t - \tau) = 0, \quad (4)$$

where the unknown function  $x$  is real-valued,  $a_k, \alpha_k \in \mathbb{R}$ , and the delay  $\tau > 0$ .

Linear systems with delays are described in the Laplace domain by transfer functions involving quasi-polynomials and then admit an infinite number of poles. These quasipolynomials have been widely studied in [59]–[61]. Studying the stability properties of *retarded* systems (they admit a finite number of poles in any right half-plane) is much easier than studying those of *neutral* systems which may exhibit an infinite number of poles, in chains asymptotic to a vertical axis possibly located in the open right half-plane or clustering the imaginary axis from left or right. Both situations prevent to get exponential stability for these systems.

Stability studies of time-delay systems exist, among them, systems with single or multiple constant delays (see for instance [5]); systems with cross-talking delays [62]; delayed difference systems (see for instance [63]). For more applications of spectral methods see [64]–[66].

To perform stability analysis, efficient methods have been proposed in frequency-domain, see, for instance, [1], [5], [67]–[71] and the references therein. Even with

the significant advances that have been reported on such topics, the question of *determining conditions on the equation parameters that guarantee asymptotic stability of solutions of linear time-invariant time-delay systems* remains still *open*.

Spectral methods, which investigate the spectrum distribution of the characteristic equations, are a powerful tool for the understanding of the asymptotic behavior of LTI time-delay system solutions by considering the roots of the corresponding characteristic equation; see [1], [5], [8], [67], [70], [88]–[90] which, for (4) equation is the quasipolynomial function  $\Delta : \mathbb{C} \rightarrow \mathbb{C}$  defined for  $s \in \mathbb{C}$  by

$$\Delta(s) = \sum_{k=0}^n a_k s^k + \alpha_k s^k e^{-\tau s}. \quad (5)$$

More precisely, the exponential behavior of solutions of equation (4) is given by the real number

$$\rho = \sup\{\Re(s) | s \in \mathbb{C}, \Delta(s) = 0\}, \quad (6)$$

called the *spectral abscissa* of the corresponding characteristic function  $\Delta$  and related to the notion of decay rate of time-delay system solutions, see [[1], Chapter 1, Theorem 6.2] for more details.

The multiplicity of a root of a quasipolynomial is bounded by the generic *Polya and Szegö bound* (denoted  $PS_B$ ), which is equal to the *degree* of the corresponding quasipolynomial, i.e., the sum of the degrees of the involved polynomials plus the number of delays; see for instance [72, Problem 206.2, page 144 and page 347]. It is worth mentioning that such a bound was recovered using structured matrices in [73] rather than the argument principle as in [72]. In particular, the degree of  $\Delta$  in (5) is  $\deg_s(\Delta) = 2n + 1$ .

From a control theory viewpoint, a recent safe control methodology called *partial pole placement* (PPP) [74], [75], based on the assignment of the closed-loop dominant solution's decay rate was investigated. In fact, it turns out that, for characteristic quasipolynomials of some time-delay systems, real roots of *maximal multiplicity* are necessarily *dominant* (roots with the largest real part), this property is known as “Generic Multiplicity-Induced-Dominancy” (GMID), it refers to special conditions on the system's free parameters (typically the control parameters) where a given characteristic root matches the spectral abscissa such that the corresponding spectral value is dominant; see for instance [50], [76]. In the case of multiple roots with strictly intermediate multiplicity, one has to seek for conditions which allow to define the admissible assignment region, this property is baptised “Intermediate Multiplicity-Induced-Dominancy”(IMID); see [50].

Thanks to this property, an ensued control strategy is proposed in [50], [77], [78], which consists in assigning a root with an admissible multiplicity once the

appropriate conditions guaranteeing its dominance are determined. Furthermore, the Multiplicity-Induced-Dominancy (MID) property may be used to tune standard controllers. For instance, in [78] it is applied to the systematic tuning of the stabilizing PID controller of a first order plant.

The MID property has been first hinted at in [51] for some low-order cases without any attempt to address the general question; see also [79] for the specific scalar first-order equations. Recent developments pursue the investigation of the MID property mainly in the single-delay case, see for instance [50], [52]–[57], [78].

Up to our knowledge, an analytical proof of the characterization of the spectral abscissa for the scalar equation with a single delay was presented and discussed for the first time in the 50s, see [79]. The dominance property is further explored and analytically shown in scalar delay equations in [52], then in second-order systems controlled by a delayed proportional controller in [53], [80], where its applicability in damping active vibrations for a piezo-actuated beam is proved. See also [81], [82] which exhibit an analytical proof for the dominance of the spectral value with maximal multiplicity for second-order systems controlled via a delayed PD controller.

Lately, the MID property has been extended to neutral differential equations, first in [83] in the context of the PID controller design for first-order delayed-plants, then in [56] where the MID property occurs for spectral values with maximal multiplicity in generic scalar neutral differential equations.

In [84], the stabilization via delayed PDA feedback and predictor feedback of the inverted pendulum is considered, where the critical length of the pendulum that limits stabilization is obtained owing to the MID property; see also [85]. It is also shown in [86] that the MID-based approach provides the critical delay, and the associated control gains are easily deduced from the characteristic equation and its derivatives.

Even though the GMID is completely characterized in [76], in general, the limits of the MID property remain an open question and further developments are required to improve the understanding of its mechanisms and benefits for a control purpose.

Three main leads remain to be addressed for the MID property:

1. the multi-delay case,
2. spectral values with non maximal admissible multiplicities,
3. the neutral case.

Up to our knowledge, the multi-delay case was first investigated in [87], where the MID property is proved to hold for the first-order retarded scalar equation with *two delays*. Next, in the context of spectral values with strictly intermediate admissible multiplicities, one may cite [50] where a discriminant-based parametric MID was investigated in the second-order retarded case with spectral values of codimensions three and four, and [77] where sufficient and necessary conditions are provided for the MID to hold in  $n$ th-order retarded systems with a finite dimensional part corresponding to realrooted plants. Further, the neutral case was addressed in some particular cases ; see [56], [57], [78].

As a matter of fact, the MID has been fully characterized, in the case where maximal multiplicity is reached, for the first-order neutral equation in [56], and for the second-order in [57] and for  $n$ th-order systems in [76]. However, for spectral values with strictly intermediate admissible multiplicities, the only contributions are provided in [78]. Indeed, the MID property is extended to codimension four in second-order time-delay neutral systems, and a systematic method for a PID stabilizing tuning for low-order delayed plants is proposed.

The aim of this manuscript is to explore the effect of multiple roots with admissible multiplicities exhibiting, under appropriate conditions, the validity of the MID property for second-order neutral time-delay differential equations with a single delay. Once that is done, we exploit the effects of time-delays on the stability of UAVs by doing a symbolic/numeric application of the MID property in the control of UAVs rotorcrafts featuring time-delays. After that, we aim at assigning dominant multiple real roots with admissible codimensions and we use the MID property for the mechanical model of human stance on rolling balance board in the sagittal plane.

The sequel of the manuscript is outlined as follows.

In Part *I*, chapter 1 gives some basic results and preliminaries in time delay systems. We discuss in chapter 2 some of the extensions of the pole placement methods for linear systems described by DDEs. In Part *II*, chapter 3, considers the MID property and focuses on second order neutral time-delay differential equations with a single delay and with the presence of real root of maximal multiplicity. After that, chapter 4, addresses the exponential stability of linear time-delay systems of neutral type by exploring the effect of multiple roots with admissible multiplicities exhibiting, under appropriate conditions, the validity of the MID property for second order neutral time-delay differential equations with a single delay. Finally, Part *III* represents two applications of the MID property. Chapter 5 exploits a symbolic/numeric application of the MID property in the control of UAVs rotorcrafts featuring time-delay, while chapter 6 considers the stabilization of a rolling balance board by means of the MID property.



## List of Publications

### 1. Journal papers:

- (a) [91] *Multiplicity-Induced-Dominancy property for second-order neutral differential equations with application in oscillation damping*, EJC 2022, **Amina Benarab**, Islam Boussaada, Karim Trabelsi and Catherine Bonnet, <https://doi.org/10.1016/j.ejcon.2022.100721>
- (b) [92] *Time-Delay Control of Quadrotor Unmanned Aerial Vehicles: A Multiplicity-Induced-Dominancy-Based Approach*, JVC 2022, José J. Castillo-Zamora, Islam Boussaada, **Amina Benarab**, and Juan Escareno, <https://journals.sagepub.com/doi/full/10.1177/10775463221082718>

### 2. Conference papers:

- (a) [93] *Over one Century of Spectrum Analysis in Delay Systems: An Overview and New Trends in Pole Placement Methods*, TDS 2022, **Amina Benarab**, Islam Boussaada, Silviu-Iulian Niculescu and Karim Trabelsi, <https://hal-centralesupelec.archives-ouvertes.fr/hal-03765146>
- (b) [57] *The MID property for a second-order neutral time-delay differential equation*, ICSTCC 2020, **Amina Benarab**, Islam Boussaada, Karim Trabelsi, Guilherme Mazanti and Catherine Bonnet, <https://ieeexplore.ieee.org/stamp/stamp.jsp?tp=&arnumber=9259779>
- (c) [94] *MID Property for Delay Systems: Insights on Spectral Values with Intermediate Multiplicity*, CDC 2022, Islam Boussaada, Guilherme Mazanti, Silviu-Iulian Niculescu and **Amina Benarab**, <https://arxiv.org/pdf/2209.06757.pdf>
- (d) [95] *Rolling Balance Board Robust Stabilization: An MID-based Design*, TDS 2022, **Amina Benarab**, Csenge A. Molnar, Islam Boussaada, Karim Trabelsi, Tamas Insperger and Silviu-Iulian Niculescu, <https://hal-centralesupelec.archives-ouvertes.fr/hal-03765149>





# **Part I**

## **Prerequisites**



# 1 - Definitions, prerequisites, and basic results

## 1.1 . Linear time-delay systems with single delay and constant coefficients

Delayed systems can be divided into three classes: retarded systems, neutral systems and advanced systems. The former have only a finite number of unstable poles in each right half-plane. The latter have only a finite number of poles in each left half-plane. Finally, the third ones have an infinite number of poles in a band around the imaginary axis; see [67] for more details.

Let us consider the functional differential equation in (4), then we classify equations of the form (4) into several categories.

**Definition 1.1.1** *An equation of the form (4) is said to be of retarded type if  $a_n \neq 0$  and  $\alpha_n = 0$ . It is said to be of neutral type if  $a_n \neq 0$  and  $\alpha_n \neq 0$ . Finally, it is said to be of advanced type if  $a_n = 0$  and  $\alpha_n \neq 0$ .*

Notice that equations of neutral or advanced type are in several ways more delicate to tackle than equations of retarded type.

In the study of linear systems with delay, we deal with transfer functions involving quasipolynomials, which are defined hereafter.

**Definition 1.1.2** *A quasipolynomial is a particular entire function  $\Delta: \mathbb{C} \rightarrow \mathbb{C}$  which may be written as follows*

$$\Delta(s) = \sum_{i=0}^k P_i(s) e^{-\tau_i s}, \quad (1.1)$$

where  $k$  is a positive integer,  $\tau_i$  ( $i = 0..k$ ) are pairwise distinct non-negative real numbers and  $P_i$  ( $i = 0..k$ ) are polynomials of degree  $d_i \geq 0$ . The degree  $\deg_s(\Delta)$  of the quasipolynomial  $\Delta$  is equal the sum of the degrees of the involved polynomials  $P_i$  plus the number of delays, i.e.,

$$\deg_s(\Delta) = k + \sum_{i=0}^k d_i. \quad (1.2)$$

The stability of a quasipolynomial  $\Delta$  results in the following way

**Definition 1.1.3** *A quasipolynomial  $\Delta$  (characteristic equation of delay system) is exponentially stable if there exists a real number  $\sigma > 0$  such that for all roots  $s_k$  of  $\Delta$ ,  $\Re(s_k) < -\sigma$ .*

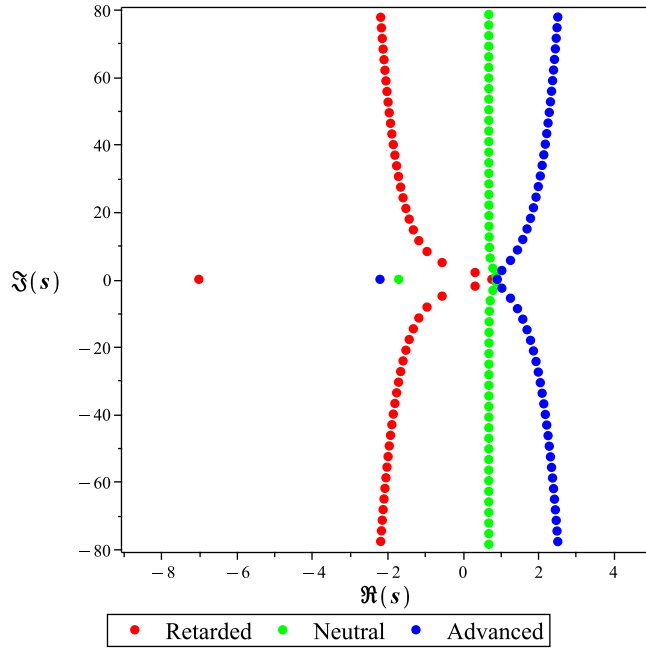


Figure 1.1: Spectrum distribution of delay equations: retarded, neutral and advanced type.

An important result in the literature, known as *Polya-Szegö bound*, shows that there exists a link between the degree of a quasipolynomial and the number of its roots in horizontal strips of the complex plane.

**Proposition 1.1.1** [72, Problem 206.2, page 144 and page 347]. *Let  $\Delta$  be a quasipolynomial of degree  $\deg_s(\Delta)$  as in (1.1), and  $\alpha, \beta \in \mathbb{R}$  be such that  $\alpha \leq \beta$ . If  $M$  is the number of roots of  $\Delta$  contained in the set  $\{s \in \mathbb{C} \mid \alpha \leq \Im(s) \leq \beta\}$  counting multiplicities, then*

$$\frac{(\tau_k - \tau_0)(\beta - \alpha)}{2\pi} - \deg_s(\Delta) \leq M \leq \frac{(\tau_k - \tau_0)(\beta - \alpha)}{2\pi} + \deg_s(\Delta). \quad (1.3)$$

Furthermore, for a given root  $s_0 \in \mathbb{C}$  of a quasipolynomial  $\Delta$ , one obtains the following link between the multiplicity of  $s_0$  and the degree of  $\Delta$ .

**Corollary 1.1.1** *Let  $\Delta$  be a quasipolynomial of degree  $\deg_s(\Delta)$ . Then, any root  $s_0 \in \mathbb{C}$  of  $\Delta$  exhibits a multiplicity at most equal to  $\deg_s(\Delta)$ .*

**Remark 1.1.1** *Corollary 1.1.1 is obtained immediately by letting  $\alpha = \beta = \Im(s_0)$  in Proposition 1.1.1. Notice also that Polya-Szegö bound has been recovered in [73] using a constructive approach based on functional Birkhoff matrices. Furthermore, if some coefficients of the polynomials  $P_i$  defined in (1.1) vanish, then a sharper bound for the multiplicity is provided in [73].*

Notice that the roots of a quasipolynomial do not change when its coefficients are all multiplied by the same nonzero number, and hence one may always assume, without loss of generality, that one nonzero coefficient of a quasipolynomial is normalized to 1. In other words, equation (4) may read as

$$x^n(t) + \sum_{k=0}^{n-1} a_k x^{(k)}(t) + \sum_{k=0}^n \alpha_k x^{(k)}(t - \tau) = 0, \quad (1.4)$$

where  $a_k, \alpha_k \in \mathbb{R}$ , and  $\tau$  is a positive delay. The corresponding characteristic equation is the following generic quasipolynomial function:

$$\Delta(s) = P_0(s) + P_\tau(s) e^{-\tau s}, \quad (1.5)$$

with

$$\begin{cases} P_0(s) &= s^n + \sum_{k=0}^{n-1} a_k s^k, \\ P_\tau(s) &= \sum_{k=0}^n \alpha_k s^k. \end{cases} \quad (1.6)$$

Notice that (1.4) is a particular case of the following time-delay system

$$\dot{\xi}(t) + B_\tau \dot{\xi}(t - \tau) = A_0 \xi(t) + A_\tau \xi(t - \tau), \quad (1.7)$$

where  $\xi(t) = (x(t), x'(t), \dots, x^{(n-1)}(t))^T \in \mathbb{R}^n$  is the state vector and  $A_0, A_\tau, B_\tau \in \mathcal{M}_n(\mathbb{R})$  are real-valued matrices which can be easily deduced from (4).

Even though the corresponding characteristic equation admits an infinite number of roots, it has some very interesting properties. One such property is the following, which holds for retarded time-delay systems (see [8]).

**Proposition 1.1.2** *Let consider the time-delay system in (1.7) with  $B_\tau = 0$ . If there exists a sequence  $(s_k)_{k \geq 1}$  of characteristic roots of (1.7) such that*

$$\lim_{k \rightarrow \infty} |s_k| \rightarrow +\infty, \quad (1.8)$$

then

$$\lim_{k \rightarrow \infty} \Re(s_k) \rightarrow -\infty. \quad (1.9)$$

Several general results on the location of roots of (4) can be found in the literature and, in particular, we refer the interested reader to [96] for a generic result on the location of the associated spectral values for an arbitrary  $n$ .

The next result plays an important role in the spectral theory of time-delay systems, it allows the construction of an envelope curve around the zeros of the characteristic equation. It collects two interesting properties, whose proofs can be found, respectively, in [8] and [97].

**Proposition 1.1.3** Consider the LTI equation (1.4), the associated system (1.7), and their characteristic quasipolynomial function  $\Delta$  given by (1.5)-(1.6).

1. If  $\alpha_n = 0$  and  $s$  is a characteristic root of system (1.7) with  $B_\tau = 0$ , then it satisfies

$$|s| \leq \|A_0 + A_\tau e^{-\tau s}\|_2. \quad (1.10)$$

2. If  $\alpha_n \neq 0$  and  $\lim_{|s| \rightarrow \infty} \left| \frac{P_\tau(s)}{P_0(s)} \right| < 1$ , then the characteristic equation  $\Delta$  defined by (1.5)-(1.6) has a finite number of unstable roots in the right half-plane.

**Remark 1.1.2**

1. In order to include all poles of a time-delay system, a new approach in [98] constructs envelopes for retarded and neutral time-delay systems.
2. Inequality (1.10), combined with the triangular inequality, provides a generic envelope curve around the characteristic roots corresponding to system (1.7). In other words, the equality case in (1.10) defines a curve in the complex plane such that all characteristic roots of  $\Delta$  are located to the left of that curve. We refer to [99] for further insights on spectral envelopes pertaining to retarded time-delay systems with a single delay.

In LTI systems whose dynamics are represented by DDEs, there exists a particular interesting property, called *Multiplicity-Induced-Dominancy (MID)* that, to the best of the authors' knowledge, was not sufficiently addressed in the open literature.

## 1.2 . The Multiplicity-Induced-Dominancy approach

The MID property consists in determining the conditions under which a given multiple complex zero of a quasipolynomial is dominant. For instance, in the generic quasipolynomial case, the real root of maximal multiplicity is necessarily the dominant (GMID). However, multiple roots with intermediate admissible multiplicities may be dominant or not. Thanks to this property, an ensued control strategy is proposed in [50], [77], which consists in assigning a root with an admissible multiplicity once appropriate conditions guaranteeing its dominancy are established. Furthermore, the MID property may be used to tune standard controllers. For instance, in [78] it is applied to the systematic tuning of the stabilizing PID controller of a first order plant. Here, we aim at assigning dominant multiple real roots with admissible codimensions.

In what follows, we give a precise definition of the *dominant root*.

**Definition 1.2.1** A spectral eigenvalue  $s_0$  is said to be a dominant (respectively, strictly dominant) root of the characteristic function  $\Delta$  given by (1.5)-(1.6), if one has  $\Re(\tilde{s}) \leq \Re(s_0)$  (respectively,  $\Re(\tilde{s}) < \Re(s_0)$ ) for any  $\tilde{s} \in \mathbb{C} \setminus \{s_0\}$ , a distinct eigenvalue of  $\Delta$ .

Notice that sufficient conditions for the dominance of simple spectral values has been proposed in [100] in the case of first-order scalar neutral equation.

**Lemma 1.2.1** [100]. Consider a characteristic equation of the form

$$Q(s) = s \left( 1 + \sum_{l=1}^m c_l e^{-\sigma_l s} \right) - a - \sum_{j=1}^k b_j e^{-h_j s} = 0, \quad (1.11)$$

where  $a, b_j (j = 1, \dots, k), c_l (l = 1, \dots, m)$  are real numbers and  $h_j (j = 1, \dots, k), \sigma_l (l = 1, \dots, m)$  are positive real numbers.

Given equation (1.11), we introduce a function  $V : \mathbb{R} \rightarrow \mathbb{R}$ , defined by,

$$V(s) = \sum_{l=1}^m |c_l| (1 + |s| \sigma_l) e^{-\sigma_l s} + \sum_{j=1}^k |b_j| e^{-h_j s}, \quad s \in \mathbb{R}. \quad (1.12)$$

Suppose that there exists a real zero  $s_0$  of equation (1.11). If  $V(s_0) < 1$ , then  $s_0$  is a real simple dominant zero of (1.11).

Note that the extension of the above result to second-order delay equations remains a challenging endeavor.

### 1.2.1 . GMID property for first-order scalar neutral equations

The GMID property consists in determining the conditions under which a given root of the characteristic function of maximal multiplicity is necessarily dominant. It is shown in [56] that the GMID property holds for the delay differential algebraic system

$$\begin{cases} \dot{x}(t) = ax(t) + by(t - \tau), \\ y(t) = cx(t) + dy(t - \tau), \end{cases} \quad (1.13)$$

where  $x(t)$  and  $y(t)$  are real-valued, and  $a, b, c, d$  are real coefficients, and whose characteristic function is given by

$$\Delta(s) = s - a - e^{-s\tau}(sd - ad + bc). \quad (1.14)$$

As a matter of fact, the maximal multiplicity, which is equal to 3, is reached at  $s_0 \in \mathbb{R}$ , and expressions of the coefficients ensuring such a configuration are determined in terms of  $s_0$  and the delay  $\tau$ . Furthermore, all complex roots of (1.14) with real-parts equal to  $s_0$  are fully characterized.

**Theorem 1.2.1** ([56]) Consider the delay differential-algebraic equation in (1.13). The explicit characteristic quasipolynomial of (1.13) is given by  $\Delta$  in (1.14). Let  $s_0 \in \mathbb{R}$ ,



- The real  $s_0$  is a root of multiplicity 3 of  $\Delta$  if, and only if, the coefficients  $a$ ,  $b$ ,  $c$ ,  $d$ , the root  $s_0$ , and the delay  $\tau$  satisfy the relations

$$\begin{cases} a = s_0 + \frac{2}{\tau}, \\ d = -e^{s_0\tau}, \\ bc = -\frac{4}{\tau}e^{s_0\tau}. \end{cases} \quad (1.15)$$

- If (1.15) is satisfied, then  $s_0$  is a dominant root of  $\Delta$ . Moreover, for every other complex root  $s$  of  $\Delta$ , one has  $\Re(s) = s_0$ .
- Let  $\Xi$  be the set

$$\Xi = \{\xi \in \mathbb{R} \mid \tan \xi = \xi\}. \quad (1.16)$$

If (1.15) is satisfied, then the set of roots of  $\Delta$  is  $\{s_0 + i\frac{2}{\tau}\xi \mid \xi \in \Xi\}$ .

### 1.2.2 . IMID property for second-order scalar neutral equations

The work in [83] aims at extending such a design approach to time-delay systems of neutral type occurring in the classical problem of PID stabilizing design for delayed plants. Namely, consider the following closed-loop plant

$$M(s) = \frac{(k_d s^2 + k_p s + k_i)e^{-s\tau}}{s^2 - ps + (k_d s^2 + k_p s + k_i)e^{-s\tau}}, \quad (1.17)$$

where  $p$  is a positive unstable pole of the open-loop plant,  $k_p, k_i, k_d$  are real parameters (gains) and  $\tau$  is the delay. In [101], it was found that the delay margin is  $\tau_{PID} = \frac{2}{p}$ ; see also [102]. Now, the corresponding characteristic function is given by

$$\Delta(s) = s^2 - ps + e^{-s\tau}(k_d s^2 + k_p s + k_i). \quad (1.18)$$

In [78], it is shown that for arbitrary real parameters  $k_p, k_i, k_d$  and arbitrary positive delay  $\tau$ , the multiplicity of a given root of (1.18) is bounded by 4. In addition, the maximal multiplicity 4 is only reached by two roots  $s_{\pm}$  for one set of given values of the gains. As a result, if  $\tau < \tau_{PID}$ , then the root  $s_+$  is dominant and guarantees stability.

### 1.3 . Partial pole placement via delay action (P3 $\delta$ )

A pole placement approach has been developed for infinite dimensional systems, in particular, delay systems and some class of partial differential equations. This approach extends the properties highlighted some years ago, and called MID property [50], [55], [76], [78]. A property called Coexisting Real Roots-Induced-Dominancy (CRRID) which consists in assigning a certain amount of real roots (typically equally spaced for simplicity) and proving that the rightmost root among the assigned roots is also the rightmost root of the characteristic quasipolynomial

[103], [104]. This property opens new prospects for the synthesis of control law.

There exist many applications of this pole placement approach, such as the modelling of Central Nervous System (CNS), the modelling of human stance in particular, vibration control along mechanical systems, etc.

We benefit from a methodological advance, called p3 $\delta$  software of partial pole placement [74], [75]. It is a Python implementation of recent methods for the stability analysis and stabilization of linear time-delay systems exploiting the delay action. Its control design strategy is based on properties of the spectral distribution of the time-delay system.

For more details on this software, one may visit: <https://iboussaa.gitlabpages.inria.fr/partial-pole-placement-via-delay-action/P3d-Home.html>, where a nice guide is available. The package and its use are described also. In addition, the user can find additional illustrative examples as well as short videos prepared to show how the software works.

#### 1.4 . Special functions in control design: Confluent hypergeometric functions

Quasipolynomial functions can be factorized in terms of a confluent hypergeometric function defined hereafter.

**Definition 1.4.1** Let  $a, b \in \mathbb{C}$  such that  $b$  is not a nonpositive integer, Kummer's confluent hypergeometric function is the entire function  $\Phi(a, b, \cdot) : \mathbb{C} \rightarrow \mathbb{C}$  defined for  $z \in \mathbb{C}$  by the series

$$\Phi(a, b, z) = \sum_{k=0}^{\infty} \frac{(a)_k z^k}{(b)_k k!}. \quad (1.19)$$

where for  $\alpha \in \mathbb{C}$  and  $k \in \mathbb{N}$ ,  $(\alpha)_k$  is the Pochhammer symbol for the ascending factorial, defined inductively as  $(\alpha)_0 = 1$  and  $(\alpha)_{k+1} = (\alpha + k)(\alpha)_k$ , for  $k \in \mathbb{N}$ .

The series in (1.19) converges for every  $z \in \mathbb{C}$  and, as presented in [105]–[107], it satisfies the *Kummer differential equation*

$$z \frac{\partial^2 \Phi}{\partial z^2}(a, b, z) + (b - z) \frac{\partial \Phi}{\partial z}(a, b, z) - a \Phi(a, b, z) = 0. \quad (1.20)$$

As discussed in [105]–[107], for every  $a, b, z \in \mathbb{C}$  such that  $\Re(b) > \Re(a) > 0$ , Kummer functions also admit the integral representation

$$\Phi(a, b, z) = \frac{\Gamma(b)}{\Gamma(a)\Gamma(b-a)} \int_0^1 e^{zt} t^{a-1} (1-t)^{b-a-1} dt, \quad (1.21)$$

where  $\Gamma$  denotes the Gamma function. This integral representation has been exploited in [55] to characterize the spectrum of some DDEs.

Kummer functions satisfy some induction relations, often called *contiguous relations*, see for instance [107]. In particular, the following relations are of interest.

**Lemma 1.4.1** ([107, p. 325]) *Let  $a, b, z \in \mathbb{C}$  with  $a \neq b$ ,  $z \neq 0$ , and  $-b \notin \mathbb{N}$ . The following relations hold:*

$$\begin{aligned}\Phi(a, b+1, z) &= \frac{-b(a+z)\Phi(a, b, z) + ab\Phi(a+1, b, z)}{z(a-b)}, \\ \Phi(a+1, b+1, z) &= -\frac{-b\Phi(a+1, b, z) + b\Phi(a, b, z)}{z}.\end{aligned}\tag{1.22}$$

Kummer confluent hypergeometric functions have close links with *Whittaker functions*. For  $k, l \in \mathbb{C}$  with  $-2l \notin \mathbb{N}^*$ , the *Whittaker function*  $\mathcal{M}_{k,l}$  is the function defined for  $z \in \mathbb{C}$  by

$$\mathcal{M}_{k,l}(z) = e^{-\frac{z}{2}} z^{\frac{1}{2}+l} \Phi\left(\frac{1}{2}+l-k, 1+2l, z\right),\tag{1.23}$$

(see, e.g., [107]). Note that, if  $\frac{1}{2}+l$  is not an integer, the function  $\mathcal{M}_{k,l}$  is a multi-valued complex function with branch point at  $z=0$ . The nontrivial roots of  $\mathcal{M}_{k,l}$  coincide with those of  $\Phi(\frac{1}{2}+l-k, 1+2l, \cdot)$  and  $\mathcal{M}_{k,l}$  satisfies the *Whittaker differential equation*

$$\varphi''(z) = \left(\frac{1}{4} - \frac{k}{z} + \frac{l^2 - \frac{1}{4}}{z^2}\right) \varphi(z).\tag{1.24}$$

Since  $\mathcal{M}_{k,l}$  is a nontrivial solution of the second-order linear differential equation (1.24), any nontrivial root of  $\mathcal{M}_{k,l}$  is necessarily simple.

In [108], Hille studies the distribution of zeros of functions of a complex variable satisfying linear second-order homogeneous differential equations with variable coefficients, as is the case for the degenerate Whittaker function  $\mathcal{M}_{k,l}$ , which satisfies (1.24). Thanks to an integral transformation defined there and called *Green–Hille transformation*, and some further conditions on the behavior of the function, Hille showed how to discard regions in the complex plane in order to preclude complex roots.

The following result, which is proved in [109] using the Green–Hille transformation from [108], gives insights on the distribution of the nonasymptotic zeros of Kummer hypergeometric functions with real arguments  $a$  and  $b$ .

**Proposition 1.4.1** ([109]) *Let  $a, b \in \mathbb{R}$  be such that  $b \geq 2$ .*

1. *If  $b = 2a$ , then all nontrivial roots  $z$  of  $\Phi(a, b, \cdot)$  are purely imaginary.*
2. *If  $b > 2a$  (resp.,  $b < 2a$ ), then all nontrivial roots  $z$  of  $\Phi(a, b, \cdot)$  satisfy  $\Re(z) > 0$  (resp.,  $\Re(z) < 0$ ).*
3. *If  $b \neq 2a$ , then all nontrivial roots  $z$  of  $\Phi(a, b, \cdot)$  satisfy*

$$(b-2a)^2 \Im(z)^2 - (4a(b-a) - 2b) \Re(z)^2 > 0.\tag{1.25}$$

## 1.5 . Insights on nonlinear time-delay systems

In this section, we recall the basic spectral theory for linear functional differential equations [1]. Let  $\mathcal{C} = \mathcal{C}([-\tau, 0], \mathbb{R}^n)$  denote the Banach space of continuous functions endowed with the supremum norm. For a function  $x : [-\tau, \infty) \rightarrow \mathbb{C}^n$ , we denote by  $x_t \in \mathcal{C}$  the function  $x_t(\theta) = x(t + \theta)$ ,  $-\tau \leq \theta \leq 0$  and  $t \geq 0$ . Consider the general autonomous neutral functional differential equations of the form

$$\frac{d}{dt} [D(x_t) + G(x_t)] = Lx_t + F(x_t), \quad (1.26)$$

where  $G$  represents the nonlinear part of the left-hand side of (1.26) ( $G$  does not contain linear terms). The nonlinear part of the right-hand side of (1.26) consists of a smooth function  $F$  satisfying  $F(0) = F'(0) = 0$  ( $F'$  denote the Fréchet derivative of  $F$ ). The operator  $D : \mathcal{C} \rightarrow \mathbb{C}^n$  is continuous, linear and atomic at zero ( $D$  is said to be atomic at  $\alpha$  if  $D$  is continuous together with its first and second Fréchet derivatives with respect to the prior data  $\phi$ ; and  $D_\phi$ , the derivative with respect to  $\phi$ , is atomic at  $\alpha$ ). The operator  $L : \mathcal{C} \rightarrow \mathbb{C}^n$  is linear and continuous and both operators are, owing to the Riesz representation theorem, defined by

$$L\phi = \int_{-\tau}^0 d\eta(\theta)\phi(\theta), \quad \text{and} \quad D\phi = \phi(0) - \int_{-\tau}^0 d\mu(\theta)\phi(\theta), \quad (1.27)$$

where  $\mu, \eta \in NBV([-\tau, 0], \mathbb{C}^{n \times n})$  are  $\mathbb{C}^{n \times n}$  matrices the elements of which are of bounded variation, normalized so that  $\mu$  is continuous at zero and  $\eta(0) = 0$ ; see Hale and Verduyn Lunel [1] for details.

The linearized equation of (1.26) is an initial value problem for a linear autonomous neutral functional differential equation is given by the following relation

$$\begin{cases} \frac{d}{dt} DX_t = LX_t, & t \geq 0, \\ X_0 = \phi, & \phi \in \mathcal{C}. \end{cases} \quad (1.28)$$

It is well-known that for any given initial function at  $\phi$ , there exists a unique solution of the initial value problem (1.28); see [110]. Namely, given the solution  $x(\cdot, \phi)$  of the initial value problem (1.28), we define the solution operator  $T(t) : \mathcal{C} \rightarrow \mathcal{C}$  by the relation

$$T(t)\phi = x_t(\cdot; \phi), \quad t \geq 0. \quad (1.29)$$

Hale and Verduyn Lunel [1] proved that the solution operator is a  $C_0$ -semigroup on  $\mathcal{C}$ , its infinitesimal generator  $A$  being

$$\begin{cases} D(\mathcal{A}) = \{\phi \in \mathcal{C} \mid \frac{d\phi}{d\theta} \in \mathcal{C}, D\frac{d\phi}{d\theta} = L\phi\}, \\ \mathcal{A}\phi = \frac{d\phi}{d\theta}. \end{cases} \quad (1.30)$$

Moreover,  $\sigma(\mathcal{A}) = P_\sigma(\mathcal{A})$  and  $s \in \sigma(\mathcal{A})$  if, and only if,  $s$  satisfies the characteristic equation  $\det \mathbb{M}(s) = 0$ ,  $\mathbb{M}$  being the characteristic matrix

$$\mathbb{M}(s) = sI - \int_{-\tau}^0 se^{s\theta} d\mu(\theta) - \int_{-\tau}^0 e^{s\theta} d\eta(\theta), \quad (1.31)$$

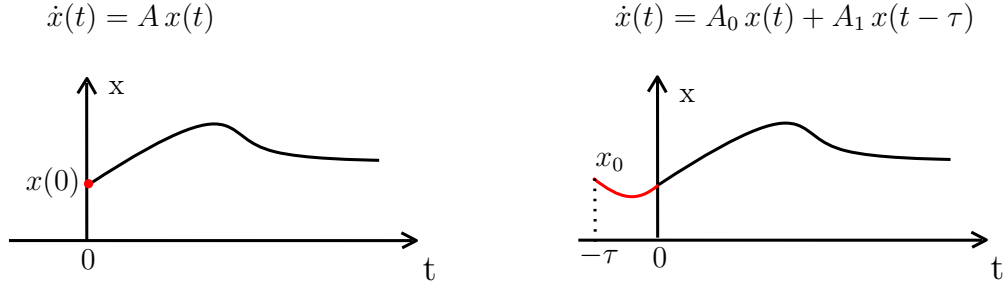


Figure 1.2: Initial value problem.

where  $\sigma(\mathcal{A})$  corresponds to the spectrum of  $\mathcal{A}$  and  $P_\sigma(\mathcal{A})$  corresponds to the point spectrum of  $\mathcal{A}$ . Two necessary results for a better understanding of the spectrum of linear time-delay systems, are given next:

- Operator  $\mathcal{A}$  only has a point spectrum:  $\sigma(\mathcal{A}) = P_\sigma(\mathcal{A})$ .
- Finitely many characteristic roots in any compact subset of  $\mathbb{C}$ .

Under these conditions, there exists a decomposition of the solution space as  $\mathcal{C} = \mathcal{C}_c \oplus \mathcal{C}_s$  where  $\mathcal{C}_c$  is  $m$ -dimensional generalized eigenspace spanned by the generalized eigenfunctions corresponding to the eigenvalues with zero real part of multiplicity  $m$ ,  $\mathcal{C}_s$  is its complement subspace in  $\mathcal{C}$ .

In the following, we describe the asymptotic behavior by the spectral approach. Let  $\Phi = \text{row}(\phi_1, \dots, \phi_m)$  denotes the basis of the generalized eigenspace  $\mathcal{C}_c$ .

Let  $\mathcal{C}^* = \mathcal{C}^*([-\tau, 0], \mathbb{R}^{n*})$ . In [1], a bilinear form associated with equation (1.28) is defined for  $\psi \in \mathcal{C}^*$  by

$$\langle \psi, \phi \rangle = \psi(0)D\phi - \int_{-\tau}^0 \int_0^\theta \psi(s - \theta) d\eta(\theta) \phi(s) ds + \int_{-\tau}^0 \int_0^\theta \psi'(s - \theta) d\mu(\theta) \phi(s) ds, \quad (1.32)$$

We can select basis  $\Psi = \text{col}(\psi_1, \dots, \psi_m)$  so as to have  $\langle \Phi, \Psi \rangle = I_{m \times m}$ .

Let  $s \in \sigma(\mathcal{A})$  be an eigenvalue of  $\mathcal{A}$ . The kernel  $\ker(sI - \mathcal{A})$  is called the eigenspace at  $s$ . Let define  $\mathcal{M}_s$  by the generalized eigenspace associated to  $s$  which is the smallest subspace containing all  $\ker((sI - \mathcal{A})^i)$  for  $i = 1, 2, \dots$ :

$$\mathcal{M}_s = \ker(sI - \mathcal{A})^{\kappa_s}, \quad (1.33)$$

where  $\kappa_s$  is the order of  $z = s$  as a pole of  $\mathbb{M}^{-1}(z)$ .

The definition of the bilinear form defined in [1] allows to establish an efficient spectral projection procedure; see [111].

From the spectral theory [1], it follows that the spectral projection onto  $\mathcal{M}_s(\mathcal{A})$  along  $\mathcal{R}((sI - \mathcal{A})^{K_s})$  can be represented by a Dunford integral

$$P_s = \frac{1}{2i\pi} \int_{\Gamma_s} (zI - \mathcal{A})^{-1} dz, \quad (1.34)$$

where  $\Gamma_s$  is a small circle such that  $s$  is the only singularity of  $(zI - \mathcal{A})^{-1}$  inside. This spectral projection is an important tool for the investigation of nonlinear systems. Indeed, Frasson [112] shows that if  $s_0 \in \mathbb{R}$  is a dominant zero of  $\mathbb{M}(s)$  of multiplicity  $n \geq 1$ , then

$$P_{s_0} \phi = 0 \implies \lim_{t \rightarrow \infty} e^{-ts_0} x(t) = 0. \quad (1.35)$$



## 2 - Existing pole placement paradigms

This chapter is an extended version of the paper [93].

### 2.1 . Introduction

*Pole placement* represents a classical method for controlling finite-dimensional linear time-invariant (LTI) systems, largely covered in the open literature. Basically, it consists of placing the poles of the closed-loop system in some predetermined loci in the complex plane. This chapter discusses some of the extensions of this method to linear systems described by delay-differential equations. Among others, the finite spectrum assignment (FSA), the algebraic pole placement (APP), the continuous pole placement (CPP) and the partial pole placement (PPP) approaches are presented and illustrated through some simple low-order dynamical systems.

Henceforth, this chapter is organized as follows. We first present the first attempts and existing pole placement paradigms (framework). Next, each section describes an existing pole placement paradigm where the main idea as well as the advantages and the drawbacks of each are discussed. Section 2.2 is devoted to the Finite Spectrum Assignment (FSA). Section 2.3 presents the Algebraic Pole Placement (APP). Section 2.4 describes the Continuous Pole Placement (CPP). Section 2.5 centers on the recent Partial Pole Placement (PPP). Finally, several examples which illustrate the described methods are given in Section 2.6.

### Overview of pioneering works on pole placement

Up to our knowledge, the first results devoted to the spectrum location of dynamical systems described by delay-differential equations (DDEs) go back to the 1920s and are due to Pólya. In point of fact, in [40], the quasipolynomial (transcendental) entire functions have been extensively studied and the asymptotic distribution of their zeros has been explored by some simple and elegant geometric approaches<sup>1</sup> which, unfortunately, have not been sufficiently exploited and extended to higher-order equations. Rather than the geometric investigation, in [41], an analytic treatment of the location of the roots of some low-order transcendental equations is given in a more precise way. Indeed, under some conditions, the roots are located in arbitrarily small sectors, and in each of these sectors the roots are additionally confined in a finite number of strips which are asymptotically of constant width.

---

<sup>1</sup>geometric determination of the characteristic roots' distribution



Later, in [113], some fundamental results concerning the zeros of quasipolynomials are obtained. In fact, necessary and sufficient conditions are given for all solutions of the transcendental function  $P(s, e^s)$  to lie in the left half-plane, where  $P(s, z)$  is a polynomial in  $s, z$ . These results are provided by extending the methods used to prove the Routh-Hurwitz criterion for the zeros of polynomials in order to be of negative real part.

Next, in the early 1950s, [79] proposed an efficient way to understand the asymptotic behaviour of solutions of first-order DDEs including a pointwise delay through the employment of the spectral method and thanks to a deep investigation of the zeros of the entire function  $g : \mathbb{C} \mapsto \mathbb{C}$ ,  $g(s) := se^s - a$  thereby providing a complete characterization of the spectrum distribution of such a first-order equation (see also [114] for further discussions). It should be mentioned that such remarkable properties appeared to be closely related to the well-known *Lambert–W functions* (see, for instance, [115] for some applications in control theory). Later, the result is generalized to the first-order DDE of *neutral* type in [90] by forging simple and direct methods for the computation of the corresponding real spectral values and for the derivation of the least upper bound of the said spectral abscissa. More recently, several works exploited Hayes results in control problems such as in delayed feedback and in stabilization problems. Unfortunately, Hayes' approach remains complicated and natural extensions to higher-order retarded or neutral DDEs do not exist.

Afterwards, a remarkable property of the spectrum distribution of low-order quasipolynomial functions with multiple spectral values has been hinted at since the late 50's in [51]. As a matter of fact, it turns out that for the first and second-order quasipolynomials, the corresponding spectral abscissa coincides with the multiple spectral value. Regrettably, despite its pioneering character, Pinney's work has made no attempt to address the general question since the employed approach seems quite difficult to extend to higher-order equations.

A classical and a standard way to count the number of unstable roots is to apply the well-known argument principle, see for instance [116]. The said count may also be obtained, in an easier and more elegant way, by the inspection of argument variation. Actually, the combination of the qualitative behavior of both the real  $\Re$  and the imaginary  $\Im$  parts (seen as real functions in the crossing frequency) of the quasipolynomial function, allows a straightforward application of the Stepan-Hassard formula [70], [117]. In fact, when a characteristic equation corresponding to a DDE of retarded type has no roots on the imaginary axis, then [118] gives a new formalism and an easy procedure to characterize the exact number of unstable roots.

## 2.2 . Finite spectrum assignment

In this section we consider the spectrum assignment via feedback for linear systems with delays, (see [42], [43]). To stabilize the system's solutions, an approach called "finite spectrum assignment" (FSA) may be used. The objective is to construct a linear feedback law which yields a finite closed-loop spectrum. Note that in [119], a reinterpretation of this approach was proposed, modeling ordinary differential equations (ODEs) with input delays as PDE-ODE interconnections. This result has enabled the design of observers, controllers, or parameter estimation methods for interconnected systems: systems with varying delays [120], cascades of PDEs [121].

### Main idea

Up to our knowledge, the FSA approach is the oldest paradigm, it is based on a predictor (integral operator) able to transform an infinite dimensional system into a finite dimensional one (the delay is compensated for by the predictor action), which is itself a remarkable property. When compared to the well-known Smith-Predictor, the FSA has the advantage of arbitrarily assigning the closed-loop poles and therefore can be applied to poorly damped and unstable processes [44], [122]. As a matter of fact, from a theoretical viewpoint, the finite spectrum assignment is a plausible methodology, however, it has several drawbacks of which the problem of robustness commented in the sequel. Two classes of systems can be considered whether the delay appears in the state or in the control.

### Description of the method

Consider the following linear system with control delays

$$\dot{x}(t) = Ax(t) + B_0 u(t) + B_1 u(t - \tau), \quad (2.1)$$

where  $x \in \mathbb{R}^n$ ,  $u \in \mathbb{R}^m$  and  $\tau$  is the delay of the system ( $\tau > 0$ ).

In [43] it is proven that the feedback of the following form

$$u(t) = F x(t) + F \int_{-\tau}^0 e^{-(\tau+\theta)A} B_1 u(t + \theta) d\theta, \quad (2.2)$$

where  $F$  is an  $m \times n$  matrix, yields a finite spectrum of the closed-loop system. The location of this spectrum can be completely controlled by the choice of  $F$  under some suitable controllability conditions. This result remains true for the more general systems governed by

$$\dot{x}(t) = Ax(t) + \int_{-\tau}^0 d\mu(\theta) u(t + \theta), \quad (2.3)$$

where  $\mu$  is an  $n \times m$  matrix function of bounded variation and the corresponding feedback has the following form

$$u(t) = Fx(t) + F \int_{-\tau}^0 \int_{\sigma}^0 e^{(\sigma-\theta)A} d\mu(\sigma) u(t+\theta) d\theta, \quad (2.4)$$

where  $\sigma$  is the integration variable of the first (outer) integral. Consider the following linear system

$$\dot{x}(t) = Ax(t) + B_0 u(t) + B_1 u(t-\tau), \quad (2.5)$$

where  $x \in \mathbb{R}^n$ ,  $u \in \mathbb{R}^m$ ,  $A \in \mathbb{R}^{n \times n}$ ,  $B_0, B_1 \in \mathbb{R}^{n \times m}$  and  $\tau$  is the delay of the system ( $\tau > 0$ ).

In [43] it is proven that the following feedback

$$u(t) = Fx(t) + F \int_{-\tau}^0 e^{-(\tau+\theta)A} B_1 u(t+\theta) d\theta, \quad (2.6)$$

where  $F$  is an  $m \times n$  matrix, yields a finite spectrum of the closed-loop system. The location of this spectrum can be completely controlled by the choice of  $F$  under some suitable controllability conditions.

A result on spectrum assignment is provided in [43]. Namely, the spectrum of the closed-loop system (2.3)-(2.4) coincides with the spectrum of the matrix  $A + B(A)F$  where

$$B(A) = \int_{-\tau}^0 e^{\sigma A} d\mu(\sigma). \quad (2.7)$$

Moreover, assuming the controllability (respectively, the stabilizability) of the pair  $(A, B(A))$ , the spectrum of the system (2.3)-(2.4) may be placed at any preassigned self-conjugate set of  $n$  points in the complex plane (respectively the unstable eigenvalues of  $A$  may be arbitrarily shifted) by a suitable choice of the matrix  $F$ .

An alternative way to stabilize the solutions of system (2.3) is the use of a dynamic feedback [43]:

$$\begin{aligned} \dot{u}(t) = & F(A - D_2)x(t) + (FB(A) + D_1)u(t) \\ & + F(A - D_2) \int_{-\tau}^0 \int_{\sigma}^0 e^{(\sigma-\theta)A} d\mu(\sigma) u(t+\theta) d\theta, \end{aligned} \quad (2.8)$$

where  $D_1$  is an  $m \times m$  matrix and  $D_2$  is an  $n \times n$  matrix. Moreover, the spectrum of the closed-loop system (2.3)-(2.8) coincides with the roots of the following equation

$$\det \left[ \mathbb{I}s - D_1 \right] \det \left[ \mathbb{I}s - A - B(A)F \right] = 0, \quad (2.9)$$

if the matrices  $D_1, D_2$  and  $F$  satisfy  $FD_2 = D_1F$ .

Moreover, if the pair  $(A, B(A))$  is controllable, then  $n$  eigenvalues of the closed-loop system may be assigned in an arbitrary self-conjugate configuration by a proper choice of matrix  $F$ .

Consider the general system governed by

$$\dot{x}(t) = \int_{-\tau}^0 d\eta(\theta)x(t+\theta) + \int_{-\tau}^0 d\mu(\theta)u(t+\theta), \quad (2.10)$$

with  $\eta$  and  $\mu$  of bounded variation. A result in [42], states that the following condition

$$\text{Rank} \left[ s\mathbb{I}_n - \int_{-\tau}^0 e^{s\theta} d\eta(\theta); \int_{-\tau}^0 e^{s\theta} d\mu(\theta) \right] = n, \quad (2.11)$$

is a necessary condition for a locally integrable control  $u(t)$  satisfying:

$$|u(t)| = o(e^{-\varepsilon t}), \quad (2.12)$$

and for some small  $\varepsilon > 0$ :

$$|x(t)| = o(e^{-\varepsilon t}), t \rightarrow \infty, \quad (2.13)$$

One can use the dynamic feedback  $\dot{u}(t) = w(t)$ , with

$$w(t) = \int_{-\tau}^0 [dK_1(\theta)]x(t+\theta) + \int_{-\tau}^0 [dK_2(\theta)]u(t+\theta). \quad (2.14)$$

Hence, condition (2.11) is also sufficient for stabilizability.

## Advantages and limitations

From a practical viewpoint, the digitization of the controller generated by the finite pole assignment is subject to a discretization which unfortunately induces the loss of the control of the closed-loop spectral values. In other words, one has spectral values that exceed the range that one has assigned (see [46], [123]) yielding the Spillover phenomena (the numerical controller parameters are not exactly the same as those computed via the analytical design method). Indeed, this has been explained by the sensitivity of the design to parameter variations. Accordingly, the instability of the difference part of the control law leads to the instability of the closed-loop system's solution, see for instance [46]. Notice also some concern with the complexity of calculations compared to other existing methods.

### 2.3 . Algebraic pole placement

In this section, we consider an algebraic design paradigm proposed and developed in [45], [124]–[126]. Such an APP approach consists in a compensation

of unstable poles by stable ones (the assigned poles). This renders the closed-loop systems' solutions exponentially stable. Its main ingredient is an appropriate division in the ring of transfer functions corresponding to pointwise or particular distributed delays, which yields fractions over  $\mathbb{R}(s, e^{-\tau s})$ .

## Main idea

Roughly speaking, the principle of this algebraic approach consists in keeping the spectral values with a real part below a chosen threshold and removing from the spectrum some undesired spectral values (typically unstable spectral values) via an Euclidean-like division. Furthermore, an additional set of spectral values is assigned to define the exponential decay rate of the closed-loop system's solution. Even if the origin of this algebraic approach is inspired from the FSA, its methodology differs in many ways.

## Description of the method

We refer to [45]. Consider the single-input delay system

$$\dot{x}(t) = \sum_{i=0}^k A_i x(t - i\tau) + \sum_{i=0}^k b_i u(t - i\tau), \quad (2.15)$$

where  $x \in \mathbb{R}^n$  is the state of the system and  $u \in \mathbb{R}$  is the output of the system. For all  $i \in \{0, \dots, k\}$ ,  $A_i \in \mathbb{R}^{n \times n}$ ,  $b_i \in \mathbb{R}^{n \times 1}$  and  $\tau > 0$  is the delay of the system. Consider the control law:

$$u(t) = \int_0^N \left( f(\theta) u(t - \theta) + g(\theta) x(t - \theta) \right) d\theta + \sum_{i=0}^M p_i x(t - i\tau), \quad (2.16)$$

where  $N \in \mathbb{R}_+$ ,  $f \in L_2([0, N], \mathbb{R})$ ,  $g \in L_2([0, N], \mathbb{R}^{1 \times n})$ ;  $M \in \mathbb{N}$  and  $\forall i \in \{1, \dots, M\}$ ,  $p_i \in \mathbb{R}$ . Applying the Laplace transform with a zero initial condition to (2.15) and (2.16), one has, respectively,

$$s x = A x + b u \quad \text{and} \quad u = F_1 u + F_2 x, \quad (2.17)$$

where

$$A = \sum_{i=0}^k A_i e^{-\tau s i}; \quad b = \sum_{i=0}^k b_i e^{-\tau s i}, \quad (2.18)$$

and

$$F_1 = \int_0^N f(\theta) e^{-\theta s} d\theta; \quad F_2 = \int_0^N g(\theta) e^{-\theta s} d\theta + \sum_{i=0}^M p_i e^{-\tau s i}. \quad (2.19)$$

In the following, we provide a definition of the finite spectrum assignability in terms of the characteristic polynomial of the closed-loop system.

**Definition 2.3.1** *If there exist  $F_1$  and  $F_2$  such that*

$$\det \begin{bmatrix} s\mathbb{I}_n - A & -b \\ -F_2 & 1 - F_1 \end{bmatrix} = \prod_{i=1}^n (s - \alpha_i), \quad (2.20)$$

*for any set of  $n$  complex numbers  $\alpha_i$  such that any  $\alpha_i \in \{\alpha_1, \dots, \alpha_n\}$  with  $\Im(\alpha_i) \neq 0$  appears in conjugate pair, then the system (2.15) is said to be finite-spectrum-assignable.*

**The ring  $\mathcal{R}[s]$ :** is a ring of transfer functions defined as the set of all the meromorphic functions in the complex plane  $\mathbb{C}$  that are of the form  $\frac{P(s, e^{-\tau s})}{Q(s)}$ , where  $Q$  is a polynomial in the Laplace complex variable  $s$ ,  $P$  is a bivariate polynomial in  $s$  and  $e^{-\tau s}$ , and  $\tau$  is a fixed positive real number. We consider the entire function which is the finite Laplace transform of a distributed delay equation, called elementary fraction [127] and defined as

$$\theta_\sigma(s) = \frac{1 - e^{(-s+\sigma)\tau}}{s - \sigma}, \quad \sigma \in \mathbb{C}. \quad (2.21)$$

The effective design of stabilizing compensates for delay-differential systems is one of the application of Bézout-domain property (see [128]–[130] and references therein).

**Remark 2.3.1** *A Bézout domain is an integral domain in which every finitely generated ideal is principal.*

**Remark 2.3.2** *We say that  $n(s, z)$  and  $d(s, z)$  over  $\mathbb{R}[s, z]$  are 2-D factor coprime if there no common 2-D factor  $r(s, z)$  over  $\mathbb{R}[s, z]$  such that  $n(s, z) = \tilde{n}(s, z) \cdot r(s, z)$ ,  $d(s, z) = \tilde{d}(s, z) \cdot r(s, z)$  and  $\deg_s(r) > 0$  or  $\deg_z(r) > 0$ .*

**Bézout-type identities:** Consider  $Q \in \mathbb{R}[s, e^{-s\tau}]^{p \times p}$ , and  $P \in \mathbb{R}[s, e^{-s\tau}]^{p \times m}$ ,  $D \in \mathbb{R}[s, e^{-s\tau}]^{m \times m}$ ,  $N \in \mathbb{R}[s, e^{-s\tau}]^{p \times m}$  which satisfy:

$$Q^{-1} \cdot P = N \cdot D^{-1}. \quad (2.22)$$

Matrices  $Q$  and  $P$  are required to be admissible. We can always find matrices  $Q, P, D$  and  $N$  that satisfy such a coprimeness condition (see [131]).

**Lemma 2.3.1** ([131], Theorem 5.1) *Let  $Q$  and  $P$  be two 2-D left-factor-coprime matrices over  $\mathbb{R}[s, e^{-s\tau}]$ . Then, there exist  $E$  a polynomial matrix in  $s$ , and two matrices  $X, Y$  over  $\mathbb{R}[s, e^{-s\tau}]$  satisfying*

$$Q \cdot X + P \cdot Y = E. \quad (2.23)$$

**Theorem 2.3.1** *If  $\text{Rank}[Q|P] = p, \forall s \in \mathbb{C}$ , then there exist  $\mathcal{X} \in \mathcal{R}[s]^{p \times p}$  and  $\mathcal{Y} \in \mathcal{R}[s]^{m \times p}$  such that*

$$Q \cdot \mathcal{X} + P \cdot \mathcal{Y} = \mathbb{I}_p. \quad (2.24)$$

**Theorem 2.3.2** ([45]) *The system (2.15) is finite-spectrum-assignable if, and only if, it is spectrally controllable, i.e.,*

$$\text{Rank} \begin{bmatrix} s\mathbb{I}_n - A & b \end{bmatrix} = n, \quad \forall s \in \mathbb{C}. \quad (2.25)$$

## Advantages and limitations

This kind of algebraic method becomes interesting when one knows beforehand the number and location of undesired spectral values.

However, in general, standard complex analysis techniques, such as the argument principle, only provide the number of undesired spectral values. In addition, the standard numerical methods only produce approximations, so that, in practice, a considerable symbolic/numeric issue arises, since the method requires their exact value. Building effective algorithms to overcome the latter symbolic/numeric issue remains challenging; the reconstruction of a polynomial characterizing an exact spectral value from a polynomial characterizing its approximation represents an additional complexity for rendering the approach systematic.

Besides, another challenging question related to this algebraic paradigm is the design of efficient and algorithmic calculations of the involved objects such as the ring elements derived from the corresponding Bézout's identity.

Solving the emphasized issues will surely break new ground for the pole placement algebraic paradigm.

### 2.4 . Continuous pole placement

To the best of our knowledge, the first “automated” pole placement for retarded time-delay systems is the numerical paradigm known as “continuous pole placement” (CPP) method introduced in [132].

#### Main idea

The CPP paradigm consists in defining a function that represents the spectral abscissa and to exploit its dependency on the controller parameters, and the control strategy can be summarized as follows: “Shift” the unstable characteristic roots from  $\mathbb{C}_+$  to  $\mathbb{C}_-$  in a “quasi-continuous” way subject to the strong constraint that, during this shifting action, stable characteristic roots are not crossing the imaginary axis from  $\mathbb{C}_-$  to  $\mathbb{C}_+$ . We refer to and references therein for further insights on the number of controlled characteristic roots (which is related to the available degrees of freedom induced by the controller structure) as well as the interpretation of CPP as a local strategy to solve an appropriate optimization problem where the objective function (rightmost root) is not differentiable. It is worth mentioning that CPP, initially applied to delay systems of retarded type, was extended to neutral systems in [133].

## Description of the method

In order to illustrate this method, we consider the investigation of the stability of the following system

$$\dot{x}(t) = Ax(t) + Bu(t - \tau), \quad (2.26)$$

where  $A \in \mathbb{R}^{n \times n}$ ,  $B \in \mathbb{R}^{n \times 1}$ ,  $x \in \mathbb{R}^n$  is the state,  $u \in \mathbb{R}$  is the input and  $\tau$  is the positive delay. Let us consider the linear control law that reads

$$u = K^T x, \quad K \in \mathbb{R}^{n \times 1}. \quad (2.27)$$

This static state feedback controller reveals the link between the CPP method and the classical pole placement method.

The CPP method consists in applying slight changes to the feedback gain so as to move the unstable eigenvalues to the left half-plane. The key steps for this method may be declined as follows. First, the rightmost eigenvalues are computed; an automatic method for doing so is provided in [134]. Second, the sensitivity of the rightmost eigenvalues with respect to changes in the feedback gain is assessed. Next, the rightmost eigenvalues are pushed in the direction of the left half-plane by applying a slight alteration to the feedback gain, owing to the aforementioned sensitivities. Lastly, the rightmost uncontrolled eigenvalues are monitored: if necessary, the number of controlled eigenvalues shall be increased ; stop when stability is reached or when the available degrees of freedom in the controller do not allow to further reduce  $\sup \Re(s)$  ; otherwise, resume step 2. These steps are resumed in the fundamental Algorithm 1.

---

### Algorithme 1 : The continuous pole placement method

---

- 1 Initialize  $m = 1$ .
  - 2 Compute the rightmost eigenvalues for the nominal delay  $\tau$ .
  - 3 Compute the sensitivity of the  $m$  rightmost eigenvalues w.r.t. changes in the feedback gain  $K$
  - 4 Move the  $m$  rightmost eigenvalues in the direction of the left half plane by applying a small change to the feedback gain  $K$ , using the computed sensitivities.
  - 5 Monitor the rightmost uncontrolled eigenvalues. If necessary, increase the number of controlled eigenvalues,  $m$ . Stop when stability is reached or when the available degrees of freedom in the controller do not allow to further reduce  $\sup \Re(s)$ . In the other case; go to step 2.
- 

**Remark 2.4.1** *The different steps of CPP method are thoroughly detailed in [132].*



## Advantages and Drawbacks

Unlike FSA method, CPP approach does not render the closed-loop system finite-dimensional, but consists instead of controlling the corresponding rightmost eigenvalues. Such an idea represents a simple generalization of the pole placement for finite-dimensional systems represented by ordinary differential equations.

### 2.5 . Partial pole placement

#### Main idea

The strategy of PPP consists in tuning standard controllers via the aforementioned MID property. Namely, one needs to determine the conditions under which a given multiple root of a the characteristic equation is dominant.

#### Description of the method

The procedure of PPP is carried out in several steps. First, conditions on the system's parameters guaranteeing the existence of a multiple root are obtained. Second, an affine change of variable is required to normalize the characteristic equation. Next, a bound on the imaginary part of roots of the normalized characteristic equation in the complex right half-plane is derived. In fact, the frequency bound is the main ingredient for the proof of the dominance, for this purpose, a pseudo-code listing the instructions to be followed to target a suitable frequency bound is given in [91]. The idea is to find an adequate truncation order of the exponential term appearing in the normalized quasipolynomial which depends only on the real part of its roots. By using a purely polynomial analysis, one is able to obtain a suitable bound of the imaginary part of the roots. Lastly, a certification of the dominance of the multiple root is established.

## Advantages and Drawbacks

Unlike the APP method, when it comes to the PPP method, *a priori* knowledge on the number of unstable roots and/or their location is not required. On the one hand, it is reported that the PPP is easy to implement and robust to uncertain delays or the model's parameters [135] and on the other hand, it applies to retarded as well as neutral systems [76]. Furthermore, it provides a procedure to assess the critical delay, see for instance [86]. The main limitation of the PPP is that the actual knowledge allows to assign the spectral abscissa only on the real axis, aside from few isolated cases, see for instance [58]), which may not be relevant in some applications. We have yet to fathom the extent of this property, notwithstanding

the fact that often small delays are required to perform the MID property which may again be a drawback in some applications.

## 2.6 . Illustrative examples

### Example 1

In order to illustrate FSA, consider the following system

$$\dot{x}(t) = x(t) + u(t - 1). \quad (2.28)$$

The characteristic equation of the open-loop system  $s - 1 = 0$  yields an unstable pole at  $s = 1$ , the open loop-system is then unstable. The feedback proposed in (2.4) reads in the case of system (2.28) as follows

$$u(t) = f x(t) + f z(t), \quad (2.29)$$

where

$$z(t) = \int_{-1}^0 e^{-(1+\theta)t} u(t + \theta) d\theta. \quad (2.30)$$

The transfer function of the system (2.30) is

$$\frac{z(s)}{u(s)} = \frac{1}{e} \int_{-1}^0 e^{(s-1)\theta} d\theta = \frac{e^{-1} - e^{-s}}{s-1}. \quad (2.31)$$

The pole  $s = 1$  is cancelled by a zero of  $e^{-1} - e^{-s}$ . The Laplace transform of (2.28)-(2.29) yields the characteristic equation of the closed-loop system

$$\begin{pmatrix} s-1 & -e^{-s} \\ -f & 1 - f \frac{e^{-1} - e^{-s}}{s-1} \end{pmatrix} \begin{pmatrix} x(s) \\ u(s) \end{pmatrix} = 0, \quad (2.32)$$

Looking for the characteristic roots amounts to computing the zeros of the determinant of the system, we have

$$(s-1) \left( 1 - f \frac{e^{-1} - e^{-s}}{s-1} \right) - f e^{-s} = 0, \quad (2.33)$$

which yields the following zero

$$s = 1 + \frac{f}{e}, \quad (2.34)$$

It is important to note that the spectrum of the closed-loop system is finite, and that the pole  $s = 1$  is not cancelled by a corresponding zero, but it is shifted from  $s = 1$  to  $s = 1 + \frac{f}{e}$  by the feedback ; see the block diagram of the closed-loop system in Figure 2.1.

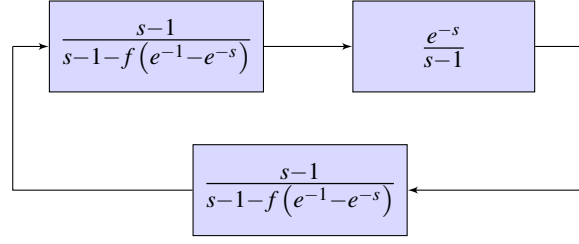


Figure 2.1: Block diagram of the closed-loop system.

### Example 2

In order to illustrate the APP method, consider the following system

$$\dot{x}(t) = A_0 x(t) + A_1 x(t-1) + b_1 u(t-1), \quad (2.35)$$

where  $x(t) = (x_1(t) \ x_2(t))^T$  and

$$A_0 = \begin{pmatrix} 0 & 0 \\ 0 & 1 \end{pmatrix}, \quad A_1 = \begin{pmatrix} 1 & -1 \\ 0 & 0 \end{pmatrix}, \quad b_1 = \begin{pmatrix} 0 \\ 1 \end{pmatrix}. \quad (2.36)$$

The above system is spectrally controllable since  $\text{Rank} [s\mathbb{I}_2 - A, b] = 2$ , where, in this case

$$A = \begin{pmatrix} e^{-s} & -e^{-s} \\ 0 & 1 \end{pmatrix}, \quad b = \begin{pmatrix} 0 \\ e^{-s} \end{pmatrix}. \quad (2.37)$$

Therefore, we can assign the poles of the system at  $-1$ . To do so, we follow [[45], proof of Theorem 9]. The condition  $(s\mathbb{I}_2 - A)^{-1} b - Nd^{-1}$  is satisfied, where

$$N = \begin{pmatrix} -e^{-2s} \\ (s - e^{-s}) e^{-s} \end{pmatrix} \quad d = (s-1)(s - e^{-s}). \quad (2.38)$$

There exist  $\mathcal{X} \in \mathcal{R}[s]$  and  $\mathcal{Y} \in \mathcal{R}^{1 \times 2}[s]$  where

$$\mathcal{X} = \frac{e^{-s} + s + e^{-2s}(2s^2 + \kappa s^2 - 2s - 1)}{s^2(s-1)}, \quad (2.39)$$

$$\mathcal{Y} = \left( \frac{-1 + (s - e^{-2s})(2s^2 + \kappa s^2 - 2s - 1)}{s^2}; \ 0 \right), \quad (2.40)$$

with  $\kappa = (-1 - e^{-s} + e^{-2s}) e^2$ , such that

$$(\mathcal{X} \ \mathcal{Y}) \cdot \begin{pmatrix} d \\ N \end{pmatrix} = 1. \quad (2.41)$$

In this example we aim to assign the poles at  $-1$ , then we take  $C = (s+1)$ . Next, we divide  $C\mathcal{Y}$  by  $(s\mathbb{I}_2 - A)$  on the left to obtain  $C\mathcal{Y} = T \cdot (s\mathbb{I}_2 - A) - F_2$

with

$$T = ((2 + \kappa) s^2 + (2 + 2\kappa) s - 3 + \kappa; -(2 + \kappa) s e^{-s} - (4 + 3\kappa) e^{-s}), \quad (2.42)$$

$$-F_2 = (-5 + \theta_0^{(1)} - 3\theta_0; -e^{-s} - 4\kappa e^{-s}). \quad (2.43)$$

Set  $H = C \mathcal{X} + T b$  which is developed as

$$H = 1 + e^{-s} \theta_0^{(1)} - (1 + 4e^{-s}) \theta_0 + 4(1 + (1 + e) e^{-s}) \theta_1 \quad (2.44)$$

As a result, a feedback law which assigns the poles of the system at  $-1$  is

$$\begin{aligned} u(t) = & 5x_1(t) + \left( 1 + \frac{4(-1 - e^{-1} + e^{-2})}{e^{-2}} \right) x_2(t-1) \\ & + \int_0^1 \left( (-\tau + 4 - 4(1 + e) e^\tau) u(t-1-\tau) \right. \\ & \left. + (1 - 4e^\tau) u(t-\tau) + (-\tau + 3) x_1(t-\tau) \right) d\tau. \end{aligned} \quad (2.45)$$

### Example 3

In order to illustrate the CPP method, we consider the system

$$\dot{x}(t) = Ax(t) + bu(t-\tau), \quad u = K^T x(t), \quad (2.46)$$

where

$$A = \begin{pmatrix} -0.08 & -0.03 & 0.2 \\ 0.2 & -0.04 & -0.005 \\ -0.06 & 0.2 & -0.07 \end{pmatrix}, \quad b = \begin{pmatrix} -0.1 \\ -0.2 \\ 0.1 \end{pmatrix}, \quad \tau = 5. \quad (2.47)$$

The open-loop system is unstable with the feedback  $u$  in (2.46) where

$$K = (0.719 \quad 1.04 \quad 1.29)^T. \quad (2.48)$$

The spectral abscissa is shown in Figure 2.2 as a function of the delay  $\tau$ . Note that the particular control law achieves stability for  $\tau = 0$ , the system is unstable for the nominal delay  $\tau = 5$ , also, the characteristic roots must cross the imaginary axis from left to right and this occurs when  $\tau_{\text{crit}} = 3.95$ . Next, we determine the delay margin, i.e. at what first value of  $\tau$ , the characteristic roots lie on the imaginary axis. Let write the characteristic equation of (2.46)-(2.47) under the form

$$\Delta(s) = P_0(s) + P_\tau(s) e^{-\tau s}, \quad (2.49)$$

where

$$P_0(s) = s^3 + 0.19s^2 + 0.03s - 0.0068, \quad (2.50)$$

$$P_\tau(s) = 0.1509s^2 + 0.070115s + 0.014. \quad (2.51)$$

A necessary and sufficient condition is that  $s = i \omega$ , with  $\omega \in \mathbb{R}$  be a solution of  $\Delta(s) = 0$  for some value of  $\tau$ , in other words,

$$P_0(i \omega) + P_\tau(i \omega) e^{-\tau i \omega} = 0. \quad (2.52)$$

Using the fact that if  $i \omega$  is a solution of (2.52), then  $-i \omega$  satisfies (2.52), i.e.

$$P_0(-i \omega) + P_\tau(-i \omega) e^{\tau i \omega} = 0. \quad (2.53)$$

Then

$$P_0(i \omega) P_0(-i \omega) - P_\tau(i \omega) P_\tau(-i \omega) = 0. \quad (2.54)$$

We define the following polynomial in  $\omega^2 = \Omega$ ,

$$\begin{aligned} \mathcal{P}(\Omega) &= P_0(i \omega) P_0(-i \omega) - P_\tau(i \omega) P_\tau(-i \omega) \\ &= \Omega^3 - 0.047 \Omega^2 + 0.002 \Omega - 0.00016. \end{aligned} \quad (2.55)$$

for which only the positive roots are of interest. Indeed, only the solution  $\omega^* = 0.227$  need be considered. The corresponding delay  $\tau_{\text{crit}}$  is the smallest positive value satisfying

$$\begin{cases} \cos(\omega \tau) = \Re \left( \frac{-P_0(i \omega)}{P_\tau(i \omega)} \right), \\ \sin(\omega \tau) = \Im \left( \frac{P_0(i \omega)}{P_\tau(i \omega)} \right), \end{cases} \quad (2.56)$$

that is

$$\begin{cases} \cos(0.227 \tau) = 0.62, \\ \sin(0.227 \tau) = 0.78. \end{cases} \quad (2.57)$$

The characteristic roots must cross the imaginary axis from left to right and this occurs when  $\tau_{\text{crit}} \approx 3.94$ .

Figure 2.3, illustrates the real parts of the rightmost spectral values of (2.46)-(2.47) as a function of the delay  $\tau$ . These figures show how the spectral abscissas progress towards the minimum for the nominal delay. One remarkable property of the system is the high sensitivity with respect to the delay changes (or eventually the change of the other parameters). Executing Algorithm 1 until to attain the minimum causes this high sensitivity with respect to the delay changes for the feedback gain. As a matter of fact, at iteration 37 (see Figure 2.3 (left)), the feedback gain obtained already reach the stability. Notice that the exponential decay rate of the closed-loop solution is smaller than for the optimum, yet less sensitive to delay changes.

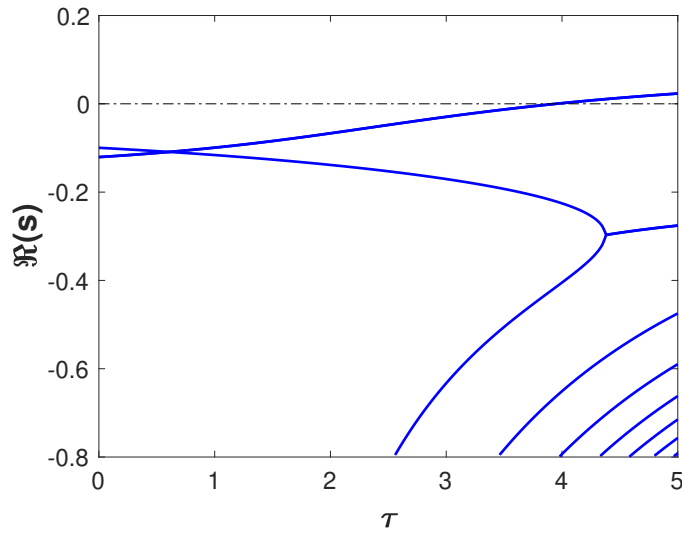


Figure 2.2: Rightmost eigenvalues of the system (2.46)–(2.47) as a function of the delay  $k = [0.719 \ 1.04 \ 1.29]^T$ .

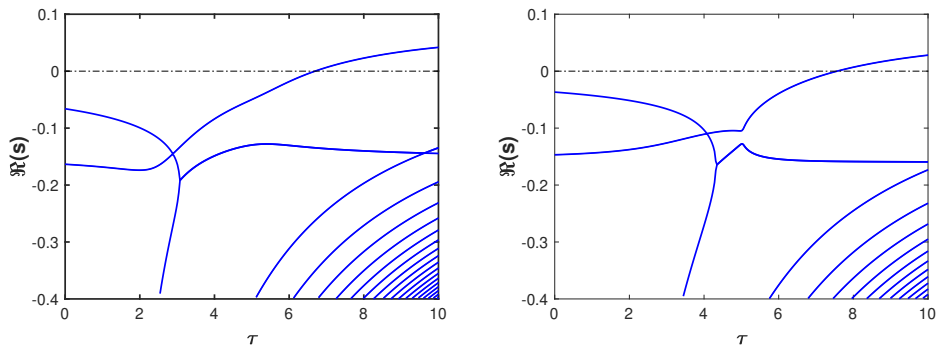


Figure 2.3: (Left) Rightmost eigenvalues of the system (2.46)–(2.47) as a function of the delay  $\tau$  for  $K = (0.712 \ 1.075 \ 0.831)^T$  at iteration 37. (Right)  $K = (0.559 \ 0.770 \ 0.694)^T$  at iteration 110.

#### Example 4

In order to understand the effect of the admissible multiplicities of spectral values on stability of the time-delay system and their characterization, Consider the problem of stabilization of the classical harmonic oscillator, by a proportional-derivative controller

$$\ddot{x}(t) + a_0 x(t) + b_1 \dot{x}(t - \tau) + b_0 x(t - \tau) = 0, \quad (2.58)$$

for which the characteristic equation is

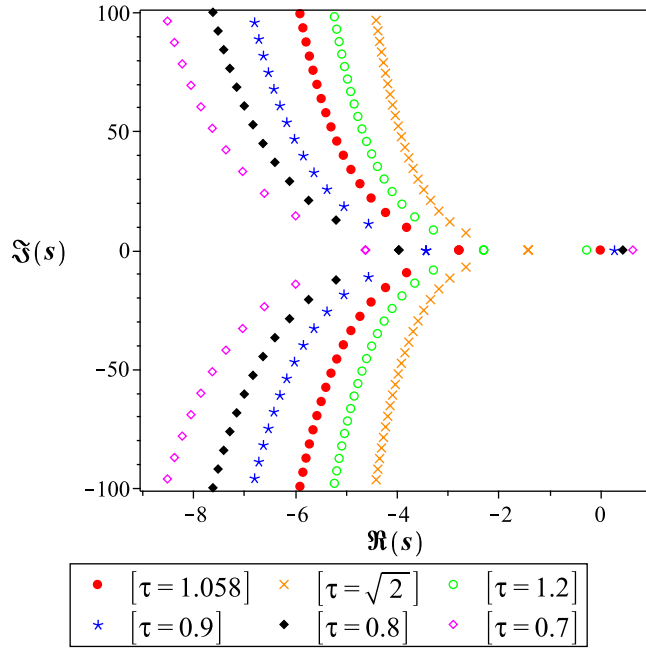


Figure 2.4: Translation of the spectrum distribution of  $\Delta_0$  according to the delay change.

$$\Delta(s) = s^2 + a_0 + (b_1 s + b_0) e^{-\tau s}, \quad (2.59)$$

the multiple spectral value of which is

$$s_{\pm} = \frac{1}{\tau} \left( -2 + \sqrt{-\tau^2 a_0 + 2} \right), \quad (2.60)$$

and the controllers' gains of which are

$$\begin{cases} b_0 = \frac{2(\tau^2 a_0 + 5\tau s_{\pm} + 3)e^{\tau s_{\pm}}}{\tau^2}, \\ b_1 = \frac{2(\tau s_{\pm} + 1)e^{\tau s_{\pm}}}{\tau}. \end{cases} \quad (2.61)$$

Under the previous conditions (2.61), the spectral value  $s = s_+$  is necessarily a dominant root for (2.59), unlike  $s_-$  which cannot be the spectral abscissa. Indeed, the multiple spectral value at  $s_-$  is always dominated by a single real root that we denote by  $s_0$ .

By substituting the gains of the controller (2.61) in the characteristic equation (2.59) where  $a_0 = 1$ , we obtain

$$\Delta_0(s) = s^2 + 1 + \left( \frac{2s(-1 - \sqrt{-\tau^2 + 2})e^{-2 - \sqrt{-\tau^2 + 2}}}{\tau} + \frac{2(-7 - 5\sqrt{-\tau^2 + 2} + \tau^2)e^{-2 - \sqrt{-\tau^2 + 2}}}{\tau^2} \right) e^{-\tau s}. \quad (2.62)$$

Now, imposing  $s = 0$  to be the real root of  $\Delta_0$ , one is able to obtain numerically the corresponding delay  $\tau_0 \approx 1.0581$  which yields a root on the imaginary axis.

Figure 2.4 presents a spectrum distribution of  $\Delta_0$  computed using `Maple`. This spectrum distribution can also be illustrated using the `QPmR` toolbox from [136]. The figure distinctly illustrates the effect of the delay on the multiple root. Actually, for the delay  $\tau = \tau_0 \approx 1.0581$  the multiple root is at  $s = 0$ , then the reduction of the value of the delay  $\tau$  pushes the roots continuously from the imaginary axis to the right.

## 2.7 . Chapter Summary

The existing pole placement paradigms were discussed. A presentation and an illustration of finite spectrum assignment, algebraic pole placement, continuous pole placement and the partial pole placement method is given, via some simple dynamical systems.





**Part II**

**Partial pole placement  
approach**



## 3 - The GMID property for second order neutral equation

This chapter is an extended version of the paper [57].

### 3.1 . Introduction

This chapter considers the Generic Multiplicity-Induced-Dominancy (GMID) property for second order neutral time-delay differential equations. Necessary and sufficient conditions for the existence of a root of maximal multiplicity are given in terms of this root and the parameters (including the delay) of the given equation. Links with dominancy of this root and with the exponential stability property of the solution of the considered equations are provided. Finally, we illustrate the obtained results on the classical oscillator control problem.

This chapter is organized as follows: Section 3.2 states a design methodology exploiting the Multiplicity-Induced-Dominancy (MID) property, the classical steps leading to the proof are recalled through a comprehensive example, the first-order neutral equation with a single delay (GMID: codimension 3). The problem setting is presented in 3.3, while the main result is presented in Section 3.4, where a classification of admissible multiplicities for second order neutral time-delay differential equation with a single delay is provided. The proof of the main result is presented in Section 3.5. Finally, Section 3.6 is dedicated to the exponential stabilization of an oscillator via delay, as an illustrative example.

### 3.2 . The MID methodology on a toy model: Codimension 3

The MID property consists of the conditions under which a given multiple complex zero of a quasipolynomial is dominant. It's proof consists of five steps. First, we establish conditions on the parameters of the system guaranteeing the existence of a multiple root. Second, an affine change of variable of the characteristic equation is performed in order to reduce the said quasipolynomial to a normalized form; the desired multiple root becomes 0 and the delay 1. Next, under the latter normalization, the characteristic equation may be easily factorized in terms of an integral expression. Hence, we derive a bound on the imaginary part of roots of the normalized quasipolynomial in the complex right half-plane. Lastly, a certification of the dominance of the multiple root is demonstrated.

The proof methodology of the MID property is resumed in Figure 3.1 and Algorithm 2 is a pseudo-code listing the instructions to be followed to target an suitable frequency bound.

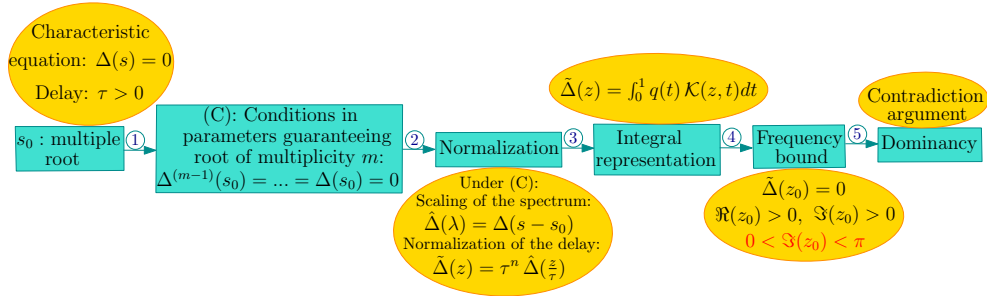


Figure 3.1: Diagram illustrating the proof methodology of the MID property for a second-order time-delay differential equation

---

**Algorithm 2** : Estimation of the MID frequency bound in second-order neutral time-delay differential equations

---

**Input** :  $\tilde{\Delta}(z) = \tilde{P}_0(z) + \tilde{P}_1(z)e^{-z}$ ; // Normalized quasipolynomial  
// Initialization

1  $ord = 0$ ; //  $ord$ : order of truncation of the Taylor expansion of

$$e^{2x} = \underbrace{1}_{ord=0} + 2x + 2x^2 + \frac{4x^3}{3} + \dots;$$

2  $dominance = false$ ;

3  $\exists z_0 = x + i\omega \in \mathbb{R}_+^* + i\mathbb{R}_+^*$  s.t.  $\tilde{\Delta}(z_0) = 0$ ;

4  $|\tilde{P}_0(x + i\omega)|^2 e^{2x} = |\tilde{P}_1(x + i\omega)|^2$ ;

5 **while**  $\sim dominance$  **do**

6      $ord = ord + 1$ ;

7      $F(\omega) = |\tilde{P}_1(x + i\omega)|^2 - |\tilde{P}_0(x + i\omega)|^2 T_{ord}(e^{2x}) > 0$ ; //  $T_{ord}(e^{2x})$ :  
Taylor expansion of  $e^{2x}$  of order =  $ord$

8      $\omega^2 = \Omega$ ;

9      $G(\Omega) = a(x)\Omega^2 + b(x)\Omega + c(x)$ ; //  $a(x) \neq 0, G(\Omega) = F(\omega)$

10  $\Omega^\pm(x) = \frac{-b(x) \pm \sqrt{b^2(x) - 4a(x)c(x)}}{2a(x)}$ ; //  $\Omega^\pm(x)$  depends on free  
parameters denoted by **param** hereafter

11 **if**  $\max_x(\max_{param}(\Omega^\pm(x))) < \pi^2$  **then**

12      $dominance = true$ ;

**Output** : Frequency bound ;

---

To illustrate the proof of the methodology of the MID property described above, we consider a model of phenomena in the bio-sciences describing the dynamics of a vector-borne disease. It is based on a simple scalar delay differential equation with a positive single delay  $\tau$ . In its linearized version, the infected host population

$x(t)$  is governed by

$$\dot{x}(t) + a_0 x(t) + a_1 x(t - \tau) = u(t), \quad (3.1)$$

where  $u$  is the delayed output-feedback:

$$u(t) = (a_1 - \alpha_0)x(t - \tau) - \alpha_1 \dot{x}(t - \tau), \quad (3.2)$$

with  $\alpha_0, \alpha_1$  are real coefficients, and  $a_1 > 0$  is called the contact rate; it represents the contact number between infected and uninfected populations. Assume that the infection of the host recovery proceeds exponentially at a rate of  $-a_0 > 0$ . The characteristic equation of (3.1) is the quasipolynomial function defined by

$$\Delta(s) = s + a_0 + (\alpha_1 s + \alpha_0) e^{-\tau s}, \quad (3.3)$$

of degree  $\deg_s(\Delta) = 3$ , The first-order neutral equation is treated in the context of delay differential-algebraic systems in [56]. In the following, we shall illustrate the dominance proof following the methodology previously described.

- GMID : spectral value of maximal admissible multiplicity (multiplicity 3):

1. Forcing multiplicity: The real  $s_0$  is a root of multiplicity 3 of  $\Delta$  if, and only if, the coefficients  $a_0, \alpha_0, \alpha_1$ , the root  $s_0$  and the delay  $\tau$  satisfy the relations below

$$\begin{cases} a_0 = -s_0 - \frac{2}{\tau}, \\ \alpha_0 = \left(-s_0 + \frac{2}{\tau}\right) e^{s_0 \tau}, \\ \alpha_1 = e^{\tau s_0}. \end{cases} \quad (3.4)$$

2. Normalization: Performing the translation and scaling of the spectrum by the following change of variables

$$\tilde{\Delta}(z) = \tau \Delta\left(\frac{z}{\tau} + s_0\right), \quad (3.5)$$

for  $z \in \mathbb{C}$ , we get the following normalized characteristic equation

$$\tilde{\Delta}(z) = z + b_0 + (\beta_1 z + \beta_0) e^{-z}, \quad (3.6)$$

with relations (3.4) normalized as follows

$$\begin{cases} b_0 = \tau (a_0 + s_0), \\ \beta_0 = \tau (\alpha_1 s_0 + \alpha_0) e^{-\tau s_0}, \\ \beta_1 = \alpha_1 e^{-\tau s_0}. \end{cases} \quad (3.7)$$

3. Integral representation: The real root  $s_0$  is a root of multiplicity 3 of  $\Delta$  if, and only if, 0 is a root of multiplicity 3 of  $\tilde{\Delta}$ . As a matter of fact, since  $\tilde{\Delta}$  is a quasipolynomial of degree  $\deg_s(\tilde{\Delta}) = 3$ , zero is a root of multiplicity 3 of  $\tilde{\Delta}$  if, and only if,

$$\tilde{\Delta}(0) = \tilde{\Delta}'(0) = \tilde{\Delta}''(0) = 0. \quad (3.8)$$

The latter identities yield a linear system whose unique solution is  $(b_0, \beta_0, \beta_1) = (-2, 2, 1)$ . From relations (3.7), one concludes that  $s_0$  is a root of multiplicity 3 of  $\Delta$  if, and only if, relations (3.4) hold. Moreover, under the latter conditions, the quasipolynomial (3.3) reduces to

$$\tilde{\Delta}(z) = \tilde{P}_0(z) + \tilde{P}_1(z) e^{-z}, \quad (3.9)$$

where

$$\tilde{P}_0(z) = z - 2 \quad \text{and} \quad \tilde{P}_1(z) = z + 2. \quad (3.10)$$

Hence, the quasipolynomial  $\tilde{\Delta}$  admits the following Fredholm integral representation

$$\tilde{\Delta}(z) = \int_0^1 q(t) \mathcal{K}(z, t) dt, \quad (3.11)$$

where

$$q(t) = t(1-t) \quad \text{and} \quad \mathcal{K}(z, t) = z^3 e^{-tz}, \quad (3.12)$$

which is easily verified via an integration by parts.

4. Frequency bound: Assume that  $z_0 = x_0 + i\omega_0 \in \mathbb{R}_+ + i\mathbb{R}_+$  is a root of  $\tilde{\Delta}$ , so that  $\tilde{\Delta}(z_0) = 0$  if, and only if,

$$|\tilde{P}_0(x_0 + i\omega_0)|^2 e^{2x_0} = |\tilde{P}_1(x_0 + i\omega_0)|^2. \quad (3.13)$$

Considering a truncation of order 1 of the exponential term  $e^{2x}$ , the latter is lower bounded by  $1 + 2x$ . Next, define

$$F(x, \omega) = |\tilde{P}_1(x + i\omega)|^2 - (1 + 2x) |\tilde{P}_0(x + i\omega)|^2, \quad (3.14)$$

where  $F > 0$  for any  $x > 0$ . The zeros of  $F$  are characterized by the first order polynomial

$$G(\Omega = \omega^2) = -2x\Omega - 2x^3 + 8x^2. \quad (3.15)$$

The polynomial function  $G$  admits a single real root  $\Omega_0(x) = -x(x-4)$ , which reaches a maximum value at  $x^* = 2$ . As a result,  $\Omega_0$  is bounded by  $\Omega^* = 4 < \pi^2$ . Thus, one obtains the desired frequency bound,

$$0 < \omega \leq 2 < \pi. \quad (3.16)$$

5. Dominancy: The purpose of the frequency bound is to prove the dominancy by a contradiction argument. For this purpose, assume that there exists  $z_0 \in \mathbb{R}_+ + i\mathbb{R}_+$  root of  $\tilde{\Delta}$ . Then, the integral representation yields

$$\int_0^1 t(1-t)e^{-tz_0} dt = 0, \quad (3.17)$$

the imaginary part of which is

$$\int_0^1 t(1-t)e^{-tx} \sin(\omega t) dt = 0. \quad (3.18)$$

Now, the frequency bound  $0 < \omega \leq \pi$  of the previous step entails that the function

$$t \mapsto t(1-t)e^{-xt} \sin(\omega t), \quad (3.19)$$

is strictly positive in  $(0, 1)$ , thereby contradicting the last equality.

### 3.3 . Problem Setting

A natural question arises. *Can one extend the result of Mazanti et al [56] to second-order neutral differential equations? Does the maximal multiplicity guarantee the dominancy for second-order neutral differential equations?*

Hence, consider the generic delay differential equation with a single delay as in (1.4) with  $n = 2$ , i.e. second-order neutral delay equation,

$$\begin{cases} \ddot{x}(t) + a_1 \dot{x}(t) + a_0 x(t) + \alpha_2 \ddot{x}(t - \tau) + \alpha_1 \dot{x}(t - \tau) + \alpha_0 x(t - \tau) = 0, \\ x(t) = \varphi(t), \quad -\tau \leq t \leq 0, \end{cases} \quad (3.20)$$

where  $a_0, a_1, \alpha_0, \alpha_1, \alpha_2 \in \mathbb{R}, \alpha_2 \neq 0, \tau > 0$ , and  $\varphi$  is a given continuously differentiable real-valued history function on the initial interval  $[-\tau, 0]$ . Its characteristic function is given by the following quasipolynomial

$$\Delta(s) = s^2 + a_1 s + a_0 + (\alpha_2 s^2 + \alpha_1 s + \alpha_0)e^{-\tau s}, \quad (3.21)$$

of degree  $\deg_s(\Delta) = 5$ . In other words, we shall investigate the validity of MID property for the above class of quasipolynomial functions.



### 3.4 . Statement of the main results

The main result we prove in this chapter is the following.

**Theorem 3.4.1** *Consider the quasipolynomial*

$$\Delta(s) = s^2 + a_1s + a_0 + (\alpha_2s^2 + \alpha_1s + \alpha_0)e^{-\tau s}. \quad (3.22)$$

1. *The real  $s_0$  is a root of multiplicity 5 of  $\Delta$  if, and only if, the coefficients  $a_0, a_1, \alpha_0, \alpha_1, \alpha_2$ , the root  $s_0$  and the delay  $\tau$  satisfy the relations*

$$\begin{cases} a_1 = -2s_0 - \frac{6}{\tau}, & a_0 = s_0^2 + \frac{6}{\tau}s_0 + \frac{12}{\tau^2}, \\ \alpha_2 = -e^{\tau s_0}, & \alpha_1 = (2s_0 - \frac{6}{\tau})e^{\tau s_0}, \\ \alpha_0 = -\left(s_0^2 - \frac{6}{\tau}s_0 + \frac{12}{\tau^2}\right)e^{\tau s_0}. \end{cases} \quad (3.23)$$

2. *If (3.23) is satisfied, then  $s_0$  is a dominant root of  $\Delta$ . Moreover, for all  $s \in \mathbb{C}$ , one has*

$$\Delta(s) = 0 \implies \Re(s) = s_0. \quad (3.24)$$

3. *If (3.23) is satisfied and  $s_0 < 0$ , then the trivial solution of (3.20) is asymptotically stable. In addition, if the history function  $\phi = {}^T(\varphi \ \varphi')$  is chosen in order for its spectral projection with respect to the generalized  $s_0$ -eigenspace to vanish identically*

$$P_{s_0}\phi = 0, \quad (3.25)$$

*then, the large-time behaviour of the trivial solution of (3.20) is*

$$\lim_{t \rightarrow \infty} e^{-s_0 t} x(t) = 0. \quad (3.26)$$

**Remark 3.4.1** *Note that item 3 of the theorem is obtained as a corollary of the MID property, unlike (1.35) in Frasson [112] where dominancy is assumed.*

**Remark 3.4.2** *Note that it suffices to let  $y(t) = x'(t)$  in (3.20), and set  $X_t = (x(t) \ y(t))^T$  and  $\phi = (\varphi \ \varphi')^T$  to reframe our problem as above:*

$$X'(t) - BX'(t - \tau) = -A_0X(t) + A_1X(t - \tau), \quad (3.27)$$

*where*

$$B = \begin{pmatrix} 0 & 0 \\ 0 & \alpha_2 \end{pmatrix}, A_0 = \begin{pmatrix} 0 & 1 \\ a_0 & a_1 \end{pmatrix}, A_1 = \begin{pmatrix} 0 & 0 \\ \alpha_0 & \alpha_1 \end{pmatrix}. \quad (3.28)$$

More precisely, as we are dealing with one discrete delay  $\tau > 0$  in our case, one has

$$\mu(\theta) = \begin{cases} -B, & \theta \leq -\tau, \\ 0, & \theta > \tau, \end{cases} \quad (3.29)$$

$$\eta(\theta) = \begin{cases} -A_1, & \theta \leq -\tau, \\ 0, & -\tau < \theta < 0, \\ -A_0, & \theta \geq 0, \end{cases} \quad (3.30)$$

with  $\mu, \eta \in NBV([- \tau, 0], \mathbb{C}^{n \times n})$ ; see [1].

### 3.5 . Proof of the main results

The proof of Theorem 3.4.1 is presented in the sequel; it follows the methodology already described in detail and applied to the toy model (3.1); see also Algorithm 2.

#### Forcing multiplicity and normalization of the characteristic function

This section covers Step 1 and 2 of the methodology.

The following lemma gives a normalization of the quasipolynomial function  $\Delta$  admitting a real root of multiplicity 5, which corresponds to conditions (3.23).

**Lemma 3.5.1** *Let  $s_0 \in \mathbb{R}$ , and consider the quasipolynomial  $\tilde{\Delta} : \mathbb{C} \rightarrow \mathbb{C}$  obtained from  $\Delta$  by the following change of variables*

$$\tilde{\Delta}(z) = \tau^2 \Delta\left(\frac{z}{\tau} + s_0\right), \quad z \in \mathbb{C}. \quad (3.31)$$

Then

$$\tilde{\Delta}(z) = z^2 + M_1 z + M_0 + (N_2 z^2 + N_1 z + N_0) e^{-z}, \quad (3.32)$$

where

$$\begin{cases} M_1 = \tau(2s_0 + a_1), & M_0 = \tau^2(s_0^2 + a_1 s_0 + a_0), \\ N_2 = \alpha_2 e^{-\tau s_0}, & N_1 = \tau(2\alpha_2 s_0 + \alpha_1) e^{-\tau s_0}, \\ N_0 = \tau^2(\alpha_2 s_0^2 + \alpha_1 s_0 + \alpha_0) e^{-\tau s_0}. \end{cases} \quad (3.33)$$

**Remark 3.5.1** *Since the expressions of  $a_0, a_1, \alpha_0, \alpha_1$  and  $\alpha_2$  in (3.23) are singular with respect to  $\tau$  as  $\tau \rightarrow 0$ , should one be interested in studying the behavior of the roots of  $\Delta$  as  $\tau \rightarrow 0$  when (3.23) is satisfied, the quasipolynomial  $\tau^2 \Delta$  may be considered instead as it exhibits the same roots as  $\Delta$ , albeit with regular coefficients.*

Before proceeding with the proof of the above theorem, it is convenient to normalize the setting using the affine change of variable  $z = \tau(s - s_0)$ . Consequently, the desired multiple root and the delay reduce to

$$s_0 = 0 \quad \text{and} \quad \tau = 1. \quad (3.34)$$

**Remark 3.5.2** *Note that under (3.34), relations (3.23) reduce to  $a_0 = 12$ ,  $a_1 = -6$ ,  $\alpha_0 = -12$ ,  $\alpha_1 = -6$ ,  $\alpha_2 = -1$ , so that the quasipolynomial (3.22) reduces to (3.35).*

Consider the following quasipolynomial function

$$\hat{\Delta}(z) = z^2 - 6z + 12 - (z^2 + 6z + 12)e^{-z}. \quad (3.35)$$

Following [56, Lemma 9], one obtains the following identity whose proof is straightforward.

**Lemma 3.5.2** *Let  $\hat{\Delta}$  be given by (3.35). Then, one has*

$$\hat{\Delta}(-z) = -e^z \hat{\Delta}(z), \quad z \in \mathbb{C}. \quad (3.36)$$

An immediate consequence of the above identity is the following symmetry property for the roots of  $\hat{\Delta}$ .

**Corollary 3.5.1** *Let  $\hat{\Delta}$  be given by (3.35) and assume that it has a root  $z_0 \in \mathbb{C}$ . Then the following equalities hold*

$$\hat{\Delta}(z_0) = \hat{\Delta}(-z_0) = \hat{\Delta}(\bar{z}_0) = \hat{\Delta}(-\bar{z}_0) = 0. \quad (3.37)$$

Consider  $\tilde{\Delta}$ , the normalized quasipolynomial, it follows immediately from relation (3.35) that  $s_0$  is a root of multiplicity 5 of  $\Delta$  if, and only if, 0 is a root of multiplicity 5 of  $\tilde{\Delta}$ . As a matter of fact, since  $\tilde{\Delta}$  is a quasipolynomial of degree  $\deg_s(\tilde{\Delta}) = 5$ , zero is a root of multiplicity 5 of  $\tilde{\Delta}$  if, and only if,

$$\tilde{\Delta}(0) = \tilde{\Delta}'(0) = \tilde{\Delta}^{(2)}(0) = \tilde{\Delta}^{(3)}(0) = \tilde{\Delta}^{(4)}(0) = 0.$$

The latter identities yield the following Cramer system

$$\begin{cases} M_0 + N_0 = 0, \\ M_1 + N_1 - N_0 = 0, \\ 2 + 2N_2 - 2N_1 + N_0 = 0, \\ -6N_2 + 3N_1 - N_0 = 0, \\ 12N_2 - 4N_1 + N_0 = 0, \end{cases} \quad (3.38)$$

whose unique solution is  $(M_0, M_1, N_0, N_1, N_2) = (12, -6, -12, -6, -1)$  as required by (3.35), thereby ending the proof of the first item of the theorem. Moreover, note that, under (3.34), one has  $\hat{\Delta} = \tilde{\Delta}$ .

## Factorization of the normalized characteristic function

This section covers Step 3 of the methodology.

The quasipolynomial  $\tilde{\Delta}$  defined in (3.35) can be factorized as

$$\hat{\Delta}(z) = \frac{1}{2}z^5 \int_0^1 q(t)e^{-zt} dt, \quad (3.39)$$

where

$$q(t) = t^2(t-1)^2. \quad (3.40)$$

In our approach, the sign constancy of the polynomial  $q$  defined previously in (3.40) for  $t \in (0, 1)$  is necessary, which is satisfied in this case for  $t \in (0, 1)$ .

## Frequency bound

This section covers Step 4 of the methodology.

We present now the main technical ingredient for the analysis of the frequency bound, which achieves Step 4 of the methodology.

**Lemma 3.5.3** *Let  $\hat{\Delta}$  be given by (3.35) and assume that it has a root  $z_0 \in \mathbb{R}^* + i\mathbb{R}$ . Then,*

$$0 < \Im(z_0) < \pi. \quad (3.41)$$

For ease of reading, the proof of the technical lemma 3.5.3 is presented in the Appendix A.

## Conclusion of the proof of Theorem 3.4.1

This section corresponds to Step 5 of the methodology.

To complete the proof (proof of item 2), it suffices to show that every root of  $\hat{\Delta}$  lies on the imaginary axis. To do so, assume that there exists a root  $z_0 \in \mathbb{C}$  of  $\hat{\Delta}$  satisfying  $\Re(z_0) \neq 0$  and set to obtain a contradiction. Writing  $z_0 = \sigma + i\omega$  for  $\sigma, \omega \in \mathbb{R}$  with  $\sigma \neq 0$ , one may assume, thanks to Corollary 3.5.1 below, that  $\sigma > 0$  and  $\omega > 0$ . Next, using the fact that  $z_0$  is a non-zero root of  $\hat{\Delta}$ , one infers from (3.39), by taking the imaginary part, the identity below

$$\int_0^1 t^2(t-1)^2 e^{-\sigma t} \sin(\omega t) dt = 0. \quad (3.42)$$

Since  $0 < \omega \leq \pi$  by Lemma 3.5.3, the function

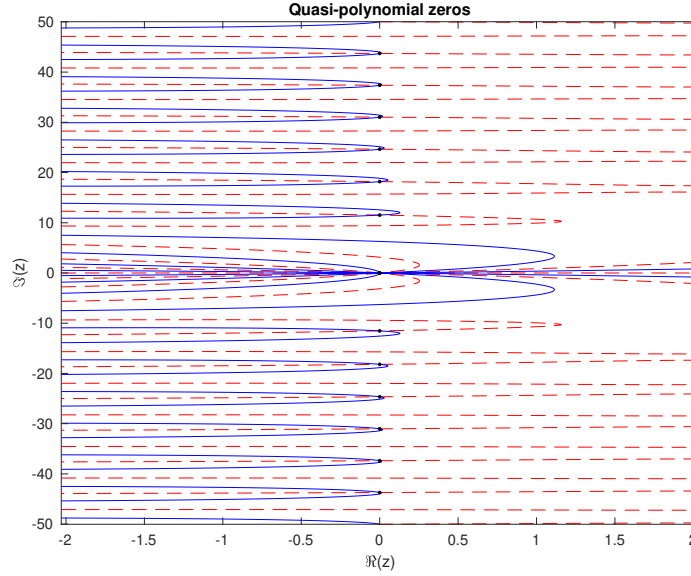


Figure 3.2: Spectrum distribution of the quasipolynomial  $\hat{\Delta}$  in (3.35).

$$t \mapsto t^2(t-1)^2 e^{-\sigma t} \sin(\omega t), \quad (3.43)$$

is strictly positive in  $(0, 1)$ , which contradicts the above equality as required to end the proof.

The third item of the main result is a direct consequence of item two and (1.35); see [112]. ■

The following result gives a description of the spectrum of  $\Delta$ .

**Theorem 3.5.1** *Let  $\Delta$  be given by (3.35). Let*

$$\mathcal{H} = \left\{ \xi \in \mathbb{R} : \tan \xi = \frac{3\xi}{3 - \xi^2} \right\}.$$

*If the relations (3.23) are satisfied, then, the set of the roots of characteristic equation (3.22) is given by*

$$\mathcal{S} = \left\{ s_0 + 2i \frac{\xi}{\tau}, \xi \in \mathcal{H} \right\}. \quad (3.44)$$

In order to prove the previous result, one needs the following lemma for which the detailed prove is presented in the Appendix.

**Lemma 3.5.4** *Let  $\Delta$  be given by (3.35) and*

$$\mathcal{H} = \left\{ \xi \in \mathbb{R} : \tan \xi = \frac{3\xi}{3 - \xi^2} \right\}$$

*Let  $\rho \in \mathbb{R}$ , then,  $i\rho$  is a root of  $\hat{\Delta}$  if and only if  $\frac{\rho}{2} \in \mathcal{H}$ .*

**Proof**[Proof of Theorem 3.5.1] Under the parameter's conditions (3.35), the roots of  $\Delta$  are defined by  $\frac{z}{\tau} + s_0$  with  $z$  us root of  $\hat{\Delta}$ . Let  $z = i\xi$ , such that  $\Delta(i\xi) = 0$  then by Lemma 3.5.4 ,  $\frac{\xi}{2} \in \mathcal{H}$ , in other words, the zeros of  $\Delta$  are

$$\left\{s_0 + \frac{z}{2} = s_0 + \frac{i\xi}{\tau}, \frac{\xi}{2} \in \mathcal{H}\right\},$$

i.e. the zeros of  $\Delta$  are given by the set

$$\left\{s_0 + \frac{2\xi i}{\tau}, \xi \in \mathcal{H}\right\}.$$

**Remark 3.5.3** The set  $\mathcal{H}$  of the real roots of the equation  $\tan(\xi) = \frac{3\xi}{3-\xi^2}$  is infinite discrete and can be as:

$$\mathcal{H} = \{\xi_k, k \in \mathbb{Z}\}$$

where  $\xi_k$  is a decreasing sequence of roots of the equation

$$\tan(\xi) = \frac{3\xi}{3-\xi^2}$$

with  $\xi_0 = 0$ . In particular,

$$\xi_k \in \left(-\frac{\pi}{2} + k\pi, (k+1)\pi + \frac{\pi}{2}\right)$$

### 3.6 . Illustrative example: exponential stabilization of an oscillator using delay action

Consider the classical oscillator control problem:

$$\ddot{x}(t) + 2\xi\omega\dot{x}(t) + \omega^2x(t) = u(t), \quad (3.45)$$

with  $u$  as the delayed output-feedback as proposed in [137]:

$$u(t) = \alpha_2\ddot{x}(t-\tau) + \alpha_1\dot{x}(t-\tau) + \alpha_0x(t-\tau), \quad (3.46)$$

$\omega$  is the frequency of the arising vibrations and  $\xi$  is the damping factor.

We proceed as in Remark 3.4.2 to reframe the problem as (3.27) with

$$B = \begin{pmatrix} 0 & 0 \\ 0 & \alpha_2 \end{pmatrix}, A_0 = \begin{pmatrix} 0 & 1 \\ \omega^2 & 2\xi\omega \end{pmatrix}, A_1 = \begin{pmatrix} 0 & 0 \\ \alpha_0 & \alpha_1 \end{pmatrix}. \quad (3.47)$$

The associated characteristic matrix reads as

$$\begin{aligned} \mathbb{M}(s) &= sI + se^{-\tau s}B - C - Ee^{-\tau s} \\ &= \begin{pmatrix} s & -1 \\ \omega^2 - \alpha_0e^{-\tau s} & s - \alpha_2se^{-\tau s} + \omega\xi - \alpha_1e^{-\tau s} \end{pmatrix}, \end{aligned} \quad (3.48)$$

so that the characteristic quasipolynomial function is

$$\Delta(s) = (-\alpha_2 s^2 - \alpha_1 s - \alpha_0) e^{-\tau s} + s^2 + 2\xi \omega s + \omega^2. \quad (3.49)$$

Following Theorem 3.4.1, we use the MID stabilizing property by forcing the multiplicity 5 of the real spectral value at:

$$s_0 = (\sigma \xi^2 - \sigma - \xi) \omega, \quad (3.50)$$

where

$$\sigma(\xi) = \sqrt{-3(\xi^2 - 1)^{-1}}, \quad (3.51)$$

and setting the delay to  $\tau = \frac{\sigma}{\omega}$ . one computes the appropriate gains:

$$\begin{cases} \alpha_0 &= -\omega^2 (4\xi^3 \sigma - 4\xi \sigma + 12\xi^2 - 13) e^{-(\xi \sigma + 3)}, \\ \alpha_1 &= -2\omega \left( 2\sqrt{-3(\xi^2 - 1)^{-1}} \sigma \xi^2 - 2\sigma - \xi \right) e^{-(\xi \sigma + 3)}, \\ \alpha_2 &= e^{-(\xi \sigma + 3)}. \end{cases} \quad (3.52)$$

Hence, we compute the spectral projection onto the generalized eigenspace  $\mathcal{M}_{s_0}$  explicitly by the Dumford integral (1.34), following [100, Section 3.2].

$$P_{s_0} \phi = \text{Res}_{s=s_0} \{ e^s \Delta^{-1}(s) \mathcal{K}(s_0) \phi \}, \quad (3.53)$$

where  $\phi = {}^T(\varphi \ \varphi') \in \mathcal{C}([-\tau, 0], \mathbb{C}^2)$  is the history function, *Res* is the residue and

$$\mathcal{K}(s_0) \phi = D\phi + \int_{-\tau}^0 [s_0 d\mu(\theta) + d\eta(\theta)] \int_0^{-\theta} e^{-sz} \phi(z + \theta) dz. \quad (3.54)$$

To illustrate the large-time behavior of the trivial solution  $x(t)$  of (3.20), we consider  $\xi = \frac{1}{2}$ ,  $\omega = 1$  and the history function

$$\begin{aligned} \varphi(\theta) &= 0.4392434197 \theta^8 + \theta^7 - 3.648426084 \theta^3 - 3.338574638 \theta^2 \\ &\quad - 0.4144356357 \theta + 0.05592390768, \end{aligned} \quad (3.55)$$

which satisfies  $P_{s_0} \phi = 0$  as in Theorem 3.4.1.3.

### 3.7 . Chapter Summary

By this chapter we extended the Multiplicity-Induced-Dominancy (MID) property to the generic (all parameters are free) second-order neutral delay equation enabling a stabilizing delayed-feedback design. The proposed design strategy has been employed to exponentially stabilize an oscillator.

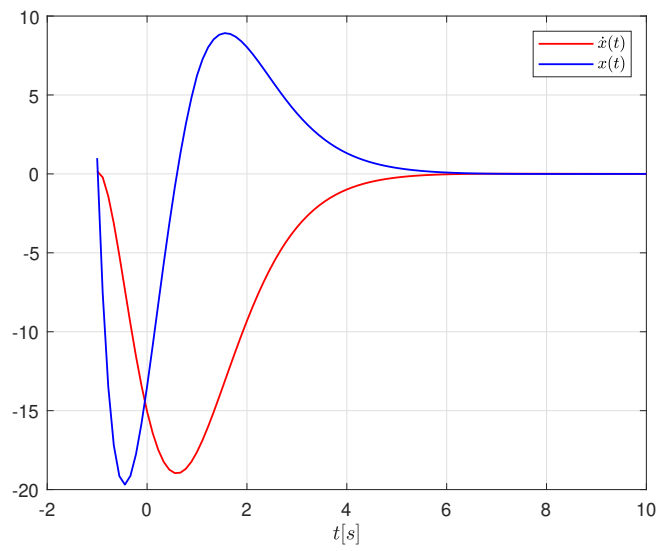


Figure 3.3: Response of the oscillator (3.45) subjected to the stabilizing MID property, with  $\xi = \frac{1}{2}$ ,  $\omega = 1$ .





## 4 - The IMID property for second order neutral equation

This chapter is an extended version of the paper [91]. It also contains a portion of the paper [94].

### 4.1 . Introduction

In this chapter we address the exponential stability of linear time-delay systems of neutral type. In general, it is quite a challenge to establish conditions on the parameters of the system in order to guarantee such a stability. It turns out that, for the characteristic equations corresponding to delay systems, the real roots of maximal multiplicity are necessarily dominant. This property is known as Generic Multiplicity-Induced-Dominancy (GMID for short) and consists in conditions under which a given real root of maximal multiplicity is necessarily dominant. However, multiple roots with intermediate admissible multiplicities may be dominant or not. As for the case of a root of strictly intermediate multiplicity, one must look for conditions on the free parameters of the system for which the former is dominant, this property is called Intermediate Multiplicity-Induced-Dominancy (IMID).

The aim of this chapter is to explore the effect of multiple roots with admissible multiplicities exhibiting, under appropriate conditions, the validity of the MID property for second-order neutral time-delay differential equations with a single delay which is a question of interest from an application viewpoint; see [85], [86]. The ensuing control methodology is summarized in a five-steps algorithm that can be exploited in the design of higher-order systems. The main ingredient of the proposed method is the dominancy proof for multiple spectral values based on frequency bounds established via integral equations. As an illustration, the stabilization of the classical oscillator benefits from the obtained results.

The sequel of the chapter is organized as follows. Section 4.2 states a design methodology exploiting the MID property, the classical steps leading to the proof are recalled through a comprehensive example, the first-order neutral equation with a single delay (IMID: codimension 2). Section 4.3 is dedicated to the problem setting. The main result is presented in Section 4.4, where a classification of admissible multiplicities for second-order neutral time-delay differential equation with a single delay is provided. Section 4.5 is dedicated to the proof of the main result. Section 4.6 is dedicated to the illustration of the obtained results on the stabilization of the classical oscillator. Finally, further remarks on the MID property (case of multiplicity 2) are given in Section 4.7.

## 4.2 . MID methodology on a toy model: Codimension 2

Let's go back to the example considered in Section 3.2 of Chapter 3. Let us recall the corresponding characteristic quasi-polynomial in (3.3):

$$\Delta(s) = s + a_0 + (\alpha_1 s + \alpha_0) e^{-\tau s}. \quad (4.1)$$

In the following, we illustrate the MID proof in the case of codimension 2.

- MID : **codimension 2:**

1. (**Forcing multiplicity**) The real  $s_0$  is a root of multiplicity 2 of  $\Delta$  if, and only if, the coefficients  $\alpha_0, \alpha_1$ , the root  $s_0$  and the delay  $\tau$  satisfy the relations below

$$\begin{cases} \alpha_0 = (\tau a_0 s_0 + \tau s_0^2 - a_0) e^{\tau s_0}, \\ \alpha_1 = (-\tau a_0 - \tau s_0 - 1) e^{\tau s_0}. \end{cases} \quad (4.2)$$

2. (**Normalization**) The normalized characteristic equation is given by

$$\tilde{\Delta}(z) = ((-\rho - 1)z - \rho) e^{-z} + z + \rho, \quad (4.3)$$

where  $\rho = \tau (s_0 + a_0)$ .

3. (**Integral representation**) The quasipolynomial  $\tilde{\Delta}$  defined in (4.3) can be factorized as

$$\tilde{\Delta}(z) = z^2 \int_0^1 q_\rho(t) e^{-tz} dt, \quad (4.4)$$

where

$$q_\rho(t) = \rho t + 1. \quad (4.5)$$

In our approach, the sign constancy of the polynomial  $q_\rho$  for  $t \in (0, 1)$  is necessary. Therefore, the following lemma gives regions in the parameter space guaranteeing the sign constancy of  $q_\rho$  for  $t \in (0, 1)$ .

**Lemma 4.2.1** *Let  $q_\rho$  be the polynomial with respect to  $t$  defined in (4.109). Then,  $q_\rho$  has a constant sign for  $t \in (0, 1)$  if, and only if,*

$$\rho \in [-1, +\infty[. \quad (4.6)$$

**Proof** The polynomial  $q_\rho$  admits one root given by  $t_0 = -\frac{1}{\rho}$ . Two cases are to be considered

- (a) If  $\rho = 0$ : in this case,  $q_\rho(t) = 1$ . As a result,  $q_\rho$  has no roots in  $(0, 1)$  which guarantees its sign constancy.

(b) If  $\rho \neq 0$ : in this case, sub-cases are to be considered with respect to the sign of  $\rho$ .

- i. If  $\rho > 0$ : in this case,  $t_0 < 0$ . Then,  $q_\rho$  has no roots in  $(0, 1)$ .
- ii. If  $\rho < 0$ : in this case,  $t_0 > 0$ . In this case, we need to look for conditions guaranteeing that  $t_0 \geq 1$ .

$$t_0 \geq 1 \iff -\frac{1}{\rho} \geq 1 \iff \rho \geq -1, \quad (4.7)$$

As a conclusion, if  $\rho < 0$ , the polynomial  $q_\rho$  has no roots for  $t \in (0, 1)$  if and only if  $\rho \in [-1, 0[$ .

The announced result is then proved. ■

#### 4. (Frequency bound)

In the following, let  $z_0 = x_0 + i\omega_0 \in \mathbb{R}_+ + i\mathbb{R}_+$  be a root of

$$\tilde{\Delta}(z) = P_0(z) + P_1(z) e^{-z}, \quad (4.8)$$

as defined in (4.3), where

$$P_0(z) = z + \rho, \quad (4.9)$$

$$P_1(z) = (-\rho - 1)z - \rho. \quad (4.10)$$

and  $z_0$  satisfy the following equality

$$|P_0(x_0 + i\omega_0)|^2 e^{2x_0} = |P_1(x_0 + i\omega_0)|^2. \quad (4.11)$$

Since  $e^{2x} > 1 + 2x$  for any  $x \in \mathbb{R}_+$  for truncation order 2 (see Algorithm 2), function

$$F_\rho(x, \omega) = |P_1(x + i\omega)|^2 - |P_0(x + i\omega)|^2 (1 + 2x), \quad (4.12)$$

satisfies  $F_\rho(x_0, \omega_0) > 0$ . Moreover, the zeros of  $F_\rho$  can be characterized by the following quadratic polynomial of degree 2 in  $\omega$

$$G_\rho(x, \omega) = a_\rho(x) \omega^2 + c_\rho(x), \quad (4.13)$$

where

$$a_\rho = -2x + 2\rho + \rho^2, \quad (4.14)$$

$$c_\rho = -2x^3 + (\rho^2 - 2\rho)x^2. \quad (4.15)$$

In order to guarantee the positivity of  $G_\rho$ , one has to investigate conditions on the signs of  $a_\rho$  as well as the discriminant of  $G_\rho$  denoted in the sequel  $\tilde{D}_\rho(x) = x^2 D_\rho(x)$  where

$$D_\rho(x) = -16x^2 + 16\rho^2x - 4(\rho^2 + 2\rho)(\rho^2 - 2\rho), \quad (4.16)$$

As a matter of fact, let  $\omega_1$  and  $\omega_2$  be the two real solutions of  $G_\rho(x, \omega) = 0$ , then  $G_\rho$  is positive if, and only if,

- $D_\rho < 0$  and  $a_\rho > 0$ , or
- $D_\rho > 0$  and  $a_\rho > 0$  and  $\omega \in \mathbb{R} - (\omega_1, \omega_2)$ , or
- $D_\rho > 0$  and  $a_\rho < 0$  and  $\omega \in (\omega_1, \omega_2)$ .

Note that in the first and second cases,  $G_\rho$  is unbounded which is not of interest in our method. Hence, we only keep the third set of conditions.

Since the coefficient in front of  $x$  in the expression of  $a_\rho$  is negative and independent of  $\rho$ , then  $a_\rho$  is negative for  $x \in \left(\frac{\rho(\rho+2)}{2}, +\infty\right)$ . The next lemma provides a characterization of regions in the parameter space guaranteeing the positivity of  $D_\rho$ .

**Lemma 4.2.2** *Let  $x^\pm = \frac{\rho^2}{2} \pm \rho$ , and  $D_\rho$  be the parametric polynomial defined in (4.16). Then,  $D_\rho$  is positive*

- for  $x \in (x^+, x^-)$ , if  $\rho \in [-1, 0)$ ,
- for  $x \in (x^-, x^+)$ , if  $\rho \in [0, +\infty)$ .

**Proof** To investigate the sign of  $D_\rho$ , we first notice that its leading coefficient is negative and independent from  $\rho$ . Next, consider  $D_\rho$ , as a polynomial in  $x$  of degree 2, we analyse its discriminant given by  $1024\rho^2$  and notice that is positive for any value of  $\rho$ . One concludes the announced result.

In the sequel we are interested in the parameter region guaranteeing the sign constancy of  $q_\rho$ , the positivity of  $D_\rho$  as well as the negativity of  $a_\rho$ , which corresponds to the candidate regions  $\rho \in [-1, +\infty)$ , for  $x \in (x^+, x^-)$ .

After having characterized the candidate regions, we present the main technical ingredient for the analysis of the frequency bound.

**Lemma 4.2.3** *Let  $\tilde{\Delta} = \tilde{\Delta}_\rho$  be the quasipolynomial given in (4.3). Consider  $\rho \in [-1, \vartheta]$ , with  $\vartheta$  is a positive number satisfies  $\vartheta \leq \frac{5}{2}$ . If  $\tilde{\Delta}$  has a root  $z_0 \in \mathbb{R}_+ + i\mathbb{R}_+$ , then*

$$0 < \Im(z_0) < \pi. \quad (4.17)$$

In addition, the root  $z_0$  may be properly assigned.

**Proof** We consider two cases

- If  $\rho \in [-1, 0]$ . Since the discriminant of the polynomial function  $G_\rho$  defined in (4.13) is positive, then  $G_\rho$  admits the following two real roots

$$\omega_\rho^\pm(x) = \mp \frac{\sqrt{-(\rho^2 + 2\rho - 2x)(\rho^2 - 2\rho - 2x)}x}{\rho^2 + 2\rho - 2x}, \quad (4.18)$$

where  $\omega_\rho^+$  denotes the greater solution (positive signal). Since  $\rho \in [-1, 0]$  and  $x > 0$ , the solution  $\omega_\rho^+$  is upper bounded with respect to  $\rho$  by the parameter-free expression

$$\omega^+(x) = \frac{x\sqrt{-4x^2 + 3}}{1 + 2x}, \quad (4.19)$$

which reaches a maximum value at  $x^* = \frac{\sqrt{3}}{2}$ . Thus,

$$\omega = \omega_\rho^+(x) \leq \omega^+(x^*) \approx 0.5899 < \pi. \quad (4.20)$$

- If  $\rho \in [0, +\infty)$ . Consider  $\rho \in [0, \vartheta]$ , with  $\vartheta > 0$  and follow the same procedure as with the previous region. The table below

$\vartheta$	1	2	2.5	3	3.5	4	10	100
$\omega^+$	1	2	3.125	4.5	6.125	8	50	5000

emphasizes the fact that an interesting frequency bound may be found only for a positive  $\vartheta$  satisfying  $\vartheta \leq \frac{5}{2}$ ; (see Figure 4.1) .

Let  $\rho \in [0, \frac{5}{2}]$ . In this case, the solution  $\omega_\rho^+$  is upper bounded with respect to  $\rho$  by the parameter-free expression

$$\omega^+(x) = \frac{1}{2}\sqrt{-4x^2 + 25x}, \quad (4.21)$$

which reaches a maximum value at  $x^* = 3.125$ . Thus,

$$\omega = \omega_\rho^+(x) \leq \omega^+(x^*) \approx 3.125 < \pi. \quad (4.22)$$

Unfortunately for  $\rho \in (\frac{5}{2}, +\infty)$ , the dominance of  $s_0$  cannot be concluded unless the order of truncation of the exponential term is increased as in Algorithm 2 in order to obtain an adequate frequency bound. ■

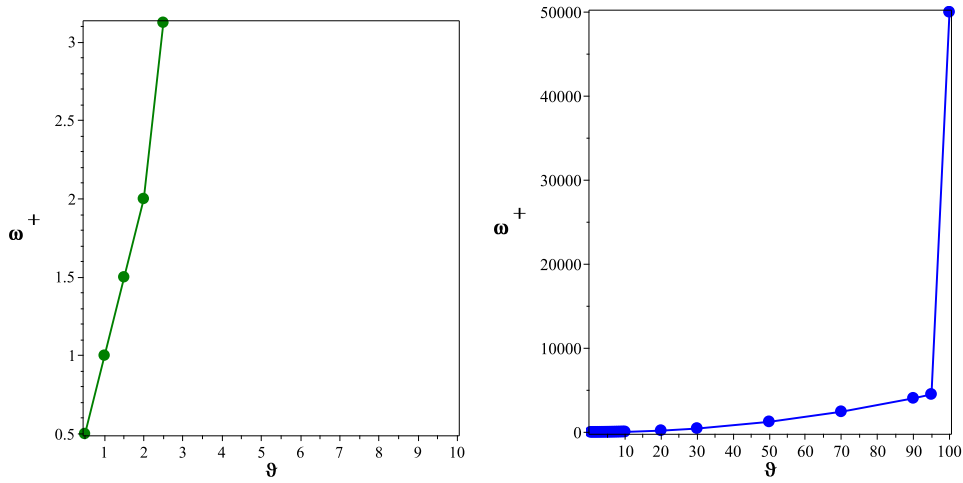


Figure 4.1: Plot emphasizes the fact that an interesting frequency bound ( $0 < \omega < \pi$ ) may be found only for a positive  $\vartheta$  satisfying  $\vartheta \leq \frac{5}{2}$ .

5. **(Dominancy)** By a contradiction argument, assume that there exists  $z_0 \in \mathbb{R}_+ + i\mathbb{R}_+$  root of  $\tilde{\Delta}$ . Then, the integral representation yields

$$\int_0^1 (\rho t + 1) e^{-tz_0} dt = 0, \quad (4.23)$$

the imaginary part of which is  $\int_0^1 t (\rho t + 1) e^{-tx} \sin(\omega t) dt = 0$ . Now, the frequency bound  $0 < \omega \leq \pi$  of the previous step entails that the function

$$t \mapsto t (\rho t + 1) e^{-xt} \sin(\omega t), \quad (4.24)$$

is strictly positive in  $(0, 1)$ , thereby contradicting the last equality.

To conclude, if relations (4.2) are satisfied and  $a_0$  satisfies the lower bound  $a_0 \geq \frac{\vartheta}{\tau}$  for a positive  $\vartheta$  satisfying  $\vartheta \leq 2.5$ , then the exponential decay  $s_0$  chosen such that

$$-a_0 - \frac{1}{\tau} \leq s_0 \leq -a_0 + \frac{\vartheta}{\tau}, \quad (4.25)$$

is necessarily negative and dominant.

### 4.3 . Problem setting

It is commonly accepted that second order linear systems capture the dynamic behavior of many natural phenomena and have found numerous applications in a variety of fields, such as vibration and structural analysis. Stabilization of solutions

to such a reduced order model represents a standard test bench to approve of new paradigms and methodologies in control design; see for instance [50].

We address the effect of the delay action on the behavior of solutions corresponding to such second-order dynamical systems. Namely, we investigate the functional differential equation in (1.4) with  $n = 2$ , which extends the study in [50]:

$$\ddot{x}(t) + a_1 \dot{x}(t) + a_0 x(t) + \alpha_2 \ddot{x}(t - \tau) + \alpha_1 \dot{x}(t - \tau) + \alpha_0 x(t - \tau) = 0, \quad (4.26)$$

where the unknown function  $x$  is real-valued,  $a_0, a_1, \alpha_0, \alpha_1, \alpha_2 \in \mathbb{R}$ ,  $\alpha_2 \neq 0$ , and the delay  $\tau > 0$ . Since the derivative of highest order appears in both, the delayed term  $\ddot{x}(t - \tau)$  and the non-delayed term  $\ddot{x}(t)$ , equation (4.26) is a delay differential equation of *neutral* type.

Time-delay systems of neutral type, which may have an infinite number of unstable poles, are more difficult to tackle than delay systems of *retarded* type (i.e. the highest order of derivation is only on the non-delayed function  $\dot{x}(t)$ ) which exhibit only a finite number of poles in any right half-plane, see for instance [50].

The characteristic function of equation (4.26) is the quasipolynomial function  $\Delta : \mathbb{C} \rightarrow \mathbb{C}$  defined for  $s \in \mathbb{C}$  by

$$\Delta(s) = s^2 + a_1 s + a_0 + (\alpha_2 s^2 + \alpha_1 s + \alpha_0) e^{-\tau s}. \quad (4.27)$$

#### 4.4 . Statement of the main result

The main result presents a classification of admissible multiplicities for a given root of the quasipolynomial (4.27).

**Theorem 4.4.1** *Consider the quasipolynomial function  $\Delta$  defined in (4.27).*

1. *GMID : spectral value of maximal admissible multiplicity*

(a) *The real  $s_0$  is a root of multiplicity 5 of  $\Delta$  if, and only if, the coefficients  $a_0, a_1, \alpha_0, \alpha_1, \alpha_2$ , the root  $s_0$  and the delay  $\tau$  satisfy the following relations*

$$\begin{cases} a_1 = -2s_0 - \frac{6}{\tau}, \\ a_0 = s_0^2 + \frac{6}{\tau} s_0 + \frac{12}{\tau^2}, \\ \alpha_2 = -e^{\tau s_0}, \\ \alpha_1 = \left(2s_0 - \frac{6}{\tau}\right) e^{\tau s_0}, \\ \alpha_0 = -\left(s_0^2 - \frac{6}{\tau} s_0 + \frac{12}{\tau^2}\right) e^{\tau s_0}. \end{cases} \quad (4.28)$$



(b) If relations (4.28) are satisfied then  $s_0$  is necessarily a dominant root of  $\Delta$ .

## 2. IMID : codimension 4

(a) Consider the following discriminant:

$$d = a_1^2 - 4a_0, \quad (4.29)$$

which corresponds to the discriminant of the finite dimensional part of the dynamical system defined by  $\Delta$ . The quasipolynomial function (4.27) admits a real root at

$$s_{\pm} = \frac{1}{\tau} \left( -\frac{a_1\tau}{2} - 3 \pm \frac{1}{2} \sqrt{\tau^2 d + 12} \right), \quad (4.30)$$

of multiplicity 4 if, and only if, the coefficients  $\alpha_0$ ,  $\alpha_1$  and  $\alpha_2$  satisfy the following relations

$$\begin{cases} \alpha_0 = \left( \left( \frac{a_1^2\tau}{2} - \tau a_0 + 6a_1 + \frac{42}{\tau} \right) s_{\pm} \right. \\ \quad \left. + \frac{\tau a_0 a_1}{2} + \frac{3a_1^2}{2} + 8a_0 + \frac{30a_1}{\tau} + \frac{54}{\tau^2} \right) e^{\tau s_{\pm}}, \\ \alpha_1 = \left( (a_1\tau + 12) s_{\pm} + 2\tau a_0 + 8a_1 + \frac{18}{\tau} \right) e^{\tau s_{\pm}}, \\ \alpha_2 = \left( 2 + \tau \left( s_{\pm} + \frac{a_1}{2} \right) \right) e^{\tau s_{\pm}}. \end{cases} \quad (4.31)$$

(b) If the relations above are satisfied, and  $a_1$ ,  $a_0$  satisfy the lower bounds  $a_0 \geq -\frac{6}{\tau^2}$  and  $a_1 \geq -\frac{6}{\tau}$ , then  $s_+$  is a dominant root of  $\Delta$ .

## 3. IMID : codimension 3

(a) The real number  $s_0$  is a root of multiplicity 3 of  $\Delta$  if, and only if, the following relations hold

$$\begin{cases} \alpha_0 = -\frac{1}{2} (\tau^2 a_1 s_0^3 + \tau^2 s_0^4 + \tau^2 a_0 s_0^2 + 2\tau s_0^3 - 2\tau a_0 s_0 + 2a_0) e^{\tau s_0}, \\ \alpha_1 = (\tau^2 a_1 s_0^2 + \tau^2 s_0^3 + \tau^2 a_0 s_0 + \tau a_1 s_0 + 3\tau s_0^2 - \tau a_0 - a_1) e^{\tau s_0}, \\ \alpha_2 = -\frac{1}{2} (\tau^2 a_1 s_0 + \tau^2 s_0^2 + a_0 \tau^2 + 2a_1 \tau + 4\tau s_0 + 2) e^{\tau s_0}. \end{cases} \quad (4.32)$$

(b) If the relations above hold and  $a_1$ ,  $a_0$  satisfy the lower bounds  $a_0 \geq \frac{\varepsilon}{4\tau^2}$  and  $a_1 \geq 0$ , where  $\varepsilon = (-10\sqrt{2} - 16)\sqrt{16\sqrt{2} - 22} + 16\sqrt{2} + 20$ , then the real root  $s_0$  chosen as follows

$$\begin{cases} s_0 \in \left( -\frac{a_1}{2} - \frac{\sqrt{d + \frac{\varepsilon}{\tau^2}}}{2}, -\frac{a_1}{2} + \frac{\sqrt{d + \frac{\varepsilon}{\tau^2}}}{2} \right) & \text{if } d < 0, \\ s_0 \in \left( -\frac{a_1}{2} - \frac{\sqrt{d + \frac{\varepsilon}{\tau^2}}}{2}, -\frac{a_1}{2} - \frac{\sqrt{d}}{2} \right) \cup \left( -\frac{a_1}{2} + \frac{\sqrt{d}}{2}, -\frac{a_1}{2} + \frac{\sqrt{d + \frac{\varepsilon}{\tau^2}}}{2} \right) & \text{otherwise,} \end{cases} \quad (4.33)$$

is a dominant root of  $\Delta$ .

From a control theory viewpoint, if instantaneous access to the state variables is not available, one option is to consider delayed controllers. In our case, the aim is to stabilize solutions of the control system

$$\ddot{x}(t) + a_1 \dot{x}(t) + a_0 x(t) = u(t), \quad (4.34)$$

by using a delayed feedback controller

$$u(t) = -\alpha_2 \ddot{x}(t - \tau) - \alpha_1 \dot{x}(t - \tau) - \alpha_0 x(t - \tau). \quad (4.35)$$

Notice that, such an idea has already been proposed in [50] with controller  $u(t) = -\alpha_1 \dot{x}(t - \tau) - \alpha_0 x(t - \tau)$  by exploiting the MID property for retarded differential equation. The above result extends such an idea to neutral equations. Furthermore, Theorem 4.4.1 offers a certified tuning of the controller's parameters allowing to assign the closed-loop dominant spectral value based on the MID strategy with appropriate admissible multiplicity. This can be done by taking into account the discriminant of the open-loop characteristic function as discussed in [50], see also [77]. Such a control strategy is part of a more general framework called partial pole placement, see for instance [75].

**Remark 4.4.1** *On the one hand, maximal multiplicity may not be reached due to the sparsity of the involved polynomial in the characteristic equation. In that case, one has to characterize the MID property in the presence of a spectral value of multiplicity strictly smaller than the maximal one. On the other hand, lowering the multiplicity relaxes the constraints on the parameters that can be fixed from the considered model ( $a_0$  and  $a_1$  in the case of equation (4.26)).*

**Remark 4.4.2** *The general case of matrix neutral differential equations (in the case where the system's coefficients are matrices) is still an unsolved open problem to the extent of the authors' knowledge. As a matter of fact, in the general case, the quasipolynomials involved exhibit multiple commensurate delays (multiples of the original system's delay) which is no trivial additional involvement. As such, only very particular instances may be treated with our approach.*

**Remark 4.4.3** *In the presence of a small perturbation, we have to deal with the splitting phenomena. From a robustness viewpoint, thanks to the continuous dependency of the spectrum distribution on the parameters' variation, one is able to estimate the perturbation bound beyond which the dominancy of the split roots is lost, see for instance [8].*

**Remark 4.4.4** *It is shown analytically that with the MID scheme, a real dominant closed-loop pole can be assigned precisely, thus guaranteeing the exponential decay rate of the system response. While achieving such transient performance, the MID design is also shown to be capable of maintaining a certain level of stability robustness against an uncertain delay, see for instance [138].*

## 4.5 . Proof of the main result

Note that for ease of reading, proofs of the technical lemmas are presented in the Appendix A.

***Proof of item 1.*** The proof of item 1 (GMID) in Theorem 4.4.1 is detailed in chapter 3; see also [57]. The normalization of the characteristic function  $\Delta$  gives

$$\tilde{\Delta}(z) = z^2 - 6z + 12 - (z^2 + 6z + 12)e^{-z}. \quad (4.36)$$

Next, the integral factorization of  $\tilde{\Delta}$  is computed to be

$$\tilde{\Delta}(z) = \frac{z^5}{2} \int_0^1 t^2(t-1)^2 e^{-zt} dt. \quad (4.37)$$

The dominance proof is established by providing an adequate frequency bound ( $\omega_0 < \pi$ ), where the considered truncation is of order 3, to show that a non-zero root of  $\tilde{\Delta}$  with non-negative real part cannot exist.

***Proof of item 2.*** Item 2 is well presented in [78]. In a similar way, the normalization of the characteristic function  $\Delta$  provides

$$\tilde{\Delta}(z) = z^2 + (\rho - 6)z - 3\rho + 12 + \left[ \left( \frac{\rho}{2} - 1 \right) z^2 + (2\rho - 6)z + 3\rho - 12 \right] e^{-z}, \quad (4.38)$$

where

$$\rho = \sqrt{12 + (a_1^2 - 4a_0)\tau^2}. \quad (4.39)$$

The integral representation of the characteristic function is

$$\tilde{\Delta}(z) = z^4 \int_0^1 q_\rho(t) e^{-tz} dt. \quad (4.40)$$

where

$$q_\rho(t) = \frac{1}{2}(t(1-t)(t(\rho-4)+2)). \quad (4.41)$$

The dominance of  $s_+$  as a root of  $\Delta$  is equivalent to the dominance of  $z=0$  as a root of  $\tilde{\Delta}$ . Consider  $z_0 = x_0 + i\omega_0 \in \mathbb{R}_+ + i\mathbb{R}_+$  as a root of

$$\tilde{\Delta}(z) = \tilde{P}_0(z) + \tilde{P}_1(z)e^{-z}, \quad (4.42)$$

as defined in (4.38), with

$$\tilde{P}_0(z) = z^2 + (\rho-6)z - 3\rho + 12, \quad (4.43)$$

$$\tilde{P}_1(z) = \left(\frac{\rho}{2} - 1\right)z^2 + (2\rho-6)z + 3\rho - 12, \quad (4.44)$$

so that

$$|\tilde{P}_0(x_0 + i\omega_0)|^2 e^{2x_0} = |\tilde{P}_1(x_0 + i\omega_0)|^2. \quad (4.45)$$

Now, define the function

$$F_\rho(x, \omega) = |\tilde{P}_1(x + i\omega)|^2 - (1 + 2x)|\tilde{P}_0(x + i\omega)|^2, \quad (4.46)$$

where  $F_\rho > 0$  since  $e^{2x} > 1 + 2x$  for any  $x > 0$ ; the order of the considered truncation order in this case is equal to 1. The zeros of  $F_\rho$  can be characterized by the quadratic polynomial

$$G_\rho(x, \Omega) = a_\rho(x)\Omega^2 + b_\rho(x)\Omega + c_\rho(x), \quad (4.47)$$

where  $\Omega = \omega^2$ ,

$$a_\rho(x) = \frac{(\rho^2 - 4\rho - 8x)}{4}, \quad (4.48)$$

$$b_\rho(x) = \frac{x^2(\rho^2 - 12\rho - 8x + 48)}{2}, \quad (4.49)$$

$$c_\rho(x) = \frac{-2x^5 + x^4(\rho - 8)(\rho - 12)}{4 + 24(\rho - 4)x^3 + 18(\rho - 4)^2x^2}. \quad (4.50)$$

The discriminant of  $G_\rho$  is positive under the condition  $\rho \in (2\sqrt{3}, 4)$  for  $x > 0$ . The polynomial function  $G_\rho$  admits two real roots denoted by  $\Omega_\rho^\pm$ , where  $\Omega_\rho^+$  is the greater solution (positive signal). Using the fact that  $\rho \in (2\sqrt{3}, 4)$ , the solution  $\Omega_\rho^+$  is upper-bounded by

$$\Omega^+(x) = -x^2 - 3\sqrt{3}x + \frac{15}{2}x + \sqrt{(-228x + 468)\sqrt{3} + 4x^2 + 369x - 810},$$

which depends only on  $x$  and reaches its maximum at  $x^* \approx 2.139$ . Thus,  $\omega^2 = \Omega_\rho^+(x) < \Omega^+(x^*) \approx 4.961 < \pi^2$ , i.e.,  $\omega < \pi$ .

***Proof of item 3.*** The completion of the proof of Theorem 4.4.1 (item 3) is presented in the sequel; it follows the methodology already described in detail in section 3 and applied to the toy model (3.1); see also Algorithm 2.

### **Forcing multiplicity and normalization of the characteristic function**

This section covers Step 1 and 2 of the general methodology introduced in Section 3.2.

The following lemma gives a normalization of the quasipolynomial function  $\Delta$  admitting a triple real root, which corresponds to conditions (4.32).

**Lemma 4.5.1** *Let  $s_0 \in \mathbb{R}$  and consider the quasipolynomial  $\tilde{\Delta} : \mathbb{C} \rightarrow \mathbb{C}$  obtained from  $\Delta$  in (4.27) by the following change of variables*

$$\tilde{\Delta}(z) = \tau^2 \Delta\left(\frac{z}{\tau} + s_0\right), \quad z \in \mathbb{C}, \quad (4.51)$$

then

$$\tilde{\Delta}(z) = \left( \left( -\frac{\delta}{2} - 1 - v \right) z^2 + (-\delta - v)z - \delta \right) e^{-z} + z^2 + v z + \delta, \quad (4.52)$$

where

$$\delta = \tau^2 (s_0^2 + a_1 s_0 + a_0), \quad \text{and} \quad v = \tau (2s_0 + a_1). \quad (4.53)$$

### **Factorization of the normalized characteristic function**

This section covers Step 3 of the general methodology introduced in Section 3.2.

The quasipolynomial  $\tilde{\Delta}$  defined in (4.52) can be factorized as

$$\tilde{\Delta}(z) = z^3 \int_0^1 q_{\delta,v}(t) e^{-tz} dt \quad \text{where} \quad q_{\delta,v}(t) = \frac{\delta}{2} t^2 + vt + 1. \quad (4.54)$$

In our approach, the sign constancy of the polynomial  $q_{\delta,v}$  defined previously for  $t \in (0, 1)$  is necessary. Therefore, the following lemma gives regions in the parameter space guaranteeing the sign constancy of  $q_{\delta,v}$  for  $t \in (0, 1)$ ; see Figure 4.2.

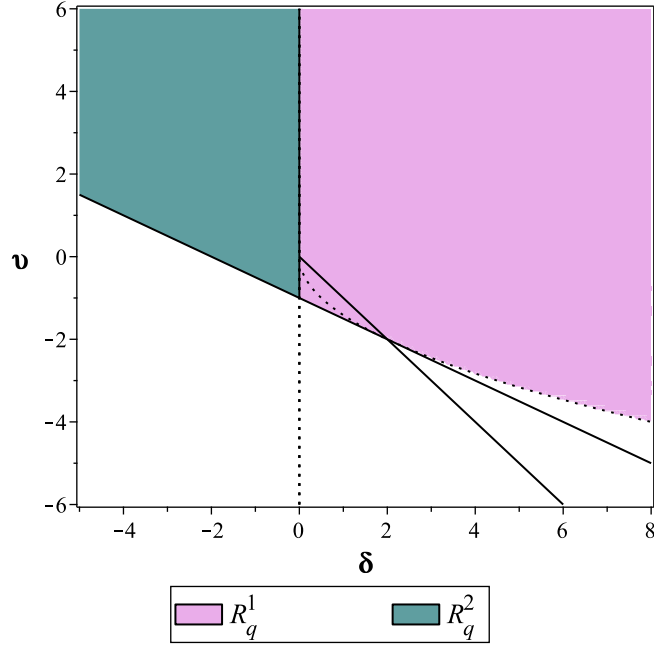


Figure 4.2: Plot of the region  $R_q$  in terms of the parameters  $(\delta, v)$  as defined in (4.56), (4.57) and (4.58).

**Lemma 4.5.2** *Let  $q_{\delta,v}$  be the quadratic polynomial with respect to  $t$  defined by (4.54). Then,  $q_{\delta,v}$  has a constant sign for  $t \in (0, 1)$  if, and only if,*

$$(\delta, v) \in R_q = R_q^1 \cup R_q^2 \cup R_q^3 \quad (4.55)$$

where

$$R_q^1 = \left\{ (\delta, v) \in \mathbb{R}^2 : \delta > 0, -\frac{\delta}{2} - 1 \leq v \leq -\delta \right\} \cup \left\{ (\delta, v) \in \mathbb{R}^2 : \delta > 0, -\sqrt{2\delta} < v \right\}, \quad (4.56)$$

$$R_q^2 = \left\{ (\delta, v) \in \mathbb{R}^2 : \delta < 0, v \geq -1 - \frac{\delta}{2} \right\}, \quad (4.57)$$

$$R_q^3 = \{(\delta, v) \in \mathbb{R}^2 : \delta = 0, v \geq -1\}. \quad (4.58)$$

### Parametric characterization of candidate regions for IMID

Now, we follow Algorithm 2 in order to tackle Step 4 of the general methodology introduced in Section 3.2.

Let  $z_0 = x_0 + i\omega_0 \in \mathbb{R}_+ + i\mathbb{R}_+$  be a root of

$$\tilde{\Delta}(z) = \tilde{P}_0(z) + \tilde{P}_1(z) e^{-z}, \quad (4.59)$$

as defined in (4.52), where

$$\tilde{P}_0(z) = z^2 + \nu z + \delta, \quad (4.60)$$

$$\tilde{P}_1(z) = \left( -\frac{\delta}{2} - 1 - \nu \right) z^2 + (-\delta - \nu) z - \delta. \quad (4.61)$$

so that  $z_0$  satisfies the following equality

$$|\tilde{P}_0(x_0 + i\omega_0)|^2 e^{2x_0} = |\tilde{P}_1(x_0 + i\omega_0)|^2. \quad (4.62)$$

Since  $e^{2x} > T_{ord}(e^{2x})$  for any  $x \in \mathbb{R}_+$  for truncation orders  $ord \in \{0, 1\}$ , function

$$F_{\delta,\nu}(x, \omega) = |\tilde{P}_1(x + i\omega)|^2 - |\tilde{P}_0(x + i\omega)|^2 T_{ord}(e^{2x}), \quad (4.63)$$

satisfies  $F_{\delta,\nu}(x_0, \omega_0) > 0$ . Moreover, the zeros of  $F_{\delta,\nu}$  can be characterized by the following quadratic polynomial

$$G_{\delta,\nu}(x, \Omega) = a_{\delta,\nu}(x) \Omega^2 + b_{\delta,\nu}(x) \Omega + c_{\delta,\nu}(x), \quad (4.64)$$

of degree  $\deg_{\Omega}(G_{\delta,\nu}) = 2$  in  $\Omega = \omega^2$  where coefficients  $a_{\delta,\nu}, b_{\delta,\nu}, c_{\delta,\nu}$  depend on the lower bound  $T_{ord}$  provided by the truncation order  $ord$ .

The region  $R_q$  is plotted in terms of the parameters  $(\delta, \nu)$  in Figure (4.2), while the analysis to obtain  $R_q$  is summarized in Figure A.5.

### Order zero truncation

In this case,  $T_0 = 1$ , hence the  $G_{\delta,\nu}$  coefficients are given by

$$\begin{cases} a_{\delta,\nu} = \frac{(2\nu+\delta+4)(2\nu+\delta)}{4}, \\ b_{\delta,\nu}(x) = 2a_{\delta,\nu}x^2 + b_{1,\delta,\nu}x, \\ c_{\delta,\nu}(x) = a_{\delta,\nu}x^4 + b_{1,\delta,\nu}x^3 + c_{2,\delta,\nu}x^2 + c_{1,\delta,\nu}x, \end{cases} \quad (4.65)$$

with,

$$b_{1,\delta,\nu} = \delta^2 + 3\nu\delta + 2\nu^2 + 2\delta, \quad (4.66)$$

$$c_{1,\delta,\nu} = 2\delta^2, \quad (4.67)$$

$$c_{2,\delta,\nu} = 2(2\nu + \delta)\delta. \quad (4.68)$$

Recall that in our approach, the condition of constancy of the sign of  $q_{\delta,\nu}$  is necessary. In addition, we need to guarantee the positivity of  $G_{\delta,\nu}$ , i.e., one has

to investigate conditions on the signs of  $a_{\delta,v}$  as well as the discriminant of  $G_{\delta,v}$  which is defined by the following second degree polynomial in  $x$

$$D_{\delta,v}(x) = (-4a_{\delta,v}c_{2,\delta,v} + b_{1,\delta,v}^2)x^2 - (4a_{\delta,v}c_{1,\delta,v})x. \quad (4.69)$$

Let define

$$\Upsilon_{\delta,v} = -4a_{\delta,v}c_{2,\delta,v} + b_{1,\delta,v}^2. \quad (4.70)$$

The following lemma provides an analysis of the sign of  $\Upsilon_{\delta,v}$ .

**Lemma 4.5.3** Consider  $\Upsilon_{\delta,v}$  given by (4.70), and let

$$v_1 = \delta_+ - \frac{1}{4}\sqrt{(\alpha_+ + \beta_+ \delta) \delta}, \quad (4.71)$$

$$v_2 = \delta_- - \frac{1}{4}\sqrt{(\alpha_- - \beta_- \delta) \delta}, \quad (4.72)$$

$$v_3 = \delta_- + \frac{1}{4}\sqrt{(\alpha_- - \beta_- \delta) \delta}, \quad (4.73)$$

$$v_4 = \delta_+ + \frac{1}{4}\sqrt{(\alpha_+ + \beta_+ \delta) \delta}, \quad (4.74)$$

where

$$\delta_1 = -\frac{\alpha_+}{\beta_+}, \quad \delta_2 = \frac{\alpha_-}{\beta_-}. \quad (4.75)$$

and

$$\alpha_{\pm} = 16(3 \pm 2\sqrt{2}), \quad \beta_{\pm} = 12\sqrt{2} \pm 17, \quad \delta_{\pm} = \frac{\delta}{4} \pm \frac{\delta}{\sqrt{2}}. \quad (4.76)$$

Then,

- $\Upsilon_{\delta,v} > 0 \iff (\delta, v) \in R_{\Upsilon^+} = R_1^{++} \cup R_2^{++} \cup R_3^{++} \cup R_1^{-+} \cup R_2^{-+} \cup R_3^{-+} \cup R_4^{-+} \cup R_5^{-+} \cup R_6^{-+}$ , where

$$R_1^{++} = \{(\delta, v) \in \mathbb{R}^2 : \delta > 0, v < v_1\}, \quad (4.77)$$

$$R_2^{++} = \{(\delta, v) \in \mathbb{R}^2 : \delta > 0, v_2 < v < v_3\}, \quad (4.78)$$

$$R_3^{++} = \{(\delta, v) \in \mathbb{R}^2 : \delta > 0, v > v_4\}, \quad (4.79)$$

$$R_1^{-+} = \{(\delta, v) \in \mathbb{R}^2 : \delta_1 < \delta < 0\}, \quad (4.80)$$

$$R_2^{-+} = \{(\delta, v) \in \mathbb{R}^2 : \delta_2 < \delta < \delta_1, v > v_4\}, \quad (4.81)$$

$$R_3^{-+} = \{(\delta, v) \in \mathbb{R}^2 : \delta_2 < \delta < \delta_1, v < v_1\}, \quad (4.82)$$

$$R_4^{-+} = \{(\delta, v) \in \mathbb{R}^2 : \delta < \delta_2, v > v_4\}, \quad (4.83)$$

$$R_5^{-+} = \{(\delta, v) \in \mathbb{R}^2 : \delta < \delta_2, v < v_1\}, \quad (4.84)$$

$$R_6^{-+} = \{(\delta, v) \in \mathbb{R}^2 : \delta < \delta_2, v_2 < v < v_3\}. \quad (4.85)$$



•  $\Upsilon_{\delta,v} < 0 \iff (\delta, v) \in R_{\Upsilon^-} = R_1^{+-} \cup R_2^{+-} \cup R_1^{-} \cup R_2^{-} \cup R_3^{-}$ , where

$$R_1^{+-} = \{(\delta, v) \in \mathbb{R}^2 : \delta > 0, v_1 < v < v_2\}, \quad (4.86)$$

$$R_2^{+-} = \{(\delta, v) \in \mathbb{R}^2 : \delta > 0, v_3 < v < v_4\}, \quad (4.87)$$

$$R_1^{-} = \{(\delta, v) \in \mathbb{R}^2 : \delta_2 < \delta < \delta_1, v_1 < v < v_4\}, \quad (4.88)$$

$$R_2^{-} = \{(\delta, v) \in \mathbb{R}^2 : \delta < \delta_2, v_3 < v < v_4\} \quad (4.89)$$

$$R_3^{-} = \{(\delta, v) \in \mathbb{R}^2 : \delta < \delta_2, v_1 < v < v_2\}. \quad (4.90)$$

We are now able to characterize the regions in the parameter space guaranteeing the positivity of the discriminant  $D_{\delta,v}$ .

**Lemma 4.5.4** *If the expression of  $\Upsilon_{\delta,v}$  defined in (4.70) is negative, then the discriminant  $D_{\delta,v}$  defined in (4.69) is positive for*

$$x \in \left(0, \frac{4a_{\delta,v}c_{1,\delta,v}}{(-4a_{\delta,v}c_{2,\delta,v} + b_{1,\delta,v}^2)}\right), \quad (4.91)$$

if, and only if,

$$(\delta, v) \in R_1^{+-}. \quad (4.92)$$

The Figure 4.3 presents the plots of the set  $R_D$ .

In the sequel, we are interested in the parameter region guaranteeing the sign constancy of  $q_{\delta,v}$  and the positivity of  $D_{\delta,v}$ , which corresponds to  $R_q \cap R_{D^+}$ . More precisely,

$$R_q \cap R_{D^+} = \bigcup_{i=1}^4 P_i, \quad (4.93)$$

where

$$\begin{cases} P_1 = \left\{ (\delta, v) \in \mathbb{R}^2 : \delta \in \left(0, \frac{2}{3+2\sqrt{2}}\right], v \in (v_1, v_2) \right\}, \\ P_2 = \left\{ (\delta, v) \in \mathbb{R}^2 : \delta \in \left(\frac{2}{3+2\sqrt{2}}, 2\right], v \in \left[-1 - \frac{\delta}{2}, v_2\right) \right\}, \\ P_3 = \left\{ (\delta, v) \in \mathbb{R}^2 : \delta \in (2, 2 + \sqrt{2}], v \in (-\sqrt{2}\delta, v_2) \right\}, \\ P_4 = \left\{ (\delta, v) \in \mathbb{R}^2 : \delta \in \left(2 + \sqrt{2}, \frac{(\sqrt{2}-4+\sqrt{16\sqrt{2}-22})^2(3+2\sqrt{2})}{4}\right), \right. \\ \left. v \in (-\sqrt{2}\delta, v_2) \right\}, \end{cases} \quad (4.94)$$

where  $v_1$  and  $v_2$  are defined in (4.71) and (4.72) respectively .

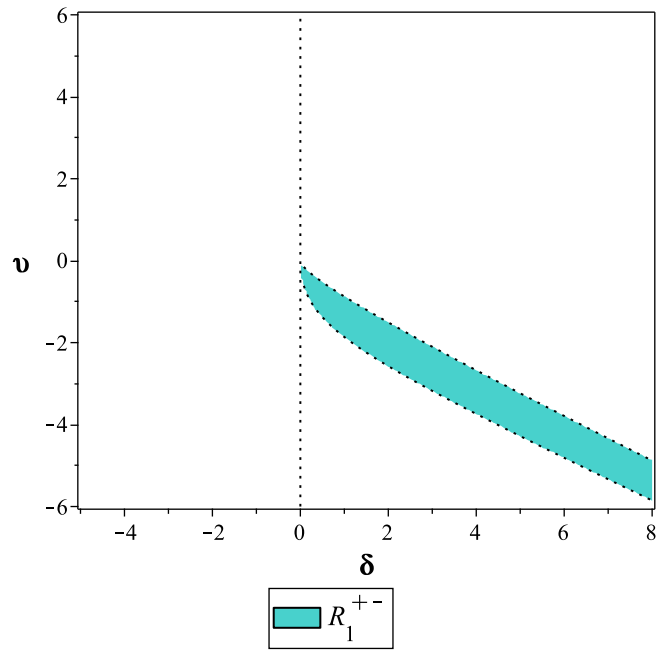


Figure 4.3: Plot represents region  $R_{D^+} = R_1^{+-}$ .

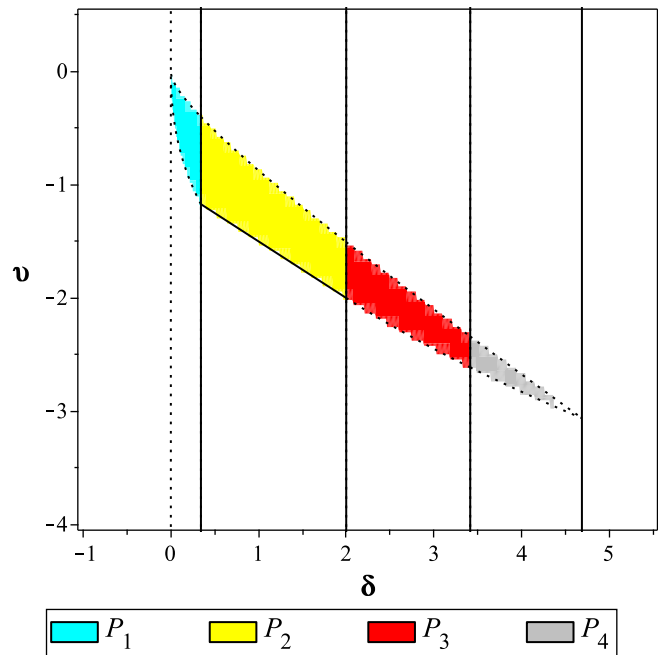


Figure 4.4: Plot shows a zoom on the regions  $P_i, i = 1..4$ .

### Order one truncation

In this case,  $T_1 = 1 + 2x$  (see Algorithm 2), which in turn allows us to define the quadratic polynomial (4.64) of degree 2 in  $\Omega = \omega^2$ , where

$$\begin{cases} a_{\delta,v}(x) = -2x + \frac{(\delta+2v)(\delta+2v+4)}{4}, \\ b_{\delta,v}(x) = -4x^3 + \frac{(\delta^2+4\delta v+4v^2+4\delta)x^2}{2} + \delta(\delta+3v+6)x, \\ c_{\delta,v}(x) = -2x^5 + \frac{(\delta^2+4\delta v+4v^2+4\delta-8v)x^4}{4} + \delta(\delta+3v-2)x^3 + 2\delta^2x^2. \end{cases} \quad (4.95)$$

In order to guarantee the positivity of  $G_{\delta,v}$ , one has to investigate conditions on the signs of  $a_{\delta,v}$  as well as the discriminant of  $G_{\delta,v}$  denoted in the sequel  $\tilde{D}_{\delta,v}(x) = x^2 D_{\delta,v}(x)$  where

$$\begin{aligned} D_{\delta,v}(x) = & -16(-v^2+4\delta)x^2 + 8\delta(\delta^2+3\delta v+v^2+6\delta+2v)x \\ & - \delta^4 - 2\delta^3v + \delta^2v^2 + 4\delta^3 + 20\delta^2v + 36\delta^2. \end{aligned} \quad (4.96)$$

As a matter of fact, let  $\Omega_{1,2}$  be the two real solutions of  $G_{\delta,v}(x, \Omega) = 0$ , then  $G_{\delta,v}$  is positive if, and only if,

$$\begin{aligned} & (D_{\delta,v} < 0 \text{ and } a_{\delta,v} > 0), \\ \text{or} \\ & (D_{\delta,v} > 0 \text{ and } a_{\delta,v} > 0 \text{ and } \Omega \in \mathbb{R} - (\Omega_1, \Omega_2)), \\ \text{or} \\ & (D_{\delta,v} > 0 \text{ and } a_{\delta,v} < 0 \text{ and } \Omega \in (\Omega_1, \Omega_2)). \end{aligned}$$

Note that in the first and second cases,  $G_{\delta,v}$  is unbounded which is not of interest in our method. Hence, we only keep the third set of conditions. Since the coefficient in front of  $x$  in the expression of  $a_{\delta,v}$  is negative and independent of  $\delta$  and  $v$ , then  $a_{\delta,v}$  is negative for  $x \in (x^*, +\infty)$ , where

$$x^* = \frac{(\delta+2v)(\delta+2v+4)}{8}. \quad (4.97)$$

The next lemma provides a characterization of regions in the parameter space guaranteeing the positivity of  $D_{\delta,v}$ .

**Lemma 4.5.5** *Let  $D_{\delta,v}$  be the parametric polynomial defined in (4.96). Then,  $D_{\delta,v}$  is positive*

- for  $x \in (-\infty, \min_{\delta,v}(x^-, x^+)) \cup (\max_{\delta,v}(x^-, x^+), +\infty)$ , if  $(\delta, v) \in R_{d^+} \cap R_{A^+}$ ,
- for  $x \in (\min_{\delta,v}(x^-, x^+), \max_{\delta,v}(x^-, x^+))$ , if  $(\delta, v) \in R_{d^+} \cap R_{A^-}$ ,

where

$$x^\pm = \frac{-8\delta(\delta^2+3\delta v+v^2+6\delta+2v) \pm \sqrt{d(\delta, v)}}{(32v^2-128\delta)}. \quad (4.98)$$

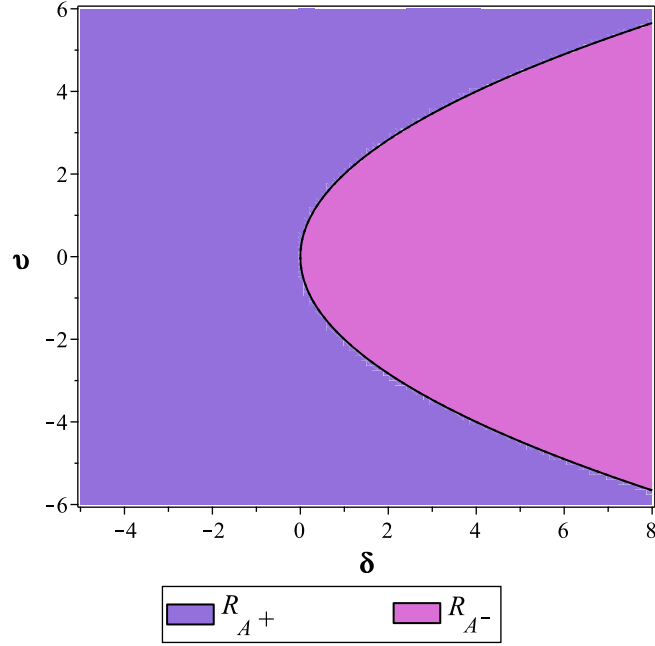


Figure 4.5: Plot represents the region  $R_{A^+} \cup R_{A^-}$ .

The set of interest here is  $R_{d^+} \cap R_{A^-}$  to which we shall add conditions guaranteeing the sign constancy of  $q_{\delta,v}$ . Hence, we characterize the intersection  $R_q \cap R_{d^+} \cap R_{A^-}$  as

$$R_q \cap R_{d^+} \cap R_{A^-} = \bigcup_{i=1}^3 \tilde{P}_i, \quad (4.99)$$

where

$$\begin{cases} \tilde{P}_1 = \left\{ (\delta, v) \in \mathbb{R}^2 : \delta \in \left( 0, \frac{2}{3+2\sqrt{2}} \right], v \in \left( -2\sqrt{\delta}, 2\sqrt{\delta} \right) \right\}, \\ \tilde{P}_2 = \left\{ (\delta, v) \in \mathbb{R}^2 : \delta \in \left( \frac{2}{3+2\sqrt{2}}, 2 \right], v \in \left[ -1 - \frac{\delta}{2}, 2\sqrt{\delta} \right) \right\}, \\ \tilde{P}_3 = \left\{ (\delta, v) \in \mathbb{R}^2 : \delta \in (2, +\infty], v \in \left( -\sqrt{2\delta}, 2\sqrt{\delta} \right) \right\}. \end{cases} \quad (4.100)$$

## Frequency bound

This section covers Step 4 of the methodology.

After having characterized the candidate regions, we present the main technical ingredient for the analysis of the frequency bound, which achieves Step 4 of the methodology.

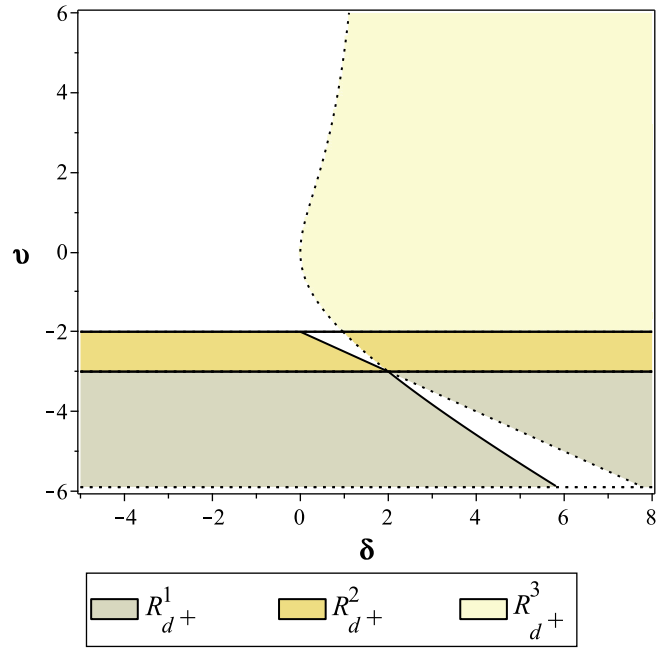


Figure 4.6: Plot represents region  $R_{d^+}$ .

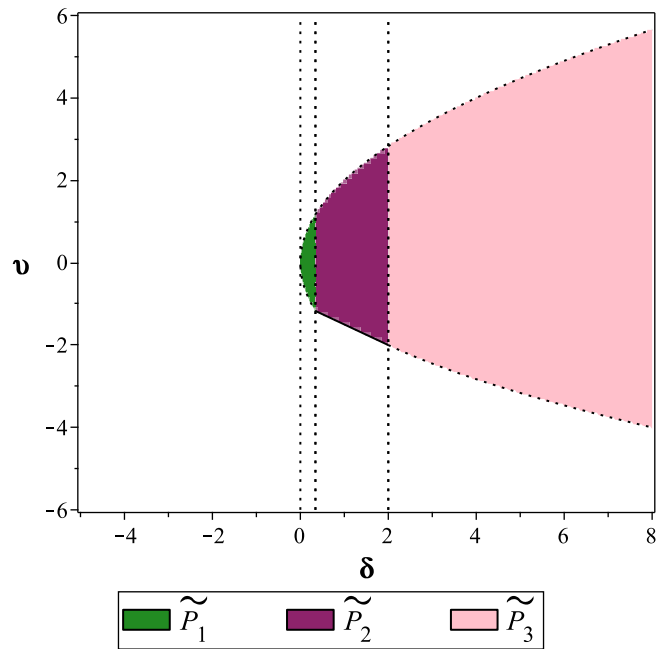


Figure 4.7: Plot represents regions  $\tilde{P}_1$ ,  $\tilde{P}_2$  and  $\tilde{P}_3$ .

**Lemma 4.5.6** Let  $\tilde{\Delta} = \tilde{\Delta}_{\delta, v}$  be the quasipolynomial given in (4.52), with  $(\delta, v) \in \tilde{P}_1 \cup \tilde{P}_2 \cup P_3 \cup P_4$ , where the regions  $\tilde{P}_1$ ,  $\tilde{P}_2$ ,  $P_3$  and  $P_4$  are given in (4.100) and (4.94)

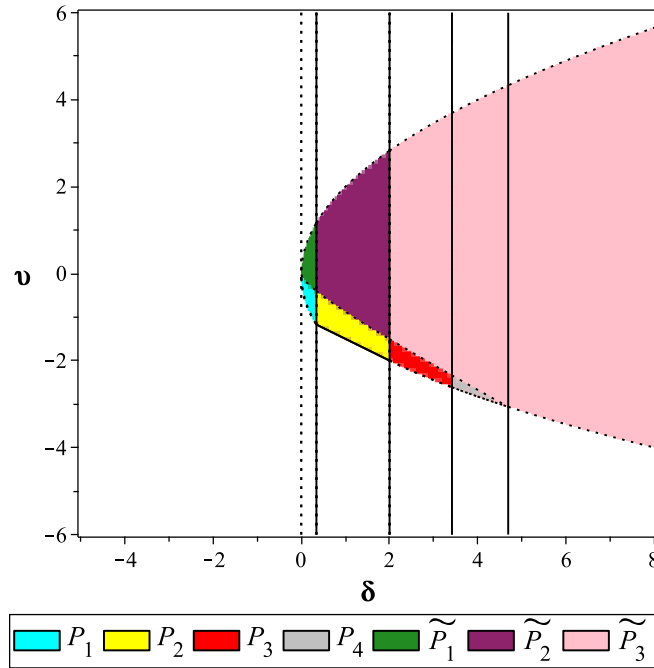


Figure 4.8: Plot shows that regions  $P_i$ ,  $i = 1..4$  obtained for an order zero truncation have been recovered and enlarged when we increased the truncation order.

respectively. If  $\tilde{\Delta}$  has a root  $z_0 \in \mathbb{R}_+ + i\mathbb{R}_+$ , then  $0 < \Im(z_0) < \pi$ . In addition, the root  $z_0$  may be properly assigned.

#### Remark 4.5.1

1. Our approach gives sufficient conditions for the dominance which are valid in regions  $P_i$ ,  $i = 3, 4$  and in regions  $\tilde{P}_i$ ,  $i = 1, 2$  which contain respectively  $P_i$ ,  $i = 1, 2$ . For each of the aforementioned regions, a frequency bound of interest ( $\omega < \pi$ ) was obtained. For region  $\tilde{P}_3$ , the truncation order needs to be increased.
2. Note that the set of conditions guaranteeing the MID obtained with a truncation of order  $k + 1$  contains the set of conditions guaranteeing the MID with a truncation of order  $k$ . As a result, higher orders of truncation shall lead to wider ranges on the conditions.

#### Conclusion of the proof of Theorem 4.4.1 (item 3)

This section corresponds to Step 5 of the general methodology introduced in Section 3.2.

After characterizing regions for which a frequency bound of interest was found, we can complete the proof of Theorem 4.4.1; this corresponds to Step 5 of the methodology.

The normalization of  $\Delta$  is given by  $\tilde{\Delta}$  in (4.52), while the factorization of  $\tilde{\Delta}$  is defined in (4.54). Using relations (A.20), one concludes that  $s_0$  is a root of multiplicity 3 of  $\Delta$  if, and only if, relations (4.32) hold, thereby ending the proof of the item (3a). To show (3b), we use the technical results previously proved. Consider  $(\delta, \nu) \in \tilde{P}_1 \cup \tilde{P}_2 \cup P_3 \cup P_4$ , the proof of the dominance is based on a contradiction. To do so, assume that there exists  $z_0 \in \mathbb{C}$  root of  $\tilde{\Delta}$  satisfying  $\Re(z_0) > 0$ . Write  $z_0 = x_0 + i\omega_0$  and using the fact that  $z_0$  is a non-zero root of  $\tilde{\Delta}$ , one may infer from (4.54) by taking the imaginary part, that

$$\int_0^1 \left( \frac{\delta}{2} t^2 + t\nu + 1 \right) \sin(t\omega_0) e^{-tx_0} dt = 0. \quad (4.101)$$

Since  $\omega_0 < \pi$  from Lemma 4.5.6, the function

$$t \mapsto \left( \frac{\delta}{2} t^2 + t\nu + 1 \right) \sin(t\omega_0). \quad (4.102)$$

is strictly positive in  $(0, 1)$ , which contradicts the above equality as required to end the proof. ■

## 4.6 . Illustrative example: classical oscillator

Consider the classical oscillator control problem:

$$\ddot{x}(t) + 2\eta\omega\dot{x}(t) + \omega^2x(t) = u(t), \quad (4.103)$$

with  $u$  as the delayed output-feedback as proposed in [137]:

$$u(t) = -\alpha_2\ddot{x}(t-\tau) - \alpha_1\dot{x}(t-\tau) - \alpha_0x(t-\tau), \quad (4.104)$$

$\eta$  is the damping factor such that  $0 < \eta < 1$ ,  $\omega$  describes the natural frequency. The characteristic equation corresponds to (4.103) is defined by

$$\Delta(s) = s^2 + 2\eta\omega s + \omega^2 + (\alpha_2s^2 + \alpha_1s + \alpha_0)e^{-\tau s}. \quad (4.105)$$

Following item 3 in Theorem 4.4.1, it shows that the real number  $s_0$  is a root of multiplicity 3 of the quasipolynomial function (4.105) if, and only if, the following relations hold

$$\begin{cases} \alpha_0 = -\frac{1}{2} (2\omega^2 + (2\eta\omega s_0^3 + \omega^2 s_0^2 + s_0^4) \tau^2 - (2\omega^2 s_0 - 2s_0^3) \tau) e^{\tau s_0}, \\ \alpha_1 = (-2\eta\omega + (2\eta\omega s_0^2 + \omega^2 s_0 + s_0^3) \tau^2 + (2\eta\omega s_0 - \omega^2 + 3s_0^2) \tau) e^{\tau s_0}, \\ \alpha_2 = -\frac{1}{2} (2 + (2\eta\omega s_0 + \omega^2 + s_0^2) \tau^2 + (4\eta\omega + 4s_0) \tau) e^{\tau s_0}. \end{cases} \quad (4.106)$$

The normalization and the integral representation of the characteristic function (4.105) are defined in (4.52) and (4.54) respectively, where in this case

$$\delta = \tau^2 (s_0^2 + 2\eta\omega s_0 + \omega^2), \quad \text{and} \quad \delta = \tau^2 ((s_0 + \eta\omega)^2 + \omega^2(1 - \eta^2)) > 0. \quad (4.107)$$

Indeed,

$$\begin{aligned} \delta &= 2\eta\omega\lambda_0 + \omega^2 + \lambda_0^2 \\ &= (\lambda_0 + \eta\omega)^2 - \eta^2\omega^2 + \omega^2 \\ &= (\lambda_0 + \eta\omega)^2 + \omega^2(1 - \eta^2) > 0. \end{aligned}$$

The integral representation is given by

$$\tilde{\Delta}(z) = z^3 \int_0^1 q_{\delta,v}(t) e^{-tz} dt, \quad (4.108)$$

where

$$q_{\delta,v}(t) = \frac{t^2\delta}{2} + vt + 1. \quad (4.109)$$

Under the expressions of  $\delta$  and  $v$ , the region in the parameter space guaranteeing the sign constancy of the polynomial  $q_{\delta,v}$  is given by  $R_q^1$  which is defined in (4.56).

In a similar way, a truncation to order 0 yields the quadratic polynomial  $G$  which is defined as in (4.65), where the region in the parameter space guaranteeing the positivity of its discriminant is given by

$$R_D = \{(\delta, v) \in \mathbb{R}^2 : \delta > 0, v_1 < v < v_2\}, \quad (4.110)$$

where  $v_1$  and  $v_2$  are given in (4.71) and (4.72) respectively.

The intersection of  $R_q^1$  and  $R_D$  is established to be given by  $\bigcup_{i=1}^4 P_i$  where  $P_i$ , for  $i = 1..4$  are respectively given in (4.94). Notice that the dominance is valid in the regions  $P_1$ ,  $P_2$  and  $P_3$ . For the region  $P_4$ , it is necessary to increase the order of truncation.

For the assignment of the root  $s_0$ , we detail the case of the region  $P_1$ , the analysis for the rest of the regions is analogue.

Considering the region  $P_1$ . We find from (4.53) that

$$v = -2\sqrt{\tau^2\omega^2(\eta^2 - 1) + \delta}, \quad (4.111)$$

On the other hand, one is able to bound (4.111) such that



$$v_1 < -2\sqrt{\tau^2 \omega^2 (\eta^2 - 1) + \delta} < v_2 \iff \delta - \frac{v_1^2}{4} < (1 - \eta^2) \omega^2 \tau^2 < \delta - \frac{v_2^2}{4}. \quad (4.112)$$

Since  $\delta \in \left(0, \frac{2}{3+2\sqrt{2}}\right]$ , it is guaranteed that  $\delta - \frac{v_1^2}{4} < \delta - \frac{v_2^2}{4}$ .

The inequality (4.112) represents condition on  $\eta$  and  $\omega$  in order to be able to assign  $s_0$ . In the following, assume that (4.112) holds.

$$\begin{aligned} 0 < \delta &\leq \frac{2}{3+2\sqrt{2}} \\ 0 < \tau^2 (s_0^2 + 2\eta \omega s_0 + \omega^2) &\leq \frac{2}{3+2\sqrt{2}} \\ 0 < \tau^2 (s_0 + \eta \omega)^2 + \tau^2 \omega^2 (1 - \eta^2) &\leq \frac{2}{3+2\sqrt{2}} \\ -\tau^2 \omega^2 (1 - \eta^2) < \tau^2 (s_0 + \eta \omega)^2 &\leq \frac{2}{3+2\sqrt{2}} - \omega^2 \tau^2 (1 - \eta^2) \end{aligned}$$

It is obvious that  $-\tau^2 \omega^2 (1 - \eta^2) < 0$  since  $0 < \eta < 1$ , in that case, we are going to consider only the right inequality, i.e.

$$\begin{aligned} \tau^2 (s_0 + \eta \omega)^2 &\leq \frac{2}{3+2\sqrt{2}} - \tau^2 \omega^2 (1 - \eta^2), \\ \tau |s_0 + \eta \omega| &\leq \sqrt{\frac{2}{3+2\sqrt{2}} - \omega^2 \tau^2 (1 - \eta^2)}, \\ -\sqrt{\frac{2}{3+2\sqrt{2}} - \tau^2 \omega^2 (1 - \eta^2)} &\leq \tau (s_0 + \eta \omega) \leq \sqrt{\frac{2}{3+2\sqrt{2}} - \tau^2 \omega^2 (1 - \eta^2)}. \end{aligned}$$

We notice that the term  $\frac{2}{3+2\sqrt{2}} - \tau^2 \omega^2 (1 - \eta^2)$  is positive due to the condition (4.112) and to the fact of  $0 < \delta \leq \frac{2}{3+2\sqrt{2}}$ .

Finally, considering the condition on  $\eta$  and  $\omega$  given in (4.112), we conclude that if the following condition in term of  $\omega$

$$\omega \geq \max \left\{ \frac{\delta}{\tau^2} - \frac{v_2^2}{4\tau^2}, \frac{1}{\tau} \sqrt{\frac{2}{3+2\sqrt{2}}} \right\}, \quad (4.113)$$

is satisfied, then we are able to assign the root  $s_0$  in the interval

$$-\eta \omega - \frac{1}{\tau} \sqrt{B} \leq s_0 \leq -\eta \omega + \frac{1}{\tau} \sqrt{B}, \quad (4.114)$$

with

$$B = \frac{2}{3+2\sqrt{2}} - \tau^2 \omega^2 (1 - \eta^2) > 0. \quad (4.115)$$

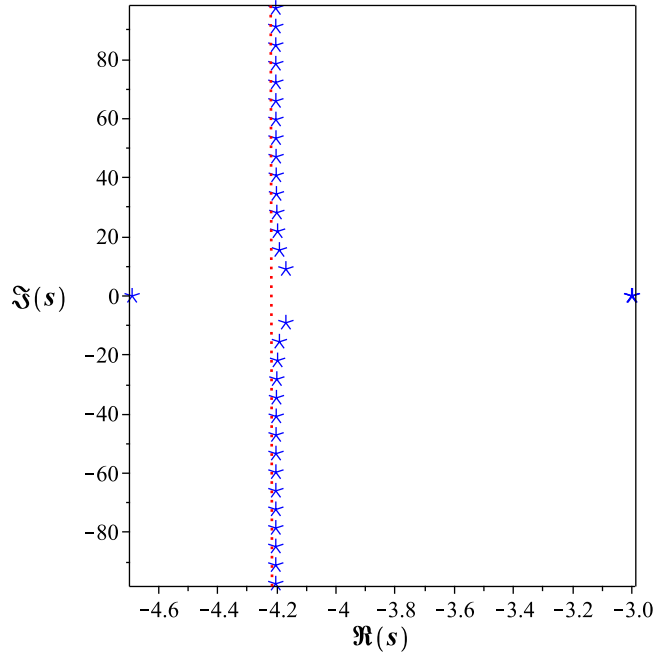


Figure 4.9: For  $\omega = 2$ ,  $\eta = \frac{1}{9}$  and  $\tau = 1$ , the plot exhibits the spectrum distribution of the quasipolynomial  $\Delta$  where the assigned rightmost triple root at  $s_0 = -3$  and the roots with large modulus are asymptotic to a vertical line  $\Re(s) \approx -\frac{1}{\tau} \log |\alpha| \approx -4.2$  ([97]).

The plot in Figure 4.9 illustrates the roots of  $\Delta$  computed numerically using Maple, while the Figure in 4.10 presents a temporal simulation with particular values of  $\omega$  and  $\eta$ .

#### 4.7 . Further remarks on the IMID: codimension 2

Consider the quasipolynomial function  $\Delta$  defined in (4.27). In Theorem 3.4.1, the quasipolynomial function  $\Delta$  has been treated in the presence of spectral values of maximal multiplicity 5. The case of intermediate multiplicities 4 and 3 was studied in Theorem 4.4.1.

The real number  $s_0$  is a root of multiplicity 2 of the quasipolynomial function  $\Delta$  if, and only if, for  $\alpha_2 = \gamma_2 e^{\tau s_0}$  the following relations hold

$$\begin{cases} \alpha_0 = (\tau s_0^3 + (\tau a_1 + \gamma_2 + 1) s_0^2 + \tau a_0 s_0 - a_0) e^{\tau s_0}, \\ \alpha_1 = (-\tau s_0^2 + (-\tau a_1 - 2\gamma_2 - 2) s_0 - \tau a_0 - a_1) e^{\tau s_0}. \end{cases} \quad (4.116)$$

The normalized quasipolynomial is given by

$$\tilde{\Delta}(z) = (\gamma_2 z^2 - (\delta + v)z - \delta) e^{-z} + z^2 + v z + \delta. \quad (4.117)$$

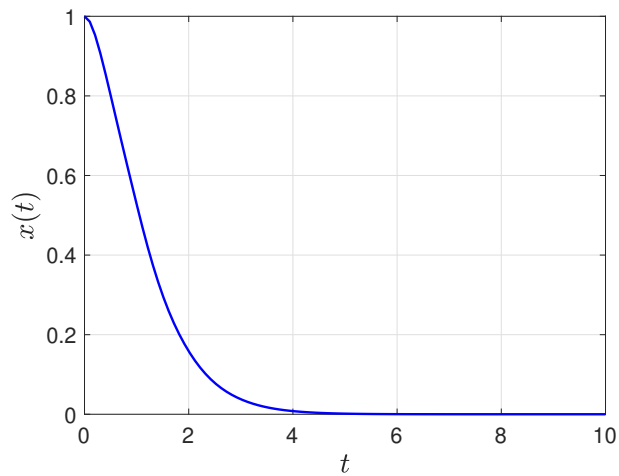


Figure 4.10: For  $\omega = 2$ ,  $\eta = \frac{1}{9}$  and  $\tau = 1$ , the plot illustrates the oscillator response with initial condition taken to be  $\varphi(t) = 1$  for  $t \in [-\tau, 0)$ .

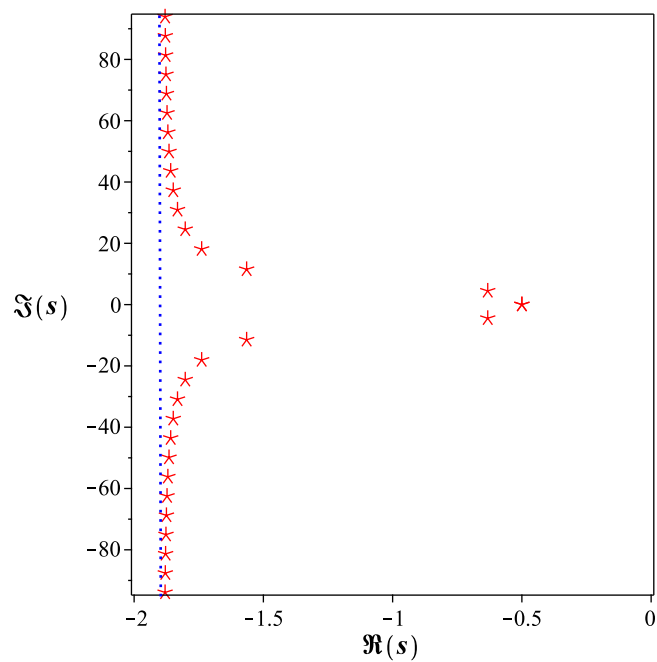


Figure 4.11: The plot illustrates for  $\omega = 2$ ,  $\eta = 0.02$  the rightmost double root of  $\Delta$  at  $s_0 = -0.5$  and the roots with large modulus asymptotic to the vertical line  $\Re(s) \approx -\frac{1}{\tau} \log |\alpha| \approx -1.88$ .

with

$$\delta = \tau^2 (s_0^2 + a_1 s_0 + a_0), \quad \text{and} \quad \nu = \tau (2s_0 + a_1). \quad (4.118)$$

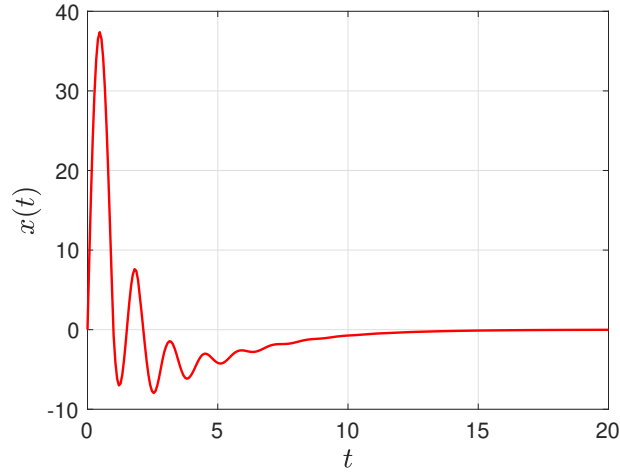


Figure 4.12: The plot is the time-response of a particular solution of (4.103) with  $\omega = 2$ ,  $\eta = 0.02$ ; the initial condition is taken to be  $\varphi(t) = t^3$  for  $t \in [-\tau, 0)$ .

The integral representation is given by

$$\tilde{\Delta}(z) = z^2 \left( 1 + \nu + \gamma_2 + \frac{\delta}{2} - z \int_0^1 \left( -\frac{\delta t^2}{2} + \nu(1-t) + \gamma_2 + \frac{\delta}{2} \right) e^{-tz} dt \right), \quad (4.119)$$

which is not the standard factorization. In fact, it is a more general form as the one described for instance in [55]. In the case of multiplicity 2, the normalized polynomial admits 3 free parameters which makes the analytic proof of the MID property quite delicate. However, we claim that even in such a case, one is able to numerically exploit such a property for rightmost spectral value assignment as is exhibited by the next example.

Consider the classical oscillator control problem (4.103). Let  $\omega = 2$  and  $\eta = 0.02$ , we choose  $s_0 = -0.5$ ,  $\tau = 1$  and  $\gamma_2 = -0.25e^{0.5}$ . Then,  $\alpha_2 \approx -0.25$  and, owing to relations (4.116), we compute  $\alpha_1 \approx -2.1471$  and  $\alpha_0 \approx -3.5891$ .

The plot in Figure 4.11 illustrates the roots of  $\Delta$  and Figure 4.12 represents a time-response of the oscillator with particular values of  $\omega$  and  $\eta$ .

#### 4.8 . Some insights on linear combinations of two kummer functions

The following results are in more detail in [94].

Consider the LTI dynamical system described by the DDE

$$x^{(n)}(t) + \sum_{k=0}^{n-1} a_k x^{(k)}(t) + \sum_{k=0}^m \alpha_k x^{(k)}(t - \tau) = 0, \quad (4.120)$$

where  $x(\cdot)$  is the real-valued unknown function,  $\tau > 0$  is the delay, and  $a_i, a_j$  are real coefficients for  $i = 1, \dots, n-1$  and  $j = 1, \dots, m$ . Notice that the DDE in (4.120) is said to be of retarded type if  $m < n$  and of neutral type if  $m = n$ . The corresponding characteristic equation is given by the quasipolynomial

$$\Delta(s) = s^n + \sum_{k=0}^{n-1} a_k s^k + \sum_{k=0}^m \alpha_k s^k e^{-\tau s}, \quad (4.121)$$

of degree  $\deg_s(\Delta) = n + m + 1$ . In the case of maximal multiplicity of a given real spectral value  $s_0$ , it was shown in [55] (case  $m = n - 1$ ) and [76] (general case  $m \leq n$ ) that  $s_0$  satisfies the GMID property.

The next lemma provides a partial step towards that goal, by providing a non-autonomous second-order differential equation having a given linear combination of Kummer functions as a solution.

**Lemma 4.8.1** *Let  $a, b$  be two complex numbers and  $\alpha$  and  $\beta$  two real numbers and define the parameter vector  $\vec{p} = (a, b, \alpha, \beta)$ . Then the complex function  $F$  defined by*

$$F(z, \vec{p}) = \alpha \Phi(a, b, z) + \beta \Phi(a, b + 1, z), \quad (4.122)$$

with  $z \notin \{0, \frac{\beta(\beta+\alpha)b^2}{(a-b)\alpha-\beta b\alpha}\}$ , satisfies the second-order differential equation

$$\frac{\partial^2 F}{\partial z^2}(z, \vec{p}) + Q(z, \vec{p}) \frac{\partial F}{\partial z}(z, \vec{p}) + R(z, \vec{p}) F(z, \vec{p}) = 0, \quad (4.123)$$

where

$$Q(z, \vec{p}) = -1 + \frac{b+1}{z} - \frac{\alpha(a\alpha - \alpha b - \beta b)}{D(z, \vec{p})}, \quad (4.124)$$

$$R(z, \vec{p}) = -\frac{N(z, \vec{p})}{D(z, \vec{p})}, \quad (4.125)$$

with

$$N(z, \vec{p}) = a((a-b)\alpha^2 - \alpha b\beta)z - \beta b(b+1)\alpha - ab^2\beta^2, \\ D(z, \vec{p}) = ((a-b)\alpha^2 - \alpha b\beta)z - \alpha b^2\beta - b^2\beta^2.$$

Note that Whittaker functions are defined in terms of Kummer functions in (1.23) by using the multiplicative factor  $e^{-\frac{\kappa}{2}z^{\frac{1}{2}+l}}$ , thanks to which the Whittaker differential equation (1.24) has no first-order term. We now proceed similarly from Kummer-type functions in order to define *Whittaker-type functions*. The next lemma can be shown by straightforward computations.

**Lemma 4.8.2** Let  $a, b$  be two complex numbers,  $\alpha, \beta$  be two real numbers,  $F$  be the function defined in (4.122), and  $Q$  and  $R$  be given by (4.124) and (4.125), respectively.

Let  $\mathcal{Q}$  be a primitive of  $\frac{Q}{2}$  and define the function  $W$  by

$$W(z, \vec{p}) = e^{\mathcal{Q}(z, \vec{p})} F(z, \vec{p}). \quad (4.126)$$

Then  $W$  satisfies the second-order differential equation

$$\frac{\partial^2 W}{\partial z^2}(z, \vec{p}) + G(z, \vec{p})W(z, \vec{p}) = 0, \quad (4.127)$$

where

$$G(z, \vec{p}) = R(z, \vec{p}) - \frac{(Q(z, \vec{p}))^2}{4} - \frac{1}{2} \frac{\partial Q}{\partial z}(z, \vec{p}). \quad (4.128)$$

In the sequel, we refer to functions  $W$  of the form (4.126) as *Whittaker-type functions*.

In what follow, Necessary and Sufficient Conditions on the parameters of the dynamical system (4.120) are provided to guarantee the existence of a characteristic root  $s_0$  with intermediate algebraic multiplicity  $n + m$ .

**Theorem 4.8.1** Let  $\tau > 0$ ,  $s_0 \in \mathbb{R}$ , and consider the quasipolynomial  $\Delta$  in (4.121). The number  $s_0$  is a root of multiplicity at least  $n + m$  of  $\Delta$  if and only if there exists  $\mathcal{A} \in \mathbb{R}$  such that

$$\Delta(s) = \frac{\tau^m (s - s_0)^{n+m}}{(m-1)!} \cdot \int_0^1 t^{m-1} (1-t)^{n-1} (1 - \mathcal{A}t) e^{-t\tau(s-s_0)} dt. \quad (4.129)$$

From Theorem 4.8.1, we are able to provide some (appropriate) sufficient conditions under which the MID property is valid for characteristic roots of multiplicity  $n + m$  of  $\Delta$ .

**Theorem 4.8.2** Let  $\tau > 0$ ,  $s_0$  and  $\mathcal{A}$  be real numbers, and  $\Delta$  be given by (4.121). Let  $F$  and  $G$  be defined respectively by (4.122) and (4.128)

Assume that, for every  $t \in (0, 1)$  and every root  $z$  of  $F(\cdot, \vec{p})$  in  $\mathbb{C}_-$ , we have  $\Re[zG(tz, \vec{p})] \geq 0$ . Then  $\lambda_0$  is a dominant root of  $\Delta$ , i.e.,  $s_0$  satisfies the MID property.

## DDEs frequency bound in the right half-plane

The main difficulty when applying Theorem 4.8.2 is to verify the technical assumption  $\Re[zG(tz, \vec{p})] \geq 0$  for every  $t \in (0, 1)$  and every root  $z$  of  $F(\cdot, \vec{p})$  in  $\mathbb{C}_-$  or, equivalently, to verify that  $\Re[zG(-tz, \vec{p})] \leq 0$  for every  $t \in (0, 1)$  and every root  $z$  of  $z \mapsto \Delta(\lambda_0 + \frac{z}{\tau})$  in  $\mathbb{C}_+$ . For that purpose, a useful technique is to establish a

priori information on the location of roots of  $\Delta$  with real part greater than  $\lambda_0$ , and in particular bounds on their imaginary parts.

To do so, a standard first step is to introduce the normalized quasipolynomial

$$\tilde{\Delta}(z) = \tau^n \Delta\left(\lambda_0 + \frac{z}{\tau}\right), \quad (4.130)$$

which can be written as

$$\tilde{\Delta}(z) = \tilde{P}_0(z) + e^{-z} \tilde{P}_\tau(z), \quad (4.131)$$

for some suitable polynomials  $\tilde{P}_0$  and  $\tilde{P}_\tau$  of degrees  $n$  and  $m$ , respectively. Hence, the problem of studying eventual roots of  $\Delta$  with real part greater than  $\lambda_0$  reduces to the study of eventual roots of  $\tilde{\Delta}$  with positive real part.

A possible strategy to do so is to notice that any root  $z$  of  $\tilde{\Delta}$  satisfies

$$|\tilde{P}_0(x + i\omega)|^2 e^{2x} = |\tilde{P}_\tau(x + i\omega)|^2, \quad (4.132)$$

where  $x = \Re(z)$  and  $\omega = \Im(z)$ . In particular, if  $z$  has nonnegative real part, then  $e^{2x} \geq T_\ell(x)$ , where, for  $\ell \in \mathbb{N}$ , the polynomial  $T_\ell$  is the truncation of the Taylor expansion of  $e^{2x}$  at order  $\ell$ , i.e.,  $T_\ell(x) = \sum_{k=0}^{\ell} \frac{(2x)^k}{k!}$ . Hence, any root  $z = x + i\omega$  of  $\tilde{\Delta}$  with nonnegative real part satisfies

$$\mathcal{F}(x, \omega) \geq 0, \quad (4.133)$$

where  $\mathcal{F}$  is the polynomial given by

$$\mathcal{F}(x, \omega) = |\tilde{P}_\tau(x + i\omega)|^2 - |\tilde{P}_0(x + i\omega)|^2 T_\ell(x). \quad (4.134)$$

In addition,  $\mathcal{F}$  only depends on  $\omega$  through  $\omega^2$  (which is a consequence of the fact that  $\tilde{P}_0$  and  $\tilde{P}_\tau$  are polynomials with real coefficients), and one may thus introduce the variable  $\Omega = \omega^2$  and define the polynomial  $H$  by setting  $H(x, \Omega) = \mathcal{F}(x, \sqrt{\Omega})$  for  $\Omega \geq 0$ . Hence, any root  $z = x + i\omega$  of  $\tilde{\Delta}$  with nonnegative real part satisfies

$$H(x, \Omega) \geq 0, \quad (4.135)$$

where  $\Omega = \omega^2$ . One can thus establish a bound on the imaginary parts of roots of  $\tilde{\Delta}$  by exploiting the polynomial inequality (4.135). This has been done for some low-order cases in [57], [91]. In particular, all these works have shown that it is sufficient to bound the absolute value of the imaginary parts of the roots in the right half-plane by  $\pi$ , as one can in general easily exclude by other arguments, such as those from Theorem 4.8.2, the possibility of having roots in the right-half plane with imaginary part at most  $\pi$ , thus concluding the proof of dominance of  $\lambda_0$ .

The procedure described in this subsection is synthetized in Algorithm 2 (see [91]), in which one increases the order of the Taylor expansion of  $e^{2x}$  until a suitable bound is found.

## 4.9 . Chapter Summary

In this chapter, we have treated the Multiplicity-Induced-Dominancy (MID) property for second order time-delay differential equations of neutral type with single-delay, i.e., the corresponding characteristic function is a quasipolynomial of degree 5. We present an algorithm as well as an overview of classification of admissible multiplicities for this class of equations. First, necessary and sufficient conditions are established, in which a real root of the characteristic function of maximal multiplicity 5 is necessarily dominant. Next, necessary and sufficient conditions have been provided in order to ensure that a given root of multiplicity 4 is the rightmost root of the characteristic function. For the case of multiplicity 3, we only provide sufficient conditions for the dominance where the number of free parameters is 2. In the latter case, we used first a truncation of the exponential function of order 0, which led to some regions where the MID property holds. To illustrate the use of the proposed algorithm, we further extended the validity area of the MID property by increasing the truncation up to order one, this allowed to enlarge the region of validity of the MID obtained with truncation of order 0. Finally, for the multiplicity 2, as the number of free parameters increases (3 free parameters), the computations become quite cumbersome from a symbolic point of view, but for the time being we used numerical approaches which can give sufficient conditions for the dominance. The obtained results have been illustrated through the delayed stabilization of the classical oscillator.





# **Part III**

## **Applications**



## 5 - Applying the MID property in the control of aerial vehicles

This chapter is a reduced version of the paper [92]. We also refer to [139].

### 5.1 . Introduction

Several application areas exist, among the actual technological surge, Unmanned Aerial Vehicles (UAVs) remain as a popular and challenging topic within the control systems and robotics scientific community. Such attractiveness relies on their friendly design and controllability criteria that have led to a wide application range such as high-precision weather monitoring, precision agriculture, swarm-based distributed perception, among others [140]–[142].

The capability of UAVs to perform accurate maneuvers is strongly dependent on the efficient synthesis and implementation of control-task-oriented algorithms. Several of these strategies take into consideration quaternion-based modeling approaches [143], image-aimed stabilization, or the well-known proportional-derivative (PD) and proportional-integral-derivative (PID) controllers [144]–[146]. In addition, robust control techniques [147] and state observers [148] have been also been used.

Among the variety of issues undermining the aerial systems performance, the study of time-delay effects remains relatively unexplored. In practice, UAVs' control systems operate in presence of time-delays arising from perception processing, decision-making, control commands and actuators' delayed dynamics. It has been proved that time-delays induce oscillatory phenomena rendering the system unstable. Nevertheless, some stabilizing effects of time-delays can be exploited to improve the system's performance [5], [32].

The stability of aerial vehicles under the influence of time-delays has been studied in different works. It is worthwhile highlighting that a considerable amount of prior works focuses on the communication and information exchange processes as the main sources of time-delays [149], [150]. In this regard, the range of solutions to overcome such an issue goes from delay-optimization approaches [151] to Backstepping and nonlinear control [152]–[154] yet, a vast variety of different approaches can be found in the literature, see for instance [2], [8], [32], [86], [155].

Amidst the novel techniques regarding time-delay systems analysis, tracking the behavior of the roots of the characteristic equation, as in [61], has led to

an increasing interest on exploiting the MID property. This property has already been suggested to solve some phenomena described by linear time-delay differential equations [73], [74], [156]. Nevertheless, the application of such findings on the domain of aerial robots control, as far as it is concerned to the authors, has not been specifically considered.

This chapter exploits the effects of time-delays on the stability of Unmanned Aerial Vehicles (UAVs). In this regard, the main contribution is a symbolic/numeric application of the Multiplicity-Induced-Dominancy (MID) property in the control of UAVs rotorcrafts featuring time-delays. The MID property is considered to address two of the most representative aerial robotic platforms: a classical quadrotor vehicle and a quadrotor vehicle endowed with tilting-rotors. The aforementioned property leads to an effective delayed feedback control design (MID tuning criteria), allowing the system to meet prescribed behavior conditions based on the placement of the rightmost root of the corresponding closed-loop characteristic function/quasipolynomial. Lastly, the results of detailed numerical simulations, including the linear and nonlinear dynamics of the vehicle, are presented and discussed to validate the proposal.

Here the MID property defines a tuning criteria of the controller gains such that a non-oscillatory transient response of the vehicle obeys a prescribed decay rate. This property is used to stabilize two popular rotorcrafts: *a classical quadrotor and a quadrotor endowing 1-Degree-Of-Freedom (DOF) tilting-rotors.*

The sequel of the chapter is outlined in the following manner: In Section 5.2, the dynamics of the quadrotor vehicles is described. Section 5.3 is devoted to the conception of the controllers that stabilize the typical quadrotor vehicle. On the other hand, Section 5.4 exposes the control strategy adopted to stabilize the UAV endowed with 1-DOF tilting-rotors. Section 5.5 provides the results of the detailed numerical simulations carried out to validate the proposals. Lastly, concluding remarks are given in Section 5.6.

## 5.2 . Quadrotor models

Let us consider the quadrotor system be depicted in Figure 5.1. The vision-based tracking system permits to know the position of the vehicle,  $\xi = [x \ y \ z]^T \in \mathbb{R}^3$ , in a conditioned environment. Such sensing strategy often takes a fraction of time  $\tau > 0$  to be executed; this issue is translated to control terms as a feedback time-delay.

The dynamics of the vehicle is described w.r.t. an inertial frame  $O_I \{x_I, y_I, z_I\}$  and a body frame  $O_b \{x_b, y_b, z_b\}$  whose origin matches the center of gravity (CoG) of the UAV. Here  $x_b, y_b, z_b$  define the roll, pitch and yaw axes and the corresponding

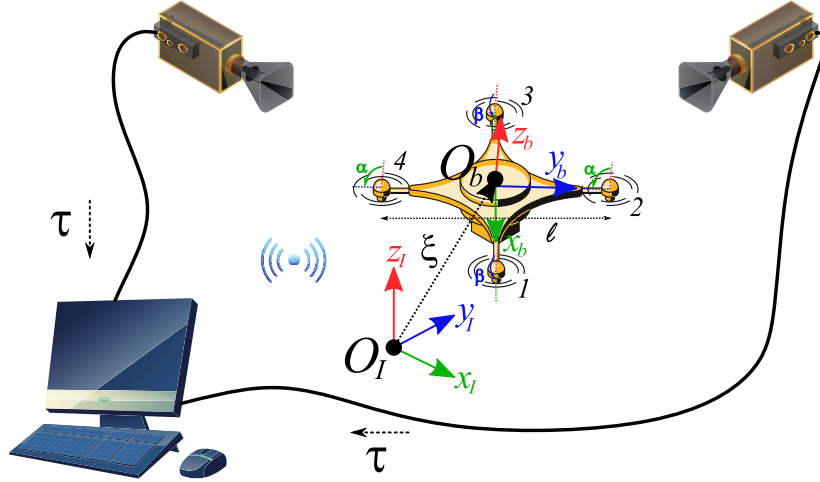


Figure 5.1: Quadrotor vehicle and vision-based tracking system (scheme conceived from figures available at [freepik.com](http://freepik.com))

principal axis of inertia which are associated to the Euler angles  $\eta = [\phi \ \theta \ \psi]^T \in \mathbb{R}^3$ , respectively. The motion of the aerial vehicle can be described, according to the Newton Euler formulation, as:

$$m_r \ddot{\xi} + m_r \mathbf{g} = \tau_\xi, \quad (5.1)$$

$$I \dot{\omega} + \omega \times (I \omega) = \tau_\omega, \quad (5.2)$$

where  $m_r > 0$  stands for the mass of the UAV and  $\mathbf{g} = [0 \ 0 \ g]^T \in \mathbb{R}^3$  does for the vector containing the constant of gravity acceleration  $g > 0$ . For a given  $\mathbf{v} \in \mathbb{R}^n$ , the function  $\text{diag} : \mathbb{R}^n \rightarrow \mathbb{R}^{n \times n}$  is defined by

$$\text{diag}(\mathbf{v}) = \begin{bmatrix} v_1 & 0 & \dots & 0 \\ 0 & v_2 & \dots & 0 \\ \vdots & \vdots & \ddots & \vdots \\ 0 & 0 & \dots & v_n \end{bmatrix}, \quad (5.3)$$

Here,  $I = \text{diag}([I_x \ I_y \ I_z]^T) \in \mathbb{R}^{3 \times 3}$  is respectively defined by the moments of inertia about the roll, pitch and yaw axis.

The angular velocity vector  $\omega = [p \ q \ r]^T \in \mathbb{R}^3$  is related to the Euler rates  $\dot{\eta}$  as follows

$$\omega = W_\eta \dot{\eta} \quad \text{and} \quad W_\eta = \begin{bmatrix} 1 & 0 & -S(\theta) \\ 0 & C(\phi) & S(\phi)C(\theta) \\ 0 & -S(\phi) & C(\phi)C(\theta) \end{bmatrix} \in \mathbb{R}^{3 \times 3}, \quad (5.4)$$

with  $C(\bullet) = \cos(\bullet)$  and  $S(\bullet) = \sin(\bullet)$ . Such an abuse of this notation is considered throughout the sequel of the manuscript.

The translational motion of the aircraft is driven by the forces comprised in the vector  $\tau_\xi \in \mathbb{R}^3$  which is defined, for the typical quadrotor, by the rotation matrix  $R_\eta \in \mathbb{R}^{3 \times 3}$  and the forces of the propellers  $f_i \geq 0$  (with  $i = 1, 2, 3, 4$ ), as:

$$\tau_\xi = R_\eta \begin{bmatrix} 0 \\ 0 \\ T = f_1 + f_2 + f_3 + f_4 \end{bmatrix}, \quad (5.5)$$

and

$$R_\eta = \begin{bmatrix} C(\theta)C(\psi) & S(\phi)S(\theta)C(\psi) - C(\phi)S(\psi) & C(\phi)S(\theta)C(\psi) + S(\phi)S(\psi) \\ C(\theta)S(\psi) & S(\phi)S(\theta)S(\psi) + C(\phi)C(\psi) & C(\phi)S(\theta)S(\psi) - S(\phi)C(\psi) \\ -S(\theta) & S(\phi)C(\theta) & C(\phi)C(\theta) \end{bmatrix},$$

For the quadrotor endowed with 1-DOF tilting-rotors, the vector  $\tau_\xi$  is rewritten in terms of  $R_\eta$ ,  $f_i$  and the tilt angles  $\alpha$  and  $\beta \in \mathbb{R}$  as:

$$\tau_\xi = R_\eta \begin{bmatrix} (f_1 + f_3)S(\beta) \\ -(f_2 + f_4)S(\alpha) \\ (f_1 + f_3)C(\beta) + (f_2 + f_4)C(\alpha) \end{bmatrix}, \quad (5.6)$$

The rotational states of the aircraft are controlled by the torques in the vector  $\tau_\omega \in \mathbb{R}^3$  which, for the typical quadrotor structure, is defined as:

$$\tau_\omega = \begin{bmatrix} \tau_\phi = \ell(f_2 - f_4)/2 \\ \tau_\theta = \ell(f_3 - f_1)/2 \\ \tau_\psi = \varepsilon(f_1 - f_2 + f_3 - f_4) \end{bmatrix}, \quad (5.7)$$

where  $\ell > 0$  denotes the diagonal motor-to-motor distance and  $\varepsilon > 0$  is a proportionality constant that relates the force  $f_i$  to the corresponding free moment  $\tau_i$  such that  $\tau_i = \varepsilon f_i$ .

For the quadrotor vehicle equipped with tilting-rotors,  $\tau_\omega$  reads as:

$$\tau_\omega = \begin{bmatrix} \ell(f_2 - f_4)C(\alpha)/2 + \varepsilon(f_1 + f_3)S(\beta) \\ \ell(f_3 - f_1)C(\beta)/2 - \varepsilon(f_2 + f_4)S(\alpha) \\ \varepsilon[(f_1 + f_3)C(\beta) - (f_2 + f_4)C(\alpha)] \end{bmatrix}, \quad (5.8)$$

### 5.3 . UAV control: The typical quadrotor case

Let the typical quadrotor vehicle be firstly addressed. It is typically assumed that the vehicle operates at low speeds in a quasi-hover state such that the Coriolis and Centripetal effects are neglected, at quasi-hovering flight ( $\phi \approx 0, \theta \approx 0$ ) and, without loss of generality,  $\psi = 0$  holds  $\forall t \geq 0$ . These considerations lead to a linear representation of (5.1), (5.2), (5.5), (5.2) and (5.7) of the form:

$$\begin{cases} X(s) = \frac{1}{m_r s^2} \theta(s) T(s), & Y(s) = -\frac{1}{m_r s^2} \phi(s) T(s), & Z(s) = \frac{1}{m_r s^2} (T(s) - m_r g), \\ \phi(s) = \frac{1}{I_x s^2} \tau_\phi(s), & \theta(s) = \frac{1}{I_y s^2} \tau_\theta(s), & \psi(s) = \frac{1}{I_z s^2} \tau_\psi(s) \end{cases} \quad (5.9)$$

which corresponds to a description of the system in the frequency domain where  $s = \sigma + j\omega$  with  $\sigma, \omega \in \mathbb{R}$ .

From (5.9), it is immediate to observe that the  $Z(s)$  and  $\psi(s)$  motions are decoupled, yet the  $X(s)$  dynamics is coupled to that of  $\theta(s)$  and the  $Y(s)$  motion is related to that of  $\phi(s)$ . In this regard, let the thrust  $T(s)$  be used as the control input to drive the system to a desired height  $Z_d(s)$  and  $\tau_\psi(s)$  does the proper to keep the yaw angle at 0. These control inputs are respectively defined, as:

$$T(s) = m_r(\mathcal{C}_z(s)E_z(s) + g), \quad \text{and} \quad \tau_\psi(s) = I_z\mathcal{C}_\psi(s)E_\psi(s), \quad (5.10)$$

where the  $z$  error reads as  $E_z(s) = Z_d(s) - e^{-\tau s}Z(s)$  since the translational states of the quadrotor are subject to a feedback time-delay  $\tau$  due to the inherent latency of the vision-based tracking system, and the  $\psi$  error stands as  $E_\psi(s) = -\psi(s)$  since  $\psi(s) = 0$ . The linear controllers  $\mathcal{C}_z(s)$  and  $\mathcal{C}_\psi(s)$  correspond to PD controllers of the form:

$$\mathcal{C}_z(s) = k_{p_z} + k_{d_z}s, \quad \text{and} \quad \mathcal{C}_\psi(s) = k_{p_\psi} + k_{d_\psi}s, \quad (5.11)$$

with  $k_{p_z}, k_{p_\psi} \in \mathbb{R}$  defined as the proportional gains and  $k_{d_z}, k_{d_\psi} \in \mathbb{R}$  standing as the derivative gains. The aforementioned control gains are tuned, as exposed in the sequel of the manuscript, by means of the MID property since a time-delay affects the corresponding dynamics.

Regarding the translational motion of the vehicle, let one consider that, for a large enough time,  $T(s) \rightarrow T_c = m_r g$  as  $Z(s) \rightarrow Z_d(s)$  [157]. The latter allows one to rewrite the equations of motion for  $X(s)$  and  $Y(s)$  in (5.9) as:

$$X(s) = \frac{1}{m_r s^2} \theta(s) T_c, \quad \text{and} \quad Y(s) = -\frac{1}{m_r s^2} \phi(s) T_c, \quad (5.12)$$

It is thus considered that  $\theta(s)$  and  $\phi(s)$  act as the control inputs for the corresponding DOF, such that the reference values are defined by linear PD controllers,  $\mathcal{C}_x(s)$  and  $\mathcal{C}_y(s)$ , as follows

$$\theta_d(s) = \frac{m_r}{T_c} \mathcal{C}_x(s) E_x(s), \quad \text{and} \quad \phi_d(s) = -\frac{m_r}{T_c} \mathcal{C}_y(s) E_y(s), \quad (5.13)$$

with

$$\mathcal{C}_x(s) = k_{p_x} + k_{d_x}s, \quad \mathcal{C}_y(s) = k_{p_y} + k_{d_y}s, \quad (5.14)$$

$$E_x(s) = X_d(s) - e^{-\tau s}X(s), \quad E_y(s) = Y_d(s) - e^{-\tau s}Y(s), \quad (5.15)$$

where the proportional gains correspond to  $k_{p_x}, k_{p_y} \in \mathbb{R}$ , and the derivative gains are denoted by  $k_{d_x}, k_{d_y} \in \mathbb{R}$ . Moreover, the reference values in (5.13) are achieved by the action of the linear PD controllers:

$$\mathcal{C}_\theta(s) = k_{p_\theta} + k_{d_\theta}s, \quad \text{and} \quad \mathcal{C}_\phi(s) = k_{p_\phi} + k_{d_\phi}s, \quad (5.16)$$



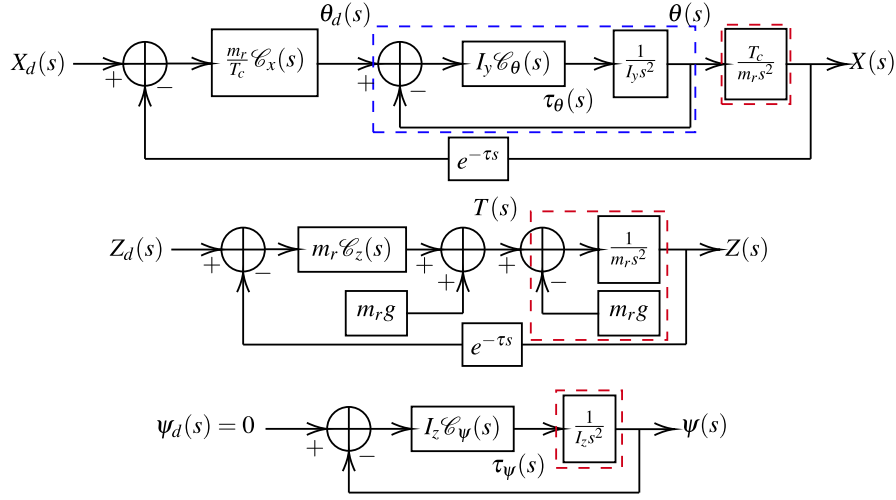


Figure 5.2: Block diagram representation of the typical quadrotor closed-loop system

such that:

$$\tau_{\theta}(s) = I_y \mathcal{C}_{\theta}(s) E_{\theta}(s), \quad \text{and} \quad \tau_{\phi}(s) = I_x \mathcal{C}_{\phi}(s) E_{\phi}(s), \quad (5.17)$$

with  $E_{\theta}(s) = \theta_d(s) - \theta(s)$  and  $E_{\phi}(s) = \phi_d(s) - \phi(s)$ . The proportional gains  $k_{p_{\theta}}, k_{p_{\phi}} \in \mathbb{R}$  as well as the derivative gains  $k_{d_{\theta}}, k_{d_{\phi}} \in \mathbb{R}$  are tuned in such a manner that the rotational dynamics is stable and faster than that of translation [157].

To synthesize the previous establishments, the  $X(s)$ ,  $Z(s)$  and  $\psi(s)$  closed-loop systems are depicted in Figure 5.2 where the dynamics of the plant is highlighted in red and the inner dynamics is surrounded by a blue dashed box. Notice that the  $Y(s)$  dynamics is omitted since it follows the same structure as that of  $X(s)$ .

### 5.3.1 . MID-property-based controllers analysis

According to Figure 5.2, the closed-loop transfer functions of each DOF can be computed such that the characteristic functions correspond to:

$$\Delta_x(s) = s^2 [s^2 + \mathcal{C}_{\theta}(s)] + e^{-\tau s} \mathcal{C}_x(s) \mathcal{C}_{\theta}(s), \quad (5.18)$$

$$\Delta_y(s) = s^2 [s^2 + \mathcal{C}_{\phi}(s)] + e^{-\tau s} \mathcal{C}_y(s) \mathcal{C}_{\phi}(s), \quad (5.19)$$

$$\Delta_z(s) = s^2 + e^{-\tau s} \mathcal{C}_z(s), \quad (5.20)$$

$$\Delta_{\psi}(s) = s^2 + \mathcal{C}_{\psi}(s), \quad (5.21)$$

Regarding (5.21), no time-delay effect is present thus, the exponential behavior of the solutions can be tuned by the proper placement of the roots of the polynomial. In this sense, it is enough that such roots rely on the left-plane of the complex space, moreover, a non-oscillatory stable system's response is achieved if the roots are real, see for instance [157]. The latter is comprised in Proposition 5.3.1 below.

**Proposition 5.3.1** *For the closed-loop dynamics described by (5.21), a non-oscillatory stable system's response is achieved and guaranteed if the controller's gains satisfy:*

$$k_{d_\psi} = s_{\psi,1} + s_{\psi,2}, \quad \text{and} \quad k_{p_\psi} = s_{\psi,1}s_{\psi,2}, \quad (5.22)$$

with  $s_{\psi,2} > s_{\psi,1} > 0$ .

**Proof** The proof is provided by the substitution of the gains given in (5.22) into (5.21) leading to:

$$s^2 + (s_{\psi,1} + s_{\psi,2})s + s_{\psi,1}s_{\psi,2} = (s + s_{\psi,1})(s + s_{\psi,2}) = 0, \quad (5.23)$$

such that the roots of the system are located at  $s = -s_{\psi,1}$  and  $s = -s_{\psi,2}$ . ■

It must be noticed that Proposition 5.3.1 can be applied to stabilize the inner-loop dynamics highlighted in blue in Figure 5.2 as the existence of negative real roots of the characteristic function of the open-loop system is essential to exploit the MID property.

Regarding the translational dynamics where the time-delay effect is found, the analysis of the  $Z(s)$  dynamics is provided at first place, afterwards, the  $X(s)$  dynamics of the vehicle is studied.

The following result, which is a direct consequence of [50], permits to characterize an assignable spectral value guaranteeing  $\sigma$ -stability as well as the corresponding controller's gains.

**Proposition 5.3.2** *For the quasipolynomial in (5.20), the following assertions hold:*

1. *The multiplicity of any given root of the quasipolynomial function is bounded by 4.*
2. *For a positive delay  $\tau$ , the quasipolynomial in (5.20) admits a real spectral value at  $s = s_{0_z}$  with algebraic multiplicity 3 if and only if:*

$$s_{0_z} = \frac{-2 + \sqrt{2}}{\tau}, \quad (5.24)$$

and the controller gains satisfy:

$$k_{p_z} = e^{\tau s_{0_z}} s_{0_z}^2 (s_{0_z} \tau + 1), \quad \text{and} \quad k_{d_z} = -e^{\tau s_{0_z}} s_{0_z} (s_{0_z} \tau + 2). \quad (5.25)$$

**Proof** The first statement of the proposition is a direct assimilation of the results presented at [73]. On the other hand, if  $s_{0_z}$  is a root with multiplicity at least 2, it follows that:  $\Delta_z(s_{0_z}) = \Delta'_z(s_{0_z}) = 0$ . By solving these equations for the control gains, the in (5.25) are obtained. The root  $s_{0_z}$  reaches a multiplicity 3 if and only if:

$$\Delta''_z(s_{0_z}) = 2 + e^{-\tau s_{0_z}} [\tau^2 (k_{d_z} s_{0_z} + k_{p_z}) - 2\tau k_{d_z}] = 0. \quad (5.26)$$

The substitution of (5.25) into (5.26) leads to (5.24). To prove that  $s_{0_z}$  is the dominant root, one may exploit the result from [50, Theorem 4.2].

■

Let one proceed to study the quasipolynomial in (5.18). In this regard, and due to the complexity of the expressions, a useful proposition based on a symbolic/numerical analysis is provided next.

### 5.3.2 . Symbolic/Numeric analysis of the MID-based controller

Firstly, to study the behavior of the system whose characteristic function corresponds to the quasipolynomial provided in (5.18), one must ensure that the delay-free part of the quasipolynomial has only real roots which occurs if:

$$k_{d_\theta}^2 > 4k_{p_\theta} > 0. \quad (5.27)$$

This condition over the gains  $k_{p_\theta}$  and  $k_{d_\theta}$  is taken into consideration to exploit the MID property as numerically/symbolically established next.

**Proposition 5.3.3** *For the quasipolynomial in (5.18), the following assertions hold:*

1. *The multiplicity of any given root of the quasipolynomial function is bounded by 7.*
2. *For a given positive delay  $\tau$ , an arbitrary root  $s_{0_x}$  with algebraic multiplicity 4 is a dominant root of (5.18) if  $s_{0_x} \in \mathbf{S}$ , where*

$$\mathbf{S} = \left\{ s_{0_x} : -\frac{3}{10\tau} < s_{0_x} < 0 \right\}, \quad (5.28)$$

*and the controller gains  $k_{p_\theta}$ ,  $k_{d_\theta}$ ,  $k_{p_x}$  and  $k_{d_x}$  satisfy:*

$$k_{p_\theta} = \lambda s_{0_x}^2, \quad k_{d_\theta} = -\frac{s_{0_x}}{9} \left( \frac{n_2 \lambda^2 - n_1 \lambda + n_0}{d_2 \lambda^2 - d_1 \lambda + d_0} \right), \quad (5.29)$$

$$k_{p_x} = \frac{s_{0_x}^2 e^{\tau s_{0_x}}}{\mathcal{C}_\theta^2(s_{0_x})} \left\{ \mathcal{C}_\theta(s_{0_x}) (\tau s_{0_x} + 1) [s_{0_x}^2 + \mathcal{C}_\theta(s_{0_x})] + s_{0_x}^2 [\mathcal{C}_\theta(s_{0_x}) + k_{p_\theta}] \right\}, \quad (5.30)$$

$$k_{d_x} = \frac{-s_{0_x} e^{\tau s_{0_x}}}{\mathcal{C}_\theta^2(s_{0_x})} \left\{ \mathcal{C}_\theta(s_{0_x}) (\tau s_{0_x} + 2) [s_{0_x}^2 + \mathcal{C}_\theta(s_{0_x})] + s_{0_x}^2 [\mathcal{C}_\theta(s_{0_x}) + k_{p_\theta}] \right\}, \quad (5.31)$$

*where  $\lambda$  is defined as the only positive real root of the following algebraic equation*

$$p_3 \lambda^3 + p_2 \lambda^2 + p_1 \lambda + p_0 = 0, \quad (5.32)$$

where

$$p_3 = 27 (s_{0_x}^2 \tau^2 + 4s_{0_x} \tau + 2)^4, \quad (5.33)$$

$$p_2 = -10s_{0_x}^9 \tau^9 - 243s_{0_x}^8 \tau^8 - 2352s_{0_x}^7 \tau^7 - 12090s_{0_x}^6 \tau^6 - 36360s_{0_x}^5 \tau^5 - 65916s_{0_x}^4 \tau^4 - 72288s_{0_x}^3 \tau^3 - 47736s_{0_x}^2 \tau^2 - 17280s_{0_x} \tau - 2592, \quad (5.34)$$

$$p_1 = (s_{0_x}^3 \tau^3 + 12s_{0_x}^2 \tau^2 + 36s_{0_x} \tau + 24) (s_{0_x}^3 \tau^3 + 18s_{0_x}^2 \tau^2 + 54s_{0_x} \tau + 24) (s_{0_x}^4 \tau^4 + 8s_{0_x}^3 \tau^3 + 24s_{0_x}^2 \tau^2 + 24s_{0_x} \tau + 12), \quad (5.35)$$

$$p_0 = - (s_{0_x}^4 \tau^4 + 8s_{0_x}^3 \tau^3 + 24s_{0_x}^2 \tau^2 + 24s_{0_x} \tau + 12) (s_{0_x}^3 \tau^3 + 12s_{0_x}^2 \tau^2 + 36s_{0_x} \tau + 24)^2. \quad (5.36)$$

with

$$n_2 = 11s_{0_x}^{12} \tau^{12} + 309s_{0_x}^{11} \tau^{11} + 3738s_{0_x}^{10} \tau^{10} + 25938s_{0_x}^9 \tau^9 + 115452s_{0_x}^8 \tau^8 + 348192s_{0_x}^7 \tau^7 + 731016s_{0_x}^6 \tau^6 + 1077408s_{0_x}^5 \tau^5 + 1105920s_{0_x}^4 \tau^4 + 771120s_{0_x}^3 \tau^3 + 347328s_{0_x}^2 \tau^2 + 90720s_{0_x} \tau + 10368, \quad (5.37)$$

$$n_1 = (s_{0_x}^3 \tau^3 + 12s_{0_x}^2 \tau^2 + 36s_{0_x} \tau + 24) (2s_{0_x}^6 \tau^6 + 39s_{0_x}^5 \tau^5 + 249s_{0_x}^4 \tau^4 + 744s_{0_x}^3 \tau^3 + 1116s_{0_x}^2 \tau^2 + 756s_{0_x} \tau + 180) (s_{0_x}^4 \tau^4 + 8s_{0_x}^3 \tau^3 + 24s_{0_x}^2 \tau^2 + 24s_{0_x} \tau + 12), \quad (5.38)$$

$$n_0 = 2 (s_{0_x}^3 \tau^3 + 6s_{0_x}^2 \tau^2 + 12s_{0_x} \tau + 6) (s_{0_x}^4 \tau^4 + 8s_{0_x}^3 \tau^3 + 24s_{0_x}^2 \tau^2 + 24s_{0_x} \tau + 12) (s_{0_x}^3 \tau^3 + 12s_{0_x}^2 \tau^2 + 36s_{0_x} \tau + 24)^2, \quad (5.39)$$

$$d_2 = 3 (2s_{0_x}^3 \tau^3 + 9s_{0_x}^2 \tau^2 + 12s_{0_x} \tau + 6) (s_{0_x}^2 \tau^2 + 4s_{0_x} \tau + 2)^4, \quad (5.40)$$

$$d_1 = (s_{0_x}^4 \tau^4 + 16s_{0_x}^3 \tau^3 + 63s_{0_x}^2 \tau^2 + 84s_{0_x} \tau + 30) (s_{0_x}^4 \tau^4 + 8s_{0_x}^3 \tau^3 + 24s_{0_x}^2 \tau^2 + 24s_{0_x} \tau + 12) (s_{0_x}^2 \tau^2 + 4s_{0_x} \tau + 2)^2, \quad (5.41)$$

$$d_0 = (s_{0_x} \tau + 2) (s_{0_x}^3 \tau^3 + 12s_{0_x}^2 \tau^2 + 36s_{0_x} \tau + 24) (s_{0_x}^4 \tau^4 + 8s_{0_x}^3 \tau^3 + 24s_{0_x}^2 \tau^2 + 24s_{0_x} \tau + 12) (s_{0_x}^2 \tau^2 + 4s_{0_x} \tau + 2)^2. \quad (5.42)$$

**Proof** The first statement of the proposition is a direct assimilation of the results presented in [73], see also [55]. Furthermore, (5.29)-(5.31) are found as in Proposition 5.3.2. In this regard, if  $s_{0_x}$  is a root with multiplicity at least 2, it follows that:

$$\Delta_x(s_{0_x}) = s_{0_x}^2 (s_{0_x}^2 + k_{d_\theta} s_{0_x} + k_{p_\theta}) + e^{-\tau s_{0_x}} (k_{d_x} s_{0_x} + k_{p_x}) (k_{d_\theta} s_{0_x} + k_{p_\theta}) = 0, \quad (5.43)$$

$$\Delta'_x(s_{0_x}) = s_{0_x} (4s_{0_x}^2 + 3k_{d_\theta} s_{0_x} + 2k_{p_\theta}) - e^{-\tau s_{0_x}} [\tau (k_{d_x} s_{0_x} + k_{p_x}) (k_{d_\theta} s_{0_x} + k_{p_\theta}) - (2k_{d_\theta} k_{d_x} s_{0_x} + k_{p_x} k_{d_\theta} + k_{p_\theta} k_{d_x})] = 0. \quad (5.44)$$

By solving (5.43) and (5.44) for the control gains  $k_{p_x}$  and  $k_{d_x}$ , the equality in (5.30) and the one in (5.31) are obtained. Moreover, the root  $s_{0_x}$  reaches a multiplicity

4 if and only if:

$$\Delta_x''(s_{0_x}) = 2(6s_{0_x}^2 + 3k_{d_\theta}s_{0_x} + k_{p_\theta}) + e^{-\tau s_{0_x}} \{ \tau^2 (k_{d_x}s_{0_x} + k_{p_x})(k_{d_\theta}s_{0_x} + k_{p_\theta}) - 2\tau(2k_{d_\theta}k_{d_x}s_{0_x} + k_{p_x}k_{d_\theta} + k_{p_\theta}k_{d_x}) + 2k_{d_x}k_{d_\theta} \} = 0, \quad (5.45)$$

$$\Delta_x'''(s_{0_x}) = 6(4s_{0_x} + k_{d_\theta}) - e^{-\tau s_{0_x}} \{ \tau^3 (k_{d_x}s_{0_x} + k_{p_x})(k_{d_\theta}s_{0_x} + k_{p_\theta}) + 3\tau^2(2k_{d_\theta}k_{d_x}s_{0_x} + k_{p_x}k_{d_\theta} + k_{p_\theta}k_{d_x}) - 6\tau k_{d_x}k_{d_\theta} \} = 0. \quad (5.46)$$

The substitution of (5.30) and (5.31) into the equations above, and the use of the routine `CellDecomposition` from the `RootFinding[Parametric]` package of computer algebra system `Maple` [158], led to (5.29) yet, one must analyse with detail the results concerning the in (5.29) and (5.32). For these ends, let one adopt the change of variable  $\varsigma = s_{0_x}\tau$  throughout (5.32)-(5.42) yielding to rewrite the expressions as follows:

$$p_3^*\lambda^3 + p_2^*\lambda^2 + p_1^*\lambda + p_0^* = 0, \quad (5.47)$$

where

$$p_3^* = 27(\varsigma^2 + 4\varsigma + 2)^4, \quad (5.48)$$

$$p_2^* = -10\varsigma^9 - 243\varsigma^8 - 2352\varsigma^7 - 12090\varsigma^6 - 36360\varsigma^5 - 65916\varsigma^4 - 72288\varsigma^3 - 47736\varsigma^2 - 17280\varsigma - 2592, \quad (5.49)$$

$$p_1^* = (\varsigma^3 + 12\varsigma^2 + 36\varsigma + 24)(\varsigma^3 + 18\varsigma^2 + 54\varsigma + 24)(\varsigma^4 + 8\varsigma^3 + 24\varsigma^2 + 24\varsigma + 12), \quad (5.50)$$

$$p_0^* = -(\varsigma^4 + 8\varsigma^3 + 24\varsigma^2 + 24\varsigma + 12)(\varsigma^3 + 12\varsigma^2 + 36\varsigma + 24)^2, \quad (5.51)$$

$$n_2^* = 11\varsigma^{12} + 309\varsigma^{11} + 3738\varsigma^{10} + 25938\varsigma^9 + 115452\varsigma^8 + 348192\varsigma^7 + 731016\varsigma^6 + 1077408\varsigma^5 + 1105920\varsigma^4 + 771120\varsigma^3 + 347328\varsigma^2 + 90720\varsigma + 10368, \quad (5.52)$$

$$n_1^* = (\varsigma^3 + 12\varsigma^2 + 36\varsigma + 24)(2\varsigma^6 + 39\varsigma^5 + 249\varsigma^4 + 744\varsigma^3 + 1116\varsigma^2 + 756\varsigma + 180)(\varsigma^4 + 8\varsigma^3 + 24\varsigma^2 + 24\varsigma + 12), \quad (5.53)$$

$$n_0^* = 2(\varsigma^3 + 6\varsigma^2 + 12\varsigma + 6)(\varsigma^4 + 8\varsigma^3 + 24\varsigma^2 + 24\varsigma + 12)(\varsigma^3 + 12\varsigma^2 + 36\varsigma + 24)^2, \quad (5.54)$$

$$d_2^* = 3(2\varsigma^3 + 9\varsigma^2 + 12\varsigma + 6)(\varsigma^2 + 4\varsigma + 2)^4, \quad (5.55)$$

$$d_1^* = (\varsigma^4 + 16\varsigma^3 + 63\varsigma^2 + 84\varsigma + 30)(\varsigma^4 + 8\varsigma^3 + 24\varsigma^2 + 24\varsigma + 12)(\varsigma^2 + 4\varsigma + 2)^2, \quad (5.56)$$

$$d_0^* = (\varsigma + 2)(\varsigma^3 + 12\varsigma^2 + 36\varsigma + 24)(\varsigma^4 + 8\varsigma^3 + 24\varsigma^2 + 24\varsigma + 12)(\varsigma^2 + 4\varsigma + 2)^2. \quad (5.57)$$

As previously mentioned, to exploit the results of [52], [77], the non-delayed part of the quasipolynomial must have only real roots which is guaranteed if (5.27)

holds, thus it follows that  $\lambda > 0$  as  $s_{0_x}^2 > 0$  and, from (5.47)-(5.57), that

$$\frac{n_2^* \lambda^2 - n_1^* \lambda + n_0^*}{d_2^* \lambda^2 - d_1^* \lambda + d_0^*} > 18\sqrt{\lambda}m \quad (5.58)$$

To ensure the existence of a given  $\lambda$  satisfying the condition above, some restrictions over  $\zeta$  (consequently over  $\tau$  and  $s_{0_x}$ ) must be established. In this regard, the analysis of the polynomial in (5.47) can be performed in any mathematical software that allows the treatment of symbolic and numerical computations. In the current case of study, Maple and its package *RootFinding[Parametric]* were used.

The aforementioned Maple package divides the space of parameters into two parts: the discriminant variety and its complement. The discriminant variety is referred as a generalization of the discriminant of a univariate polynomial and contains those parameter values leading to non-generic solutions, meanwhile, its complement can be expressed as a finite union of open cells such that the number of real solutions of the system is constant on each cell. In this manner, all parameter values leading to generic solutions of the system can be described. The underlying techniques used are Gröbner bases, polynomial real root finding, and cylindrical algebraic decomposition, see for instance [158]–[161]. Further details of the package and its implementation are available at [162]. Thus, considering (5.58) and the fact that  $\lambda > 0$ , the cell decomposition of (5.47) provides three  $\zeta$  intervals where the conditions holds. These intervals are defined by

$$\begin{aligned} \varphi_1(\zeta) = & \zeta^{12} - 78\zeta^{10} - 120\zeta^9 + 2772\zeta^8 + 13824\zeta^7 + 8208\zeta^6 - 105408\zeta^5 \\ & - 357696\zeta^4 - 546048\zeta^3 - 456192\zeta^2 - 207360\zeta - 41472 \end{aligned} \quad (5.59)$$

$$\varphi_2(\zeta) = \zeta^2 + 4\zeta + 2, \quad \varphi_3(\zeta) = \zeta^3 + 9\zeta^2 + 18\zeta + 6 \quad (5.60)$$

and their real roots, such that

$$\zeta_{\varphi_1,1} \approx -0.8478574488 < \zeta < \zeta_{\varphi_2,2} \approx -0.5857864376 \quad (5.61)$$

$$\zeta_{\varphi_2,2} \approx -0.5857864376 < \zeta < \zeta_{\varphi_3,3} \approx -0.4157745568 \quad (5.62)$$

$$\zeta_{\varphi_3,3} \approx -0.4157745568 < \zeta < 0 \quad (5.63)$$

where  $\zeta_{\varphi_i,j}$  denotes the  $j$ -th real root of the projection polynomial  $\varphi_i(\zeta)$  (considering that the real roots are arranged in increasing order). For instance, only the conditions over  $\zeta$  that ensure the existence of a proper  $\lambda$  have been given thus, one shall investigate the dominance of the corresponding roots within the intervals. As suggested in [73], [77], if the quasipolynomial in (5.18) possesses a root of multiplicity at least 4, an integral representation can be adopted. The computation of the control gains as previously performed, allows one to establish a negative real root of multiplicity 4 thus, the substitution of (5.29)-(5.31) into (5.18) yields to:

$$\Delta_x(s; s_{0_x}, \tau) = (s - s_{0_x})^4 \left( 1 + \int_0^1 e^{-(s-s_{0_x})\tau v} \frac{\tau R_{3,x}(s_{0_x}; \tau v)}{3!} dv \right) \quad (5.64)$$

such that:

$$\begin{aligned}
R_{3,x}(s_{0_x}; \tau v) = & s_{0_x} \left[ s_{0_x}^3 \tau^3 v^3 \left( 1 + \lambda - \frac{1}{9} \frac{n_2 \lambda^2 - n_1 \lambda + n_0}{d_2 \lambda^2 - d_1 \lambda + d_0} \right) + 6s_{0_x}^2 \tau^2 v^2 \left( 2 + \lambda - \frac{1}{6} \frac{n_2 \lambda^2 - n_1 \lambda + n_0}{d_2 \lambda^2 - d_1 \lambda + d_0} \right) + \right. \\
& \left. 6s_{0_x} \tau v \left( 6 + \lambda - \frac{1}{3} \frac{n_2 \lambda^2 - n_1 \lambda + n_0}{d_2 \lambda^2 - d_1 \lambda + d_0} \right) + 2 \left( 12 - \frac{1}{3} \frac{n_2 \lambda^2 - n_1 \lambda + n_0}{d_2 \lambda^2 - d_1 \lambda + d_0} \right) \right] \quad (5.65)
\end{aligned}$$

The results in [52] provide a necessary and sufficient condition for the dominance of a given multiple root (of maximal multiplicity) in the first-order case. The main idea of the cited work is used in the current case of study to get sufficient conditions for the dominance of the quadruple root at  $s_{0_x}$ , such that if:

$$\left| \frac{\tau R_{3,x}(s_{0_x}; \tau v)}{3!} \right| \leq 1 \quad \forall 0 < v < 1 \quad (5.66)$$

holds,  $s_{0_x}$  is the dominant root of (5.18). Nevertheless, to keep the consistency of the proof, one may rewrite (5.66) in terms of  $\zeta$  as follows:

$$|R_{3,x}^*(\zeta; v)| \leq 1 \quad \forall 0 < v < 1 \quad (5.67)$$

with

$$\begin{aligned}
R_{3,x}^*(\zeta; v) = & \frac{1}{6} \left[ \zeta^4 v^3 \left( 1 + \lambda - \frac{1}{9} \frac{n_2^* \lambda^2 - n_1^* \lambda + n_0^*}{d_2^* \lambda^2 - d_1^* \lambda + d_0^*} \right) \right. \\
& \left. + 6\zeta^3 v^2 \left( 2 + \lambda - \frac{1}{6} \frac{n_2^* \lambda^2 - n_1^* \lambda + n_0^*}{d_2^* \lambda^2 - d_1^* \lambda + d_0^*} \right) + \right. \\
& \left. 6\zeta^2 v \left( 6 + \lambda - \frac{1}{3} \frac{n_2^* \lambda^2 - n_1^* \lambda + n_0^*}{d_2^* \lambda^2 - d_1^* \lambda + d_0^*} \right) + 2\zeta \left( 12 - \frac{1}{3} \frac{n_2^* \lambda^2 - n_1^* \lambda + n_0^*}{d_2^* \lambda^2 - d_1^* \lambda + d_0^*} \right) \right] \quad (5.68)
\end{aligned}$$

Due to the high order of the polynomials involved in the definition of  $R_{3,x}^*(\zeta; v)$ , an analysis of its behavior results complex and computationally expensive. Instead, a numerical analysis implies less computational resources and can provide enough and sufficient information to validate the proposal. In this regard, Figure 5.3 exposes the plots of  $R_{3,x}^*(\zeta; v)$  for a given  $\zeta$  within each of the intervals in (5.61)-(5.63) such that  $v$  varies from 0 to 1 in order to verify (5.67).

The results depicted in Figure 5.3 show that for a given  $\zeta$  within the intervals in (5.61) and (5.62), the condition in (5.67) does not hold. On the other hand, for a given  $\zeta$  within the interval in (5.63), one can obtain a bound over  $\zeta$  such that (5.67) holds. By solving  $R_{3,x}^*(\zeta; v=0) = 1$ , one finds that the aforementioned condition is satisfied if  $0 > \zeta > -0.3109805570$  which ends the proof. ■

Notice that the numerical study revealed that for any  $\zeta$  within the intervals in (5.61)-(5.63), the dominance of  $s_{0_x}$  holds (as illustrated in Figure 5.4) yet, the analytic extension of the proof implies a further and more complex analysis that comprehends the definition of more inequalities and conditions over the integral. Time-domain representation is given in Figure 5.5.

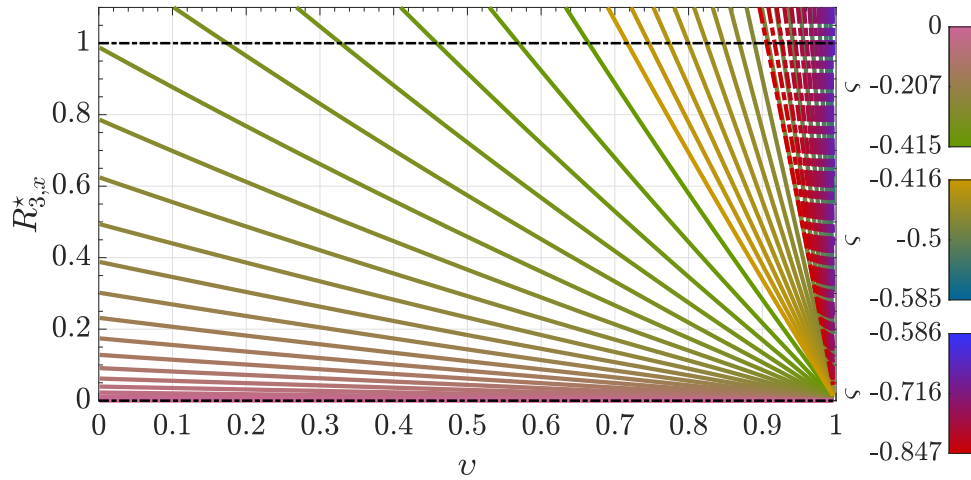


Figure 5.3: Behavior of  $R_{3,x}^*(\zeta; v)$  within the interval  $0 < v < 1$ . Numerical evidence of the dominance of the root  $s_{0_x}$  within the intervals in (5.61)-(5.63) with  $\tau = 0.1$  [s]

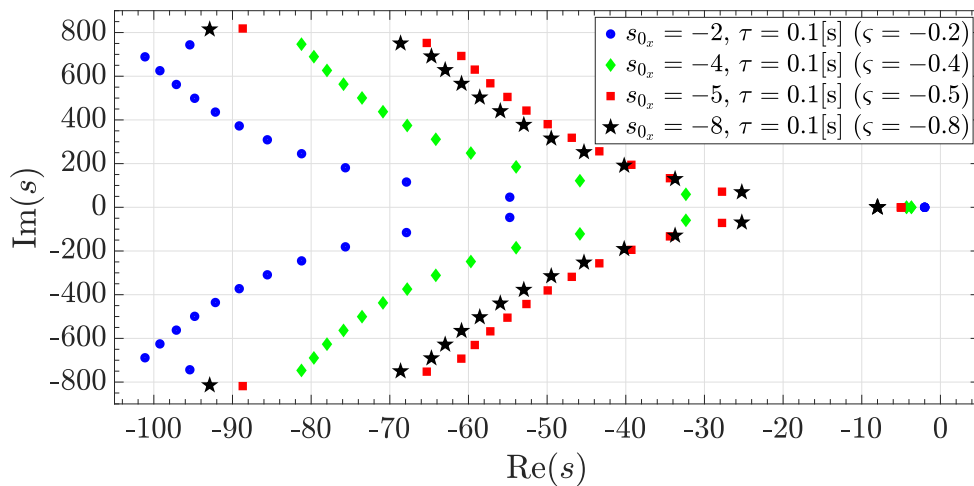


Figure 5.4: Spectral distribution of the roots

#### 5.4 . UAV control: the tilting-rotors case

The analysis of the quadrotor endowed with tilting-rotors takes into consideration the prescribed linearized conditions established in Section 5.3, additionally, the small-angle approximation is extended to the tilt angles of the rotors  $\beta, \alpha$ , i.e.  $C_\beta \approx 1$ ,  $S_\beta \approx \beta$ ,  $C_\alpha \approx 1$  and  $S_\alpha \approx \alpha$ . In this regard, the dynamic model in (5.1), (5.2), (5.6) and (5.8) is linearized such that the corresponding representation in



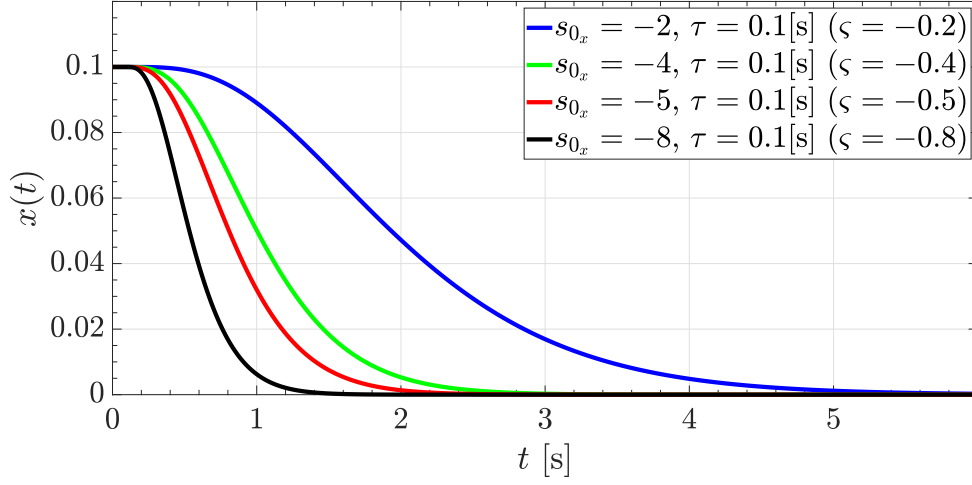


Figure 5.5: Time-domain solution

the frequency domains reads as:

$$\left\{ \begin{array}{l} X(s) = \frac{1}{m_r s^2} ((F_{p_1}(s) + F_{p_3}(s)) \beta(s)), \\ Y(s) = \frac{1}{m_r s^2} (-(F_{p_2}(s) + F_{p_4}(s)) \alpha(s)) \\ Z(s) = \frac{1}{m_r s^2} (T(s) - m_r g), \\ \psi(s) = \frac{1}{I_z s^2} \tau_\psi(s), \\ \phi(s) = \frac{1}{I_x s^2} (\tau_\phi(s) + \rho_\phi(s)), \\ \theta(s) = \frac{1}{I_y s^2} (\tau_\theta(s) + \rho_\theta(s)) \end{array} \right. \quad (5.69)$$

It has been assumed that the rotational dynamics is faster than that of translation such that for a large enough time,  $\phi(s)T(s)$ ,  $\theta(s)T(s) \rightarrow 0$  since  $\phi(s)$ ,  $\theta(s)$ ,  $\psi(s) \rightarrow 0$ . Additionally, the influence of the free-moments  $\varepsilon(F_{p_1}(s) + F_{p_3}(s))\beta(s)$  and  $-\varepsilon(F_{p_2}(s) + F_{p_4}(s))\alpha(s)$  is considered as a disturbance and denoted instead as  $\rho_\phi(s)$  and  $\rho_\theta(s)$ , respectively. In addition, it can be appreciated that the 6 DOFs of the current quadrotor vehicle are decoupled which permits a separate treatment. Additionally, the linearization holds if the vehicle operates at  $\phi, \theta, \psi \approx 0$  thus, the attitude controllers must keep the vehicle at such operational point.

As in Section 5.3, the  $Z(s)$  and  $\psi(s)$  dynamics is addressed firstly as they provide valuable information used in the sequel of the procedure. Thus, let  $T(s)$  and  $\tau_\psi(s)$  be used as the respective control inputs for  $Z(s)$  and  $\psi(s)$  in (5.69). Regarding the  $\phi(s)$  and  $\theta(s)$  motions of the vehicle, the corresponding control inputs  $\tau_\phi(s)$

and  $\tau_\theta(s)$  are defined as

$$\tau_\phi(s) = I_x \mathcal{C}_\phi^*(s) E_\phi(s) \quad \text{and} \quad \tau_\theta(s) = I_y \mathcal{C}_\theta^*(s) E_\theta(s) \quad (5.70)$$

where

$$\mathcal{C}_\phi^*(s) = k_{d_\phi} s + k_{p_\phi} + \frac{k_{i_\phi}}{s} \quad \text{and} \quad \mathcal{C}_\theta^*(s) = k_{d_\theta} s + k_{p_\theta} + \frac{k_{i_\theta}}{s} \quad (5.71)$$

correspond to linear PID controllers with gains  $k_{p_\phi}, k_{p_\theta}, k_{d_\phi}, k_{d_\theta}, k_{i_\phi}, k_{i_\theta} > 0$  since the presence of disturbances could be neutralized by the effects of the integral term. These controllers can be tuned by means of spectral methods.

As in Section 5.3, it is assumed that  $\tau_\psi(s) \rightarrow 0$  and  $T(s) \rightarrow T_c = m_r g$  thus, from the in (5.5), (5.2) and (5.7),  $F_{p1}(s) + F_{p3}(s) \rightarrow T_c/2$  and  $F_{p2}(s) + F_{p4}(s) \rightarrow T_c/2$ . The latter is translated to (5.69) as follows:

$$X(s) = \frac{T_c}{2m_r s^2} \beta(s) \quad \text{and} \quad Y(s) = -\frac{T_c}{2m_r s^2} \alpha(s) \quad (5.72)$$

These assumptions lead to define  $\alpha(s)$  and  $\beta(s)$  as the control inputs that drive the translational states of the system such that:

$$\alpha(s) = -\frac{2m_r}{T_c} \mathcal{C}_y(s) E_y(s) \quad \text{and} \quad \beta(s) = \frac{2m_r}{T_c} \mathcal{C}_x(s) E_x(s) \quad (5.73)$$

with  $\mathcal{C}_x(s)$ ,  $\mathcal{C}_y(s)$ ,  $E_x(s)$  and  $E_y(s)$  being linear PD controllers and the error signals as in (5.14)-(5.15).

The dynamics of the servomotors are neglected since, according to the results reported in the literature (see for instance [163]–[166]), it is relatively faster than that of the overall aircraft. Thus, the  $\alpha(s)$  and  $\beta(s)$  angles are assumed to be instantaneously tracked.

Lastly, the  $X(s)$  and  $\theta(s)$  closed-loop dynamics of the quadrotor with tilting-rotors is depicted as block diagrams in Figure 5.6. The diagram blocks regarding the  $Z(s)$  and  $\psi(s)$  dynamics coincide with those of the typical quadrotor vehicle shown in Figure 5.2.

From Figure 5.6, and recalling that the effect of the time-delay  $\tau$  affects only the translational motion, one can find that the characteristic quasipolynomials of the concerned degrees of freedom are:

$$\begin{cases} \Delta_x(s : k_{p_x}, k_{d_x}, \tau) = s^2 + e^{-\tau s} \mathcal{C}_x(s), \\ \Delta_y(s : k_{p_y}, k_{d_y}, \tau) = s^2 + e^{-\tau s} \mathcal{C}_y(s), \\ \Delta_z(s : k_{p_z}, k_{d_z}, \tau) = s^2 + e^{-\tau s} \mathcal{C}_z(s). \end{cases} \quad (5.74)$$

Since the three characteristic quasipolynomials above have the form of that in (5.20), Proposition 5.3.2 is used to tune the controller gains.

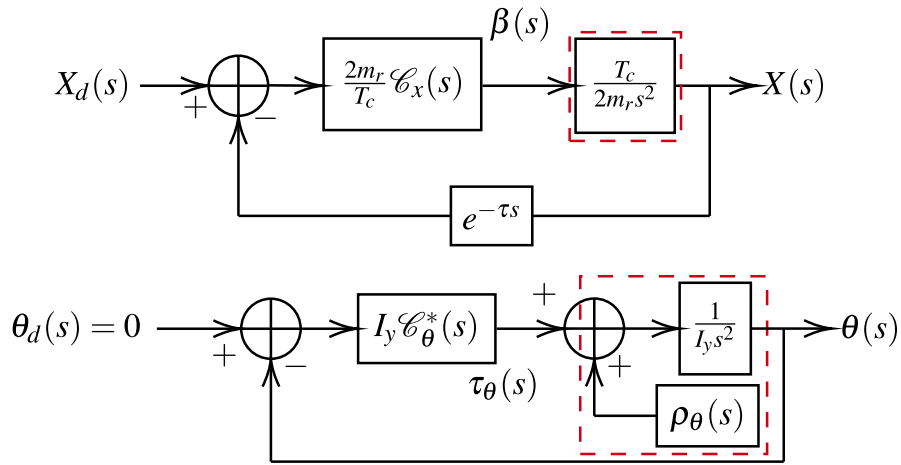


Figure 5.6: Block diagram representation of the quadrotor with tilting-rotors closed-loop system

## 5.5 . Simulation results

The actual section provides the results validating the proposed control scheme and tuning criteria. In this regard, a set of detailed numerical simulations, including the full nonlinear dynamics and the linearized one, was conducted. The parameters

Table 5.1: Parameters of the UAVs

Parameter	Nominal value
$m_r$	0.675 kg
$I_x, I_y$	0.271 kg m <sup>2</sup>
$I_z$	0.133 kg m <sup>2</sup>
$\ell$	0.45 m
$g$	9.81 m/s <sup>2</sup>
$\varepsilon$	0.34 m

Table 5.2: Control gains: Typical quadrotor

DOF	$k_p$	$k_d$
$x, y$	1.658539	1.842677
$z$	7.91223	4.611587
$\phi, \theta$	10.80751	10.65158
$\psi$	10	15
* $x, y$	2.8	2.15
* $z$	8.1	3.64

of the vehicles are listed in Table 5.1 meanwhile, the translational references to be achieved and tracked can be found as:

$$\left\{ \begin{array}{l} x_d(t) = \begin{cases} 0 & 0 \leq t < 20 \\ \frac{20-t}{10} & 20 < t < 30 \\ \frac{t-30}{5} - 1 & 30 < t < 40 \\ 1 - \frac{t-40}{10} & 40 < t < 50 \\ 0 & 50 < t \leq 70 \end{cases} \\ y_d(t) = \begin{cases} 0 & 0 \leq t < 10 \\ 1 & 10 < t < 20 \\ 1 - \frac{t-20}{5} & 20 < t < 30 \\ -1 & 30 < t < 40 \\ \frac{t-40}{5} - 1 & 40 < t < 50 \\ 0 & 50 < t \leq 70 \end{cases} \\ z_d(t) = \begin{cases} 2 & 0 \leq t < 30 \\ 2 - \frac{t-30}{10} & 30 < t < 40 \\ 1 & 40 < t < 60 \\ 0 & 60 < t \leq 70 \end{cases} \end{array} \right. \quad (5.75)$$

where  $x_d(t)$ ,  $y_d(t)$  and  $z_d(t)$  (given in [m]) denote the corresponding references and  $t \geq 0$  stands for the time (in seconds [s]).

The study was conducted within the MATLAB/Simulink<sup>®</sup> 2018b environment, running on an equipment with an 8GB RAM and an Inter<sup>®</sup> Core™ i5-8250 CPU @ 1.60 GHz & 1.80 GHz processor. Finally, the simulations took into consideration a time-delay  $\tau$  of 0.1 [s]. Further details concerning the controller gains and the behavior of each system are provided in the upcoming subsections.

### 5.5.1 . The typical quadrotor case

With base on Proposition 5.3.2, the controller of the altitude ( $z$ ) was tuned. The rightmost root was found to be  $s_{0_z} \approx -5.85786437$ . On the other hand, for the  $x$  and  $y$  controllers, Proposition 5.3.3 was used such that  $s_{0_x} = s_{0_y} = -2$ . The results of the tuning criteria led to the control gains summarized in Table 5.2 where the gains denoted by a  $\star$  where computed (for comparison purposes) with base on

Table 5.3: Control gains: Quadrotor endowed with titling rotors

DOF	$k_p$	$k_d$	$k_i$
$x, y, z$	7.91223	4.611587	
$\phi, \theta$	10	15	0.5
$\psi$	10	15	
$\star x, y, z$	8.1	3.64	

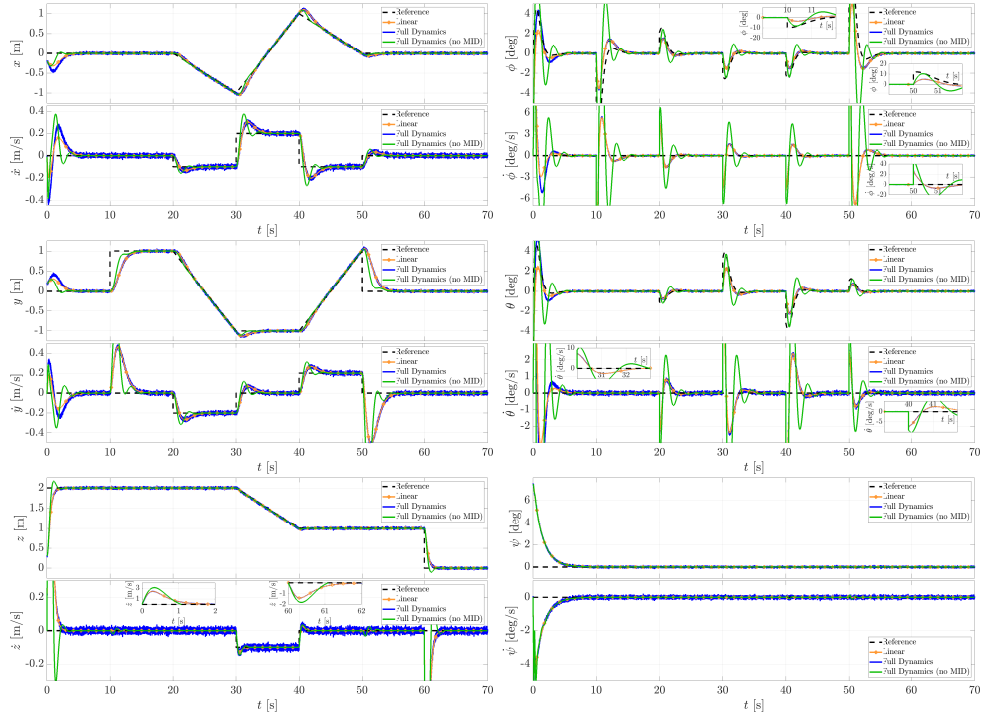


Figure 5.7: Motion of the typical quadrotor vehicle: Left) Translational states. Right) Rotational states.

the results at [167] such that it was considered that  $\sigma_{x,y,z} = s_{0_{x,y,z}}$  to apply the  $\sigma$ -stability criteria. In this matter, it is worth highlighting that with the given control gains  $s_{\phi,1} = s_{\theta,1} \approx -9.515844632$  and  $s_{\phi,2} = s_{\theta,2} \approx -1.135739338$  such that  $s_{\theta,1} < s_{0_x} < s_{\theta,2}$  (respectively  $s_{\phi,1} < s_{0_y} < s_{\phi,2}$ ) thus, the overall dynamics of the system can be considered to be slightly faster than that of the inner loop but still bounded. The results of the numerical simulation depicted throughout Figure 5.7 suggest that such difference is acceptable since the UAV achieves and successfully tracks the desired references.

In Figure 5.7, the left-column results correspond to the vehicle's translational motion, while the right-column plots exhibit the UAV's rotational behavior. In this regard, the black signals stand for the reference values, the blue noisy signals correspond to the response of the nonlinear system and the orange lines describe the behavior of the linearized system. The signals in green depict the behavior of the vehicle whose controllers were tuned with base on the results of [167].

As it can be appreciated in Figure 5.7, the vehicle reaches the desired translational references, moreover, the performance of the nonlinear system matches that of the vehicle whose dynamics is provided by the linear model. Nevertheless, one may pay special attention to the  $z$  motion as the behavior of the vehicle differs; in this sense, the vehicle with nonlinear dynamics experiences some disturbances related to the real couplings existing due to the inherent nature of the UAV, however,

the vehicle converges to the reference value in a relatively short time. Regarding the rotational motion of the quadrotor, depicted in Figure 5.7, it comes to be evident to relate the corresponding peaks on the signals to the corresponding translation DOFs at which they are coupled, such that a change in the desired orientation occurs as the translational desired behavior changes.

In comparison with previous results (see for instance [157], [168]) and the ones depicted in green in Figure 5.7, the vehicle operates with no overshoot or oscillation during the transient phase. The latter occurs as the real part of the dominant roots, for the case depicted in green, is lesser than the corresponding  $\sigma$  yet, these roots have an imaginary component since it is impossible, to know the exact location of the dominant roots meanwhile, the MID tuning criteria allows one to place the dominant roots exactly over the real axis. A similar behavior can be appreciated in the response of the quadrotor with tilting rotors.

### 5.5.2 . The tilting-rotors case

As discussed in Section 5.4, to tune the controllers regarding this quadrotor, Proposition 5.3.2 was used thus, the control gains in Table 5.3 were found. The results of the simulation are depicted throughout Figure 5.8 such that the translational motion is described by the plots at the left, and the plots at the right column depict the rotational states of the corresponding vehicle. The response of the servomotors is also depicted in the corresponding figures.

In comparison with the typical quadrotor vehicle, the translational states of the system seem to follow a similar behavior than that previously obtained, nevertheless, Figure 5.8 shows the existence of a coupling between the three DOFs, in this sense, one may recall the considerations assumed during the linearization and controllers conception such that the couplings are related to the tilting-rotors and the rotational dynamics.

Regarding the rotational motion of the system, depicted in Figure 5.8, it can be appreciated that the states of the system remain near to 0 [deg] as the servomotors' action permits to decouple the rotational and translational motions, at some point and under specific constrains. Nonetheless, the yaw angle seems to present a large deviation from the desired value due to the influence of the servomotors actuation which was neglected during the conception of the controllers yet, the orientation tends to be stabilized with no considerable consequence.

## 5.6 . Chapter Summary

In this chapter, the MID property has been exploited to tune stabilizing controllers of two representative aerial robotic systems. It has been shown by detailed numerical simulations that, by means of the MID property, the effects of the time-delayed feedback that degrade the translational's motion of the vehicles can be mitigated since a proper assignment of the rightmost root of the characteristic function can be performed. As a consequence, the system's convergence rate is

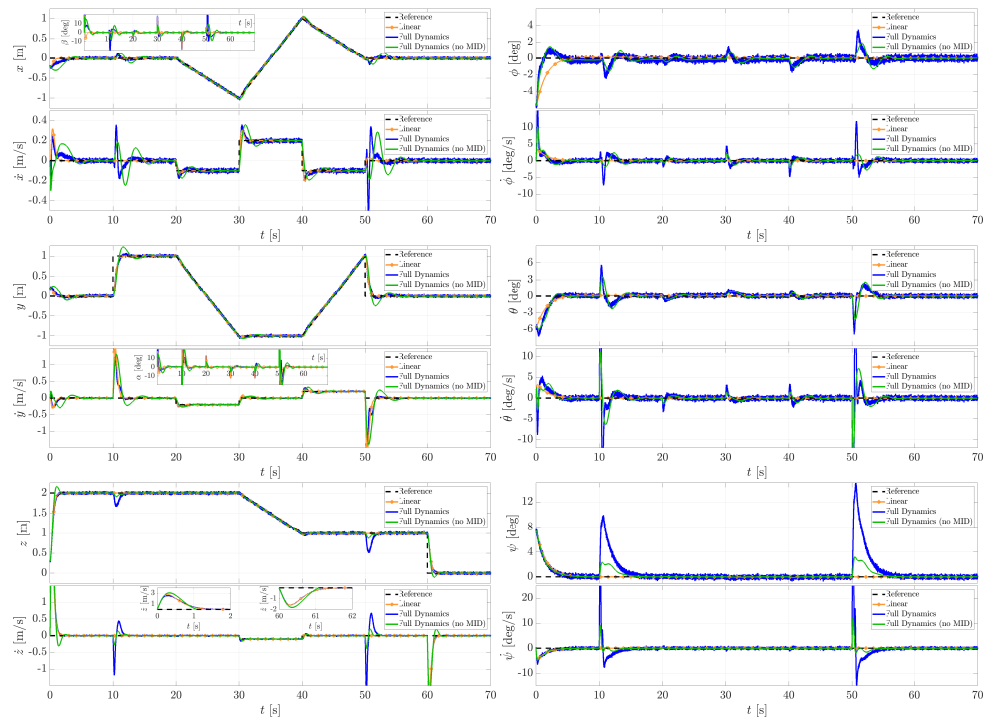


Figure 5.8: Motion of the quadrotor vehicle endowed with tilting-rotors: Left) Translational states. Right) Rotational states.

guaranteed to follow a prescribed behavior such that a fast non-oscillatory response is appreciated. Specific conditions and their corresponding proofs were introduced and detailed, leading to the control gains with respect to the time-delay value. The latter could equally serve as a tuning methodology proposal whether a time-delay can be induced in the feedback loop.

## 6 - Bio-mechanical perspectives: Modeling the CNS Action

This chapter is an extended version of the paper [95]

### 6.1 . Introduction

Another area of application exists, such as, human stance. In fact, the comprehension of human stance is a subject of growing interest since a principal contributor to falls among older adults is an age-related decline in balance. As a matter of fact, in older adults, falls are amongst the most common causes of accidental deaths, and in non-fatal cases the costs related to the treatment of fall-related sequelae are increasing as a consequence of the growing age of populations.

The passive biomechanics of human stance are unstable as they are comprised of interconnected inverted pendulums that are each unstable. The human stance system is the sensorimotor system that permits us to stand upright, walk, etc. Balance may be defined as the ability to maintain equilibrium in a gravitational field by keeping or returning the center of body mass over its base of support [169]. As such, successfulness of balance may be measured by the ability to perform quiet stance, compensatory postural reactions and anticipatory postural responses. This ability is also assessed by reaction time or the controller of the central nervous system (CNS). Hence, simple balancing tasks may be investigated by a mechanical analysis. Stick balancing on fingertip [16], [18], quiet standing [25], [170]–[174], ball and beam balancing [175] and standing on a balance board [176]–[178] have been deeply researched. Indeed, inquiries are based on the mechanical model of a single inverted pendulum, more complex tasks require multi-Degree-Of-Freedom (DOF) models.

The balance board has a configurable geometry: the radius  $R$  of the wheels and the elevation  $h$  between the top of the wheel and the board can be adjusted. Preliminary computations and experiments performed by human subjects showed that the aforementioned parameters highly affect the stabilizability of the associated mathematical model. Standing on the balance board becomes harder as the wheel radius and the board elevation decrease. In case of greater radii ( $R > 100$  mm), balancing subjects use the musculature at the ankle to maintain the equilibrium, so that the human body can be considered as a single inverted pendulum. In contrast, hip strategy is dominant for smaller radii, which indicates a double inverted pendulum model for the human body. In this work, greater wheel radii are considered and therefore a 2-DOF mechanical model is analyzed involving the balance board



and the human body.

Note that even though reaction delays of different sensory systems are different, they are still at the same scale [179]. Consequently, in most of the studies related to human stance, the delays associated with different sensory organs are assumed to be the same [17], [176]. In case of quiet stance, the feedback delay is estimated to be 100-200 ms [20], [180]. Balancing on an unstable, moving surface such as the balance board or skateboard is a more complicated task, therefore the reaction time is higher: 150-300 ms [17], [176], [181].

This chapter considers the stabilization of a rolling balance board by means of the multiplicity-induced-dominancy property. A 2-DOF mechanical model of a human stance on a rolling balance board is analyzed in the sagittal plane. The human body is modeled by an inverted pendulum which connects to the balance board through the ankle joint. The system is stabilized by the ankle torque managed by the central nervous system (CNS). The action of the CNS is modeled by a delayed full state feedback: a pointwise delay stands for all latencies in the neuromechanical system (reaction time, neuromechanical lag, etc.). The aim of the chapter is to achieve a good occurrence in terms of the decay rate, it shows the links with dominancy and with the exponential stability property of the solution in other words, we aim at assigning dominant multiple real roots with admissible codimensions and the MID property is utilized for the mechanical model of human stance on rolling balance board in the sagittal plane.

The chapter is organized as follows. In Section 6.2, human stance on a rolling balance board in the sagittal plane model is described. Section 6.3 is devoted to the mathematical model. The main result is presented in Section 6.4. Finally, Section 6.5 is dedicated to the illustration of the obtained result.

## 6.2 . Mechanical model

Human stance on a rolling balance board in the sagittal plane is described by a 2-DOF mechanical model as shown in Figure 6.1. Similar mechanical models involving a double inverted pendulum can be found in the corresponding literature for various human stance tasks [86], [182]–[185]. The human body is modeled as a homogeneous rigid bar and the balance board is assumed to roll on the horizontal ground. The mass and the height of the human body are denoted by  $m_h$  and  $l$  respectively, therefore the mass moment of inertia of the human body becomes  $I_h = m_h l^2 / 12$  for the center of gravity.

The ankle height is denoted by  $f$  (see Figure 6.1). The ankle joint is located on the left side of the symmetry axis of the balance board expressed by distance

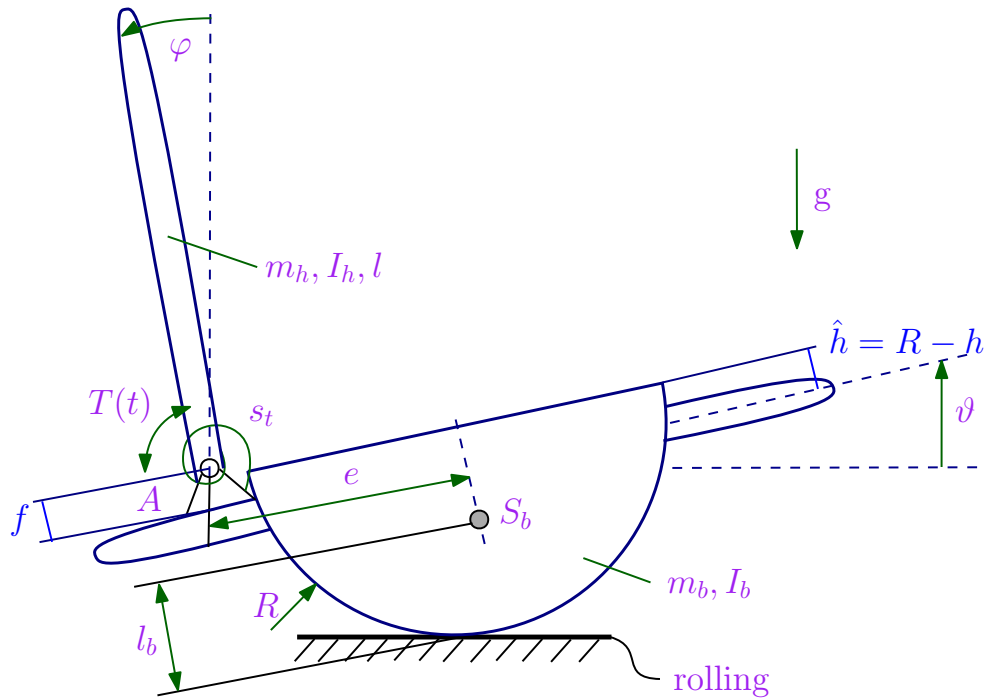


Figure 6.1: 2-DOF mechanical model of human stance on a uniaxial rolling balance board in the sagittal plane.

$e$ . The intrinsic ankle stiffness was considered as a torsional spring of constant stiffness

$$s_t = 0.8m_h g \frac{l}{2}, \quad (6.1)$$

following [185]–[187].

Experimental estimation of the passive damping at the ankle joint is more uncertain than that of the passive stiffness and it also changes with age [174], [188]. Moreover, in case of a single inverted pendulum model subject to delayed PD feedback, the effect of passive damping on the critical delay is negligible [189]. Therefore, here, passive damping at the ankle joint is neglected.

The elements of the balance board were made from plywood with 21 mm thickness. The geometry of the balance board was designed so that two parameters, the wheel radius  $R$  and the board elevation  $h$ , can be adjusted. The difficulty of standing on the balance board can be influenced by these two parameters. The location of the center of gravity  $l_b$ , the mass  $m_b$  and the mass moment of inertia  $I_b$  of the balance board were calculated based on the actual set of the adjustable parameters  $R$  and  $h$ .

The governing equation of the motion was derived with Lagrange's equation

of the second kind and were linearized about the upper unstable equilibrium. The linearized equation of motion reads

$$\mathbf{M}\ddot{\mathbf{q}}(t) + \mathbf{S}\mathbf{q}(t) = \mathbf{Q}(t), \quad (6.2)$$

where  $\mathbf{M}$  is the mass matrix,  $\mathbf{S}$  is the stiffness matrix, and  $\mathbf{Q}(t)$  stands for the vector of generalized forces. The vector of generalized coordinates is

$$\mathbf{q}(t) = \begin{bmatrix} \varphi(t) \\ \vartheta(t) \end{bmatrix} \quad (6.3)$$

where  $\varphi$  is the inclination angle of the human body and  $\vartheta$  is the inclination angle of the balance board, both measured from the equilibrium position. The vector of generalized forces reads

$$\mathbf{Q}(t) = \mathbf{H}T(t), \quad (6.4)$$

where

$$\mathbf{H} = \begin{bmatrix} 1 \\ -1 \end{bmatrix}. \quad (6.5)$$

The operation of the central nervous system (CNS) was modeled as full state feedback  $[\mathbf{q}(t), \dot{\mathbf{q}}(t)]^T$  with a constant lumped delay, which involves all the latencies (reaction time, neuromuscular lag) in the feedback loop. The control torque acts at the ankle joint and becomes

$$T(t) = P_\varphi\varphi(t - \tau) + D_\varphi\dot{\varphi}(t - \tau) + P_\vartheta\vartheta(t - \tau) + D_\vartheta\dot{\vartheta}(t - \tau) \quad (6.6)$$

where  $P_\varphi$ ,  $P_\vartheta$ ,  $D_\varphi$  and  $D_\vartheta$  are the proportional and derivative control gains for  $\varphi$  and  $\vartheta$ ; see [14].

### 6.3 . Mathematical model

The system can be written in state space form by introducing

$$\mathbf{x}(t) = [\mathbf{q}(t), \dot{\mathbf{q}}(t)]^T \quad (6.7)$$

Reformulation of (6.2) gives a compact form:

$$\dot{\mathbf{x}}(t) = \mathbf{A}\mathbf{x}(t) + \mathbf{B}\mathbf{u}(t), \quad (6.8)$$

with

$$\mathbf{u}(t) = \mathbf{K}\mathbf{x}(t - \tau) \quad (6.9)$$

where

$$\mathbf{K} = [P_\varphi \quad P_\vartheta \quad D_\varphi \quad D_\vartheta]. \quad (6.10)$$

The state matrix is

$$\mathbf{A} = \begin{bmatrix} \mathbf{0} & \mathbf{I} \\ -\mathbf{M}^{-1}\mathbf{S} & \mathbf{0} \end{bmatrix} \quad (6.11)$$

where  $\mathbf{0}$  and  $\mathbf{I}$  stand for the  $2 \times 2$  zero and identity matrices and the input matrix is

$$\mathbf{B} = [0 \quad 0 \quad (\mathbf{M}^{-1}\mathbf{H})^T]^T \quad (6.12)$$

The characteristic equation of (6.8)-(6.9) can be given in the form

$$\det(\lambda\mathbf{I} - \mathbf{A} - \mathbf{BK}e^{-s\tau}) = 0, \quad (6.13)$$

which reduces to

$$\begin{cases} \Delta(s) = P_0(s) + P_\tau(s)e^{-s\tau}, & \text{with} \\ P_0(s) = s^4 + a_2s^2 + a_0, & \text{and} \\ P_\tau(s) = b_3s^3 + b_2s^2 + b_1s + b_0. \end{cases} \quad (6.14)$$

Note that in particular,  $P_0(s)$  is a polynomial which has either real roots or complex conjugate roots. It is important to recall that for this type of model, the approach proposed in [77] does not work since it requires a real-rooted polynomial  $P_0$ . Since  $a_0$  is typically a negative parameter, the change of variables ( $\tilde{s} \rightarrow \sqrt[4]{-a_0}s$ ) allows to reduce the analysis to the normalized characteristic function:

$$\begin{cases} \tilde{\Delta}(\tilde{s}) = \tilde{P}_0(\tilde{s}) + \tilde{P}_\tau(\tilde{s})e^{-\tilde{s}\tilde{\tau}} & \text{with} \\ \tilde{P}_0(\tilde{s}) = \tilde{s}^4 + \tilde{a}_2\tilde{s}^2 - 1 & \text{and} \\ \tilde{P}_\tau(\tilde{s}) = \tilde{b}_3\tilde{s}^3 + \tilde{b}_2\tilde{s}^2 + \tilde{b}_1\tilde{s} + \tilde{b}_0, \end{cases}$$

where

$$\begin{cases} \tilde{\tau} = \sqrt[4]{-a_0}\tau, \\ \tilde{a}_2 = a_2/\sqrt{-a_0}, \\ \tilde{b}_k = b_k/(-a_0)^{\frac{4-k}{4}} \quad \text{for } k \in \{0, \dots, 3\}. \end{cases} \quad (6.15)$$

For the sake of simplicity, the symbol  $\tilde{\cdot}$  is omitted. In the sequel, the normalized quasipolynomial function is studied:

$$\Delta(s) = s^4 + a_2s^2 - 1 + (b_3s^3 + b_2s^2 + b_1s + b_0)e^{-s\tau} \quad (6.16)$$

where  $a_2$  stands for the plant parameter which contains all the stiffness and inertial terms. Coefficients  $b_k$  can be considered as control parameters since they are the linear combination of the control gains:

$$b_0 = b_0(P_\varphi, P_\vartheta), \quad (6.17)$$

$$b_1 = b_1(D_\varphi, D_\vartheta), \quad (6.18)$$

$$b_2 = b_2(P_\varphi, P_\vartheta), \quad (6.19)$$

$$b_3 = b_3(D_\varphi, D_\vartheta). \quad (6.20)$$

Finally, the transformation (6.15) is used to reconstruct the appropriate stabilizing conditions for (6.14).

**Remark 6.3.1** *It should be mentioned that the particular structure of the system's dynamics does not allow the use of any of the existing MID results straightforwardly. Thus, for instance, due to the sparsity of the open-loop transfer function, the generic MID cannot be reached and the characterization of the generic MID proposed in [55] does not apply. Moreover, the corresponding plant is not real rooted but its roots are located on real and imaginary axis and the ideas and the approach proposed in [77] cannot apply.*

#### 6.4 . Main results

**Theorem 6.4.1** *Let  $\Delta$  be the quasipolynomial given in (6.16). If the parameters  $a_2$  and  $\tau$  are left free, then the maximal multiplicity of a given root  $s_0$  of (6.16) is 5.*

**Proof** It is recovered that the admissible multiplicity of a real spectral values of the characteristic quasipolynomial is bounded by the generic *Pólya and Szegő bound*, which is equal to the degree of the corresponding quasipolynomial. In particular, according to Definition 1.1.2, the degree of  $\Delta$  in (6.16) is equal to  $\deg_s(\Delta) = PS_B = 8$ . On the other hand, due to the sparsity of the open-loop polynomial ( $P_0(s) = s^4 + a_2s^2 - 1$ ), such a bound cannot be reached. ■

**Theorem 6.4.2** *The root  $s_0$  of (6.16) has multiplicity 5 if, and only if, the system parameters satisfy:*

$$b_k = e^{s_0 \tau} \tau^{k-4} f_k(s_0, \tau), \quad k \in \llbracket 0, 3 \rrbracket \quad (6.21)$$

where  $f_k$  are polynomials in  $s_0$  parametrized in  $a_2$  and  $\tau$  which will be given later, such that,  $f_0$  and  $f_1$  are of degree less than or equal to 3 while  $f_2$  and  $f_3$  are of degree 3. Moreover, if (6.21) is satisfied then  $s_0$  is necessarily dominant).

**Proof** First, the vanishing of the quasipolynomial  $\Delta$  given in (6.16) yields the elimination of the exponential term as a rational function in  $s$ :

$$e^{-\tau s} = -\frac{P_0(s)}{P_\tau(s)} \quad (6.22)$$

where

$$P_0(s) = s^4 + a_2 s^2 - 1, \quad (6.23)$$

$$P_\tau(s) = b_3 s^3 + b_2 s^2 + b_1 s + b_0. \quad (6.24)$$

Next, to investigate potential roots with algebraic multiplicity 5, one substitutes the obtained equality (6.22) in the ideal  $\mathcal{I}_5$  generated by the first four derivatives of  $\Delta$ , that is,  $\mathcal{I}_5 = \langle \partial_s \Delta, \partial_s^2 \Delta, \partial_s^3 \Delta, \partial_s^4 \Delta \rangle$ . This allows to investigate the variety of four algebraic equations in 7 unknowns  $a_2, s, \tau, (b_k)_{k \in \llbracket 0, 3 \rrbracket}$ :

$$P_0(s) P_\tau(s) \tau + P_0'(s) P_\tau(s) - P_\tau'(s) P_0(s) = 0, \quad (6.25)$$

$$-P_0(s) P_\tau(s) \tau^2 + 2P_0'(s) P_0(s) \tau + P_0^{(2)}(s) P_\tau(s) - P_\tau^{(2)}(s) P_0(s) = 0, \quad (6.26)$$

$$P_0(s) P_\tau(s) \tau^3 - 3P_0'(s) P_0(s) \tau^2 + 3P_0^{(2)}(s) P_0(s) \tau + 24s P_\tau(s) = 0, \quad (6.27)$$

$$-P_0(s) P_\tau(s) \tau^4 + 4P_0'(s) P_0(s) \tau^3 - 6P_0^{(2)}(s) P_0(s) \tau^2 = 0. \quad (6.28)$$

The obtained system is a linear system in the unknowns  $(b_k)_{k \in \llbracket 0, 3 \rrbracket}$ . Using standard elimination techniques, one obtains a set of three solutions; the first one, asserts that  $b_k = 0$  for  $k \in \llbracket 0, 3 \rrbracket$ , the second one corresponds to  $s$  as a root of the open-loop polynomial ( $s^4 + a_2 s^2 - 1 = 0$ ) with  $b_2 = -s^3 b_1 - s^2 b_0 - s a_2 b_1 - s b_3 - a_2 b_0$ , which is inconsistent with respect to the transcendental-term elimination (6.22). So that, these two solutions are discarded. The last solution corresponds to  $s = s_0$  as a real root of an elimination polynomial of degree 4 in  $s$ , and  $b_k, k \in \llbracket 0, 3 \rrbracket$  as rational functions in  $(s_0, \tau)$  given by

$$b_k = e^{s_0 \tau} \tau^{k-4} f_k(s_0, \tau), \quad k \in \llbracket 0, 3 \rrbracket, \quad (6.29)$$

with

$$f_k(s_0, \tau) = \sum_{j=0}^3 \alpha_{k,j}(\tau) \tau^j s_0^j, \quad k \in \llbracket 0, 3 \rrbracket, \quad (6.30)$$

The coefficients of the delay-dependent polynomials  $f_k, k \in \llbracket 0, 3 \rrbracket$  are given by:

$$\alpha_{0,3} = -\frac{23P_0''(0)\tau^2}{6} + \frac{2348}{3}, \quad (6.31)$$

$$\alpha_{0,2} = \left(-\frac{(P_0''(0))^2}{12} - \frac{2}{3}\right)\tau^4 - \frac{5P_0''(0)\tau^2}{6} + 5268, \quad (6.32)$$

$$\alpha_{0,1} = \left(-\frac{2(P_0''(0))^2}{3} + \frac{26}{3}\right)\tau^4 + \frac{806P_0''(0)\tau^2}{3} + 7992, \quad (6.33)$$

$$\alpha_{0,0} = 2056 + \frac{P_0''(0)\tau^6}{6} + \left(-\frac{(P_0''(0))^2}{3} - \frac{254}{3}\right)\tau^4 + 510P_0''(0)\tau^2, \quad (6.34)$$

$$\alpha_{1,3} = -\frac{P_0''(0)\tau^2}{2} + 196, \quad \alpha_{1,2} = \frac{5P_0''(0)\tau^2}{2} + 1380, \quad (6.35)$$

$$\alpha_{1,1} = 2\tau^4 + 74P_0''(0)\tau^2 + 2136, \quad (6.36)$$

$$\alpha_{1,0} = -22\tau^4 + 138P_0''(0)\tau^2 + 552, \quad (6.37)$$

$$\alpha_{2,3} = 18, \quad (6.38)$$

$$\alpha_{2,2} = \frac{P_0''(0)\tau^2}{2} + 138, \quad (6.39)$$

$$\alpha_{2,1} = \frac{15P_0''(0)\tau^2}{2} + 228, \quad (6.40)$$

$$\alpha_{2,0} = \frac{29P_0''(0)\tau^2}{2} - 2\tau^4 + 60, \quad (6.41)$$

$$\alpha_{3,3} = \frac{2}{3}, \quad (6.42)$$

$$\alpha_{3,2} = 6, \quad \alpha_{3,1} = \frac{P_0''(0)\tau^2}{6} + 12, \quad (6.43)$$

$$\alpha_{3,0} = \frac{P_0''(0)\tau^2}{2} + 4, \quad (6.44)$$

which concludes the announced result. ■

In our approach, we derive a bound on the imaginary part of roots of the quasipolynomial in the complex right half-plane. In fact, Algorithm 2 gives an appropriate bound on the imaginary part of the characteristic roots (see [91]).

## 6.5 . Illustration example

For the sake of simplicity, case  $e = 0$  is analyzed. Consequently, the upper (unstable) equilibrium becomes  $\mathbf{q}_0 = \mathbf{0}$ . The human mass and height are set to  $m_h = 70$  kg,  $l = 1.7$  m, the wheel radius is  $R = 0.25$  m, the board elevation is  $\hat{h} = 0$ .

Numerical simulations were performed in order to analyze the dynamics of the human body and the balance board for different combinations of control gains. First, the delay was fixed to  $0.1$  s [174], [190], [191] and the characteristic root  $s_0$

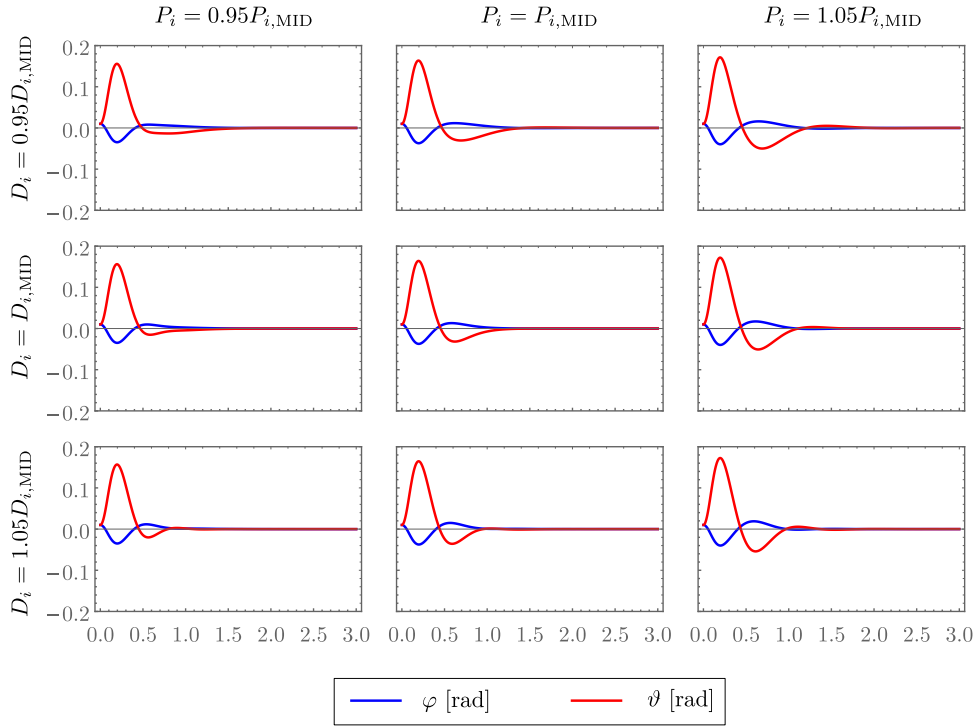


Figure 6.2: 2-DOF mechanical model of human stance on a uniaxial rolling balance board in the sagittal plane.

Table 6.1: Result of MID-based control design

Parameter	Value
$P_{\varphi,\text{MID}}$	2854.4
$P_{\vartheta,\text{MID}}$	1040.34
$D_{\varphi,\text{MID}}$	1082.98
$D_{\vartheta,\text{MID}}$	335.735
$s_0$	-1.63368
$a_2$	7.421572

with multiplicity 5 was determined. Next, the corresponding control parameters  $b_0, b_1, b_2, b_3$  and also the control gains  $P_{\varphi}, P_{\vartheta}, D_{\varphi}, D_{\vartheta}$  were calculated. The results are summarized in Table 6.1. The control gains obtained by the MID-based control design are denoted by  $P_{i,\text{MID}}$  and  $D_{i,\text{MID}}$ , where  $i = \varphi, \vartheta$ . The corresponding time history of human body and balance board angle were determined by numerical simulation. Then, numerical simulations determined the control gains  $P_{\varphi}, P_{\vartheta}$ , and  $D_{\varphi}, D_{\vartheta}$  perturbed by  $\pm 5\%$ . The numerical results can be seen in Figure 6.2.

The initial function over  $t \in (-\tau, 0)$  interval was set to the constant value of



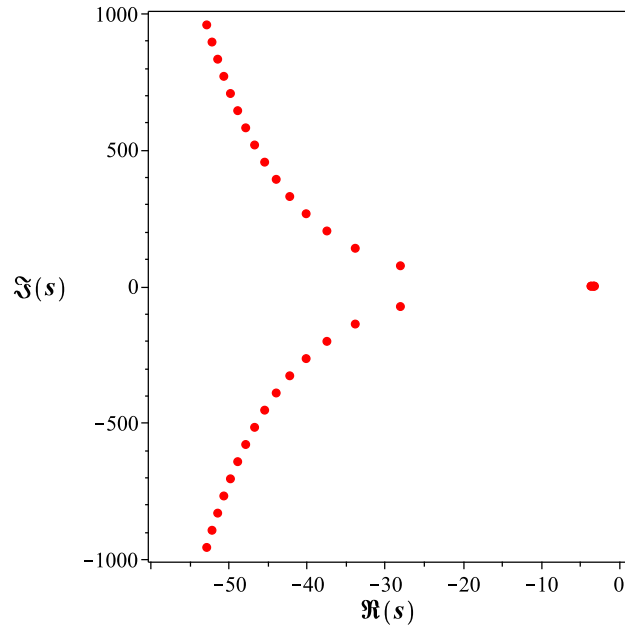


Figure 6.3: Spectrum distribution of the characteristic equation

0.01 rad both for the human body and the balance board angle. One can observe in the middle subplot of Figure 6.2 that the fastest decay rate of the solution is associated with  $P_{\varphi,\text{MID}}$ ,  $P_{\vartheta,\text{MID}}$ ,  $D_{\varphi,\text{MID}}$ ,  $D_{\vartheta,\text{MID}}$  gains obtained by the intermediate MID property.

Figure 6.3 shows the characteristic roots in the considered case.

## 6.6 . Chapter Summary

In this chapter, we extend the validity of the control-oriented MID property. As a matter of fact, the result in [77] applies only for systems with real-rooted open-loop characteristic polynomial. Here, we have employed the MID property to  $P_0(s)$ , a plant not only exhibiting real roots but also complex conjugate roots. Furthermore, a biomechanical application of the MID is considered. A 2-DOF mechanical model of a human stance on a rolling balance board is analyzed in the sagittal plane. The human body is modeled by an inverted pendulum which connects to the balance board through the ankle joint. The system is stabilized by the ankle torque managed by the central nervous system (CNS). The action of the CNS is modeled by a delayed full state feedback.

## 7 - Conclusion and Prospects

### 7.1 . Conclusion

In this dissertation, we considered the problem of exponential stability of linear time-delay systems of neutral type by means of the Multiplicity-Induced-Dominancy (MID) approach. Roughly, this spectral property asserts that, in some cases, the characteristic root with maximal multiplicity is necessarily the rightmost root of the spectrum, that is, this given root of the characteristic function matches the spectral abscissa so that the associated spectral value is dominant.

To cite and assess what has been done on the MID property so far, let us consider the following generic time-delay equation

$$\sum_{k=0}^n a_k x^{(k)}(t) + \sum_{k=0}^m \alpha_k x^{(k)}(t - \tau) = 0, \quad (7.1)$$

where  $x$  is real-valued,  $a_k, \alpha_k \in \mathbb{R}$ , and the delay  $\tau > 0$ . The above time-delay equation in (7.1) is of **retarded** type if  $m < n$  and is of **neutral** type if  $n = m$ .

The MID property proved to be successful in the tackling of the following cases:

1. Time-delay systems of retarded type:
  - The case:  $(n,m)=(2,0)$  in [53]
  - The case:  $(n,m)=(2,1)$  in [50], [82]
  - The case of  $\forall n \in \mathbb{N}$  and  $m = n - 1$  in [55], [156]
2. Time-delay systems of neutral type:
  - The case:  $(n,m)=(1,1)$  in [56]

Note that there are more published results on the time-delay systems of retarded type than neutral time-delay systems. In our work, we focus more on the study of the MID property for neutral time-delay equations. We first extended the result in [56] to the case of  $(n,m) = (2,2)$ ; see [57]. For spectral values of second-order neutral time-delay equations with strictly intermediate admissible multiplicities, the only contributions are provided in [78] where the MID property is extended to codimension 4 i.e. a given root is of intermediate multiplicity equal to 4. We extended in a second step the result in [78], where we improved the understanding and the characterization of the MID property for second-order neutral time-delay equations in the presence of real spectral values with any admissible multiplicity; see [91]. In fact, we explored the effect of multiple roots with admissible multiplicities exhibiting, under appropriate conditions, the validity of the MID property for second-order

neutral time-delay differential equations with a single delay. We summarized the MID methodology in a five-steps algorithm:

1. Forcing multiplicity (maximal or intermediate)
2. Normalization of the characteristic function
3. Factorization of the characteristic function (integral representation)
4. Frequency bound
5. Dominancy

that may be extended to tackle the design of higher-order systems.

More recently, the MID property was shown in the case of arbitrary  $n \geq m$ ; which covers the case of neutral equations; see [76].

As an illustration, we successfully applied this methodology to:

1. Unmanned Aerial Vehicles (UAVs)
2. Human stance control on a rolling balance board

As a matter of fact, we first exploited the effects of time-delays on the stability of UAVs; see [92]. Namely, we provided a symbolic/numeric application of the MID property in the control of UAVs rotorcrafts featuring time-delays. Secondly, we considered the stabilization of a rolling balance board by means of the MID property; see [95]. We extended the validity of the control-oriented MID property and we achieved a good occurrence in terms of decay rate. We also showed the links with dominancy and with the exponential stability property of the solution.

## 7.2 . Prospects

In this dissertation, we terminated the study of the stabilization of time-delay systems of neutral type up to degree 2, and that allows to cover some interesting applications; see above. However, this does not prevent us from opening up to other interesting questions which revolves around our approach. Hereafter, some of these open questions are described.

**Real-time implementation:** We investigated the effects of time-delays on the stability of UAVs [92], where symbolic/numeric application of the MID property is provided. Up to our knowledge, a similar analytical and/or symbolic/numerical method to accurately determine the gains of the controllers for quadrotors, under

the conditions herein considered, is not available in current related literature. As a short-term application, we would like to try in the near future to organize the experimental validation of the approach for the quadrotors.

**Further extensions of the MID property:** After having worked on some extensions of the MID property, we are still curious to look at other extensions. Several configurations of the MID property are of our interest:

- In the application part of our results, we were interested in human stance problems. We therefore applied the MID property to stabilize the rolling balance board. Indeed, the result in [77] applied only for systems with real-rooted open-loop characteristic polynomial. Relaxing such a requirement to systems with open-loop characteristic polynomials having not only real roots but also complex conjugate roots is a further theoretical development that we would like to investigate.
- In our results, we basically extended the results on the MID property to second-order time-delay equations. So far, the extensions we have made suggest to investigate the MID property for *higher orders* in configurations of admissible spectral values of strictly intermediate multiplicity. Furthermore, a more ambitious endeavour would be the extension of the result in [76] to arbitrary neutral equations. However, this may require an indepth knowledge of hypergeometric functions.
- Further questions arise. *Is it possible to choose the systems' parameters in such a way there exist a complex number  $s_0$  and its complex conjugate  $\bar{s}_0$  multiple characteristics roots? Under this choice of the systems' parameters, do  $s_0$  and its complex conjugate  $\bar{s}_0$  are necessarily dominants roots?* These questions are considered in [58] for second order time-delay equation of retarded type (GMID case). Therefore, another important point in theory is to extend the MID property to complex conjugate roots of intermediate multiplicity (IMID case).

**MID property for multi-delay (commensurate delays) equations:**

As mentioned in the introduction, the MID property has been shown for the case of a delayed scalar differential equation of retarded type with two delays; see [87], However, the question of extending the results on the MID property to a neutral time-delay equation with two (or more) delays remains open. This suggest to investigate and explore the GMID property for multi-delay equations. In this regard, let consider the simplest case, generic time-delay scalar equation of neutral type:

$$\dot{x}(t) + a_0x(t) + \alpha_1 \dot{x}(t - \tau_1) + \alpha_0x(t - \tau_1) + \beta_1 \dot{x}(t - \tau_2) + \beta_0x(t - \tau_1) = 0, \quad (7.2)$$

where  $a_0$  and  $\alpha_i, \beta_i$  for  $i = 0, 1$  are real coefficients and  $\tau_i$  for  $i = 0, 1$  are positive delays. The corresponding characteristic equation of (7.2) is given by the following quasipolynomial function

$$\Delta(s) = s + a_0 + (\alpha_1 s + \alpha_0) e^{-\tau_1 s} + (\beta_1 s + \beta_0) e^{-\tau_2 s} \quad (7.3)$$

of degree  $\deg_s(\Delta) = 5$ . Let  $s_0$  be a real root of maximal multiplicity 5 (GMID) of  $\Delta$  in (7.3). Then, the quasipolynomial function  $\Delta$  can be factorized as follow:

$$\Delta(s) = (s - s_0)^5 \int_0^1 \left( q_1(t) e^{-\tau_1 (s - s_0) t} + q_2(t) e^{-\tau_2 (s - s_0) t} \right) dt, \quad (7.4)$$

where  $q_1$  and  $q_2$  are two polynomials depending in  $t$  and in the two parameters (delays)  $\tau_1$  and  $\tau_2$ .

The techniques we use in our approach do not apply directly to the system described above. However, this does not prevent us from writing our quasipolynomial function under the form of a linear combination of hypergeometric functions which have different arguments. In fact, the quasipolynomial function  $\Delta$  can be written under the following combination:

$$\Delta(z) = \alpha \Phi(a, b, \tau_1 z) + \beta \Phi(a, b, \tau_2 z). \quad (7.5)$$

Unfortunately there exist no results that give informations about the distribution of the zeros of this kind of linear combination of hypergeometric functions. Therefore, thinking about methodologies for analysing the integrals in (7.4) and finding other ways to generalise is of our interest.

**Nonlinear time-delay problems:** We could be interested in time-delay nonlinear problems [192]–[196] which intervene in problems very close to what we have already investigated until now. For instance, consider the problem of quenching the oscillations occurring in the Duffing oscillator:

$$\ddot{x}(t) + 2\eta\omega\dot{x}(t) + \omega^2 x(t) + \gamma x^3(t) + u(t - \tau) = 0. \quad (7.6)$$

where  $\eta$  is the damping factor ( $0 < \eta < 1$ ),  $\omega$  describes the natural frequency,  $\gamma$  corresponds to the nonlinearity coefficient,  $\alpha_0, \alpha_1$ , and  $\alpha_2$  ( $\alpha_2 \neq 0$ ) are real coefficients of the delayed external force given by

$$u(t) = \alpha_2 \ddot{x}(t - \tau) + \alpha_1 \dot{x}(t - \tau) + \alpha_0 x(t - \tau). \quad (7.7)$$

The controller structure we consider relies on the knowledge of the position  $x(t)$ , the speed  $\dot{x}(t)$  and the acceleration  $\ddot{x}(t)$ , all of which are delayed. This naturally yields a neutral functional differential equation. We are interested in exploiting the MID property in tuning the gains of such a controller to render the linearized closed-loop system stable, which, in particular, enables the explicit derivation of the delay margin.

When the delay reaches the latter critical value, the spectrum is strictly dominated by a multiple root at zero (with geometric multiplicity one) making the trivial equilibrium point non hyperbolic and of Bogdanov-Takens type. The resulting configuration may be tackled by approximating the local nonlinear infinite dimensional dynamics by the corresponding finite dimensional dynamics occurring in the center manifold. Hence, it is important to establish a parametric analysis on the controller gains to investigate the central dynamics stability.



## A - Proofs of some technical lemmas

**Proof**[ of Lemma 3.5.3] Let  $z_0 = \sigma + i\omega \in \mathbb{R}^* + i\mathbb{R}$  be as in the statement. Thanks to Corollary 3.5.1, one may assume that  $\sigma > 0$ . Since  $z_0$  is a root of  $\hat{\Delta}$ , one has

$$e^{z_0}(z_0^2 - 6z_0 + 12) = z_0^2 + 6z_0 + 12, \quad (\text{A.1})$$

and therefore, in particular,

$$|e^{z_0}|^2 |z_0^2 - 6z_0 + 12|^2 = |z_0^2 + 6z_0 + 12|^2, \quad (\text{A.2})$$

which in turn yields

$$(\omega^4 + (2\sigma^2 - 12\sigma + 12)\omega^2 + \sigma^4 - 12\sigma^3 + 60\sigma^2 - 144\sigma + 144)e^{2\sigma} = \omega^4 + (2\sigma^2 + 12\sigma + 12)\omega^2 + \sigma^4 + 12\sigma^3 + 60\sigma^2 + 144\sigma + 144. \quad (\text{A.3})$$

Furthermore, since  $e^{2\sigma}$  is lower bounded by  $1 + 2\sigma + 2\sigma^2 + \frac{4}{3}\sigma^3$ , one deduces that

$$\begin{aligned} & (2\sigma + 2\sigma^2 + \frac{4}{3}\sigma^3)\omega^4 + ((2\sigma^2 - 12\sigma + 12)(1 + 2\sigma + 2\sigma^2 + \frac{4}{3}\sigma^3) - 2\sigma^2 - 12\sigma \\ & - 12)\omega^2 + (\sigma^4 - 12\sigma^3 + 60\sigma^2 - 144\sigma + 144)(1 + 2\sigma + 2\sigma^2 + \frac{4}{3}\sigma^3) \\ & - \sigma^4 - 12\sigma^3 - 60\sigma^2 - 144\sigma - 144 < 0. \end{aligned} \quad (\text{A.4})$$

Now, setting  $\Omega = \omega^2$ , we define  $f : \Omega \in \mathbb{R} \rightarrow \mathbb{R}$  the following second degree polynomial

$$\begin{aligned} f(\Omega) &= (2x + 2x^2 + \frac{4}{3}x^3)\Omega^2 + ((2x^2 - 12x + 12)(1 + 2x + 2x^2 + \frac{4}{3}x^3) - 2x^2 - 12x \\ & - 12)\Omega + (x^4 - 12x^3 + 60x^2 - 144x + 144)(1 + 2x + 2x^2 + \frac{4}{3}x^3) - x^4 - 12x^3 \\ & - 60x^2 - 144x - 144, \end{aligned} \quad (\text{A.5})$$

the discriminant of which is given by

$$D(x) = x^5 \tilde{D}(x), \quad \text{where} \quad \tilde{D}(x) = -\frac{256}{3}x^3 + 256x^2 + 320x + 768. \quad (\text{A.6})$$

Since  $x > 0$ , the sign of the discriminant  $D$  is equal to that of  $\tilde{D}$ , which admits a unique real root given by



$$x_0 = \frac{(59 + 8\sqrt{43})^{\frac{2}{3}} + 2(59 + 8\sqrt{43})^{\frac{1}{3}} + 9}{2(59 + 8\sqrt{43})^{\frac{1}{3}}}, \quad (\text{A.7})$$

owing to the Cardan-Tartaglia method. Hence, the discriminant  $D$  admits zero as solution and a unique non-zero real solution  $x_0$ , on the one hand. On the other hand, it is negative in the interval  $(x_0, +\infty)$  and tends towards  $-\infty$  at  $\infty$ . Consequently, the discriminant  $D$  is strictly positive for every  $x \in (0, x_0)$ .

In what follows, one is only interested in the latter interval in which the discriminant  $D$  is strictly positive. In this case,  $f$  must admit two real roots, given by

$$\Omega_{\pm}(x) = \frac{(-2x^3 + 9x^2 \pm 2\sqrt{-12x^4 + 36x^3 + 45x^2 + 108x + 3x})x}{2x^2 + 3x + 3}. \quad (\text{A.8})$$

The aim, now, is to determine a bound for the square of the frequency  $\Omega$ . First, One may remark that the quantity given by

$$\Omega_+(x) - \Omega_-(x) = \frac{8x\sqrt{-3(x^3 - 3x^2 - \frac{15}{4}x - 9)}}{2x^2 + 3x + 3} \quad (\text{A.9})$$

is strictly positive for every  $x \in (0, x_0)$ , so that  $\Omega_+$  is the greatest solution. Therefore, we shall investigate the maximum of the branch  $\Omega_+$ , by studying the vanishing of its first derivative, i.e.,

$$\begin{aligned} \Omega'_+(x) = & - \frac{6x(4x^4 - 15x^2 - 45x - 9)\sqrt{-4x(x^3 - 3x^2 - \frac{15}{4}x - 9)}}{(-4x^4 + 12x^3 + 15x^2 + 36x)^{\frac{1}{3}}(2x^2 + 3x + 3)^2} \\ & - \frac{8\sqrt{3}x(6x^5 + 9x^4 - \frac{27x^3}{2} - \frac{297x^2}{4} - 108x - \frac{243}{2})}{(-4x^4 + 12x^3 + 15x^2 + 36x)^{\frac{1}{3}}(2x^2 + 3x + 3)^2} = 0. \end{aligned} \quad (\text{A.10})$$

Or, equivalently, one may investigate the vanishing of its numerator, that is,

$$\begin{aligned} & -((24x^4 - 90x^2 - 270x - 54)\sqrt{-4x(x^3 - 3x^2 - \frac{15}{4}x - 9)} + 8\sqrt{3}(6x^5 + 9x^4 \\ & - \frac{27x^3}{2} - \frac{297x^2}{4} - 108x - \frac{243}{2}))x = 0. \end{aligned} \quad (\text{A.11})$$

By isolating the term  $\sqrt{-4x(x^3 - 3x^2 - \frac{15}{4}x - 9)}$

$$\begin{aligned} & -48(2x - 3)(8x^7 - 36x^6 - 18x^5 + 81x^4 + 594x^3 - 243x^2 - 1188x - 2916) \\ & (2x^2 + 3x + 3)^2 = 0. \end{aligned} \quad (\text{A.12})$$

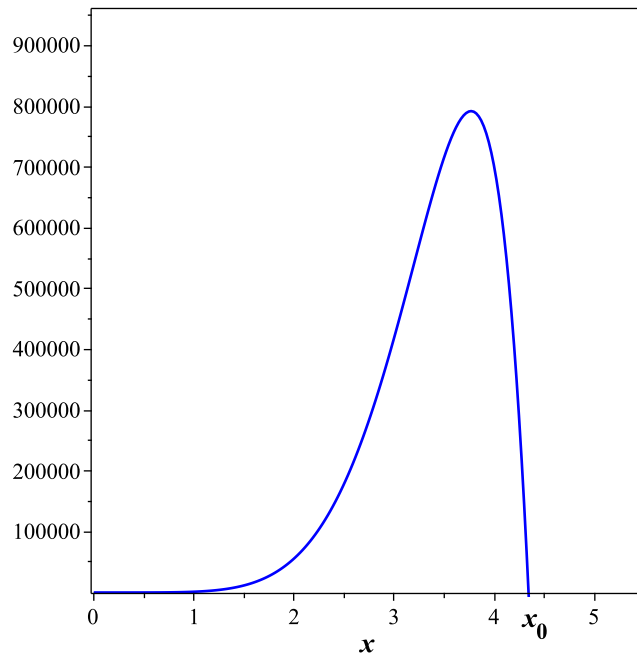


Figure A.1: The discriminant  $D$  of  $f$ .

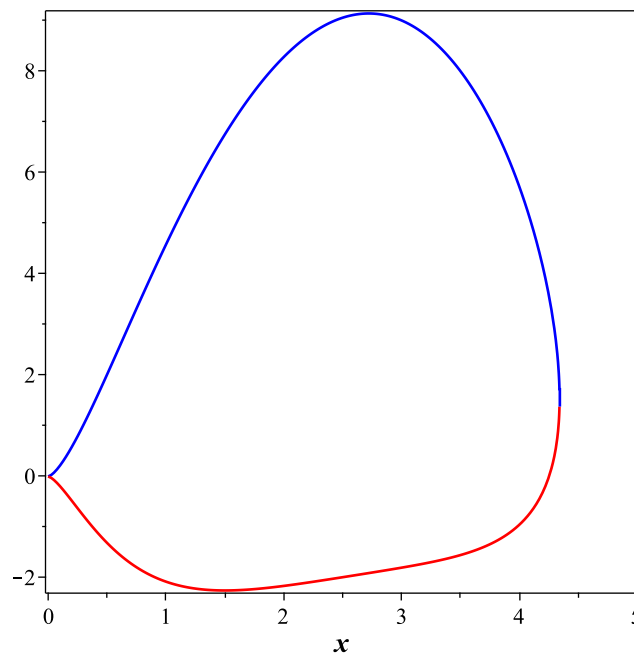


Figure A.2: Graph of  $\Omega_+$  (red) and  $\Omega_-$  (blue).

The polynomial  $2x - 3$  admits one positive root,  $x_1^* = \frac{3}{2}$ , corresponding to the point which minimizes the solution  $\Omega_-$ , while the polynomial  $2x^2 + 3x + 3$  is strictly

positive. Hence, let us investigate the polynomial

$$P(x) = 8x^7 - 36x^6 - 18x^5 + 81x^4 + 594x^3 - 243x^2 - 1188x - 2916. \quad (\text{A.13})$$

To do so, we need to lower the degree to 4 by computing its third-order derivative

$$P^{(3)}(x) = 1680x^4 - 4320x^3 - 1080x^2 + 1944x + 3564, \quad (\text{A.14})$$

the discriminant of which is negative. More precisely, it admits exactly two real roots denoted by  $x_{3,1}$  and  $x_{3,2}$  and which may be explicitly computed by the Ferrari method. Furthermore, one may remark that  $0 < x_{3,1} < x_{3,2} < x_0$ . As a result, the above polynomial has an alternating sign, which means that the second-order derivative of  $P$ , i.e.,

$$P''(x) = 336x^5 - 1080x^4 - 360x^3 + 972x^2 + 3564x - 486, \quad (\text{A.15})$$

has an alternating monotonicity. Namely, it increases from  $P''(0) < 0$  to  $P''(x_{3,1}) > 0$ , it decreases from  $P''(x_{3,1})$  to  $P''(x_{3,2}) < 0$  and by computing its limit at  $\infty$ , one may see that it increases again from  $P''(x_{3,2})$  to  $\infty$ . Then, one deduces that the polynomial given in (A.15) admits three positive roots denoted by  $x_{2,1}$ ,  $x_{2,2}$  and  $x_{2,3}$ . Approximating these roots by a numerical algorithm, one infers that  $x_{2,1} < x_{3,1} < x_{2,2} < x_{3,2} < x_{2,3} < x_0$ . Along the same lines, one may deduce that the derivative of  $P$ ,

$$P'(x) = 56x^6 - 216x^5 - 90x^4 + 324x^3 + 1782x^2 - 486x - 1188, \quad (\text{A.16})$$

admits one positive root, denoted by  $x_{1,1}$  such that  $x_{2,1} < x_{1,1} < x_{3,1}$ . Then, with the same analysis, one may also deduce that the polynomial  $P$  admits a unique positive root denoted by  $x_2^*$  such that  $x_{2,3} < x_2^* < x_0$ .

Using a numerical algorithm, one may approximate this unique solution by  $\{x_2^* \approx 2.72\}$ , which corresponds to the point that maximizes the solution  $\Omega_+$  at  $\Omega_+^* \approx 9.13$ . As a result,  $\omega$  is bounded by  $\omega^* \approx 3.02$ , that is,  $0 < \omega \leq 3.02 < \pi$  as required.

The spectrum distribution of the characteristic function  $\hat{\Delta}$  is represented in Figure 3.2 which permits to visualize the zero-level curves of the real and imaginary parts of the quasipolynomial  $\hat{\Delta}$  over the complex plane, see for instance [197].

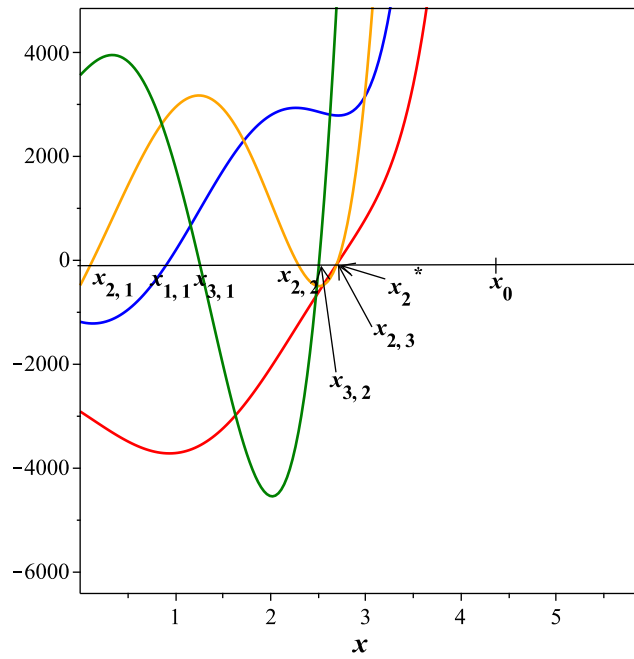


Figure A.3: Graphs of  $P$  (red),  $P'$  (blue),  $P^2$  (brown) and  $P^3$  (green).

**Proof**[of lemma 3.5.4]

Note that if  $i\rho$  is a root of  $\hat{\Delta}$ , then

$$\begin{aligned}
\hat{\Delta}(i\xi) = 0 &\iff (-\xi^2 + 12 + \xi^2 C(\xi) - 6\xi S(\xi) - 12C(\xi)) \\
&\quad + i(-6\xi - \xi^2 S(\xi) - 6\xi C(\xi) + 12S(\xi)) = 0 \\
\hat{\Delta}(i\xi) = 0 &\iff (-\xi^2 + 12 + \xi^2 C(\xi) - 6\xi S(\xi) - 12C(\xi)) \\
&\quad + i(-6\xi - \xi^2 S(\xi) - 6\xi C(\xi) + 12S(\xi)) = 0 \\
&\iff \begin{cases} -\xi^2 + 12 + \xi^2 C(\xi) - 6\xi S(\xi) - 12C(\xi) = 0 \\ -6\xi - \xi^2 S(\xi) - 6\xi C(\xi) + 12S(\xi) = 0 \end{cases} \\
&\iff \begin{cases} -\xi^2 + 12 + (\xi^2 - 12)C(\xi) - 6\xi S(\xi) = 0 \\ (-\xi^2 + 12)S(\xi) - 6\xi C(\xi) - 6\xi = 0 \end{cases} \\
&\iff R_{-\xi} \begin{pmatrix} \xi^2 - 12 \\ -6\xi \end{pmatrix} = \begin{pmatrix} \xi^2 - 12 \\ 6\xi \end{pmatrix} \\
&\iff R_{-\frac{\xi}{2}} R_{-\frac{\xi}{2}} \begin{pmatrix} \xi^2 - 12 \\ -6\xi \end{pmatrix} = \begin{pmatrix} \xi^2 - 12 \\ 6\xi \end{pmatrix} \\
&\iff R_{-\frac{\xi}{2}} \begin{pmatrix} \xi^2 - 12 \\ -6\xi \end{pmatrix} = R_{-\frac{\xi}{2}}^{-1} \begin{pmatrix} \xi^2 - 12 \\ 6\xi \end{pmatrix} \\
&\iff R_{-\frac{\xi}{2}} \begin{pmatrix} \xi^2 - 12 \\ -6\xi \end{pmatrix} = R_{\frac{\xi}{2}} \begin{pmatrix} \xi^2 - 12 \\ 6\xi \end{pmatrix} \\
&\iff -(\xi^2 - 12)S\left(\frac{\xi}{2}\right) - 6\xi C\left(\frac{\xi}{2}\right) = (\xi^2 - 12)S\left(\frac{\xi}{2}\right) + 6\xi C\left(\frac{\xi}{2}\right) \\
&\iff -2(\xi^2 - 12)S\left(\frac{\xi}{2}\right) = 12\xi C\left(\frac{\xi}{2}\right) \\
&\iff (12 - \xi^2)S\left(\frac{\xi}{2}\right) = 6\xi C\left(\frac{\xi}{2}\right) \\
&\iff (12 - \xi^2) \frac{S\left(\frac{\xi}{2}\right)}{C\left(\frac{\xi}{2}\right)} = 6\xi \\
&\iff \frac{S\left(\frac{\xi}{2}\right)}{C\left(\frac{\xi}{2}\right)} = \frac{6\xi}{12 - \xi^2} \\
&\iff \tan\left(\frac{\xi}{2}\right) = \frac{6\xi}{12 - \xi^2}
\end{aligned}$$

where  $C(\bullet) = \cos(\bullet)$ ,  $S(\bullet) = \sin(\bullet)$  and

$$R_{\xi} = \begin{pmatrix} C(\xi) & -S(\xi) \\ S(\xi) & C(\xi) \end{pmatrix} \quad (\text{A.17})$$

such that the following properties hold

$$R_{\xi}^{-1} = R_{\xi}, \quad R_{\xi_1 + \xi_2} = R_{\xi_1} \cdot R_{\xi_2}. \quad (\text{A.18})$$

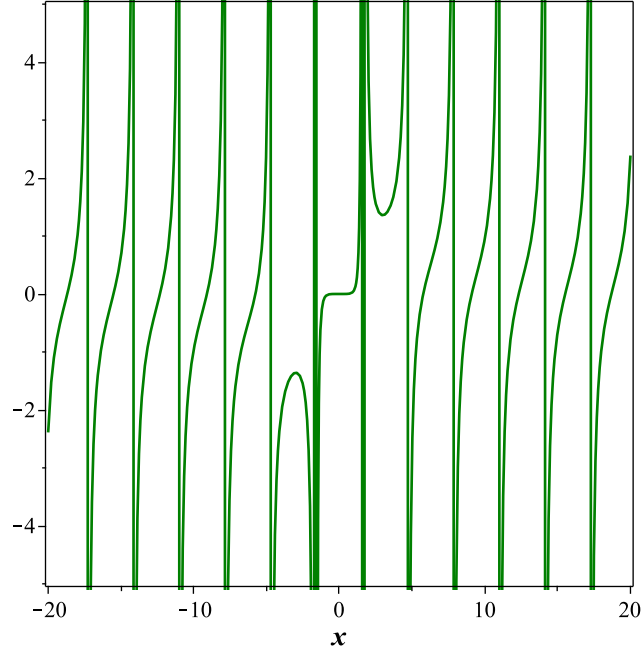


Figure A.4: Plot of solutions of the equation  $\tan(\xi) = \frac{3\xi}{3-\xi^2}$ .

**Proof**[of lemma 4.5.1] It follows immediately from the normalization that  $s_0$  is a root of multiplicity 3 of  $\Delta$  if, and only if, 0 is a root of multiplicity 3 of  $\tilde{\Delta}$ . As a matter of fact, zero is a root of multiplicity 3 of  $\tilde{\Delta}$  if, and only if,  $\tilde{\Delta}(0) = \tilde{\Delta}'(0) = \tilde{\Delta}^{(2)}(0) = 0$ . Hence, we obtain the linear system

$$b_0 + \beta_0 = -\beta_0 + \beta_1 + b_1 = 2 + \beta_0 - 2\beta_1 + 2\beta_2 = 0 \quad (\text{A.19})$$

whose solution is  $(\beta_0, \beta_1, \beta_2) = (-b_0, -b_0 - b_1, -1 - \frac{b_0}{2} - b_1)$ , where

$$\begin{cases} b_0 = (s_0^2 + a_1 s_0 + a_0) \tau^2, \\ b_1 = 2\tau (s_0 + \frac{1}{2} a_1) \\ \beta_0 = \tau^2 (\alpha_2 s_0^2 + \alpha_1 s_0 + \alpha_0) e^{-s_0 \tau}, \\ \beta_1 = 2\tau (\alpha_2 s_0 + \frac{1}{2} \alpha_1) e^{-s_0 \tau}, \\ \beta_2 = \alpha_2 e^{-s_0 \tau}, \end{cases} \quad (\text{A.20})$$

which completes the proof. ■

**Proof**[ of lemma 4.5.2] The polynomial  $q_{\delta,v}$  admits two roots given by

$$t^{\pm} = \frac{(-v \pm \sqrt{v^2 - 2\delta})}{\delta}. \quad (\text{A.21})$$

Since, for  $v^2 - 2\delta < 0$ , the polynomial  $q_{\delta,v}$  does not admit real roots, then  $q_{\delta,v}$  has a constant sign in  $(0, 1)$ . If  $v^2 - 2\delta \geq 0$ , then  $q_{\delta,v}$  admits two real roots  $t^{\pm}$ ; sub-cases are to be considered with respect to the sign of  $\delta$ .

1. If  $\delta > 0$ , then  $t^- \leq t^+$  and the assumption  $v^2 - 2\delta \geq 0$  is equivalent to  $v \leq -\sqrt{2\delta}$  or  $v \geq \sqrt{2\delta}$ . Since  $\delta > 0$ , one has

$$\begin{aligned} \delta > 0 &\iff \underbrace{v^2 - 2\delta}_{\geq 0 \text{ by assumption}} < v^2 \\ &\iff \sqrt{v^2 - 2\delta} < |v| \\ &\iff \frac{1}{\delta} \left( -|v| + \sqrt{v^2 - 2\delta} \right) < 0. \end{aligned}$$

The latter inequality is split in two cases.

- (a) If  $v \geq \sqrt{2\delta}$ , then  $t^+ < 0$ . As a result,  $q_{\delta,v}$  has no roots in  $(0, 1)$  which guarantees its sign constancy.
- (b) If  $v \leq -\sqrt{2\delta}$ , then  $t^- > 0$ . In this case, we need to look for conditions guaranteeing that  $t^- \geq 1$ .

$$\begin{aligned} t^- \geq 1 &\iff \frac{1}{\delta} \left( -v - \sqrt{v^2 - 2\delta} \right) \geq 1 \\ &\iff -v - \sqrt{v^2 - 2\delta} \geq \delta \quad (\text{since } \delta > 0) \\ &\iff \sqrt{v^2 - 2\delta} \leq \underbrace{-\delta - v}_{\geq 0 \implies -\delta \geq v} \\ &\iff v^2 - 2\delta \leq (\delta + v)^2 \\ &\iff v^2 - 2\delta \leq \delta^2 + 2\delta v + v^2 \\ &\iff -2\delta - \delta^2 - 2\delta v \leq 0 \\ &\iff 2\delta + \delta^2 + 2\delta v \geq 0 \\ &\iff \underbrace{\delta}_{>0} (2v + 2 + \delta) \geq 0 \\ &\iff -1 - \frac{\delta}{2} \leq v. \end{aligned}$$

Consequently,  $t^- \geq 1$  if, and only if,

$$-\frac{\delta}{2} - 1 \leq v \leq -\delta, \quad \forall \delta > 0. \quad (\text{A.22})$$

As a conclusion, if  $\delta > 0$ , then the quadratic polynomial  $q_{\delta,v}$  has constant sign for  $t \in (0,1)$  if, and only if,  $(\delta, v) \in \mathbb{R}_q^1$ .

2. If  $\delta < 0$ , then the assumption  $v^2 - 2\delta \geq 0$  is obviously satisfied and we can notice that  $t^- > 0$ ,  $t^+ < 0$  and  $t^- > t^+$ . In this case, we need to look for conditions under which  $t^- \geq 1$ .

$$\begin{aligned} t^- \geq 1 &\iff \frac{1}{\delta} \left( -v - \sqrt{v^2 - 2\delta} \right) \geq 1 \\ &\iff \sqrt{v^2 - 2\delta} \geq -\delta - v \end{aligned} \quad (\text{A.23})$$

As a conclusion, the condition under which  $t^- \geq 1$  which is equivalent to  $\sqrt{v^2 - 2\delta} \geq -\delta - v$ .

Now, consider two cases.

- (a) If  $-\delta - v \geq 0$ , then  $\sqrt{v^2 - 2\delta} \geq -\delta - v$  is equivalent to

$$-\frac{\delta}{2} - 1 \leq v \leq -\delta, \quad \forall \delta < 0. \quad (\text{A.24})$$

- (b) If  $-\delta - v < 0$ , then  $\sqrt{v^2 - 2\delta} \geq -\delta - v$  is immediately satisfied, so that  $t^- \geq 1$  if

$$v > -\delta, \quad \forall \delta < 0. \quad (\text{A.25})$$

As a conclusion, if  $\delta < 0$ , then the quadratic polynomial  $q_{\delta,v}$  has constant sign for  $t \in (0,1)$  if, and only if,  $(\delta, v) \in \mathbb{R}_q^2$ .

3. If  $\delta = 0$ , then the quadratic polynomial reduces to  $q_{\delta,v}(t) = vt + 1$  which reduces to 1 for  $v = 0$ .

Next, if we assume that  $v \neq 0$ , then  $q_{\delta,v}$  admits one real root given by  $t_0 = -\frac{1}{v}$ . As a matter of fact, one has  $t_0 < 0$  when  $v \leq 0$  and  $t_0 \geq 1$  when  $-1 \leq v < 0$ . Hence,  $q_{\delta,v}$  has constant sign for  $t \in (0,1)$  if, and only if,  $(\delta, v) \in \mathbb{R}_q^3$ .

The announced result is proved. ■



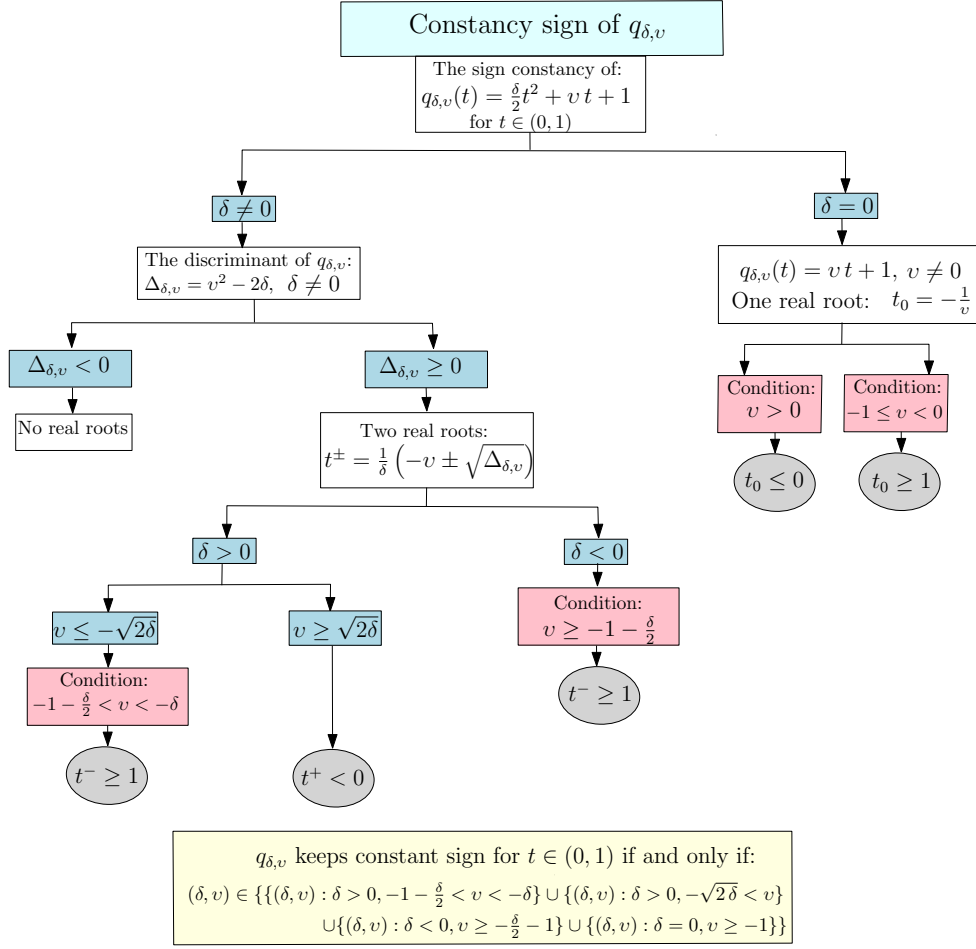


Figure A.5: Diagram representing conditions in parameter space guaranteeing the constancy sign of  $q_{\delta,v}$ .

**Proof**[of lemma 4.5.3] We compute the expression of  $\Upsilon_{\delta,v}$  in terms of  $\delta$  and  $v$ ,

$$\Upsilon_{\delta,v} = -2(2v + \delta + 4)(2v + \delta)^2\delta + (\delta^2 + 3v\delta + 2v^2 + 2\delta)^2. \quad (\text{A.26})$$

As a fourth-degree polynomial with respect to  $v$ ,  $\Upsilon_{\delta,v}$  admits 4 roots.

1. **Case  $\delta > 0$ :** The roots are real such that  $v_1 < v_2 < v_3 < v_4$ , see (4.71-4.74), and

$$\Upsilon_{\delta,v} = 4(v - v_1)(v - v_2)(v - v_3)(v - v_4). \quad (\text{A.27})$$

As a result,

$$\bullet \Upsilon_{\delta,v} > 0 \iff (\delta, v) \in R_1^{++} \cup R_2^{++} \cup R_3^{++};$$

- $\Upsilon_{\delta,v} < 0 \iff (\delta, v) \in R_1^{+-} \cup R_2^{+-}$

2. **Case  $\delta < 0$ :** Consider  $\delta_1$  and  $\delta_2$  given in (4.76). In this case,  $v_1$  and  $v_4$  are well defined for  $\delta \in (-\infty, \delta_1)$ , as for  $v_2$  and  $v_3$  are well defined for  $\delta \in (-\infty, \delta_2)$ . Notice that  $v_1$  and  $v_4$  form a parabola of vertex  $(\delta_1, \delta_+)$ , and that  $v_2$  and  $v_3$  form a parabola of vertex  $(\delta_2, \delta_-)$ , this leads to

- $\Upsilon_{\delta,v} > 0 \iff (\delta, v) \in R_1^{-+} \cup R_2^{-+} \cup R_3^{-+} \cup R_4^{-+} \cup R_5^{-+} \cup R_6^{-+};$

- $\Upsilon_{\delta,v} < 0 \iff (\delta, v) \in R_1^{--} \cup R_2^{--} \cup R_3^{--}.$  ■

**Proof**[of lemma 4.5.4] Considering  $D_{\delta,v}$  as a polynomial of degree 2 with respect to  $x$ , it admits two roots  $x_1 = 0$  and

$$x_2 = \frac{4a_{\delta,v}c_{1,\delta,v}}{-4a_{\delta,v}c_{2,\delta,v} + b_{1,\delta,v}^2}. \quad (\text{A.28})$$

The term  $a_{\delta,v}$  as a polynomial of degree  $\deg_v(a_{\delta,v}) = 2$  with respect to  $v$ , admits 2 real roots given by

$$v \in \left\{ -\frac{\delta}{2} - 2, -\frac{\delta}{2} \right\}, \quad (\text{A.29})$$

so that  $a_{\delta,v}$  is negative if, and only if,

$$(\delta, v) \in R_{a^-} = \left\{ (\delta, v) \in \mathbb{R}^2 : -\frac{\delta}{2} - 2 < v < -\frac{\delta}{2} \right\} \quad (\text{A.30})$$

and positive elsewhere. Note that the region  $R_{a^-}$  is of interest in our analysis. Now, we investigate the sign of  $x_2$  taking into account the signs of  $a_{\delta,v}$  and  $\Upsilon_{\delta,v}$ . Namely, since coefficient  $c_{2,\delta,v} > 0$ , then  $x_2$  is positive if, and only if,

$$(a_{\delta,v} > 0 \text{ and } \Upsilon_{\delta,v} > 0) \text{ or } (a_{\delta,v} < 0 \text{ and } \Upsilon_{\delta,v} < 0),$$

so that  $x_2$  is positive if, and only if,

$$(\delta, v) \in R_{a^-} \cap \{R_1^{+-} \cup R_2^{+-} \cup R_1^{-+} \cup R_2^{-+} \cup R_3^{-+}\} = R_1^{+-}. \quad (\text{A.31})$$

If  $\Upsilon_{\delta,v} > 0$ , then  $D_{\delta,v} > 0$  for  $x \in (-\infty, 0) \cup (x_2, +\infty)$ . As a result, if  $\Upsilon_{\delta,v} < 0$ , then  $D_{\delta,v} > 0$  for  $x \in (0, x_2)$  if, and only if,  $(\delta, v) \in R_1^{+-}$ , as expected. ■

**Proof**[ of lemma 4.5.5] To investigate the sign of  $D_{\delta,v}$ , we first study the sign of its leading coefficient that we denote by

$$A(\delta, v) = 16v^2 - 64\delta, \quad (\text{A.32})$$

a polynomial in  $\delta$  of degree 1, which admits one positive root at  $\delta = \frac{v^2}{4}$ . As a result,  $A(\delta, v)$  is positive if, and only if,

$$(\delta, v) \in R_{A^+} = \left\{ (\delta, v) \in \mathbb{R}^2 : \delta \leq \frac{v^2}{4} \right\} \quad (\text{A.33})$$

and negative if

$$(\delta, v) \in R_{A^-} = \mathbb{R}^2 - R_{A^+}. \quad (\text{A.34})$$

To study the sign of  $D_{\delta,v}$ , as a polynomial in  $x$  of degree  $\deg_x(D_{\delta,v})2$ , we analyse its discriminant which is given by

$$d(\delta, v) = 64(\delta + 2v + 4)(\delta^3 + 4\delta^2v + 4\delta v^2 + 4\delta^2 + 8\delta v - 8v^2 + 36\delta)\delta^2. \quad (\text{A.35})$$

Now, consider

$$d_1(\delta, v) = \delta + 2v + 4, \quad (\text{A.36})$$

as a polynomial in  $\delta$  of degree  $\deg_\delta(d_1) = 1$ , it admits one real root at  $\delta = -2v - 4$ . Next, consider

$$d_2(\delta, v) = (\delta^3 + 4\delta^2v + 4\delta v^2 + 4\delta^2 + 8\delta v - 8v^2 + 36\delta), \quad (\text{A.37})$$

as polynomial in  $\delta$  of degree  $\deg_\delta(d_2) = 3$ , it admits two conjugate roots and, for  $v \in (-1 - 2\sqrt{6}, +\infty)$  one real root

$$\delta^* = \frac{1}{3}\Gamma - \frac{4}{3}(-v^2 - 2v + 23)/\Gamma, \quad (\text{A.38})$$

where

$$\Gamma = \sqrt[3]{8v^3 + 132v^2 + 600v + 584 + 12\sqrt{\tilde{\Gamma}}}, \quad (\text{A.39})$$

with  $\tilde{\Gamma} = 12v^5 + 213v^4 + 1284v^3 + 2988v^2 + 3456v + 7776$ . In the sequel, we shall assume that  $v \in (-1 - 2\sqrt{6}, +\infty)$  which allows to conclude that  $d(\delta, v)$  is positive if,  $(\delta, v) \in R_{d^+} = R_{d^+}^1 \cup R_{d^+}^2 \cup R_{d^+}^3$  where

$$R_{d^+}^1 = \left\{ (\delta, \nu) \in \mathbb{R}^2 : \delta \in \{(-\infty, \delta^*] \cup (-2\nu - 4, \infty)\}, \nu \in (-1 - 2\sqrt{6}, -3] \right\}, \quad (\text{A.40})$$

$$R_{d^+}^1 = \left\{ (\delta, \nu) \in \mathbb{R}^2 : \delta \in (-\infty, -2\nu - 4], \nu \in (-3, -2] \right\}, \quad (\text{A.41})$$

$$R_{d^+}^1 = \left\{ (\delta, \nu) \in \mathbb{R}^2 : \delta \in (\delta^*, \infty), \nu \in (-3, \infty) \right\}. \quad (\text{A.42})$$

■

**Proof**[ of lemma 4.5.6]

Consider  $(\delta, v) \in \tilde{P}_1 \cup \tilde{P}_2 \cup P_3 \cup P_4$ . Since the discriminant of the polynomial function  $G_{\delta, v}$  defined in (4.64-4.65) is positive, then  $G_{\delta, v}$  admits the following two real roots

$$\begin{aligned} \Omega_{\delta, v}^{\pm}(x) = & -\frac{(\delta^2 x + 4 v x \delta + 4 v^2 x + 2 \delta^2 + 6 \delta v + 4 \delta x - 8 x^2 + 12 \delta) x}{\delta^2 + 4 \delta v + 4 v^2 + 4 \delta + 8 v - 8 x} \\ & \pm \frac{\sqrt{\tilde{D}_{\delta, v}(x)}}{\frac{\delta^2}{2} + 2 \delta v + 2 v^2 + 2 \delta + 4 v - 4 x}, \end{aligned} \quad (\text{A.43})$$

where  $\Omega_{\delta, v}^+$  denotes the greater solution (positive signal). We deal with each of the considered regions separately hereafter.

1. **Region  $\tilde{P}_1$ .** Since  $v \in (-2\sqrt{\delta}, 2\sqrt{\delta})$  and  $x > 0$ , the solution  $\Omega_{\delta, v}^+$  is upper bounded with respect to  $v$  by the parameter expression

$$\Omega_{\delta}^+(x) = \frac{h_{1, \delta}(x) - 2x \sqrt{h_{2, \delta}(x)}}{h_{3, \delta}(x)} \quad (\text{A.44})$$

where

$$h_{1, \delta}(x) = 8x^3 + (-\delta^2 + 8\delta^{\frac{3}{2}} - 20\delta)x^2 + (-2\delta^2 + 12\delta^{\frac{3}{2}} - 12\delta)x, \quad (\text{A.45})$$

$$h_{2, \delta}(x) = x(8\delta^3 + 48\delta^{\frac{5}{2}} + 80\delta^2 + 32\delta^{\frac{3}{2}}) - \delta^4 - 4\delta^{\frac{7}{2}} + 8\delta^3 + 40\delta^{\frac{5}{2}} \quad (\text{A.46})$$

$$+ 36\delta^2, \quad (\text{A.47})$$

$$h_{3, \delta}(x) = -8x + \delta^2 - 8\delta^{\frac{3}{2}} + 20\delta - 16\sqrt{\delta}. \quad (\text{A.48})$$

Next, we obtain the following parameter-free upper bound for  $\Omega_{\delta}^+$

$$\Omega^+(x) = \frac{8x^3}{-8x - 4} \quad (\text{A.49})$$

$$+ \frac{2x}{8x + 4} \sqrt{\frac{x(111872\sqrt{2} + 158208)}{(1 + \sqrt{2})^{11}} + \frac{1989312 + 1406656\sqrt{2}}{(1 + \sqrt{2})^{15}}} \quad (\text{A.50})$$

which reaches a maximum value at  $x^* \approx 0.5791$ . Thus,

$$\omega^2 = \Omega_{\delta, v}^+(x) \leq \Omega^+(x^*) \approx 0.3970 < \pi^2, \quad (\text{A.51})$$

i.e.,  $\omega_0 < \pi$ .

Now, we shall detail the assignment of  $s_0$ . From (4.53), we infer that

$$v = -\sqrt{(a_1^2 - 4a_0) \tau^2 + 4\delta} \quad (\text{A.52})$$

for which the following condition needs to be satisfied

$$\delta \geq \left(a_0 - \frac{a_1^2}{4}\right) \tau^2 \quad (\text{A.53})$$

On the other hand, using the fact of  $v \in (-2\sqrt{\delta}, 2\sqrt{\delta})$ , one is able to bound (A.52) in the following way

$$-2\sqrt{\delta} < -\sqrt{(a_1^2 - 4a_0) \tau^2 + 4\delta} < 2\sqrt{\delta} \quad (\text{A.54})$$

which is equivalent to

$$-4\delta < (a_1^2 - 4a_0) \tau^2 < 0 \quad (\text{A.55})$$

The above inequality represents the condition of compatibility in terms of  $a_1$  and  $a_0$  for the assignment of  $s_0$ .

We shall assume henceforth that it holds.

Now, since  $0 < \delta \leq \frac{2}{3+2\sqrt{2}}$  from (A.55), we get

$$0 < \tau^2 (s_0^2 + a_1 s_0 + a_0) \leq \frac{2}{3+2\sqrt{2}}. \quad (\text{A.56})$$

To analyze the previous inequality, we consider each inequality separately below.

(a) **Condition**  $\tau^2 (s_0^2 + a_1 s_0 + a_0) > 0$ . By solving  $\tau^2 (s_0^2 + a_1 s_0 + a_0) = 0$  with respect to  $s_0$ , two roots are obtained:

$$s_{0,A}^{\pm} = -\frac{a_1}{2} \pm \frac{1}{2} \sqrt{a_1^2 - 4a_0} \quad (\text{A.57})$$

So that, two cases are to be considered.

- If  $a_1^2 - 4a_0 < 0$ , then there is no change of the sign, and the set of solution is then given by  $\mathbb{R}$ .
- If  $a_1^2 - 4a_0 \geq 0$ , then

$$s_0 \in \left(-\infty, s_{0,A}^-\right) \cup \left(s_{0,A}^+, +\infty\right). \quad (\text{A.58})$$

(b) **Condition**  $\tau^2 (s_0^2 + a_1 s_0 + a_0) \leq \frac{2}{3+2\sqrt{2}}$ . By solving

$$\tau^2 (s_0^2 + a_1 s_0 + a_0) = \frac{2}{3+2\sqrt{2}} \quad (\text{A.59})$$

with respect to  $s_0$ , we obtain two roots:

$$s_{0,B}^{\pm} = -\frac{a_1}{2} \pm \frac{1}{2} \sqrt{a_1^2 - 4a_0 + \frac{-16\sqrt{2} + 24}{\tau^2}}. \quad (\text{A.60})$$

Since  $\delta \geq \left(a_0 - \frac{a_1^2}{4}\right) \tau^2$  from (A.53), it's guaranteed that

$$a_1^2 - 4a_0 + \frac{-16\sqrt{2} + 24}{\tau^2} \geq 0 \quad (\text{A.61})$$

without any additional condition. Indeed, from (A.53), one has

$$-4\delta + 24 - 16\sqrt{2} \leq (a_1^2 - 4a_0) \tau^2 + 24 - 16\sqrt{2}. \quad (\text{A.62})$$

On the other hand, since  $0 < \delta \leq \frac{2}{3+2\sqrt{2}}$ , one has

$$0 < -\frac{8}{3+2\sqrt{2}} + 24 - 16\sqrt{2} \leq -4\delta + 24 - 16\sqrt{2} < 24 - 16\sqrt{2} \quad (\text{A.63})$$

which guarantee that (A.61) holds. The set of solution in the considered case is given by

$$s_0 \in [s_{0,B}^-, s_{0,B}^+]. \quad (\text{A.64})$$

Finally, the intersection between the set of solutions obtained for the two cases is given by

$$\begin{cases} s_0 \in [s_{0,B}^-, s_{0,B}^+] & \text{if } a_1^2 - 4a_0 < 0 \\ s_0 \in \left\{ \left( -\infty, s_{0,A}^- \right) \cup \left( s_{0,A}^+, +\infty \right) \right\} \cap [s_{0,B}^-, s_{0,B}^+] & \text{otherwise} \end{cases}$$

Now, bearing in mind that

$$s_{0,B}^- < s_{0,A}^- < s_{0,A}^+ < s_{0,B}^+ \quad (\text{A.65})$$

In this case, we conclude that

$$\left\{ \left( -\infty, s_{0,A}^- \right) \cup \left( s_{0,A}^+, +\infty \right) \right\} \cap [s_{0,B}^-, s_{0,B}^+] = [s_{0,B}^-, s_{0,A}^-] \cup \left( s_{0,A}^+, s_{0,B}^+ \right). \quad (\text{A.66})$$



It amounts to conclude that

$$\begin{cases} s_0 \in [s_{0,B}^-, s_{0,B}^+] & \text{if } a_1^2 - 4a_0 < 0 \\ s_0 \in [s_{0,B}^-, s_{0,A}^-) \cup (s_{0,A}^+, s_{0,B}^+] & \text{otherwise} \end{cases}$$

Finally, for the exponential decay  $s_0$  has to be negative, so we impose that that  $s_{0,A}^+ < 0$  and  $s_{0,B}^+ < 0$ .

Analysing the sign of  $s_{0,A}^+$  and  $s_{0,B}^+$ , we deduce that  $s_{0,A}^+$  is negative if and only if

$$a_0 \geq 0 \text{ and } a_1 \geq 0 \quad (\text{A.67})$$

and that  $s_{0,B}^+$  is negative if and only if

$$a_0 \geq \frac{-4\sqrt{2}+6}{\tau^2} \text{ and } a_1 \geq 0 \quad (\text{A.68})$$

It turns out that  $s_0 < 0$  if and only if  $a_1 \geq 0$  and  $a_0 \geq \frac{-4\sqrt{2}+6}{\tau^2}$ .

Finally, we conclude that if the conditions in term of  $a_1$  and  $a_0$

$$a_0 \geq \frac{-4\sqrt{2}+6}{\tau^2} \text{ and } a_1 \geq 0 \quad (\text{A.69})$$

are satisfied, then we are able to assign the root  $s_0$  such that

$$\begin{cases} s_0 \in [s_{0,B}^-, s_{0,B}^+] & \text{if } a_1^2 - 4a_0 < 0 \\ s_0 \in [s_{0,B}^-, s_{0,A}^-) \cup (s_{0,A}^+, s_{0,B}^+] & \text{otherwise} \end{cases} \quad (\text{A.70})$$

2. **Region  $\tilde{P}_2$ .** Since  $v \in [-1 - \delta/2, 2\sqrt{\delta}]$  and  $x > 0$ , the solution  $\Omega_{\delta,v}^+$  is upper bounded with respect to  $v$  by the parameter expression  $\Omega_{\delta}^+(x)$  which is upper bounded with respect to  $\delta$  by the parameter-free expression

$$\Omega^+(x) = \frac{1}{-8x-4} \left( 8x^3 + \frac{(-20-8\sqrt{2})x^2}{3+2\sqrt{2}} + \frac{(-32-24\sqrt{2})x}{(3+2\sqrt{2})^2} \right) \quad (\text{A.71})$$

$$-2x\sqrt{192+x(384+256\sqrt{2})+128\sqrt{2}} \quad (\text{A.72})$$

The latter expression of  $\Omega^+$  depends only in  $x$  and reaches a maximum value on  $x^* \approx 1.9018$ . Thus,  $\omega^2 = \Omega_{\delta,v}^+(x) < \Omega^+(x^*) \approx 6.7190 < \pi^2$ , which implies  $\omega_0 < \pi$ . To assign the root  $s_0$  in this case, we proceed as with the previous region  $\tilde{P}_1$  and conclude that if the following conditions in term of  $a_1$  and  $a_0$

$$a_0 \geq \frac{2}{\tau^2} \text{ and } a_1 \geq 0 \quad (\text{A.73})$$

are satisfied, then we are able to assign the root  $s_0$  such that

$$s_0 \in \left[ s_{0,C}^-, s_{0,B}^- \right) \cup \left( s_{0,B}^+, s_{0,C}^+ \right] \quad (\text{A.74})$$

where

$$s_{0,C}^\pm = -\frac{a_1}{2} \pm \frac{1}{2} \sqrt{a_1^2 - 4a_0 + \frac{8}{\tau^2}}. \quad (\text{A.75})$$

3. **Region  $\tilde{P}_3$ .** Consider  $\delta \in (2, \vartheta)$ , with  $\vartheta > 0$  and follow the same procedure as with previous regions. The table below

$\vartheta$	2.001	2.2	2.3	2.5
$\Omega^+$	8.7083	9.7402	10.2747	11.3748

emphasizes the fact that an interesting frequency bound may be found only for a positive  $\delta$  close to 2, which is not interesting for continuing the next step. Unfortunately for  $\delta \in (2, \infty)$ , the dominance of  $s_0$  cannot be concluded unless the order of truncation of the exponential term is increased as in Algorithm 2 in order to obtain an adequate frequency bound.

4. **Region  $P_3 \cup P_4$ .** Since  $v \in (-\sqrt{2\delta}, v_2)$  and  $x > 0$ , the solution  $\Omega_{\delta,v}^+$  is upper bounded with respect to  $v$  by the parameter expression  $\Omega_\delta^+$ , a function the expression of which we have avoided writing because of its length, this function  $\Omega_\delta^+$  itself can be upper bounded with respect to  $\delta$  by the parameter-free expression

$$\Omega^+(x) = \frac{h_1(x) - 2x\sqrt{h_2(x)}}{(-8x - 4)} \quad (\text{A.76})$$

where

$$h_1(x) = 8x^3 + \left( (-4\sqrt{2} + 6) \sqrt{41 - 28\sqrt{2} + 40\sqrt{2} - 66} \right) x^2 - 8x, \quad (\text{A.77})$$

$$h_2(x) = -64x^2 + x \left( (-3184\sqrt{2} - 4512) \sqrt{16\sqrt{2} - 22 + 2720\sqrt{2} + 3680} \right) \quad (\text{A.78})$$

$$+ (4016\sqrt{2} + 5664) \sqrt{16\sqrt{2} - 22 - 3104\sqrt{2} - 4384}. \quad (\text{A.79})$$

The latter expression of  $\Omega^+$  reaches a maximum value at  $x^* \approx 1.5514$ . Thus,  $\omega^2 = \Omega_{\delta,v}^+(x) < \Omega^+(x^*) \approx 5.1031 < \pi^2$ , i.e.,  $\omega_0 < \pi$ .

To assign the root  $s_0$  in this case, we analyse in a similar way as in the previous cases and we conclude that if the following conditions in term of  $a_1$  and  $a_0$

$$a_0 \geq \frac{(-10\sqrt{2} - 16) \sqrt{16\sqrt{2} - 22 + 16\sqrt{2} + 20}}{4\tau^2} \quad \text{and} \quad a_1 \geq 0 \quad (\text{A.80})$$

are satisfied, then we are able to assign the root  $s_0$  such that

$$s_0 \in \left( s_{0,D}^-, s_{0,C}^- \right) \cup \left( s_{0,C}^+, s_{0,D}^+ \right) \quad (\text{A.81})$$

where

$$s_{0,D}^\pm = -\frac{a_1}{2} \pm \frac{1}{2} \sqrt{a_1^2 - 4a_0 + \frac{(-10\sqrt{2} - 16) \sqrt{16\sqrt{2} - 22 + 16\sqrt{2} + 20}}{\tau^2}}. \quad (\text{A.82})$$

The proof is complete. ■

## Bibliography

- [1] J. K. Hale and S. M. V. Lunel, *Introduction to functional differential equations*, ser. Applied Mathematics Sciences. Springer Verlag, New York, 1993, vol. 99.
- [2] K. Gu, J. Chen, and V. L. Kharitonov, *Stability of time-delay systems*. Springer Science & Business Media, 2003.
- [3] K. Gopalsamy, *Stability and oscillations in delay differential equations of population dynamics*. Springer Science & Business Media, 2013, vol. 74.
- [4] W. Michiels and S.-I. Niculescu, *Stability and stabilization of time-delay systems*, ser. Advances in Design and Control. SIAM, 2007, vol. 12, pp. xxii+378.
- [5] R. Sipahi, S.-I. Niculescu, C. T. Abdallah, W. Michiels, and K. Gu, "Stability and stabilization of systems with time delay," *IEEE Control Systems Magazine*, vol. 31, no. 1, pp. 38–65, 2011.
- [6] K. L. Cooke, "Differential—difference equations," in *International Symposium on Nonlinear Differential Equations and Nonlinear Mechanics*, Elsevier, 2012, p. 155.
- [7] O. Diekmann, S. A. Van Gils, S. M. Lunel, and H.-O. Walther, *Delay equations: functional-, complex-, and nonlinear analysis*. Springer Science & Business Media, 2012, vol. 110.
- [8] W. Michiels and S.-I. Niculescu, *Stability, control, and computation for time-delay systems: an eigenvalue-based approach*. SIAM, 2014.
- [9] T. Vyhlidal, J.-F. Lafay, and R. Sipahi, *Delay systems: From theory to numerics and applications*. Springer Science & Business Media, 2013, vol. 1.
- [10] R. Sipahi, T. Vyhlidal, S.-I. Niculescu, and P. Pepe, *Time delay systems: Methods, applications and new trends*. Springer, 2012.
- [11] G. Valmorbidia, A. Seuret, I. Boussaada, and R. Sipahi, *Delays and interconnections: Methodology, algorithms and applications*. Springer, 2019.
- [12] S.-I. Niculescu, *Delay effects on stability: a robust control approach*. Springer Science & Business Media, 2001, vol. 269.
- [13] V. B. Kolmanovskii and V. R. Nosov, *Stability of functional differential equations*. Elsevier, 1986, vol. 180.

- [14] G. Stepan, "Delay effects in the human sensory system during balancing," *Philosophical Transactions of the Royal Society A: Mathematical, Physical and Engineering Sciences*, vol. 367, no. 1891, pp. 1195–1212, 2009.
- [15] J. R. Chagdes, S. Rietdyk, J. M. Haddad, *et al.*, "Limit cycle oscillations in standing human posture," *Journal of biomechanics*, vol. 49, no. 7, pp. 1170–1179, 2016.
- [16] P. Kowalczyk, P. Glendinning, M. Brown, G. Medrano-Cerda, H. Dallali, and J. Shapiro, "Modelling human balance using switched systems with linear feedback control," *Journal of The Royal Society Interface*, vol. 9, no. 67, pp. 234–245, 2012.
- [17] B. Varszegi, D. Takacs, G. Stepan, and S. J. Hogan, "Stabilizing skateboard speed-wobble with reflex delay," *Journal of The Royal Society Interface*, vol. 13, no. 121, p. 20160345, 2016.
- [18] T. Insperger and J. Milton, "Sensory uncertainty and stick balancing at the fingertip," *Biological Cybernetics*, vol. 108, no. 1, pp. 85–101, 2014.
- [19] L. Zhang, G. Stepan, and T. Insperger, "Saturation limits the contribution of acceleration feedback to balancing against reaction delay," *Journal of the Royal Society Interface*, vol. 15, no. 138, p. 20170771, 2018.
- [20] Y. Asai, Y. Tasaka, K. Nomura, T. Nomura, M. Casadio, and P. Morasso, "A model of postural control in quiet standing: robust compensation of delay-induced instability using intermittent activation of feedback control," *PLoS One*, vol. 4, no. 7, 2009.
- [21] J. L. Cabrera and J. G. Milton, "On-off intermittency in a human balancing task," *Physical Review Letters*, vol. 89, no. 15, p. 158702, 2002.
- [22] N. Yoshikawa, Y. Suzuki, K. Kiyono, and T. Nomura, "Intermittent feedback-control strategy for stabilizing inverted pendulum on manually controlled cart as analogy to human stick balancing," *Frontiers in computational neuroscience*, vol. 10, p. 34, 2016.
- [23] P. Gawthrop, I. Loram, H. Gollee, and M. Lakie, "Intermittent control models of human standing: similarities and differences," *Biological Cybernetics*, vol. 108, no. 2, pp. 159–168, 2014.
- [24] J. Milton, J. L. Townsend, M. A. King, and T. Ohira, "Balancing with positive feedback: the case for discontinuous control," *Philosophical Transactions of the Royal Society A: Mathematical, Physical and Engineering Sciences*, vol. 367, no. 1891, pp. 1181–1193, 2009.

- [25] T. Nomura, S. Oshikawa, Y. Suzuki, K. Kiyono, and P. Morasso, "Modeling human postural sway using an intermittent control and hemodynamic perturbations," *Mathematical biosciences*, vol. 245, no. 1, pp. 86–95, 2013.
- [26] J. Milton, R. Meyer, M. Zhvanetsky, S. Ridge, and T. Insperger, "Control at stability's edge minimizes energetic costs: expert stick balancing," *Journal of The Royal Society Interface*, vol. 13, no. 119, p. 20160212, 2016.
- [27] T. Insperger, J. Milton, and G. Stepan, "Semi-discretization and the time-delayed pda feedback control of human balance," *IFAC-PapersOnLine*, vol. 48, no. 12, pp. 93–98, 2015.
- [28] D. Lehotzky and I. Tamas, "Emberi egyensulyozas mechanikai modellezese PIDA szabalyozo segitsegevel," *Biomechanica Hungarica*, vol. 7, no. 1, pp. 24–33, 2014.
- [29] D. Lehotzky, "Numerical methods for the stability and stabilizability analysis of delayed dynamical systems," Ph.D. dissertation, Budapest University of Technology and Economics, 2016.
- [30] G. Orosz, R. E. Wilson, and G. Stépán, *Traffic jams: dynamics and control*, 2010.
- [31] V. L. Kharitonov, S.-I. Niculescu, J. Moreno, and W. Michiels, "Static output feedback stabilization: necessary conditions for multiple delay controllers," *IEEE transactions on automatic control*, vol. 50, no. 1, pp. 82–86, 2005.
- [32] S.-I. Niculescu and W. Michiels, "Stabilizing a chain of integrators using multiple delays," *IEEE Transactions on Automatic Control*, vol. 49, no. 5, pp. 802–807, 2004.
- [33] K. A. Astrom and R. M. Murray, *Feedback Systems: An Introduction for Scientists and Engineers*. Princeton Univ. Press (2nd edition), 2009.
- [34] A. C. Antoulas, E. D. Sontag, and Y. Yamamoto, "Controllability and observability," in *Wiley Encyclopedia of Electrical Electronics Engineering*, Wiley & Sons, 2001, pp. 264–281.
- [35] F. Al-Musallam, K. Ammari, and B. Chentouf, "Asymptotic behavior of a 2d overhead crane with input delays in the boundary control," *ZAMM-Journal of Applied Mathematics and Mechanics/Zeitschrift fur Angewandte Mathematik und Mechanik*, vol. 98, no. 7, pp. 1103–1122, 2018.

- [36] K. Ammari and B. Chentouf, "Further results on the asymptotic behavior of a 2d overhead crane with input delays: exponential convergence," *arXiv preprint arXiv:1804.06765*, 2018.
- [37] D. Bresch-Pietri and F. Di Meglio, "Prediction-based control of linear input-delay system subject to state-dependent state delay-application to suppression of mechanical vibrations in drilling," *IFAC-PapersOnLine*, vol. 49, no. 8, pp. 111–117, 2016.
- [38] —, "Prediction-based control of linear systems subject to state-dependent state delay and multiple input-delays," in *2017 IEEE 56th Annual Conference on Decision and Control (CDC)*, IEEE, 2017, pp. 3725–3732.
- [39] D. Bresch-Pietri, N. Petit, and M. Krstic, "Prediction-based control for nonlinear state-and input-delay systems with the aim of delay-robustness analysis," in *2015 54th IEEE Conference on Decision and Control (CDC)*, IEEE, 2015, pp. 6403–6409.
- [40] G. Pólya, "Geometrisches über die verteilung der nullstellen gewisser ganzer transzenderter funktionen," 1920. [Online]. Available: <https://publikationen.badw.de/de/003395469>.
- [41] R. E. Langer, "The asymptotic location of the roots of a certain transcendental equation," *Trans. Am. Math. Soc.*, vol. 31, no. 4, pp. 837–844, 1929.
- [42] A. Olbrot, "Stabilizability, detectability, and spectrum assignment for linear autonomous systems with general time delays," *IEEE Trans. Automat. Contrl*, vol. 23, no. 5, pp. 887–890, 1978.
- [43] A. Manitius and A. Olbrot, "Finite spectrum assignment problem for systems with delays," *IEEE Trans. Automat. Contrl*, vol. 24, no. 4, pp. 541–552, 1979.
- [44] Q.-G. Wang, T. H. Lee, and K. K. Tan, *Finite-spectrum assignment for time-delay systems*. Springer Science & Business Media, 1998, vol. 239.
- [45] D. Brethé and J. Loiseau, "An effective algorithm for finite spectrum assignment of single-input systems with delays," *Math. Comput. Simul*, vol. 45, no. 3-4, pp. 339–348, 1998.
- [46] K. Engelborghs, M. Dambrine, and D. Roose, "Limitations of a class of stabilization methods for delay systems," *IEEE Trans. Automat. Contrl*, vol. 46, no. 2, pp. 336–339, 2001.
- [47] J. Ackermann, "The design of linear control systems in the state space," *At-Automatisierungstechnik*, vol. 20, pp. 297–300, 1972.

- [48] T. Vyhlídal, W. Michiels, and P. Zitek, "Quasi-direct pole placement for time delay systems applied to a heat transfer set-up," *IFAC Proceedings Volumes*, vol. 42, no. 14, pp. 325–330, 2009, 8th IFAC Workshop on TDS.
- [49] Y. Ram, J. Mottershea, and M. Tehrani, "Partial pole placement with time delay in structures using the receptance and the system matrices," *Linear. Algebra. Appl.*, vol. 434, no. 7, pp. 1689–1696, 2011.
- [50] I. Boussaada, S.-I. Niculescu, A. El Ati, R. Pérez-Ramos, and K. L. Trabelsi, "Multiplicity-induced-dominancy in parametric second-order delay differential equations: analysis and application in control design," *ESAIM - Control Optim. Calc. Var.*, 2019.
- [51] E. Pinney, *Ordinary difference-differential equations*. Univ. California Press, 1958, pp. xii+262.
- [52] I. Boussaada, H. U. Ünal, and S.-I. Niculescu, "Multiplicity and stable varieties of time-delay systems: a missing link," in *Proceedings of the 22nd ISMTNS*, Minneapolis, MN, USA, Jul. 2016, pp. 188–194.
- [53] I. Boussaada, S. Tliba, S.-I. Niculescu, H. U. Ünal, and T. Vyhlídal, "Further remarks on the effect of multiple spectral values on the dynamics of time-delay systems. application to the control of a mechanical system," *Linear Algebra and its Applications*, vol. 542, pp. 589–604, 2018.
- [54] A. Ramírez, S. Mondié, R. Garrido, and R. Sipahi, "Design of proportional-integral-retarded (PIR) controllers for second-order LTI systems," *IEEE Trans. Automat. Control*, vol. 61, no. 6, pp. 1688–1693, 2016, issn: 0018-9286.
- [55] G. Mazanti, I. Boussaada, and S.-I. Niculescu, "Multiplicity-induced-dominancy for delay-differential equations of retarded type," *Journal of Differential Equations*, vol. 286, pp. 84–118, 2021.
- [56] G. Mazanti, I. Boussaada, S.-I. Niculescu, and Y. Chitour, "Effects of roots of maximal multiplicity on the stability of some classes of delay differential-algebraic systems: the lossless propagation case," *IFAC-PapersOnLine*, vol. 54, no. 9, pp. 764–769, 2021.
- [57] A. Benarab, I. Boussaada, K. Trabelsi, G. Mazanti, and C. Bonnet, "The MID property for a second-order neutral time-delay differential equation," in *2020 24th ICSTCC*, 2020, pp. 202–207.



- [58] G. Mazanti, I. Boussaada, S.-I. Niculescu, and T. Vyhlídal, "Spectral dominance of complex roots for single-delay linear equations," *IFAC-PapersOnLine*, vol. 53, no. 2, pp. 4357–4362, 2020, 21st IFAC World Congress.
- [59] N. G. Chebotarev and N. N. Meiman, "The routh-hurwitz problem for polynomials and entire functions," *Trudy Matematicheskogo Instituta imeni VA Steklova*, vol. 26, pp. 3–331, 1949.
- [60] A. Ronkin, "Quasipolynomials," *Functional Analysis and Its Applications*, vol. 12, no. 4, pp. 321–323, 1978.
- [61] I. Boussaada and S.-I. Niculescu, "Tracking the algebraic multiplicity of crossing imaginary roots for generic quasipolynomials: a vandermonde-based approach," *IEEE Transactions on Automatic Control*, vol. 61, no. 6, pp. 1601–1606, 2015.
- [62] N. Olgac, T. Vyhlídal, and R. Sipahi, "Exact stability analysis of neutral systems with cross-talking delays," *IFAC Proceedings Volumes*, vol. 39, no. 10, pp. 175–180, 2006.
- [63] S. Damak, M. Di Loreto, and S. Mondié, "Stability of linear continuous-time difference equations with distributed delay: constructive exponential estimates," *International Journal of Robust and Non-linear Control*, vol. 25, no. 17, pp. 3195–3209, 2015.
- [64] T. Vyhlídal, N. Olgac, and V. Kucera, "Delayed resonator with acceleration feedback—complete stability analysis by spectral methods and vibration absorber design," *Journal of Sound and Vibration*, vol. 333, no. 25, pp. 6781–6795, 2014.
- [65] D. Pilbauer, T. Vyhlídal, and N. Olgac, "Delayed resonator with distributed delay in acceleration feedback—design and experimental verification," *IEEE/ASME Transactions on Mechatronics*, vol. 21, no. 4, pp. 2120–2131, 2016.
- [66] T. Vyhlídal, D. Pilbauer, B. Alikoç, and W. Michiels, "Analysis and design aspects of delayed resonator absorber with position, velocity or acceleration feedback," *Journal of Sound and Vibration*, vol. 459, p. 114 831, 2019.
- [67] R. Bellman and K. Cooke, *Differential-difference equations*. New York: Academic Press, 1963, pp. xvi+462.
- [68] K.-L. Cooke and P. van den Driessche, "On zeroes of some transcendental equations," *Funkcial. Ekvac.*, vol. 29, no. 1, pp. 77–90, 1986.

- [69] K. Walton and J. E. Marshall, "Direct method for tds stability analysis," *IEE Proceedings D - Control Theory and Applications*, vol. 134, no. 2, pp. 101–107, 1987.
- [70] G. Stépán, *Retarded Dynamical Systems: Stability and Characteristic Functions*, ser. Pitman research notes in mathematics series. Longman Sci. and Tech., 1989.
- [71] N. Olgac and R. Sipahi, "An exact method for the stability analysis of time delayed linear time-invariant (lti) systems.," *IEEE Transactions on Automatic Control*, vol. 47, no. 5, pp. 793–797, 2002.
- [72] G. Pólya and G. Szegő, *Problems and Theorems in Analysis, Vol. I: Series, Integral Calculus, Theory of Functions*. New York, Heidelberg, and Berlin: Springer-Verlag, 1972.
- [73] I. Boussaada and S.-I. Niculescu, "Characterizing the codimension of zero singularities for time-delay systems," *Acta Applicandae Mathematicae*, vol. 145, no. 1, pp. 47–88, 2016.
- [74] I. Boussaada, G. Mazanti, S.-I. Niculescu, J. Huynh, F. Sim, and M. Thomas, "Partial pole placement via delay action: a python software for delayed feedback stabilizing design," in *2020 24th International Conference on System Theory, Control and Computing (ICSTCC)*, IEEE, 2020, pp. 196–201.
- [75] I. Boussaada, G. Mazanti, S.-I. Niculescu, A. Leclerc, J. Raj, and M. Perraudin, "New features of P3delta software: partial pole placement via delay action," *IFAC-PapersOnLine*, vol. 54, no. 18, pp. 215–221, 2021, 16th IFAC Workshop on Time Delay Systems TDS 2021.
- [76] I. Boussaada, G. Mazanti, and S.-I. Niculescu, "The generic multiplicity-induced-dominancy property from retarded to neutral delay-differential equations: when delay-systems characteristics meet the zeros of kummer functions," *Comptes Rendus. Mathématique*, vol. 360, no. G4, pp. 349–369, 2022.
- [77] T. Balogh, I. Boussaada, T. Insperger, and S.-I. Niculescu, "Conditions for stabilizability of time-delay systems with real-rooted plant," *International Journal of Robust and Nonlinear Control*, vol. 32, no. 6, pp. 3206–3224, 2022.
- [78] D. Ma, I. Boussaada, J. Chen, C. Bonnet, S.-I. Niculescu, and J. Chen, "Pid control design for first-order delay systems via mid pole placement: performance vs. robustness," *Automatica*, vol. 137, p. 110 102, 2022.

- [79] N. D. Hayes, "Roots of the transcendental equation associated with a certain difference-differential equation," *Journal of the London Mathematical Society*, vol. s1-25, no. 3, pp. 226–232, 1950, issn: 1469-7750.
- [80] I. Boussaada, S.-I. Niculescu, S. Tliba, and T. Vyhlídal, "On the coalescence of spectral values and its effect on the stability of time-delay systems: application to active vibration control," *Procedia IUTAM*, vol. 22, no. Supplement C, pp. 75–82, 2017.
- [81] I. Boussaada, S.-I. Niculescu, and K. Trabelsi, "Toward a decay rate assignment based design for time-delay systems with multiple spectral values," in *Proceeding of the 23rd International Symposium on Mathematical Theory of Networks and Systems*, 2018, pp. 864–871.
- [82] I. Boussaada and S.-I. Niculescu, "On the dominance of multiple spectral values for time-delay systems with applications," *IFAC-PapersOnLine*, vol. 51, no. 14, pp. 55–60, 2018.
- [83] D. Ma, I. Boussaada, C. Bonnet, S.-I. Niculescu, and J. Chen, "Multiplicity-induced-dominancy extended to neutral delay equations: towards a systematic pid tuning based on rightmost root assignment," in *2020 American Control Conference (ACC)*, IEEE, 2020, pp. 1690–1695.
- [84] B. A. Kovacs and T. Insperger, "Critical parameters for the robust stabilization of the inverted pendulum with reaction delay: state feedback versus predictor feedback," *International Journal of Robust and Nonlinear Control*, 2021.
- [85] T. G. Molnar and T. Insperger, "On the robust stabilizability of unstable systems with feedback delay by finite spectrum assignment," *Journal of Vibration and Control*, vol. 22, no. 3, pp. 649–661, 2016.
- [86] C. A. Molnar, T. Balogh, I. Boussaada, and T. Insperger, "Calculation of the critical delay for the double inverted pendulum," *Journal of Vibration and Control*, vol. 27, no. 3-4, pp. 356–364, 2021.
- [87] S. Fueyo, G. Mazanti, I. Boussaada, Y. Chitour, and S.-I. Niculescu, "Insights into the multiplicity-induced-dominancy for scalar delay-differential equations with two delays," *IFAC-PapersOnLine*, vol. 54, no. 18, pp. 108–114, 2021.
- [88] K. L. Cooke and P. Van Den Driessche, "On zeroes of some transcendental equations," *Funkcialaj Ekvacioj*, vol. 29, no. 1, pp. 77–90, 1986.

- [89] K. Engelborghs and D. Roose, "On stability of lms methods and characteristic roots of delay differential equations," *SIAM Journal on Numerical Analysis*, vol. 40, no. 2, pp. 629–650, 2002.
- [90] E. M. Wright, "Stability criteria and the real roots of a transcendental equation," *J. Soc. Indust. Appl. Math.*, vol. 9, pp. 136–148, 1961, issn: 0368-4245.
- [91] A. Benarab, I. Boussaada, K. Trabelsi, and C. Bonnet, "Multiplicity-induced-dominancy property for second-order neutral differential equations with application in oscillation damping," *European Journal of Control*, p. 100 721, 2022.
- [92] J. J. Castillo-Zamora, I. Boussaada, A. Benarab, and J. Escareno, "Time-delay control of quadrotor unmanned aerial vehicles: a multiplicity-induced-dominancy-based approach," *Journal of Vibration and Control*, p. 10 775 463 221 082 718, 2022.
- [93] A. Benarab, I. Boussaada, S.-I. Niculescu, and K. Trabelsi, "Over one century of spectrum analysis in delay systems: an overview and new trends in pole placement methods," in *17th IFAC Workshop on Time Delay Systems (TDS)*, 2022.
- [94] I. Boussaada, G. Mazanti, S.-I. Niculescu, and A. Benarab, "Mid property for delay systems: insights on spectral values with intermediate multiplicity," *Conference on Decision and Control (CDC)*, 2022.
- [95] A. Benarab, C. A. Molnar, I. Boussaada, K. Trabelsi, T. Insperger, and S.-I. Niculescu, "Rolling balance board robust stabilization: a mid-based design," in *17th IFAC Workshop on Time Delay Systems (TDS)*, 2022.
- [96] F. G. Boese, "Stability with respect to the delay: on a paper of K. L. Cooke and P. van den Driessche," *Journal of Mathematical Analysis and Applications*, vol. 228, no. 2, pp. 293–321, 1998.
- [97] J. R. Partington and C. Bonnet, " $H_\infty$  And bibo stabilization of delay systems of neutral type," *Systems & Control Letters*, vol. 52, no. 3-4, pp. 283–288, 2004.
- [98] C. B. Cardeliquio, A. R. Fioravanti, C. Bonnet, and S.-I. Niculescu, "Stability and stabilization through envelopes for retarded and neutral time-delay systems," *IEEE Transactions on Automatic Control*, vol. 65, no. 4, pp. 1640–1646, 2019.
- [99] T. Mori and H. Kokame, "Stability of  $\dot{x}(t) = Ax(t) + Bx(t - \tau)$ ," *IEEE Transactions on Automatic Control*, vol. 34, pp. 460–462, 1989.

- [100] M. V. Frasson and S. M. V. Lunel, "Large time behaviour of linear functional differential equations," *Integral Equations and Operator Theory*, vol. 47, no. 1, pp. 91–121, 2003.
- [101] G. Silva, A. Datta, and S. Bhattacharyya, "New results on the synthesis of pid controllers," *IEEE transactions on automatic control*, vol. 47, no. 2, pp. 241–252, 2002.
- [102] D. Ma and J. Chen, "Delay margin of low-order systems achievable by pid controllers," *IEEE Transactions on Automatic Control*, vol. 64, no. 5, pp. 1958–1973, 2018.
- [103] S. Amrane, F. Bedouhene, I. Boussaada, and S.-I. Niculescu, "On qualitative properties of low-degree quasipolynomials: further remarks on the spectral abscissa and rightmost-roots assignment," *Bulletin mathématique de la Société des Sciences Mathématiques de Roumanie*, vol. 61, no. 4, pp. 361–381, 2018.
- [104] F. Bedouhene, I. Boussaada, and S.-I. Niculescu, "Real spectral values coexistence and their effect on the stability of time-delay systems: vandermonde matrices and exponential decay," *Comptes Rendus. Mathématique*, vol. 358, no. 9-10, pp. 1011–1032, 2020.
- [105] H. Buchholz, *The confluent hypergeometric function with special emphasis on its applications*, ser. Springer Tracts in Natural Philosophy. Springer-Verlag, 1969, vol. 15, pp. xviii+238.
- [106] A. Erdélyi, W. Magnus, F. Oberhettinger, and F. Tricomi, *Higher transcendental functions. Vol. 1*. Robert E. Krieger Publishing Co., Inc., Melbourne, Fla., 1981, pp. xiii+302, isbn: 0-89874-069-X.
- [107] F. Olver, D. Lozier, R. Boisvert, and C. Clark, Eds., *NIST Handbook of Mathematical Functions*. U.S. Department of Commerce, National Institute of Standards and Technology, Washington, DC; Cambridge University Press, Cambridge, 2010, pp. xvi+951, isbn: 978-0-521-14063-8.
- [108] E. Hille, "Oscillation theorems in the complex domain," *Trans. Am. Math. Soc*, vol. 23, no. 4, pp. 350–385, 1922.
- [109] I. Boussaada, G. Mazanti, and S.-I. Niculescu, "Some remarks on the location of non-asymptotic zeros of Whittaker and Kummer hypergeometric functions," *Bull. Sci. Math.*, vol. 174, Paper No. 103093, 2022.
- [110] R. Driver, D. Sasser, and M. Slater, "The equation  $x'(t) = ax(t) + bx(t - \tau)$  with "small" delay," *The American Mathematical Monthly*, vol. 80, no. 9, pp. 990–995, 1973.

- [111] M. Frasson, "Large time behaviour of neutral delay systems," Ph.D. dissertation, Leiden University, 2005.
- [112] M. Frasson, "Large time behaviour for functional differential equations with dominant eigenvalues of arbitrary order," *Journal of mathematical analysis and applications*, vol. 360, no. 1, pp. 278–292, 2009.
- [113] L. Pontryagin, "On zeros of some transcendental functions (in russian)," *Izvestiya, Akad. Nauk SSSR, Ser. Math*, vol. 6, pp. 115–134, 1942.
- [114] E. Wright, "Solution of the equation  $zez = a$ ," *Bulletin of the American Mathematical Society*, vol. 65, no. 2, pp. 89–93, 1959.
- [115] S. Yi, P. W. Nelson, and A. G. Ulsoy, *Time-delay systems: analysis and control using the Lambert W function*. World Scientific, 2010.
- [116] L. V. Ahlfors, *Complex Analysis*, 3-rd. McGraw-Hill, 1979.
- [117] B. Hassard, "Counting roots of the characteristic equation for linear delay-differential systems," *Journal of Differential Equations*, vol. 136, no. 2, pp. 222–235, 1997.
- [118] G. Stépán, "On the stability of linear differential equations with delay," *Coll. Math. Soc. J. Bolyai*, vol. 30, pp. 971–984, 1979.
- [119] M. Krstic and A. Smyshlyaev, "Backstepping boundary control for first-order hyperbolic pdes and application to systems with actuator and sensor delays," *Systems & Control Letters*, vol. 57, no. 9, pp. 750–758, 2008.
- [120] D. Bresch-Pietri, "Commande robuste de systèmes à retard variable: contributions théoriques et applications au contrôle moteur," Ph.D. dissertation, Ecole Nationale Supérieure des Mines de Paris, 2012.
- [121] J. Auriol, F. Di Meglio, and F. Bribiesca-Argomedo, "Delay robust state feedback stabilization of an underactuated network of two interconnected pde systems," in *2019 American Control Conference (ACC)*, IEEE, 2019, pp. 593–599.
- [122] K. Watanabe and M. Ito, "A process-model control for linear systems with delay," *IEEE Transactions on Automatic control*, vol. 26, no. 6, pp. 1261–1269, 1981.
- [123] S. Mondié and W. Michiels, "Finite spectrum assignment of unstable time-delay systems with a safe implementation," *IEEE Trans. Automat. Contrl*, vol. 48, no. 12, pp. 2207–2212, 2003.

- [124] D. Brethé and J. Loiseau, "A result that could bear fruit for the control of delay-differential systems," in *Proc. 4th IEEE Mediterranean Symp. Control Automation*, 1996, pp. 168–172.
- [125] D. Brethé, "Stabilization and observation of neutral-type delay systems," *IFAC Proceedings Volumes*, vol. 30, no. 6, pp. 865–870, 1997.
- [126] J. J. Loiseau, "Algebraic tools for the control and stabilization of time-delay systems," *Annu. Rev. Control*, vol. 24, pp. 135–149, 2000.
- [127] E. Kamen, P. Khargonekar, and A. Tannenbaum, "Proper stable bezout factorizations and feedback control of linear time-delay systems," *International Journal of Control*, vol. 43, no. 3, pp. 837–857, 1986.
- [128] E. Emre and P. Khargonekar, "Regulation of split linear systems over rings: coefficient-assignment and observers," *IEEE Transactions on Automatic Control*, vol. 27, no. 1, pp. 104–113, 1982.
- [129] D. O'Connor and T. Tarn, "On stabilization by state feedback for neutral differential difference equations," *IEEE Transactions on Automatic Control*, vol. 28, no. 5, pp. 615–618, 1983.
- [130] L. Pandolfi, "Stabilization of neutral functional differential equations," *Journal of Optimization Theory and Applications*, vol. 20, no. 2, pp. 191–204, 1976.
- [131] M. Morf, B. C. Lévy, and S.-Y. Kung, "New results in 2-d systems theory, part i: 2-d polynomial matrices, factorization, and coprimeness," *Proceedings of the IEEE*, vol. 65, no. 6, pp. 861–872, 1977.
- [132] W. Michiels, K. Engelborghs, P. Vansevenant, and D. Roose, "Continuous pole placement for delay equations," *Automatica J. IFAC*, vol. 38, no. 5, pp. 747–761, 2002, issn: 0005-1098.
- [133] W. Michiels and T. Vyhldal, "An eigenvalue based approach for the stabilization of linear time-delay systems of neutral type," *Automatica*, vol. 41, no. 6, pp. 991–998, 2005.
- [134] K. Engelborghs and D. Roose, "Numerical computation of stability and detection of hopf bifurcations of steady state solutions of delay differential equations," *Advances in Computational Mathematics*, vol. 10, no. 3, pp. 271–289, 1999.

- [135] W. Michiels, I. Boussaada, and S.-I. Niculescu, "An explicit formula for the splitting of multiple eigenvalues for nonlinear eigenvalue problems and connections with the linearization for the delay eigenvalue problem," *SIAM Journal on Matrix Analysis and Applications*, vol. 38, no. 2, pp. 599–620, 2017.
- [136] T. Vyhlidal and P. Zitek, "Mapping based algorithm for large-scale computation of quasi-polynomial zeros," *IEEE Transactions on Automatic Control*, vol. 54, no. 1, pp. 171–177, 2009.
- [137] T. Insperger, J. Milton, and G. Stépán, "Acceleration feedback improves balancing against reflex delay," *Journal of the Royal Society Interface*, vol. 10, no. 79, p. 20120763, 2013.
- [138] W. Michiels, I. Boussaada, and S.-I. Niculescu, "An explicit formula for the splitting of multiple eigenvalues for nonlinear eigenvalue problems and connections with the linearization for the delay eigenvalue problem," *SIAM Journal on Matrix Analysis and Applications*, vol. 38, no. 2, pp. 599–620, 2017.
- [139] J. d. J. C. Zamora, "Design, modeling and control of a multi-drone system for aerial manipulation," Ph.D. dissertation, Université Paris-Saclay, 2021.
- [140] F. Ruggiero, V. Lippiello, and A. Ollero, "Aerial manipulation: a literature review," *IEEE Robotics and Automation Letters*, vol. 3, no. 3, pp. 1957–1964, 2018.
- [141] H. Shakhathreh, A. H. Sawalmeh, A. Al-Fuqaha, *et al.*, "Unmanned aerial vehicles (uavs): a survey on civil applications and key research challenges," *IEEE Access*, vol. 7, pp. 48 572–48 634, 2019.
- [142] T. Cabreira, L. Brisolaro, and P. R. Ferreira, "Survey on coverage path planning with unmanned aerial vehicles," *Drones*, vol. 3, no. 1, p. 4, 2019.
- [143] J. Alvarez-Munoz, N. Marchand, J. Guerrero-Castellanos, J. Tellez-Guzman, J. Escareno, and M. Rakotondrabe, "Rotorcraft with a 3dof rigid manipulator: quaternion-based modeling and real-time control tolerant to multi-body couplings," *International Journal of Automation and Computing*, vol. 15, no. 5, pp. 547–558, 2018.
- [144] W. Wang, K. Nonami, M. Hirata, and O. Miyazawa, "Autonomous control of micro flying robot," *Journal of Vibration and Control*, vol. 16, no. 4, pp. 555–570, 2010.



- [145] J. J. Castillo-Zamora, K. A. Camarillo-Gomez, G. I. Perez-Soto, and J. Rodriguez-Resendiz, "Comparison of pd, pid and sliding-mode position controllers for v-tail quadcopter stability," *Ieee Access*, vol. 6, pp. 38 086–38 096, 2018.
- [146] J. J. Castillo-Zamora, K. A. Camarillo-Gómez, G. I. Pérez-Soto, J. Rodríguez-Reséndiz, and L. A. Morales-Hernández, "Mini-auv hydrodynamic parameters identification via cfd simulations and their application on control performance evaluation," *Sensors*, vol. 21, no. 3, p. 820, 2021.
- [147] R. Jiao, W. Chou, Y. Rong, and M. Dong, "Anti-disturbance attitude control for quadrotor unmanned aerial vehicle manipulator via fuzzy adaptive sigmoid generalized super-twisting sliding mode observer," *Journal of Vibration and Control*, vol. 28, no. 11-12, pp. 1251–1266, 2022.
- [148] J. J. C. Zamora, J. Escareno, I. Boussaada, J. Stephant, and O. Labbani-Igbida, "Nonlinear control of a multilink aerial system and asekf-based disturbances compensation," *IEEE Transactions on Aerospace and Electronic Systems*, vol. 57, no. 2, pp. 907–918, 2020.
- [149] J. Morales, G. Rodriguez, G. Huang, and D. Akopian, "Toward uav control via cellular networks: delay profiles, delay modeling, and a case study within the 5-mile range," *IEEE Transactions on Aerospace and Electronic Systems*, vol. 56, no. 5, pp. 4132–4151, 2020.
- [150] M. Sharma and I. Kar, "Control of a quadrotor with network induced time delay," *ISA transactions*, vol. 111, pp. 132–143, 2021.
- [151] L. Li, M. Wang, K. Xue, *et al.*, "Delay optimization in multi-uav edge caching networks: a robust mean field game," *IEEE Transactions on Vehicular Technology*, 2020.
- [152] M. Liu, L. Zhang, P. Shi, and Y. Zhao, "Fault estimation sliding-mode observer with digital communication constraints," *IEEE Transactions on Automatic Control*, vol. 63, no. 10, pp. 3434–3441, 2018.
- [153] Y. Ding, Y. Wang, and B. Chen, "A practical time-delay control scheme for aerial manipulators," *Proceedings of the Institution of Mechanical Engineers, Part I: Journal of Systems and Control Engineering*, vol. 235, no. 3, pp. 371–388, 2021.

- [154] Y. Kartal, K. Subbarao, N. R. Gans, A. Dogan, and F. Lewis, "Distributed backstepping based control of multiple uav formation flight subject to time delays," *IET Control Theory & Applications*, vol. 14, no. 12, pp. 1628–1638, 2020.
- [155] O. Mofid, S. Mobayen, C. Zhang, and B. Esakki, "Desired tracking of delayed quadrotor uav under model uncertainty and wind disturbance using adaptive super-twisting terminal sliding mode control," *ISA transactions*, 2021.
- [156] G. Mazanti, I. Boussaada, and S.-I. Niculescu, "On qualitative properties of single-delay linear retarded differential equations: characteristic roots of maximal multiplicity are necessarily dominant," *IFAC-PapersOnLine*, vol. 53, no. 2, pp. 4345–4350, 2020.
- [157] E. Steed, E. Quesada, L. Rodolfo, G. Carrillo, A. N. Ramirez, and S. Mondie, "Algebraic dominant pole placement methodology for unmanned aircraft systems with time delay," *IEEE Transactions on Aerospace and Electronic Systems*, vol. 52, no. 3, pp. 1108–1119, 2016.
- [158] D. Lazard and F. Rouillier, "Solving parametric polynomial systems," *Journal of Symbolic Computation*, vol. 42, no. 6, pp. 636–667, 2007.
- [159] F. Rouillier, "Solving zero-dimensional systems through the rational univariate representation," *Applicable Algebra in Engineering, Communication and Computing*, vol. 9, no. 5, pp. 433–461, 1999.
- [160] D. Lazard, "Computing with parameterized varieties," in *Algebraic geometry and geometric modeling*, Springer, 2006, pp. 53–69.
- [161] G. Moroz, "Sur la décomposition réelle et algébrique des systèmes dépendant de paramètres," Ph.D. dissertation, Université Pierre et Marie Curie-Paris VI, 2008.
- [162] J. Gerhard, D. J. Jeffrey, and G. Moroz, "A package for solving parametric polynomial systems," *ACM Communications in Computer Algebra*, vol. 43, no. 3/4, pp. 61–72, 2010.
- [163] M. Ryll, H. H. Bühlhoff, and P. R. Giordano, "A novel overactuated quadrotor unmanned aerial vehicle: modeling, control, and experimental validation," *IEEE Transactions on Control Systems Technology*, vol. 23, no. 2, pp. 540–556, 2014.

- [164] A.-W. A. Saif, A. Aliyu, M. Al Dhaifallah, and M. Elshafei, "Decentralized backstepping control of a quadrotor with tilted-rotor under wind gusts," *International Journal of Control, Automation and Systems*, vol. 16, no. 5, pp. 2458–2472, 2018.
- [165] M. J. Gerber and T.-C. Tsao, "Twisting and tilting rotors for high-efficiency, thrust-vectoring quadrotors," *Journal of Mechanisms and Robotics*, vol. 10, no. 6, 2018.
- [166] I. Al-Ali, Y. Zweiri, N. AMoosa, T. Taha, J. Dias, and L. Senevirtane, "State of the art in tilt-quadrotors, modelling, control and fault recovery," *Proceedings of the Institution of Mechanical Engineers, Part C: Journal of Mechanical Engineering Science*, vol. 234, no. 2, pp. 474–486, 2020.
- [167] J. J. Castillo-Zamora, J. E. Hernández-Díez, I. Boussaada, J. Escareno, and J. U. Alvarez-Muñoz, "A preliminary parametric analysis of pid delay-based controllers for quadrotor uavs," in *2021 International Conference on Unmanned Aircraft Systems (ICUAS)*, IEEE, 2021, pp. 28–37.
- [168] Z. Xu, M. Xu, Y. Wu, Q. Chen, and E. Zhang, "Distributed hunting problem of multi-quadrotor systems via bearing constraint method subject to time delays," *Journal of the Franklin Institute*, vol. 357, no. 12, pp. 7537–7555, 2020.
- [169] F. B. Horak, "Clinical measurement of postural control in adults," *Physical therapy*, vol. 67, no. 12, pp. 1881–1885, 1987.
- [170] C. W. Eurich and J. G. Milton, "Noise-induced transitions in human postural sway," *Physical Review E*, vol. 54, no. 6, p. 6681, 1996.
- [171] P. Kowalczyk, S. Nema, P. Glendinning, I. Loram, and M. Brown, "Auto-regressive moving average analysis of linear and discontinuous models of human balance during quiet standing," *Chaos: An Interdisciplinary Journal of Nonlinear Science*, vol. 24, no. 2, p. 022 101, 2014.
- [172] C. Maurer and R. J. Peterka, "A new interpretation of spontaneous sway measures based on a simple model of human postural control," *Journal of neurophysiology*, vol. 93, no. 1, pp. 189–200, 2005.
- [173] T. Kiemel, Y. Zhang, and J. J. Jeka, "Identification of neural feedback for upright stance in humans: stabilization rather than sway minimization," *Journal of Neuroscience*, vol. 31, no. 42, pp. 15 144–15 153, 2011.

- [174] J. H. Pasma, T. A. Boonstra, J. van Kordelaar, V. V. Spyropoulou, and A. C. Schouten, "A sensitivity analysis of an inverted pendulum balance control model," *Frontiers in Computational Neuroscience*, vol. 11, p. 99, 2017.
- [175] G. Buza, J. Milton, L. Bencsik, and T. Insperger, "Establishing metrics and control laws for the learning process: ball and beam balancing," *Biological Cybernetics*, pp. 1–11, 2020.
- [176] J. R. Chagdes, S. Rietdyk, M. H. Jeffrey, N. Z. Howard, and A. Raman, "Dynamic stability of a human standing on a balance board," *Journal of biomechanics*, vol. 46, no. 15, pp. 2593–2602, 2013.
- [177] D. R. Cruise, J. R. Chagdes, J. J. Liddy, *et al.*, "An active balance board system with real-time control of stiffness and time-delay to assess mechanisms of postural stability," *Journal of biomechanics*, vol. 60, pp. 48–56, 2017.
- [178] E. Chumacero-Polanco and J. Yang, "Basin of attraction and limit cycle oscillation amplitude of an ankle-hip model of balance on a balance board," *Journal of biomechanical engineering*, vol. 141, no. 11, 2019.
- [179] R. R. Zana and A. Zelei, "Introduction of a complex reaction time tester instrument," *Periodica Polytechnica Mechanical Engineering*, vol. 64, no. 1, pp. 20–30, 2020.
- [180] A. D. Goodworth and R. J. Peterka, "Influence of stance width on frontal plane postural dynamics and coordination in human balance control," *Journal of Neurophysiology*, vol. 104, no. 2, pp. 1103–1118, 2010.
- [181] C. A. Molnar, A. Zelei, and T. Insperger, "Human balancing on rolling balance board in the frontal plane," *IFAC-PapersOnLine*, vol. 51, no. 14, pp. 300–305, 2018.
- [182] B. J. Pinter, R. van Swigchem, A. J. " van Soest, and L. A. Rozen-daal, "The dynamics of postural sway cannot be captured using a one-segment unverted pendulum model: A PCA on segment rotations during unperturbed stance," *J. Neurophysiol.*, vol. 100, pp. 3197–3208, 2008.
- [183] Y. Suzuki, T. Nomura, M. Casadio, and P. Morasso, "Intermittent control with ankle, hip, and mixed strategies during quiet standing: a theoretical proposal based on a double inverted pendulum model," *Journal of Theoretical Biology*, vol. 310, pp. 55–79, 2012.

- [184] P. Morasso, A. Cherif, and J. Zenzeri, "Quiet standing: the single inverted pendulum model is not so bad after all," *PloS One*, vol. 14, no. 3, 2019.
- [185] C. A. Molnar, A. Zelei, and T. Insperger, "Rolling balance board of adjustable geometry as a tool to assess balancing skill and to estimate reaction time delay," *Journal of the Royal Society Interface*, vol. 18, no. 176, p. 20200956, 2021.
- [186] I. D. Loram and M. Lakie, "Direct measurement of human ankle stiffness during quiet standing: the intrinsic mechanical stiffness is insufficient for stability," *The Journal of Physiology*, vol. 545, no. 3, pp. 1041–1053, 2002.
- [187] M. Casadio, P. G. Morasso, and V. Sanguineti, "Direct measurement of ankle stiffness during quiet standing: implications for control modelling and clinical application," *Gait & posture*, vol. 21, no. 4, pp. 410–424, 2005.
- [188] M. Cenciarini, P. J. Loughlin, P. J. Sparto, and M. S. Redfern, "Stiffness and damping in postural control increase with age," *IEEE Transactions on biomedical engineering*, vol. 57, no. 2, pp. 267–275, 2009.
- [189] G. Gyebroszki, G. Csernák, J. G. Milton, and T. Insperger, "The effects of sensory quantization and control torque saturation on human balance control," *Chaos: An Interdisciplinary Journal of Nonlinear Science*, vol. 31, no. 3, p. 033145, 2021.
- [190] T. Kiemel, K. S. Oie, and J. J. Jeka, "Slow dynamics of postural sway are in the feedback loop," *Journal of neurophysiology*, vol. 95, no. 3, pp. 1410–1418, 2006.
- [191] A. Zelei, J. Milton, G. Stepan, and T. Insperger, "Response to perturbation during quiet standing resembles delayed state feedback optimized for performance and robustness," *Scientific Reports*, vol. 11, no. 1, pp. 1–13, 2021.
- [192] S. A. Campbell, "Calculating centre manifolds for delay differential equations using maple™," in *Delay differential equations*, Springer, 2009, pp. 1–24.
- [193] S. A. Campbell and Y. Yuan, "Zero singularities of codimension two and three in delay differential equations," *Nonlinearity*, vol. 21, no. 11, p. 2671, 2008.

- [194] M. A. Babram, M. Hbid, and O. Arino, "Approximation scheme of a center manifold for functional differential equations," *Journal of mathematical analysis and applications*, vol. 213, no. 2, pp. 554–572, 1997.
- [195] M. A. Babram, O. Arino, and M. Hbid, "Computational scheme of a center manifold for neutral functional differential equations," *Journal of mathematical analysis and applications*, vol. 258, no. 2, pp. 396–414, 2001.
- [196] I. Boussaada, I.-C. Morărescu, and S.-I. Niculescu, "Inverted pendulum stabilization: characterization of codimension-three triple zero bifurcation via multiple delayed proportional gains," *Systems & Control Letters*, vol. 82, pp. 1–9, 2015.
- [197] T. Vyhlídal and P. Zítek, "Qpmr-quasi-polynomial root-finder: algorithm update and examples," in *Delay systems*, Springer, 2014, pp. 299–312.